

Shasta River Model Development DRAFT

April 2026

Prepared for:



State Water Resources Control Board
1001 I St, Sacramento, CA 95814

Prepared by:



Paradigm Environmental
9320 Chesapeake Drive, Suite 100
San Diego, CA 92123

This Page Intentionally Left Blank

EXECUTIVE SUMMARY

This report provides a detailed discussion of the configuration and calibration of a coupled surface/groundwater model which was developed for the Shasta River Watershed to facilitate the advancement of three broad objectives: (i) more reliable water supplies, (ii) the restoration of important species and habitat, and (iii) a more resilient, sustainably managed water resources system (water supply, water quality, flood protection, and environment) that can better withstand inevitable and unforeseen pressures in the coming decades. This study builds upon decades of research and data collection in the Shasta River watershed and provides an evaluation platform for (1) simulating existing instream flows that integrate current water management activities and consumptive uses, (2) evaluating the range of impacts of alternative management scenarios. The Loading Simulation Program in C++ (LSPC) was used to characterize surface hydrology and the Modular Three-Dimensional Finite-Difference Groundwater Flow Model (MODFLOW) was used to characterize groundwater hydrology. The coupled surface/groundwater modeling approach allowed for a comprehensive evaluation of the effects of diverse water-budget components including precipitation (rainfall and snow), evapotranspiration, diversions, irrigation, groundwater pumping, and groundwater storage. The calibrated LSPC/MODFLOW model calibration achieved a qualitative score of “satisfactory” or better for a range of metrics assessing goodness-of-fit between simulated values and observations. During calibration, LSPC and MODFLOW parameters were intentionally constrained to plausible ranges to avoid overfitting. In so doing, larger-than-anticipated differences in model prediction often revealed gaps in model configuration that prompted further investigation and refinement throughout the model development cycle. This approach, combined with satisfactory calibration performance, ensures that the model remains physically meaningful. As a result, the model is reliable for meeting project objectives, provides confidence in water-budget estimates, and can be used to support informed management decisions.

Acronyms

AGWO	Active Groundwater Outflow
BMP	Best Management Practices
CDEC	California Data Exchange Center
CDF	Cumulative Distribution Function
CDFW	California Department of Fish and Wildlife
DEM	Digital Elevation Model
DEP	Estimated Bankfull-Depth
DCIA	Directly Connected Impervious Area
DWR	California Department of Water Resources
EIA	Effective Impervious Area
ET	Evapotranspiration
GHCN	Global Historical Climatology Network
GIS	Geographic Information System
GW	Groundwater Inflow
HRU	Hydrologic Response Unit
HSG	Hydrologic Soil Group
IFWO	Interflow Outflow Volume
LiDAR	Light Detection and Ranging
LSM	Land Surface Model
LSPC	Loading Simulation Program in C++
MWCD	Montague Water Conservation District
MIA	Mapped Impervious Area
MRLC	Multi-Resolution Land Consortium
NASA	National Aeronautics and Space Administration
NED	National Elevation Dataset
NSE	Nash-Sutcliffe Model Efficiency Coefficient
NHD	National Hydrography Dataset
NLCD	National Land Cover Database

NLDAS	North American Land Data Assimilation System
NRCS	Natural Resources Conservation Service
NSIDC	National Snow & Ice Data Center
PBIAS	Percent Bias
PEST	Parameter ESTimation
POI	Point of Interest
PRISM	Parameter-elevation Regressions on Independent Slopes Model
RAWS	Remote Automated Weather Stations
SNODAS	Snow Data Assimilation System
SNOTEL	Snow Telemetry
SSURGO	Soil Survey Geographic Database
STATSGO	State Soil Geographic Database
SURO	Surface Outflow Volume
SWRCB	State Water Resources Control Board
UCSB	University of California at Santa Barbara
USDA	United States Department of Agriculture
USFS	United States Forest Service
USGS	United States Geological Survey
WBD	Watershed Boundary Dataset

Contents

1	Introduction.....	1
1.1	Study Objectives	2
1.2	Integrated Modeling Approach	3
1.3	Model Overview	5
1.4	Model Development Cycle	6
2	Model Segmentation	8
2.1	Subwatershed Delineation	8
2.2	Refinements to Subwatershed Routing.....	13
2.3	Cross-Section Analysis	14
2.3.1	Identifying Representative Reach Segments.....	14
2.3.2	Cross-Section Characterization Methodology	14
2.3.3	Extrapolating Cross-Sections for Reaches Without Observed LiDAR.....	18
2.4	Hydrologic Response Unit Development.....	19
2.4.1	Digital Elevation Model	21
2.4.2	Land Cover	22
2.4.3	Percent Impervious Cover	24
2.4.4	Percent Canopy Cover	25
2.4.5	Hydrologic Soil Group	27
2.4.6	Bedrock and Hydrogeology	28
2.5	HRU Data Processing	35
2.5.1	Slope Groups.....	36
2.5.2	Land Cover Groups	37
2.5.3	Hydrologic Soil Groups.....	39
2.5.4	Geology Groups	41
2.6	Hydrologic Response Units	44
2.6.1	Directly Connected Impervious Area	47
2.6.2	Secondary HRU Attributes.....	49
3	Meteorological Boundary Conditions.....	51
3.1	Subwatershed Gage Assignment	53
3.1.1	Elevation and Aspect Analysis.....	55
4	Integrated Groundwater Model	59
4.1	Domain and Discretization	62
4.2	Simulation Period	62

4.3	Aquifer Properties	64
4.4	Recharge	69
4.5	Lake Shastina	71
4.6	Streams and Springs	72
4.7	Shallow Groundwater Discharge	73
4.8	Groundwater Pumping.....	75
4.9	Canal Leakage	77
4.10	Additional Boundary Conditions	78
5	Model Approach & Performance	78
5.1	Model Approach.....	78
5.2	Additional Model Configuration.....	79
5.2.1	Consumptive Use Assumptions	79
5.2.2	Riparian Evapotranspiration.....	92
5.3	Metrics for Model Evaluation.....	93
6	Model Calibration & Validation.....	96
6.1	Observed Snowpack.....	96
6.2	Snow Calibration	99
6.3	Snow Validation	104
6.4	Observed Streamflow	109
6.5	LSPC Initial Streamflow Calibration.....	111
6.6	MODFLOW Calibration	116
6.6.1	Groundwater Heads.....	116
6.6.2	Lake Shastina	119
6.6.3	Minor Spring Flow.....	121
6.6.4	Aquifer Parameters	123
6.7	Calibration: Coupled LSPC-MODFLOW Streamflow.....	125
6.8	Validation: Coupled LSPC-MODFLOW Streamflow	129
6.9	Validation: Intermediate Network Locations	133
7	Unimpaired Flow Scenario.....	138
8	Application Guidelines and Considerations.....	146
9	Summary and Conclusions	148
10	References	148

Figures

Figure 1-1. Integrated modeling approach for the Shasta River watershed.	4
Figure 1-2. Hydrology model schematic for land segments (based on Stanford Watershed Model). ..	6
Figure 1-3. Conceptual schematic of model development cycle proposed for assessing instream flow needs in the Shasta River watershed.	8
Figure 2-1. Initial Shasta River Watershed Points of Interest	10
Figure 2-2. Example comparison of original and dissolved tailwater neighborhoods datasets.	11
Figure 2-3. Shasta River subwatersheds initial delineation (left) and final delineation (right) which incorporated tailwater neighborhoods.	12
Figure 2-4. Department of Water Resources Land and Water Use Map near Table Rock. Black lines and arrows indicate direction for ditches, canals, and natural channels.	13
Figure 2-5. Example cross-section representations in LSPC.	15
Figure 2-6. Bare Earth LiDAR cross section for Station 2380.	16
Figure 2-7. Bare Earth LiDAR cross section for Station 1920.	16
Figure 2-8. LiDAR data coverage within the Shasta River watershed area and example cross-sections for stations 2380 and 1920.	17
Figure 2-9. Correlations of sampled LiDAR bank-full width and depth vs. upstream drainage area within the Shasta River watershed area.	18
Figure 2-10. Organizational relationship of HRUs, subwatersheds & model parameterization.	20
Figure 2-11. Elevation of the Shasta River watershed.	21
Figure 2-12. NLCD 2011 land cover in the Shasta River watershed.	23
Figure 2-13. Irrigated areas within the Shasta River watershed by water source.	24
Figure 2-14. NLCD 2011 percent impervious cover in the Shasta River watershed.	25
Figure 2-15. NLCD 2011 percent tree canopy cover in the Shasta River watershed.	26
Figure 2-16. SSURGO hydrologic soil groups within the Shasta River watershed.	28
Figure 2-17. Simplified geologic map of the Shasta River watershed. Major groundwater springs and agricultural irrigation diversions are shown.	29
Figure 2-18. Alluvial aquifers recognized within the Shasta River watershed and water provider boundaries.	33
Figure 2-19. Big Springs Complex.	34
Figure 2-20. Major groundwater springs and surface water diversions of the Shasta Valley.	35
Figure 2-21. Slope Categories within the Shasta River watershed.	37

Figure 2-22. Land Use Categories within the Shasta River watershed.	39
Figure 2-23. Soil Categories within the Shasta River watershed.	41
Figure 2-24. Geology groups within the Shasta River watershed. “Unclassified” represents land cover that was not stratified by geology (i.e., water, wetland, and developed area [about 5.4% of watershed area]).....	43
Figure 2-25. HRU categories map of the Shasta River watershed.	46
Figure 2-26. Translation Sequence from MIA to DCIA.	47
Figure 2-27. Mapped and directly connected impervious area relationships (Sutherland, 2000).	48
Figure 3-1. Annual average PRISM rainfall depths with NLDAS and PRISM centroids.	54
Figure 3-2. Annual average rainfall by subwatershed (from PRISM and NLDAS gridded data).	55
Figure 3-3. Overlay of PRISM centroids with NED-derived elevation and aspect.	56
Figure 3-4. Average annual PRISM rainfall vs. centroid elevation (with median elevation).	57
Figure 3-5. Box plots of average annual rainfall variability by elevation and aspect.	57
Figure 3-6. Median rainfall (vertical axis) vs. elevation and aspect (horizontal plane).....	58
Figure 4-1. Schematic of coupled hydrology model components, interactions, and application.....	59
Figure 4-2. LSPC hydrology model processes, parameters, and timeseries.....	60
Figure 4-3. Overview of key model development components for LSPC and MODFLOW.	61
Figure 4-4. Top elevations of the Shasta River watershed MODFLOW model.	63
Figure 4-5. Bottom elevation and geological attributes for MODFLOW layer 1 in the Shasta River watershed.	65
Figure 4-6. Bottom elevation and geological attributes for MODFLOW layer 2 in the Shasta River watershed.	66
Figure 4-7. Bottom elevation and geological attributes for MODFLOW layer 3 in the Shasta River watershed.	67
Figure 4-8. Bottom elevation and geological attributes for MODFLOW layer 4 in the Shasta River watershed.	68
Figure 4-9. Annual average recharge (GWI) sent from LSPC to MODFLOW grids.	70
Figure 4-10. Ratio of annual average GWI to PREC for MODFLOW grid cells.....	71
Figure 4-11. Average shallow groundwater discharge per MODFLOW grid cell.	74
Figure 4-12. Shasta Valley surface ponds in the vicinity of modeled shallow groundwater discharges.	75
Figure 4-13. Annual average volumes of groundwater pumping and recharge (due to canal leakage) within the Shasta River watershed.....	76

Figure 4-14. Annual average rates of groundwater pumping and recharge due to canal leakage within the Shasta River watershed.	77
Figure 5-1. Process for model calibration to minimize propagation of uncertainty.	79
Figure 5-2. Monthly average surface water, groundwater, and total volumes pumped for irrigation within the Shasta River watershed.....	80
Figure 5-3. Monthly groundwater (top) and surface water (bottom) irrigation depth distributions, with crop and pasture medians, across irrigated subwatersheds.	81
Figure 5-4. Irrigation districts, service areas, canals, and ditches within the Shasta River watershed.	83
Figure 5-5. Schematic of major water features and consumptive uses in the Shasta River watershed.	84
Figure 5-6. MWCD Parks Creek diversion channel.....	85
Figure 5-7. Validation of flow and diversion volumes in the MWCD Parks Creek diversion channel.	86
Figure 5-8. Montague Canal and nearby irrigated fields.	87
Figure 5-9. Early model calibration comparison, prior to MODFLOW and consumptive uses (irrigation withdrawals, groundwater pumping, and diversions), showed close agreement at the Montague Gage during the 2014-2015 drought period.....	88
Figure 5-10. Pacey pumping and canal leakage losses within Shasta River watershed.	89
Figure 5-11. Percent of irrigated HRU area subject to an irrigation rate by water source type. The unadjusted Crop and Pasture irrigated areas are shown in the legend.	90
Figure 5-12. Summary of non-irrigation surface water diversions used in the LSPC model.....	91
Figure 5-13. Cumulative distribution of average percent canopy within a 10-m stream buffer.	92
Figure 5-14. Distribution of monthly Forest TAET for all modeled subwatersheds vs. average Riparian ET.....	93
Figure 6-1. SNOTEL and CDEC stations in the vicinity of the Shasta River watershed.	98
Figure 6-2. Modeled and observed snowpack time series for Big Red Mountain (Station ID: BRM).	103
Figure 6-3. Modeled and observed average monthly snowpack values for Big Red Mountain (Station ID: BRM).	103
Figure 6-4. Modeled and observed snowpack time series for CDEC snow survey data at Parks Creek.	105
Figure 6-5. Modeled and observed snowpack time series for CDEC snow survey data at Mt. Shasta.	105

Figure 6-6. Modeled and observed average monthly snowpack values for CDEC snow survey data at Parks Creek.	106
Figure 6-7. Modeled and observed average monthly snowpack values for CDEC snow survey data at Mt. Shasta.	106
Figure 6-8. CDF comparing annual average snow depth by percent of watershed area.	107
Figure 6-9. Modeled average annual snowpack in the Shasta River watershed. Red dots represent grid cells selected for comparison with the UCSB snow model.	108
Figure 6-10. Modeled LSPC vs. USCB daily snowpack depth (GRID 15201029).	109
Figure 6-11. Modeled LSPC vs. USCB daily snowpack depth (GRID 21903228).	109
Figure 6-12. Streamflow stations within the Shasta River watershed by agency.	110
Figure 6-13. SHASTA R NR YREKA CA (11517500) - Hydrology calibration: Simulated vs. observed normalized monthly streamflow.	114
Figure 6-14. SHASTA R NR YREKA CA (11517500) - Hydrology calibration: Simulated vs. observed normalized monthly streamflow.	114
Figure 6-15. SHASTA R NR YREKA CA (11517500) - Hydrology calibration: Average normalized monthly streamflow.	115
Figure 6-16. SHASTA R NR YREKA CA (11517500) - Hydrology calibration: Simulated vs. observed streamflow duration curves.	115
Figure 6-17. Head contours comparing observed data for Spring 1954 (Mack, 1960) (Black Lines) and model generated steady-state conditions (Green Lines) representing initial conditions for WY 1991.	117
Figure 6-18. Simulated and observed monthly groundwater head values. The coefficient of efficiency, R^2 , and the index of agreement, d , were calculated following methods presented by Legates and McCabe (1999).	119
Figure 6-19. Lake Shastina observed and simulated values.	120
Figure 6-20. Simulated water budget for Lake Shastina.	121
Figure 6-21. Location of springs represented as drain (red) or streams (green) in MODFLOW.	122
Figure 6-22. SHASTA R NR YREKA CA (11517500) - Hydrology calibration: Simulated vs. observed normalized monthly streamflow.	126
Figure 6-23. SHASTA R NR YREKA CA (11517500) - Hydrology calibration: Simulated vs. observed normalized monthly streamflow.	126
Figure 6-24. SHASTA R NR YREKA CA (11517500) - Hydrology calibration: Average normalized monthly streamflow.	127
Figure 6-25. SHASTA R NR YREKA CA (11517500) - Hydrology calibration: Simulated vs. observed streamflow duration curves.	127

Figure 6-26. SHASTA R NR YREKA CA (11517500) - Hydrology validation: Simulated vs. observed normalized monthly streamflow.	130
Figure 6-27. SHASTA R NR YREKA CA (11517500) - Hydrology validation: Simulated vs. observed normalized monthly streamflow.	130
Figure 6-28. SHASTA R NR YREKA CA (11517500) - Hydrology validation: Average normalized monthly streamflow.	131
Figure 6-29. SHASTA R NR YREKA CA (11517500) - Hydrology validation: Simulated vs. observed streamflow duration curves.....	131
Figure 6-30. Big Springs Creek Water Wheel (105SRBSWW) - Hydrology calibration: Average normalized monthly streamflow	134
Figure 6-31. Big Springs Creek Water Wheel (105SRBSWW) - Hydrology calibration: Simulated vs. observed streamflow duration curves.....	135
Figure 6-32. Long-term Trends in Groundwater Recharge (1896-2024).	136
Figure 6-33. SHASTA R NR MONTAGUE CA (11517000) - Hydrology calibration: Simulated vs. observed streamflow duration curves.....	137
Figure 7-1. Selected unimpaired flow locations within Shasta River Watershed.	139
Figure 7-2. Flow at Yreka: comparison between unimpaired and baseline flow conditions.....	140
Figure 7-3. Flow at mainstem between Big Springs and Parks Creek: comparison between unimpaired and baseline flow conditions.	141
Figure 7-4. Flow at mainstem between Dwinnell Reservoir and Parks Creek: comparison between unimpaired and baseline flow conditions.	142
Figure 7-5. Flow at Little Shasta River Near Montague Gage: comparison between unimpaired and baseline flow conditions.	143
Figure 7-6. Flow at Parks Creek location: comparison between unimpaired and baseline flow conditions.....	144
Figure 7-7. Flow at Big Springs: comparison between unimpaired and baseline flow conditions...	145

Tables

Table 2-1. Manning's n values for natural channels ¹	19
Table 2-2. Summary of input datasets detailing data source and type	20
Table 2-3. NLCD 2011 land cover classifications & areas in the Shasta River watershed.....	22
Table 2-4. NRCS Hydrologic soil group descriptions.....	27
Table 2-5. Shasta Valley Groundwater Basin.	32
Table 2-6. Slope HRU groups and area distribution for Shasta River watershed.....	36
Table 2-7. Land Cover HRU groups and area distribution for Shasta River watershed	38
Table 2-8. HSG category HRU groups and area distribution for Shasta River watershed.....	40
Table 2-9. Geologic HRU groups and area distribution for Shasta River watershed	42
Table 2-10. Percent land cover distribution by HRU category for the Shasta River watershed	45
Table 2-11. Mapped Impervious Area compared with Effective Impervious Area.	49
Table 2-12. Summary of Forest Land Cover Classification by Forest HRU category.....	51
Table 3-1. Climate parameters evaluated during the initial inventory.	53
Table 3-2. Median rainfall (and distribution of PRISM centroids) by elevation and aspect	58
Table 5-1. Summary of performance metrics used to evaluate hydrology calibration.....	95
Table 6-1. Summary of observed snowpack data reviewed for the Shasta River watershed	97
Table 6-2. Typical and possible parameter values for snow calibration (Source: EPA 2000).....	100
Table 6-3. Calibrated snow parameter ranges by land use group and soil type.....	101
Table 6-4. Snowpack simulation Nash-Sutcliffe (NSE), PBIAS (percent bias), and R-squared value for modeled vs. observed snowpack at the Big Red Mountain SNOTEL location.	102
Table 6-5. Upstream drainage area characteristics for selected streamflow stations	111
Table 6-6. Parameters and ranges used in automated calibration.....	112
Table 6-7. Typical and possible parameter values for hydrology calibration (Source: EPA 2000) ..	113
Table 6-8. Observed and simulated flow rates for springs (drains or streams) within the MODFLOW model.....	123
Table 6-9. Calibrated aquifer parameters used in the Shasta River watershed MODFLOW model	124
Table 6-10. SHASTA R NR YREKA CA (11517500) - Hydrology calibration: Percent bias statistical metric for predicted vs observed volumes.....	128
Table 6-11. SHASTA R NR YREKA CA (11517500) - Hydrology calibration: Statistical metric for monthly predicted vs observed volumes.....	128

Table 6-12. SHASTA R NR YREKA CA (11517500) - Hydrology validation: Percent bias statistical metric for predicted vs observed volumes.....	132
Table 6-13. SHASTA R NR YREKA CA (11517500) - Hydrology calibration: Statistical metric for monthly predicted vs observed volumes.....	133
Table 6-14. Summary of PBIAS by season and flow regime for additional validation gages.....	134
Table 6-15. Big Springs Creek Water Wheel (105SRBSWW) - Hydrology calibration: Percent bias statistical metric for predicted vs observed volumes.....	135
Table 6-16. SHASTA R NR MONTAGUE CA (11517000) - Hydrology calibration: Percent bias statistical metric for predicted vs observed volumes.....	138

Appendices

Appendix A: Watershed Delineation

Appendix B: Channel Properties

Appendix C: HRU Summary

Appendix D: Streamflow Data

Appendix E: Snow Calibration

Appendix F: Calibrated LSPC Parameters

Appendix G: Groundwater Hydrographs

Appendix H: Hydrology Calibration

Appendix I: Hydrology Validation

Appendix J: Hydrology Validation Intermediate Network Locations

ACKNOWLEDGEMENTS

The following project team members supported Paradigm Environmental, Inc. in the preparation of this report:

S.S. Papadopoulos & Associates

1 INTRODUCTION

The California Natural Resources Agency, the California Environmental Protection Agency, and the California Department of Food and Agriculture developed the California Water Action Plan (WAP), released on January 22, 2014. The WAP has been developed to meet three (3) broad objectives:

1. More reliable water supplies;
2. The restoration of important species and habitat; and
3. A more resilient, sustainably managed water resources system (water supply, water quality, flood protection, and environment) that can better withstand inevitable and unforeseen pressures in the coming decades.

Action Four (4) of the WAP, to “Protect and Restore Important Ecosystems,” contains the following sub-action:

“The State Water Resources Control Board and the Department of Fish and Wildlife will implement a suite of individual and coordinated administrative efforts to enhance flows statewide in at least five stream systems that support critical habitat for anadromous fish. These actions include developing defensible, cost-effective, and time-sensitive approaches to establish instream flows using sound science and a transparent public process. When developing and implementing this action, the State Water Resources Control Board and the Department of Fish and Wildlife will consider their public trust responsibility and existing statutory authorities such as maintaining fish in good condition.”

Through a coordinated effort between the State Water Resources Control Board (State Water Board) and California Department of Fish and Wildlife (CDFW), the following five (5) priority stream systems have been identified as a starting point for the WAP effort:

1. Shasta River, tributary to the Klamath River, Siskiyou County
2. South Fork Eel River, tributary to the Eel River, Humboldt and Mendocino Counties
3. Mark West Creek, tributary to the Russian River, Sonoma County
4. Mill Creek, tributary to the Sacramento River, Shasta and Tehama Counties
5. Ventura River, Santa Barbara and Ventura Counties

The State Water Board and CDFW have been working to identify potential actions that may be taken to enhance and establish instream flow for anadromous fish in these five (5) priority streams and other streams of importance to the WAP objectives. The development of hydrologic characterization models is one of the first efforts that the State Water Board will work on to better understand water supply, water demand, and instream flow in the priority watersheds.

This document specifically focuses on the Shasta River watershed, and documents data and assumptions for model development, describes methods and assumptions for model parameterization, presents model calibration results, and summarizes limitations and important considerations for developing future management scenarios.

1.1 Study Objectives

The State Water Board identified the following key study objectives to be addressed with the hydrologic model:

- ▼ Estimate existing instream flows¹ at multiple points of interest (POI) throughout the mainstem Shasta River and its tributaries where no flow measurement data are available.
- ▼ Predict unimpaired flow² at each POI that would occur with no water diversions, pumping, or storage.
- ▼ Depict how water use and other human activities affect the water balance and instream flows.
- ▼ Ensure the model simulation period is long enough to capture the variability of the full range of water year types from drought to flood years.
- ▼ Simulate groundwater pumping and surface-subsurface interactions to understand groundwater effects on instream flows.

In addition, the State Water Board identified other model capabilities that should be considered in the current study to support future studies and planning efforts. Although these capabilities may require future model refinements or linkages to other models, the base hydrologic modeling system will be developed in a manner that supports these potential future upgrades or linkages. Additional capabilities of interest include:

- ▼ Support assessments of habitat for important species.
- ▼ Represent the water rights priority system to evaluate water management scenarios.
- ▼ Simulate climate change and future water demand.
- ▼ Simulate water quality or the ability to link the surface water hydrology model to separate water quality models.

¹ For this model, “existing instream flows” are defined as the flows estimated by the model using the most recent and complete land use and water use data at the time of model development.

² Unimpaired flow is the flow that would have occurred had the natural flow regime remained unaltered in rivers instead of being stored in reservoirs, imported, exported, or diverted. Unimpaired flow is a modeled flow generally based on historical gage data with factors applied to primarily remove the effects of dams and diversion within the watersheds. Unimpaired flow differs from full natural flow in that the modeled unimpaired flow does not remove changes that have occurred such as channelization and levees, loss of floodplain and wetlands, deforestation, and urbanization. Where no diversion, storage, or consumptive use exists in the watershed, the historical gage data is often assumed to represent unimpaired flow.

1.2 Integrated Modeling Approach

Main modeling components include:

- ▼ Watershed model that integrates surface and subsurface hydrology, hydromodifications, surface diversions, and irrigation and non-irrigation consumptive uses
- ▼ Groundwater model to represent complex geology, lateral water movements, change in groundwater storage, groundwater recharge, spring outflow to streams, groundwater pumping, and surface water – groundwater interaction.

This modeling effort provides comprehensive, transparent, and reproducible methods for evaluating impacts and benefits of water management of instream flows. The model was developed from 2018 through 2025. The Paradigm modeling team included S.S. Papadopoulos & Associates Inc (SSPA) for Modular Three-Dimensional Finite-Difference Groundwater Flow Model (MODFLOW) and geology expertise from Stillwater Sciences. The model was also developed in collaboration with the California State Water Resources Control Board, Stockholm Environmental Institute (SEI), and Larry Walker Associates (LWA).

To address the above objectives, the Loading Simulation Program in C++ (LSPC) was selected as the watershed modeling platform. MODFLOW was coupled with LSPC to increase subsurface resolution to address complex geology and surface-groundwater interactions. Supporting information used for model development included:

- ▼ Detailed spatial and temporal information including land use, topography, geology, stream hydrography, and meteorological boundary conditions for model segmentation
- ▼ Observed snowpack and streamflow data for model calibration
- ▼ Irrigation infrastructure data including points of diversion canal conveyance pathways, and estimated places of use
- ▼ Spatial and temporal irrigation demand estimates developed by Davids Engineering (Davids Engineering, 2020)
- ▼ Spatial and temporal estimates of groundwater pumping
- ▼ Non-irrigation consumptive use and return flows from the Electronic Water Rights Management System (eWRIMS)

Figure 1-1 presents a conceptual schematic of the integrated modeling approach and key components for the Shasta River watershed. A full description of the model is provided in the following section. In an earlier parallel modeling effort, CE-QUAL-W2 was used to model stream temperature; however, that component has not been updated with recent refinements to the watershed model. This report documents the technical approaches used to configure and calibrate the integrated watershed-groundwater hydrology model, and the integration of consumptive use assumptions.

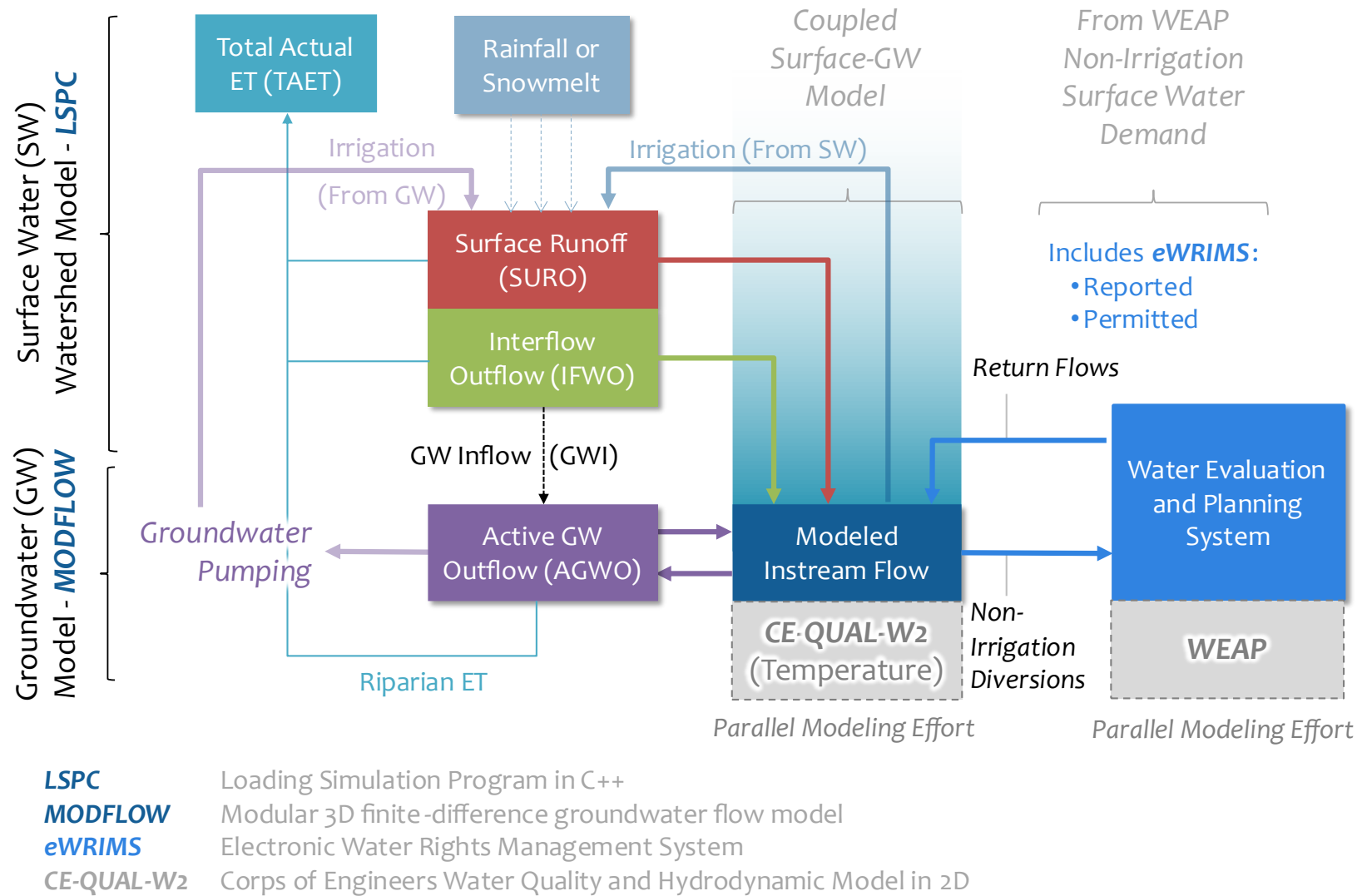


Figure 1-1. Integrated modeling approach for the Shasta River watershed.

1.3 Model Overview

LSPC is an open-source, process-based watershed modeling system developed by the U.S. Environmental Protection Agency (EPA) for simulating watershed hydrology, temperature, sediment erosion and transport, and water quality processes from both upland contributing areas and receiving streams (USEPA 2017a, 2017b).

Fundamentally, a watershed model is a series of algorithms for representing the interaction between meteorology and the landscape, resulting in surface and subsurface flows that transport pollutants downstream. The LSPC model simulates flow accumulation in stream networks. Although water quality is not among the current study objectives, the model can be expanded in the future to also simulate the transport of pollutants, which may be deposited or scoured from the stream bed, sorbed, and/or transformed due to various chemical and biological processes. LSPC is capable of dynamically simulating flow, sediments, nutrients, metals, dissolved oxygen, temperature, and other pollutants for pervious and impervious lands and waterbodies of varying sizes.

LSPC algorithms were developed from a subset of those in the Hydrologic Simulation Program FORTTRAN (HSPF) (Bicknell et al. 1997). The hydrologic portion of HSPF is based on the Stanford Watershed Model (Crawford and Linsley 1966), one of the pioneering watershed models. LSPC is built upon a relational database platform, enabling the collation of diverse datasets to produce robust representations of natural systems. LSPC integrates GIS outputs, comprehensive data storage and management capabilities, the original HSPF algorithms, and a data analysis/post-processing system into a PC-based Windows environment.

Figure 1-2 is a generalized schematic of the underlying hydrology model (Stanford Watershed Model) used in LSPC. The schematic represents land-based processes for a single land unit in the model, which is referred to herein as a hydrologic response unit (HRU). The schematic shows the major processes that influence hydrology, which in turn influence water quality. Some of the parameters shown in the schematic represent state variables and others represent rates. All HRUs within a subwatershed are simulated in parallel and routed to the associated routing segment—there are no lateral connections between HRUs in LSPC; therefore, LSPC alone is limited in its ability to simulate groundwater movement springs, and impacts of groundwater pumping on recharge to streams. The green box in Figure 1-2 highlights model components in LSPC that were supplemented by MODFLOW to help overcome those limitations. The details of model integration are described in Sections 4 and 5. Model calibration strikes a balance between capturing differences in physical characteristics and explaining those differences with available data, while managing the size and complexity of the model. Wherever tradeoffs arose during model development and calibration, decisions err on the side of that which produces better low-flow predictions to support minimum flow requirements and critical conditions for instream temperature.

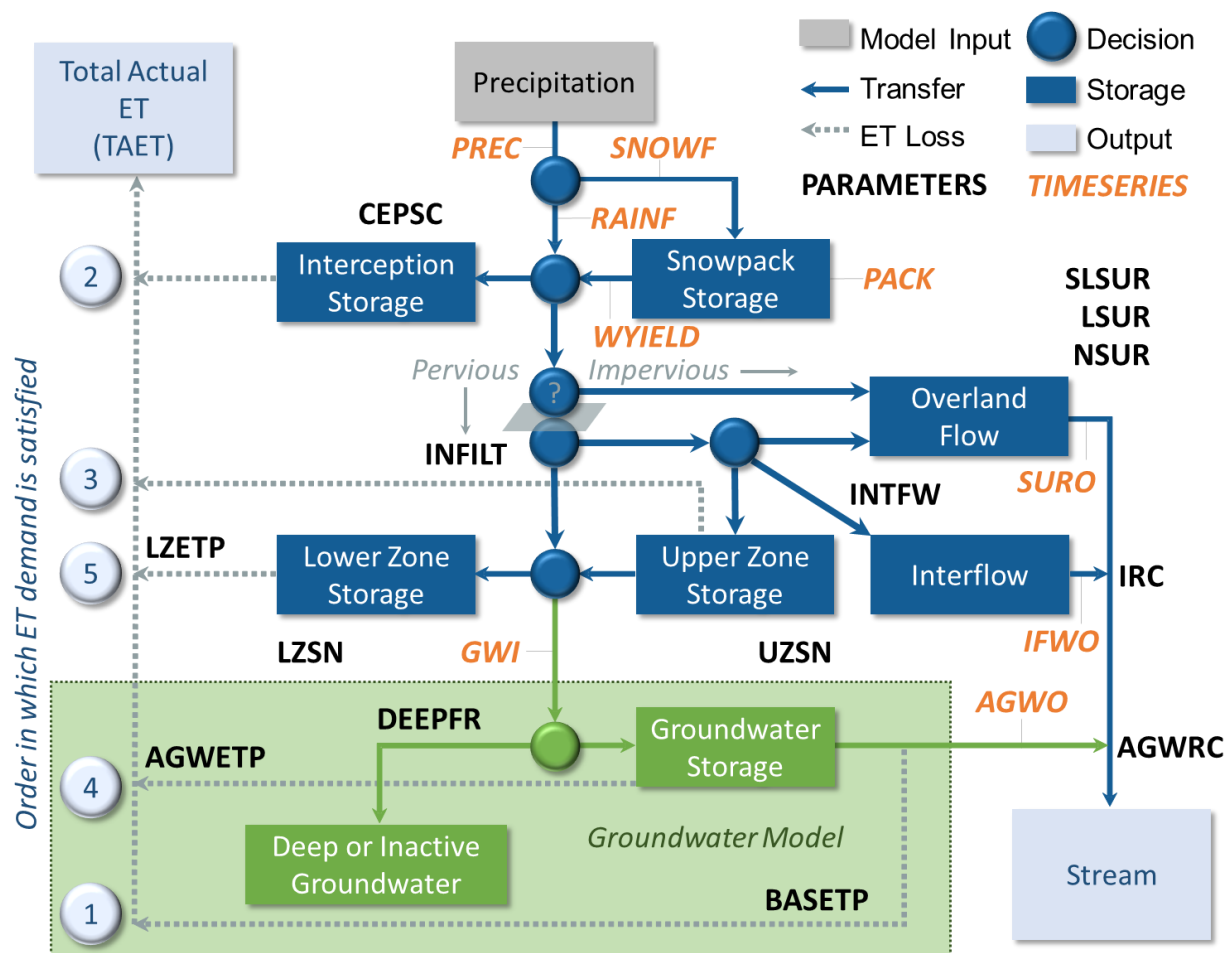


Figure 1-2. Hydrology model schematic for land segments (based on Stanford Watershed Model).

1.4 Model Development Cycle

The Shasta River modeling approach builds upon insights gained from several years of research, data collection and modeling efforts in the region and incorporates several key model configuration components and calibration approaches. Detailed descriptions of those components are described in the sections below. They include:

- ▼ Model Segmentation (Section 2), including:
 - Delineation of subwatershed boundaries,
 - Reach segmentation, cross sections, and network routing,
 - Land segments and associated hydrological responses
- ▼ Meteorological Boundary Conditions (Section 3)
- ▼ Groundwater Model Integration (Section 4)
- ▼ Modeling Approach and Performance (Section 5)
- ▼ Model Calibration and Validation (Section 6)
- ▼ Unimpaired Flow Scenario (Section 7)
- ▼ Limitations and Recommendations (Section 8)

Figure 1-3 is a schematic of the adaptive model development cycle adopted for assessing and integrating the required datasets for simulation, and how they relate to the overall model calibration

and validation process and study objectives. The gray arrows show the connections between the various stages of model development. The cycle can be summarized in six interrelated steps:

1. **Assess Available Data.** Compile and assess data to be used for land representation, source characterization, meteorological boundary conditions, etc. This includes insights from previous modeling efforts that can be leveraged and incorporated.
2. **Define Model Domain.** Determine model segmentation and discretization needed to simulate hydrology and water quality at temporal and spatial scales appropriate for supporting decisions across the watershed.
3. **Set Boundary Conditions.** Set spatial and temporal model inputs, especially meteorological data, for establishing the conditions that drive variation in hydrology and water quality.
4. **Represent Processes.** Select the processes and pathways to be represented by the algorithms in the model based on the intended application (e.g., which pollutants to simulate).
5. **Confirm Predictions.** Adjust model parameters to characterize a complex physical environment in a simplified modeling framework, mostly through comparison to local observations, past relevant studies, and best professional judgment.
6. **Assess Data Gaps.** Modeled responses and/or unsatisfactory model performance can indicate the influence of unrepresented physical processes in the modeled system. A well-designed model can be adapted for future applications as new information about the system becomes available. Depending on the study objectives, data gaps sometimes provide a sound basis for further data collection efforts to refine the model, which cycles back to Step 1.

The Shasta River watershed model uses a regional calibration approach with consistent methods and assumptions for model parameterization across the watershed. The approach prioritizes configuration over calibration by investigating and expressing known physical characteristics of the watershed explicitly wherever possible and practical, and only leaving responses that cannot be explained by physical characteristics to model calibration. These steps are organized into two primary efforts: model configuration (green boxes) and model calibration and validation (blue), described below in Section 6.

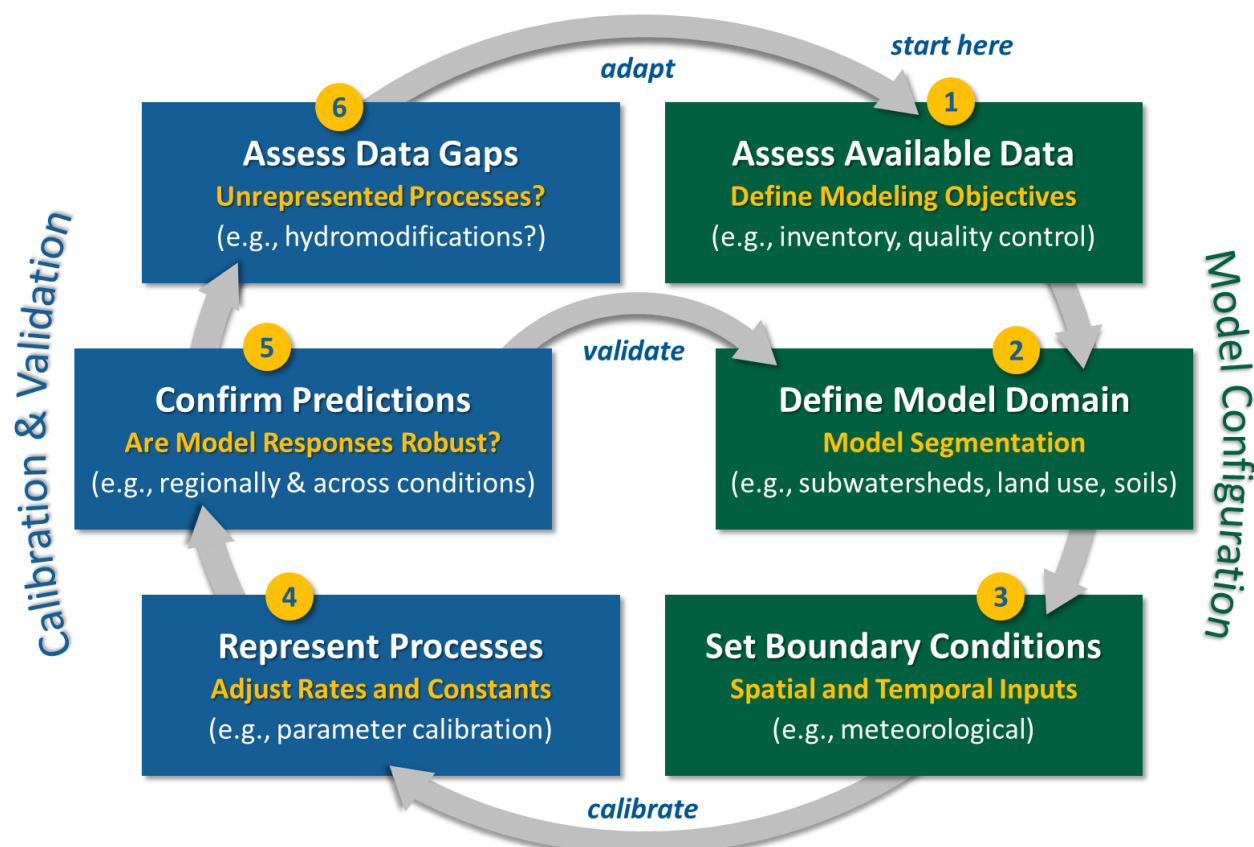


Figure 1-3. Conceptual schematic of model development cycle proposed for assessing instream flow needs in the Shasta River watershed.

2 MODEL SEGMENTATION

Model segmentation refers to basic building blocks for the definition of the surface water model domain. It includes subwatershed delineation, reach segments (cross-sections, hydraulic characteristics, and routing network), and HRUs. Model segmentation for the coupled groundwater model is presented in Section 4 (Integrated Groundwater Model).

2.1 Subwatershed Delineation

Developing the Shasta River Loading Simulation Program C++ (LSPC)/MODLFOW model began with a subwatershed delineation to establish the model domain. The subwatershed delineation was informed by points of interest (POI) and tailwater neighborhoods provided by the State Water Resources Control Board (SWRCB). Initially, 307 POI were identified; some of the POI correspond to locations of instream monitoring gages, while others are points in the flow network that correspond to known diversions or threatened habitats. Points of interest that align with monitoring stations allow for direct comparison of model-predicted and observed streamflow for model calibration and validation. The initial set of 307 POI was reduced to 149 POI, which included 96 high priority SWRCB POI and 53 additional POI to reflect stream network connectivity (Figure 2-1). The base layer for the subwatershed delineation was the National Hydrography Dataset *Plus*, version 2 (NHDPlusV2) dataset (U.S. Geological Survey, 2018) NHDPlusV2 integrates spatial data from the

National Elevation Dataset (NED) and the Watershed Boundary Dataset (WBD) to produce several high-resolution geospatial data products for delineation. For the Shasta River delineation, NHDPlusV2 flow direction, flow accumulation, and catchments files for California region 18c were identified and downloaded. The goal of this effort was to delineate subwatershed outlets that aligned with the POI identified by the SWRCB, while preserving stream routing/connectivity and modeling efficiency. The pre-delineated NHDPlusV2 subwatershed boundaries were used to validate the spatial extent and connectivity of subwatersheds resulting from this process.

The process for subwatershed delineation included the following steps:

1. Creating stream flowlines from the NHDPlusV2 flow accumulation file and delineating the Shasta River watershed using flow accumulation and streamline information.
2. Verifying that the spatial extent of the delineated Shasta River watershed aligned with catchments downloaded from NHDPlusV2 and the outermost watershed boundary.
3. Snapping SWRCB POI locations with nearby major confluences as applicable and adding new POI as needed to preserve stream network connectivity.
4. Delineating subwatersheds using the final set of POI from the previous step.

Several POI delineations required review and resolution in coordination with the SWRCB—these are discussed in Appendix A. The initial, POI-based delineation resulted in 141 subwatersheds and included outlets for all the identified POI and preserved stream connectivity and routing requirements for the model.

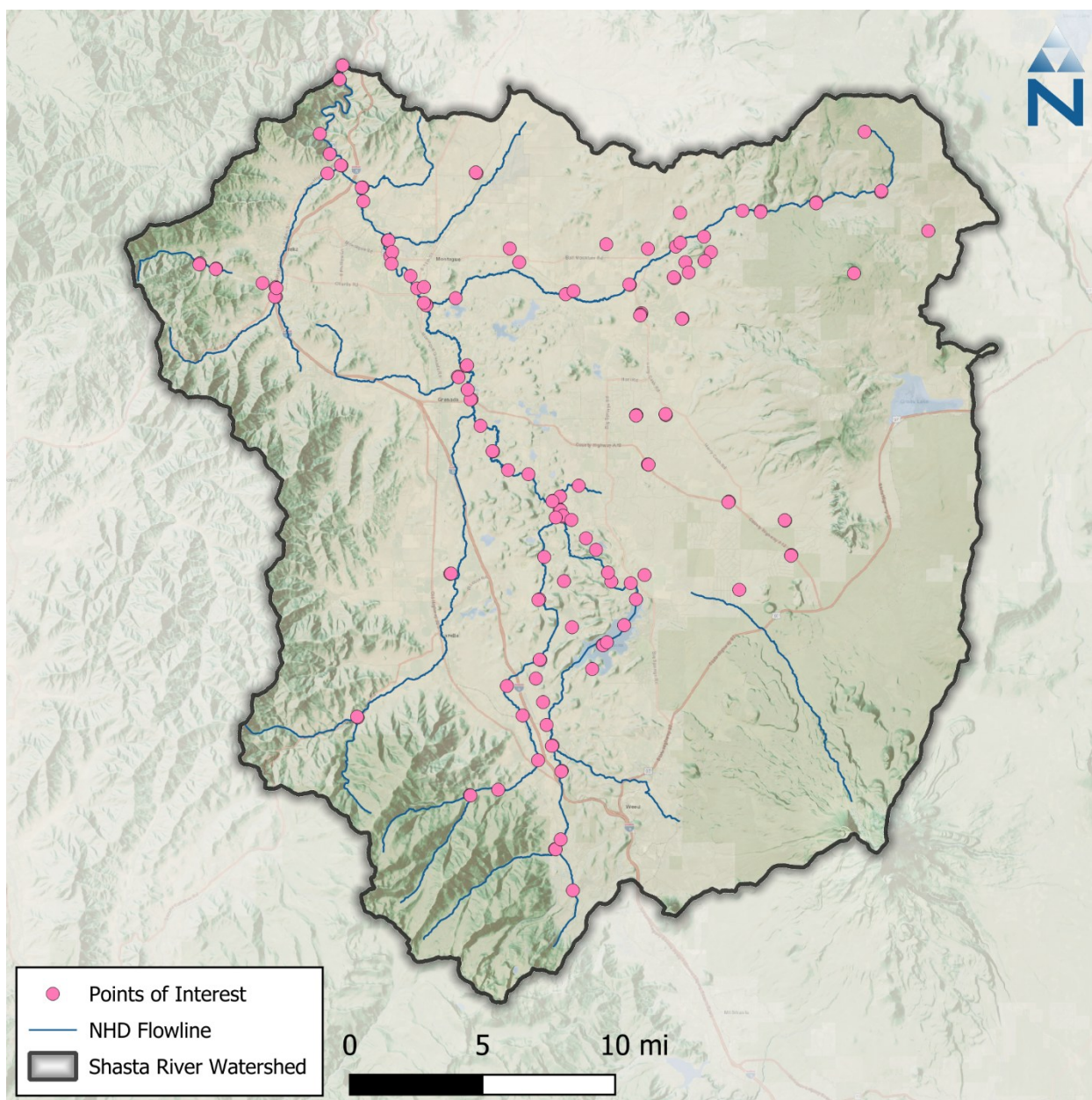


Figure 2-1. Initial Shasta River Watershed Points of Interest

The watersheds were further refined using available tailwater neighborhood information provided by the SWRCB. The Shasta tailwater neighborhoods are LiDAR-derived areas in which surface water runoff used for irrigation returns to a stream or river. This water is initially diverted out of the Shasta River and its tributaries then conveyed via ditches or pipes to an irrigation site. While much of the irrigation water is taken up by plants, evaporated, or infiltrated, some of it runs off the land as tailwater. Tailwater return flows have been identified as a primary factor impacting stream temperatures in the Shasta River watershed (Shasta Valley Resource Conservation District, 2017). The original tailwater neighborhood watersheds ranged in size from 0.6 to 1,828 acres. These watersheds were combined along the ~1 km (0.6 miles) CE-QUAL-W2 channel segments developed for the temperature modeling component of this project (see Paradigm Environmental, 2022). Figure 2-2 presents an example of the original and dissolved tailwater neighborhoods. Figure 2-3 shows the initial

set of subwatersheds, which were informed by the POI and the final delineation that also incorporated the dissolved tailwater neighborhoods. The final delineation consisted of 261 subwatersheds.

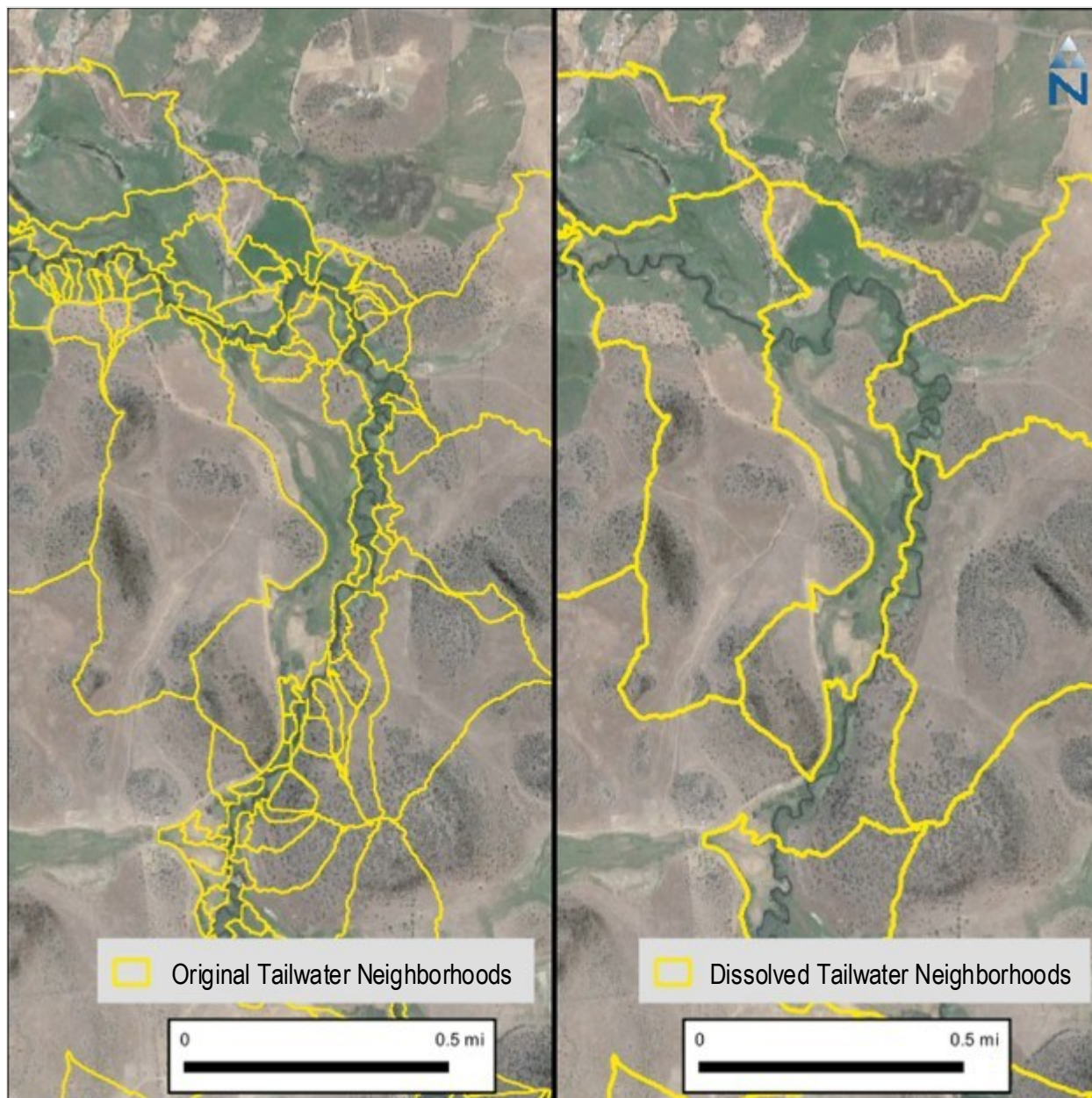


Figure 2-2. Example comparison of original and dissolved tailwater neighborhoods datasets.

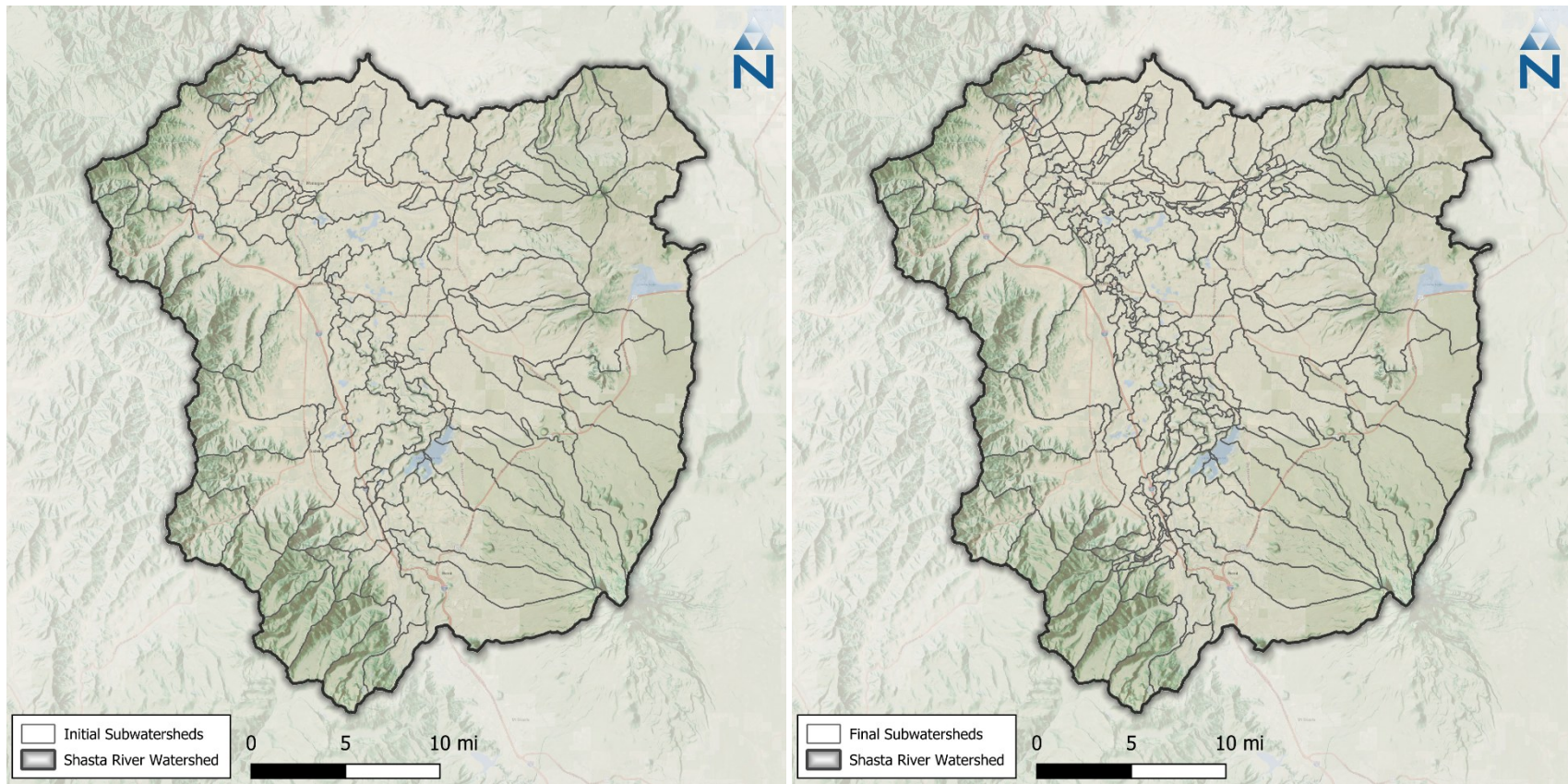


Figure 2-3. Shasta River subwatersheds initial delineation (left) and final delineation (right) which incorporated tailwater neighborhoods.

2.2 Refinements to Subwatershed Routing

Surface water routing in the Shasta River can be complex, influenced by several ditches, canals, and other man-made structures. To improve the accuracy of LSPC watershed routing, Land and Water Use maps from California Department of Water Resources, published for the Shasta Valley in 1958 were used. The maps contain information on location of irrigation land as well as flow direction of streams, canals, and natural channels. Figure 2-4 presents a sample of the information portrayed in these maps for a location near the Table Rock formation in the Shasta Valley.

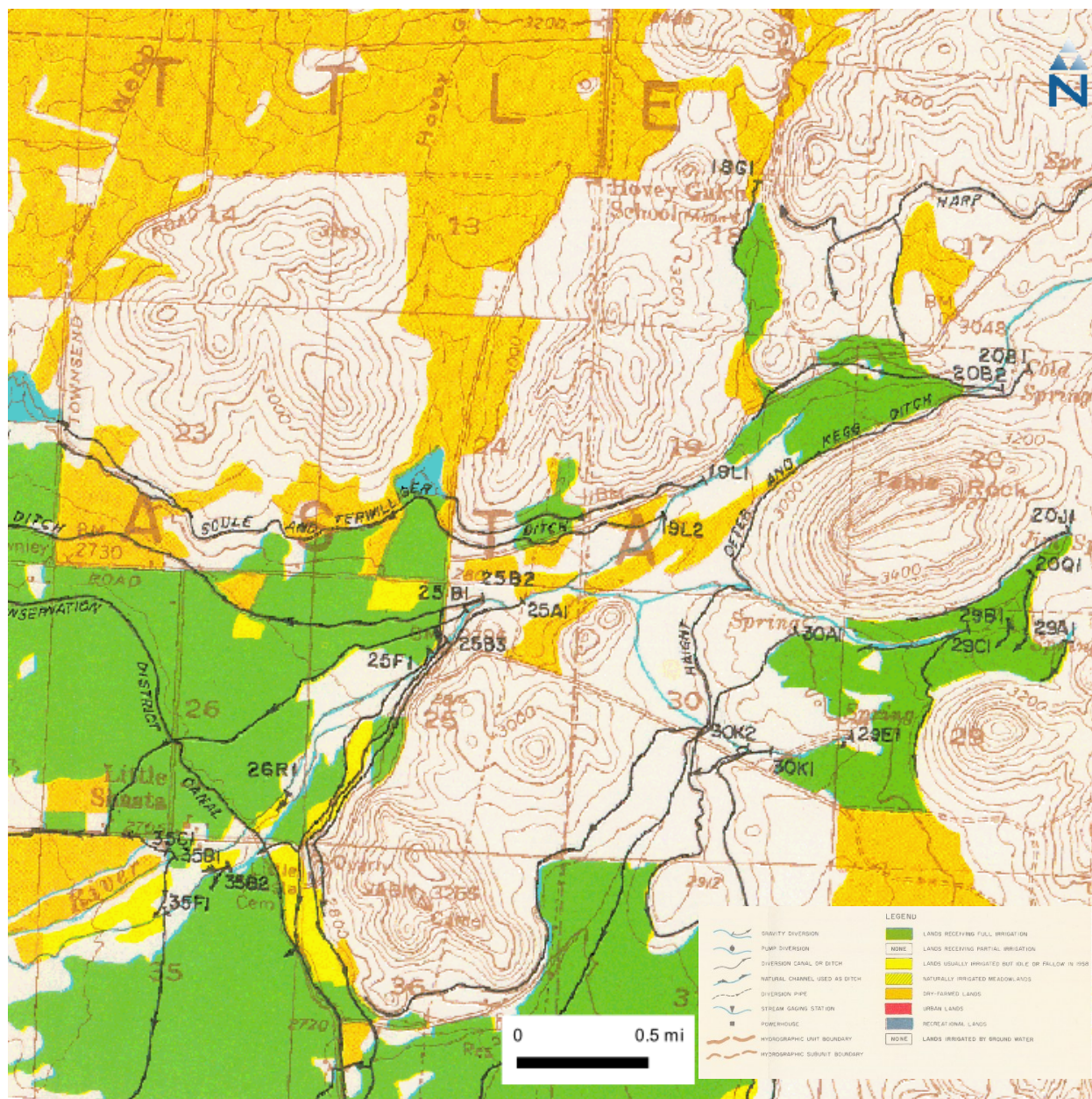


Figure 2-4. Department of Water Resources Land and Water Use Map near Table Rock. Black lines and arrows indicate direction for ditches, canals, and natural channels.

2.3 Cross-Section Analysis

Once watersheds have been delineated, the physical stream properties (e.g., depth, width) within each watershed need to be specified so that water can be routed from upstream to downstream areas. Within the Shasta River watershed model, surface flow is conveyed through a reach network with one representative reach segment for each subwatershed. Within a subwatershed, water from all other upstream physical conveyances is routed directly to the top of and through the representative stream segment. Stream segments are represented in the model as having the same cross-section for the entire length of the reach. Where available, Light Detection And Ranging (LiDAR) data were used to estimate physical characteristics for the representative reach segment. LiDAR data were also used to develop empirical relationships between channel geometry and watershed characteristics, and these relationships were applied in areas where high resolution remote sensing data were unavailable.

2.3.1 Identifying Representative Reach Segments

After representative reach segments were identified for each subwatershed, the length and average slope of each reach segment was calculated from the GIS spatial features. For cases where segments were downstream of a confluence, forming a “Y” with two upstream subwatersheds, the leg connecting the subwatershed with the greatest upstream drainage area was selected as the representative reach segment. The length and slope properties were derived using the reach segment GIS line feature and Digital Elevation Model (DEM) or LiDAR, and recorded as attributes of the line feature as follow:

- ▼ **SLength:** the 3-dimensional surface length of stream segments in the LiDAR point cloud.
- ▼ **Shape_Leng:** the 2-dimension surface length of stream segments field which has slightly smaller values than “SLength.”
- ▼ **Avg_Slope:** the average slope of reach segments.
- ▼ **Source:** the source of data used to calculate slope/length values. For the segments that have full coverage of LiDAR data (for both the starting point and ending point of the stream segment), a 1-ft DEM extracted from LiDAR data has been used (62 stream segments, mainly along the mainstem). For other stream segments, a 10-m DEM has been used (87 stream segments).

2.3.2 Cross-Section Characterization Methodology

The default cross-section representation in LSPC is a symmetrical trapezoidal channel defined using the terms shown in Figure 2-5. Alternatively, when observed cross-section data are available, (x, y) transect coordinates can replace the lower trapezoid, as shown in the bottom panel of Figure 2-5. The channel area above the estimated bank-full width (DEP) is still modeled using the upper-trapezoid parameters. Because the cross-section is modeled as uniform across the entire reach segment, a weighted average of multiple cross-sections along the segment or an extrapolation from several measured cross-sections may be more representative than using a single cross-section measured at one point along the stream segment.

Representative cross sections were estimated from transects of the LiDAR data along the mainstem of the Shasta River, along with a few of the tributary confluences near the mainstem that were within the LiDAR sampling buffer. The high-resolution LiDAR dataset (1-ft resolution) was flown by Terrapoint LLC in January, 2008. The primary purpose for acquiring the LiDAR dataset was to use as a planning and design tool to develop agricultural tailwater reduction projects in the Shasta Valley.

The data were used to develop the Tailwater Neighborhood geometric network discussed in section 2.1. Figure 2-8 shows LiDAR data boundary and coverage. Figure 2-6 and Figure 2-7 are examples of the bare-earth LiDAR cross-section at stations 2380 and 1920, respectively. Station 2380 is a tributary, while Station 1920 is along the mainstem. The upstream drainage area for station 2380 is approximately double the upstream drainage area for station 1920, but they both approach the confluence at similar slopes. Figure 2-8 shows LiDAR data coverage and highlights stations 2380 and 1920.

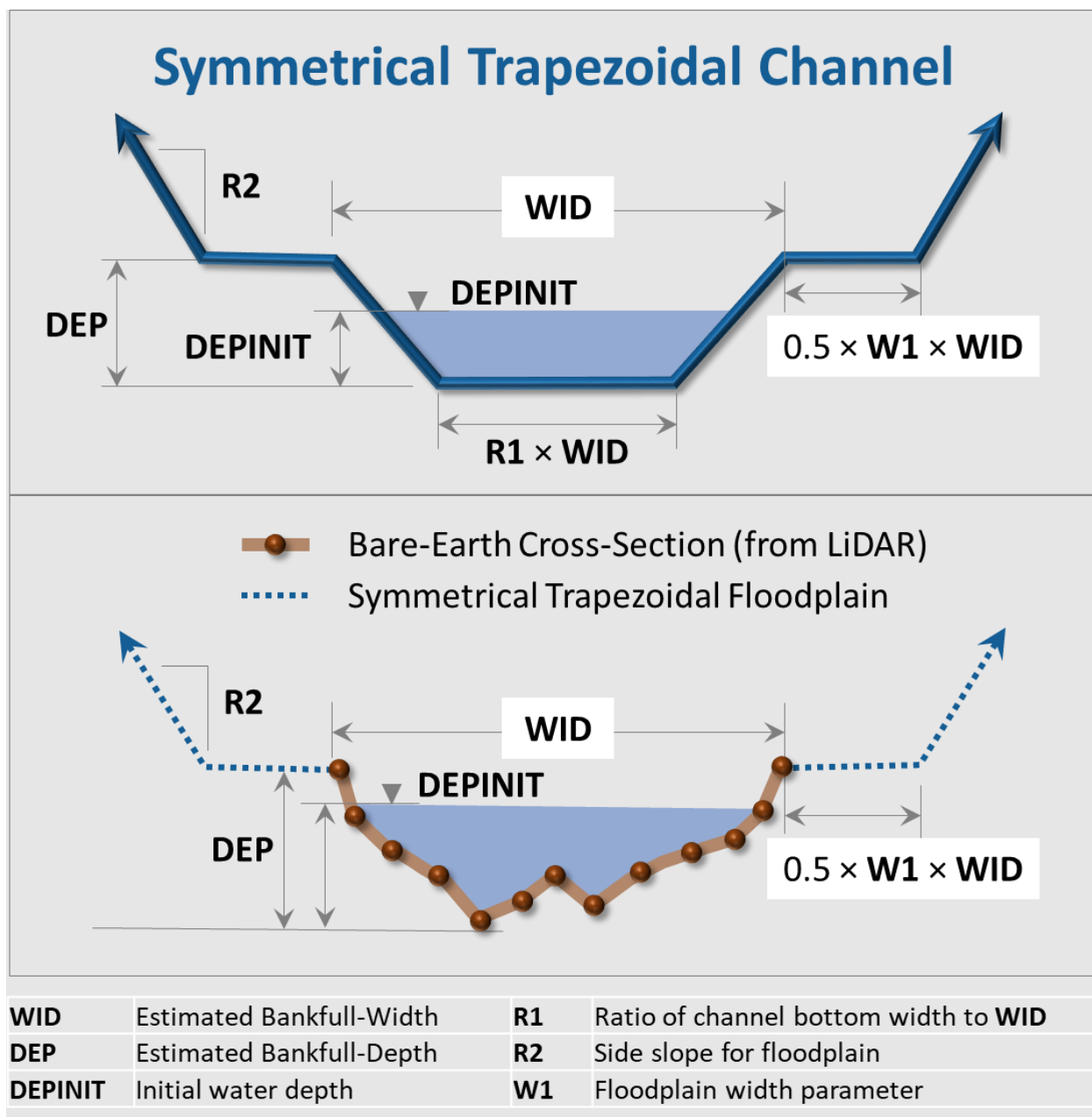


Figure 2-5. Example cross-section representations in LSPC.

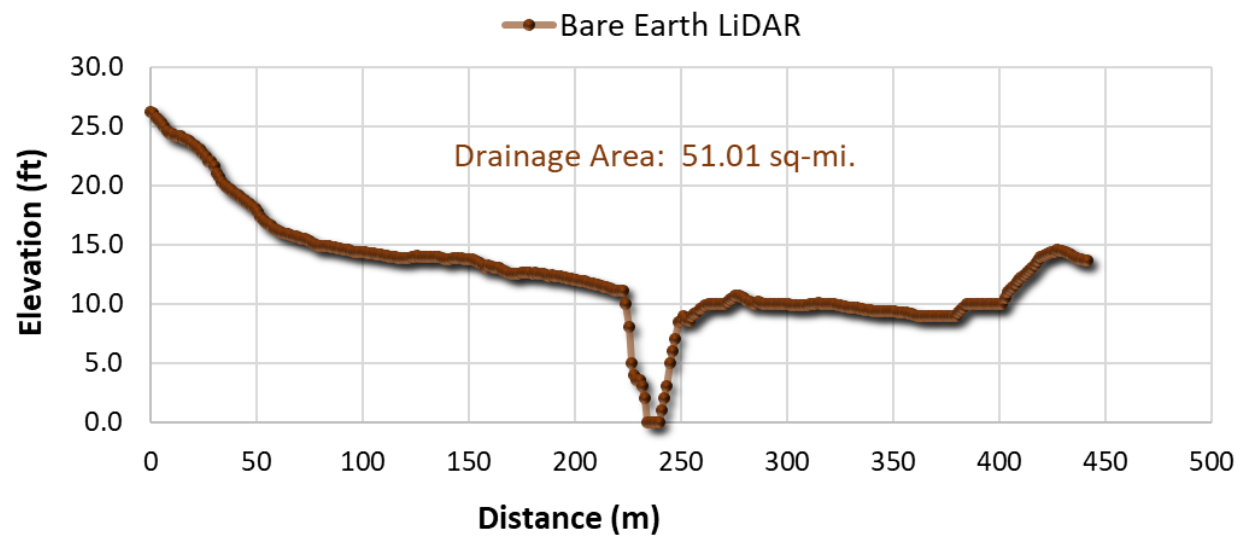


Figure 2-6. Bare Earth LiDAR cross section for Station 2380.

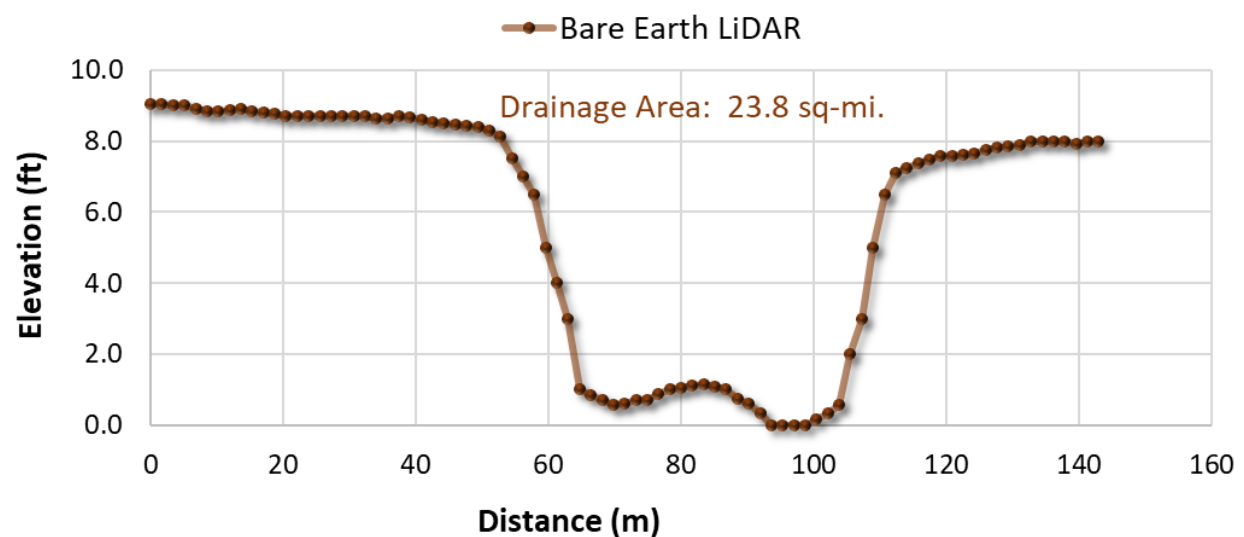


Figure 2-7. Bare Earth LiDAR cross section for Station 1920.

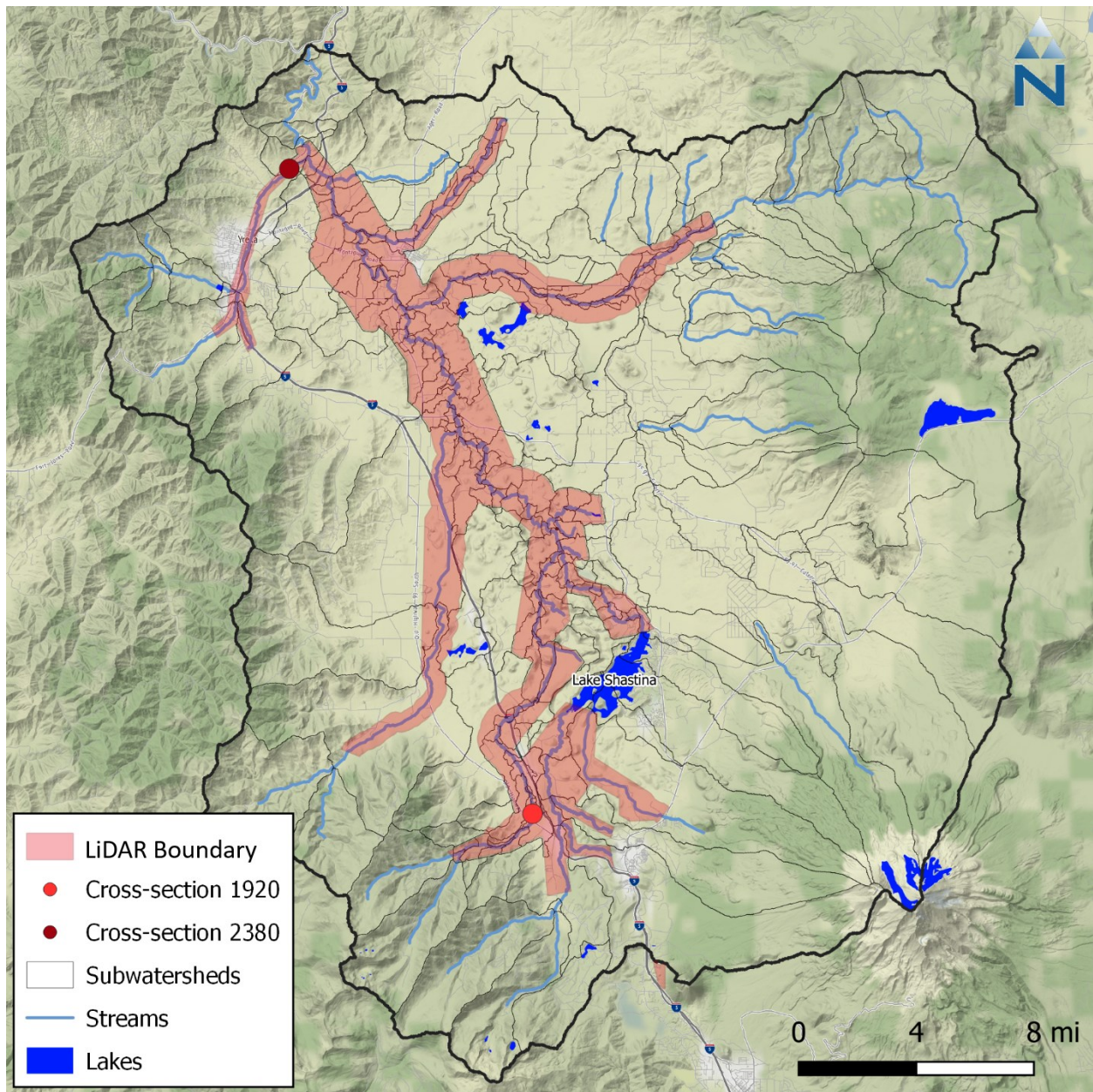


Figure 2-8. LiDAR data coverage within the Shasta River watershed area and example cross-sections for stations 2380 and 1920.

2.3.3 Extrapolating Cross-Sections for Reaches Without Observed LiDAR

It is common practice when developing large-scale watershed models to estimate cross-sectional properties (e.g. bank-full discharge, cross-sectional area, and bank-full depth and width) as a function of cumulative upstream drainage area (Bent & Waite, 2013; McCandless, 2003b, 2003a; McCandless & Everett, 2002). Several studies have developed regression relationships for estimating those properties with spatial analysis of multiple cross-sections. The literature generally shows strongest correlations (highest R^2 values) between bank-full discharge and upstream drainage area, followed by cross-sectional area, and then bank-full depth and width. That finding is intuitively consistent with the continuity equation, $Q = VA$, because flow (Q) is a product of both cross-sectional area (A) and velocity (V), while V is a function of longitudinal slope and channel properties. This suggests that while upstream drainage area is a robust predictor of bank-full discharge, longitudinal slope, the sinuous path of the channel, and other physical properties should be considered when estimating bank-full depth and width terms.

Observed LiDAR cross-sections were used to estimate the bank-full depths and widths. Other physical properties such as slope and composition of bed soils affect channel migration and the shape of the cross-section both spatially and temporally. The relative widths of the left and right banks of the river also change along the sinuous path of the reach segments. Because the model assumes a uniform symmetrical shape for the cross-section, the correlations derived above provide a consistent positive relationship for estimating the central tendency for the cross-sectional area, with deeper-and-wider channels estimated for outlets with larger upstream drainage areas. Sampling multiple cross-sections at regular intervals along the representative reach would likely provide additional data points for estimating the average width and depth for each segment. The R^2 value (0.82) for the width function is higher than the R^2 (0.66) of the depth function, which might suggest that other physical factors such as the longitudinal slope of the channel at the sampled transect may influence the depth more so than the width. Depth is also the smaller term of the two; therefore, a function based on depth will be more sensitive to variations than one based on width.

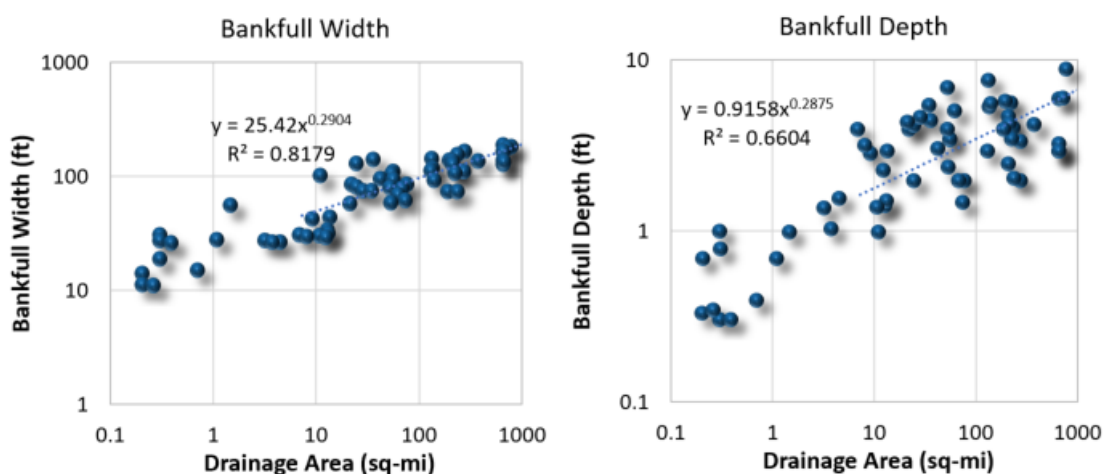


Figure 2-9. Correlations of sampled LiDAR bank-full width and depth vs. upstream drainage area within the Shasta River watershed area.

Using the two generalized functions derived in Figure 2-9, the upstream drainage area for all 62 transects were estimated and compared against the measured data. Appendix B summarizes channel properties for each of those reach segments, sorted by upstream drainage area.

The Manning equation, $Q = VA = \left(\frac{1.49}{n}\right) AR^{\frac{2}{3}} \sqrt{S}$ is used in LSPC/MODFLOW to calculate discharge as a function of cross-sectional area (A), wetted perimeter (R), bank-full velocity (V), longitudinal slope (S), and a channel roughness coefficient. An initial estimate of $n = 0.045$ was used for all reach segment, this value has been used in previous modeling efforts in the region (Deas et al., 2003). Table 2-1 presents typical Manning's n value for a variety of channel types. Calibration did not result in a need to adjust the initial value.

Table 2-1. Manning's n values for natural channels¹

Natural Channel Description ²	Manning's n		
	Min.	Avg.	Max.
a. clean, straight, full stage, no rifts or deep pools	0.03	0.03	0.03
b. same as above, but more stones and weeds	0.03	0.04	0.04
c. clean, winding, some pools and shoals	0.03	0.04	0.05
d. same as above, but some weeds and stones	0.04	0.05	0.05
e. same as above, lower stages, more ineffective, slopes and sections	0.04	0.05	0.06
f. same as "d" with more stones	0.05	0.05	0.06
g. sluggish reaches, weedy, deep pools	0.05	0.07	0.08
h. very weedy reaches, deep pools, or floodways with heavy stand of timber and underbrush	0.08	0.1	0.15

1: Data Source: (Chow, 1959)

2: Applies to natural streams with top width at flood stage < 100 ft.)

2.4 Hydrologic Response Unit Development

Hydrologic Response Units (HRUs) are the core hydrologic modeling land units in LSPC/MODFLOW. Each HRU represents areas of similar physical characteristics attributable to hydrological processes. Spatial or geological characteristics such as land cover, soils, geology, and slope/steepness are typically used to define HRUs. Those four datasets were the primary attributes used in the Shasta River watershed for classifying HRUs. The areal combination of primary characteristics ultimately determines the number of meaningful HRU categories considered for the model. Some consolidation of HRUs is required to balance the need for spatial resolution with model simulation efficiency. Figure 2-10 shows the organizational relationship of HRUs, subwatersheds, and model parameterization. Secondary attributes are properties (e.g., canopy cover and impervious cover) that are summarized by HRU to estimate numerical values for the model. This section describes the component layers and the overlay methodology used to derive HRUs for the Shasta River watershed.

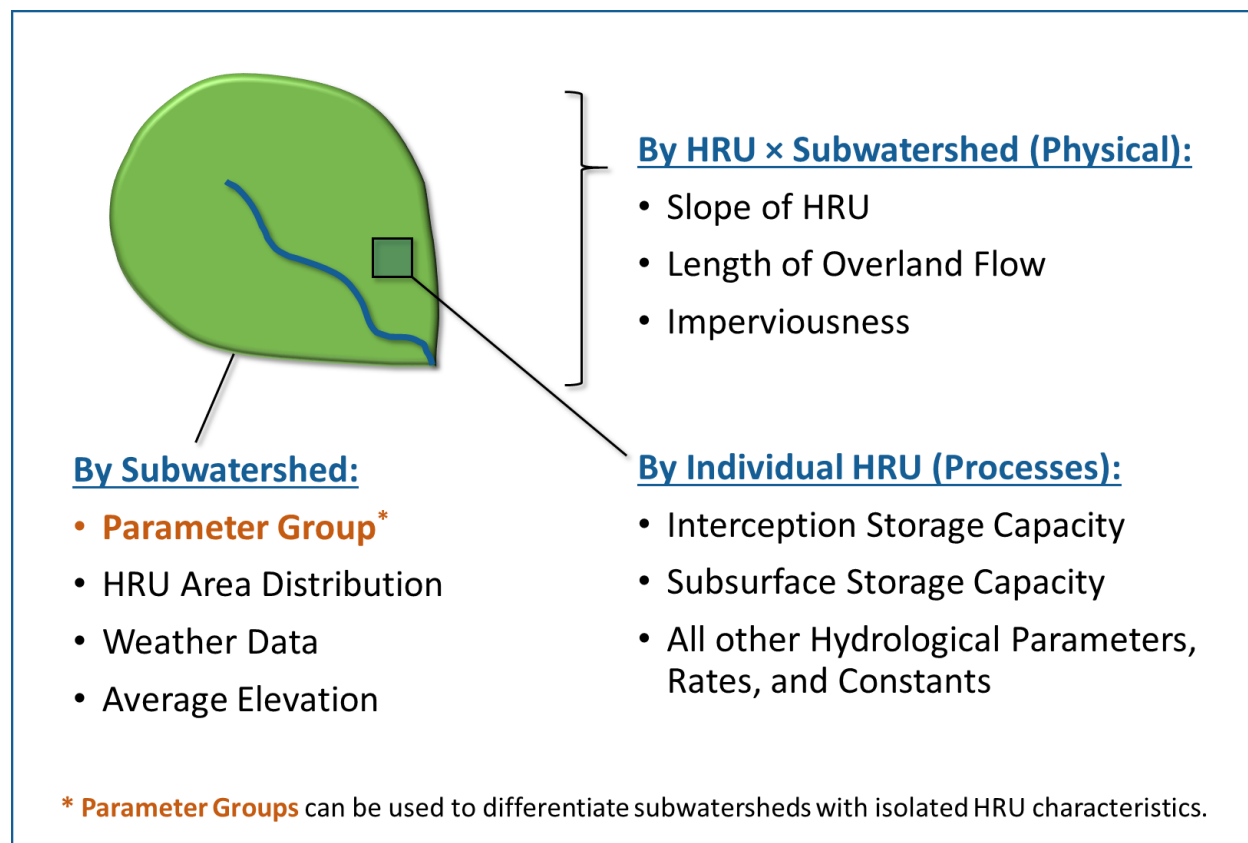


Figure 2-10. Organizational relationship of HRUs, subwatersheds & model parameterization.

Table 2-2 lists the spatial data used in HRU analyses along with the corresponding data sources. The data are representative of conditions between 2011 and 2016. All data layers were downloaded from publicly available data sources at no cost. The following subsections provide detailed descriptions of each HRU component dataset shown in Table 2-2.

Table 2-2. Summary of input datasets detailing data source and type

GIS Layer	Data Source (Reference)	Description
Digital Elevation Model	USGS NED (Gesch et al., 2014)	2013 – 30m resolution grid
Land Cover	NLCD (Homer et al., 2015)	2011 – 30m resolution grid
Irrigated Areas	DWR (DWR, 2019)	2019 polygon layer
Percent Imperviousness	NLCD (Xian et al., 2011)	2011 – 30m resolution grid
Percent Tree Canopy	NLCD (Coulston et al., 2013)	2011 – 30m resolution grid
Soil Survey Geographic Database (SSURGO)	USDA (NRCS, 2016a)	2016 polygon layer
State Soil Geographic Database (STATSGO)	USDA (NRCS, 2016b)	2016 polygon layer
Bedrock Geology	USGS, DWR (McLaughlin et al., 2000; Wagner & Saucedo, 1987)	Lithologic units

2.4.1 Digital Elevation Model

The United States Geological Survey (USGS) publishes DEMs expressing landscape elevation through a raster grid data product with 30-meter horizontal resolution and a Root Mean Square Error (RMSE) of 1.89m associated with vertical accuracy (Gesch et al., 2014). The Shasta River watershed ranges in elevation from less than 700 meters along the riverbed in the northern part of the watershed to over 2,000 meters at the highest elevation peaks in the southern portion of the watershed and along the eastern edge (Figure 2-11). As a geoprocessing input, the DEM was used to calculate slope as a derived data product.

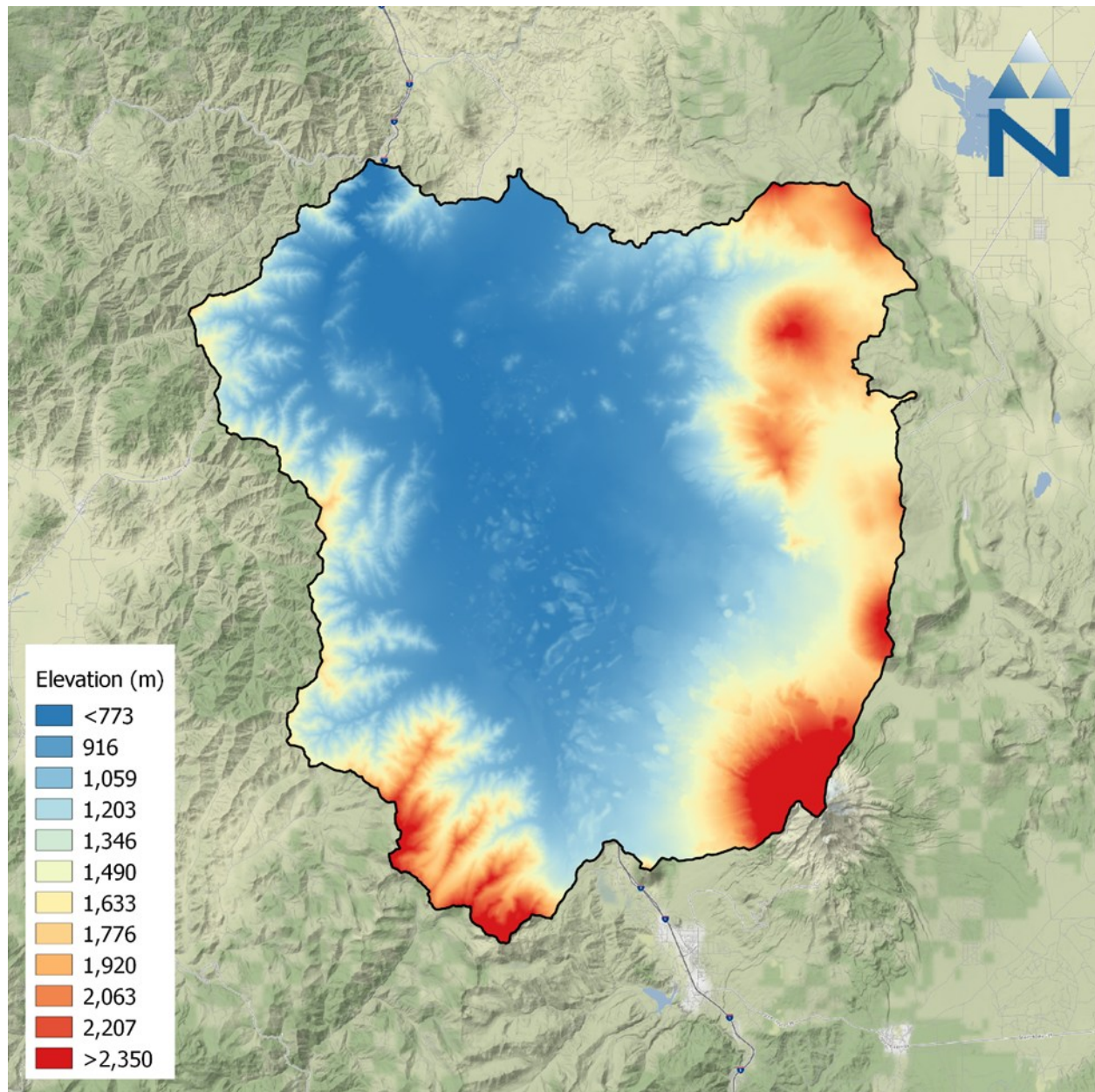


Figure 2-11. Elevation of the Shasta River watershed.

2.4.2 Land Cover

The primary source of land cover data for this effort was the 2011 National Land Cover Database (NLCD) maintained by the Multi-Resolution Land Consortium (MRLC), a joint effort between multiple federal agencies. The primary objective of the MRLC NLCD is to provide a current data product in the public-domain which provides a consistent characterization of land cover across the United States. The first iteration of the NLCD dataset was released in 1992. Since the 2001 NLCD version, a consistent 16-class land cover classification scheme has been adopted nationwide. The 2011 NLCD adopted this 16-class scheme at a 30-meter grid resolution. The minimum mapping unit is 5 30-m pixels (1.1 acres) for most land cover classes, except urban (1 pixel, 0.2 acres) and cropland and hay/pasture (12 pixels, 2.7 acres) (Homer et al., 2015).

Table 2-3 summarizes the composite land cover distribution within the Shasta River watershed; Table 2-11 shows the NLCD 2011 land cover. Within the watershed, Evergreen forest is the dominant land cover classification, making up 35.57% of the total watershed area. When combined with evergreen forest, the undeveloped categories of deciduous forest, mixed forest, shrub, and grass account for close to 77% of the total watershed area. Developed land cover makes up less than 5% of the total watershed area and is classified mostly as “Developed, Open Space,” which suggests that much of the developed area is dispersed.

Table 2-3. NLCD 2011 land cover classifications & areas in the Shasta River watershed

NLCD Class	Classification Description	Area (acres)	Area (%)
11	Open Water	1,687.75	0.33%
12	Perennial Ice/Snow	378.74	0.07%
21	Developed, Open Space ¹	9,998.39	1.97%
22	Developed, Low Intensity ¹	6,726.97	1.32%
23	Developed, Medium Intensity ¹	1,848.32	0.36%
24	Developed, High Intensity ¹	343.60	0.07%
31	Barren Land	17,114.10	3.37%
41	Deciduous Forest	1,490.71	0.29%
42	Evergreen Forest	180,668.84	35.57%
43	Mixed Forest	607.58	0.12%
52	Shrub/Scrub	119,431.78	23.51%
71	Grassland/Herbaceous	91,155.95	17.95%
81	Pasture/Hay	21,761.03	4.28%
82	Cultivated Crops	53,297.16	10.49%
90	Woody Wetlands	34.25	0.01%
95	Emergent Herbaceous Wetlands	1,393.08	0.27%
Total		507,938.23	100.00%

Data Source: 2011 National Land Cover Database (Homer et al. 2015)

1: Imperviousness: Open Space (<20%); Low Intensity (20-49%); Medium Intensity (50-79%); High Intensity (≥80%).

Color Gradient:

Lowest	Low	Med	High	Highest
--------	-----	-----	------	---------

Together, cultivated crops and pasture/hay land uses make up 14.77% of the total watershed area. These land cover classes can be further discretized based on the source of irrigation water (i.e., surface water, groundwater, mixed surface and groundwater, and recycled water) as shown in Figure 2-13. This information is represented in the DWR Statewide Crop Mapping Datasets (DWR, 2019); Larry Walker Associates worked to ground truth the water source data as part of the Siskiyou County Sustainable Groundwater Management Act compliance effort. It should be noted that some of the areas classified as “irrigated” in this dataset are actually waterbodies (e.g., Lake Shastina and Grass Lake). The intersection of irrigated cropland and pasture and associated consumptive use estimates is presented in Section 5.2.1

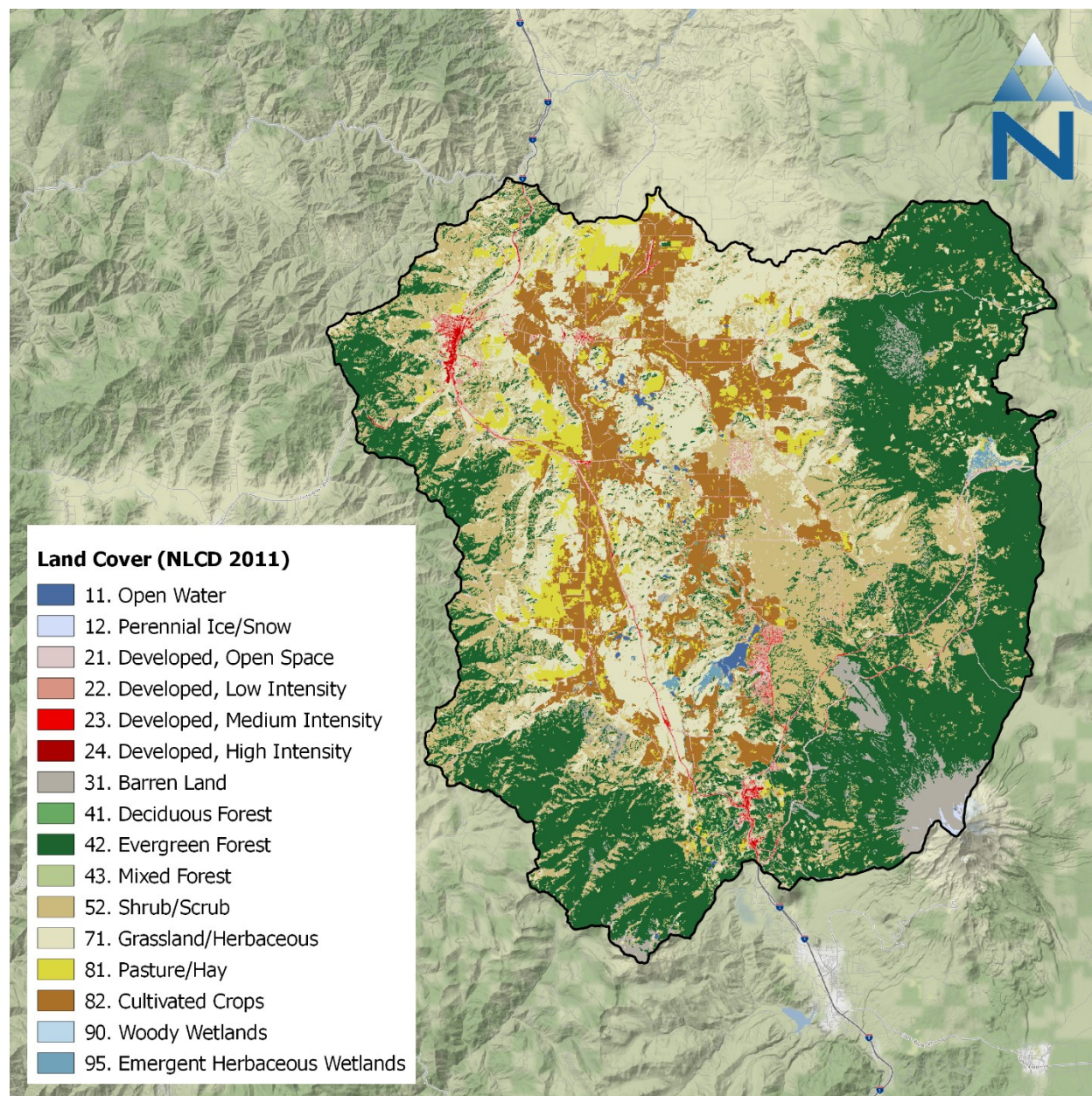


Figure 2-12. NLCD 2011 land cover in the Shasta River watershed.

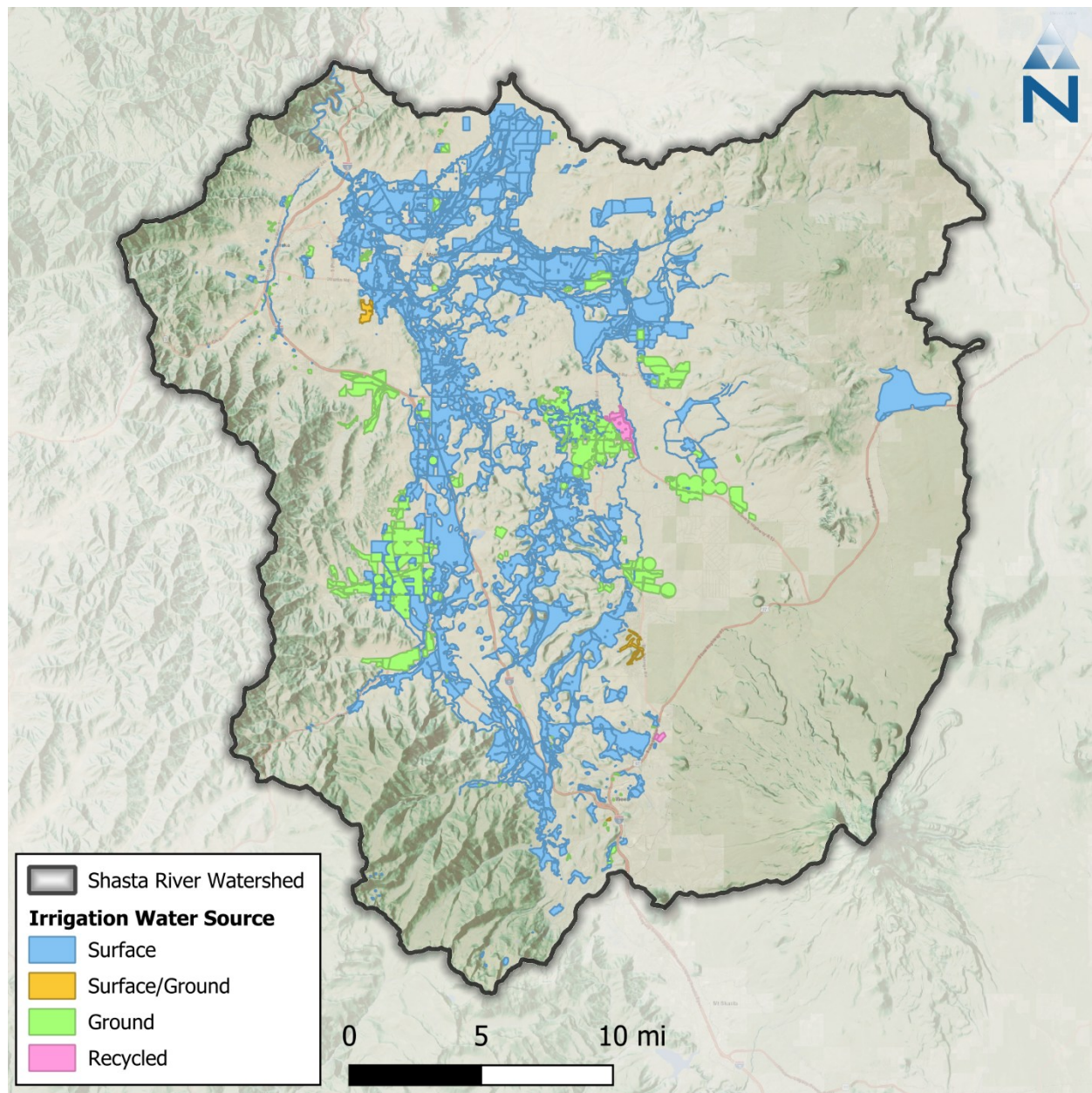


Figure 2-13. Irrigated areas within the Shasta River watershed by water source.

2.4.3 Percent Impervious Cover

MRLC publishes a developed impervious cover dataset as a companion to the NLCD land cover. This dataset is also provided as a raster with a 30-meter grid resolution. Impervious cover is expressed in each raster pixel as a percentage of total area ranging from 0 to 100 percent. Figure 2-14 shows the NLCD 2011 developed impervious cover dataset for the Shasta River watershed. Because this dataset provides impervious cover estimates for areas classified as *developed*, non-zero values in Figure 2-14 closely align with developed areas in Figure 2-12 (NLCD classification codes 21 through 24).

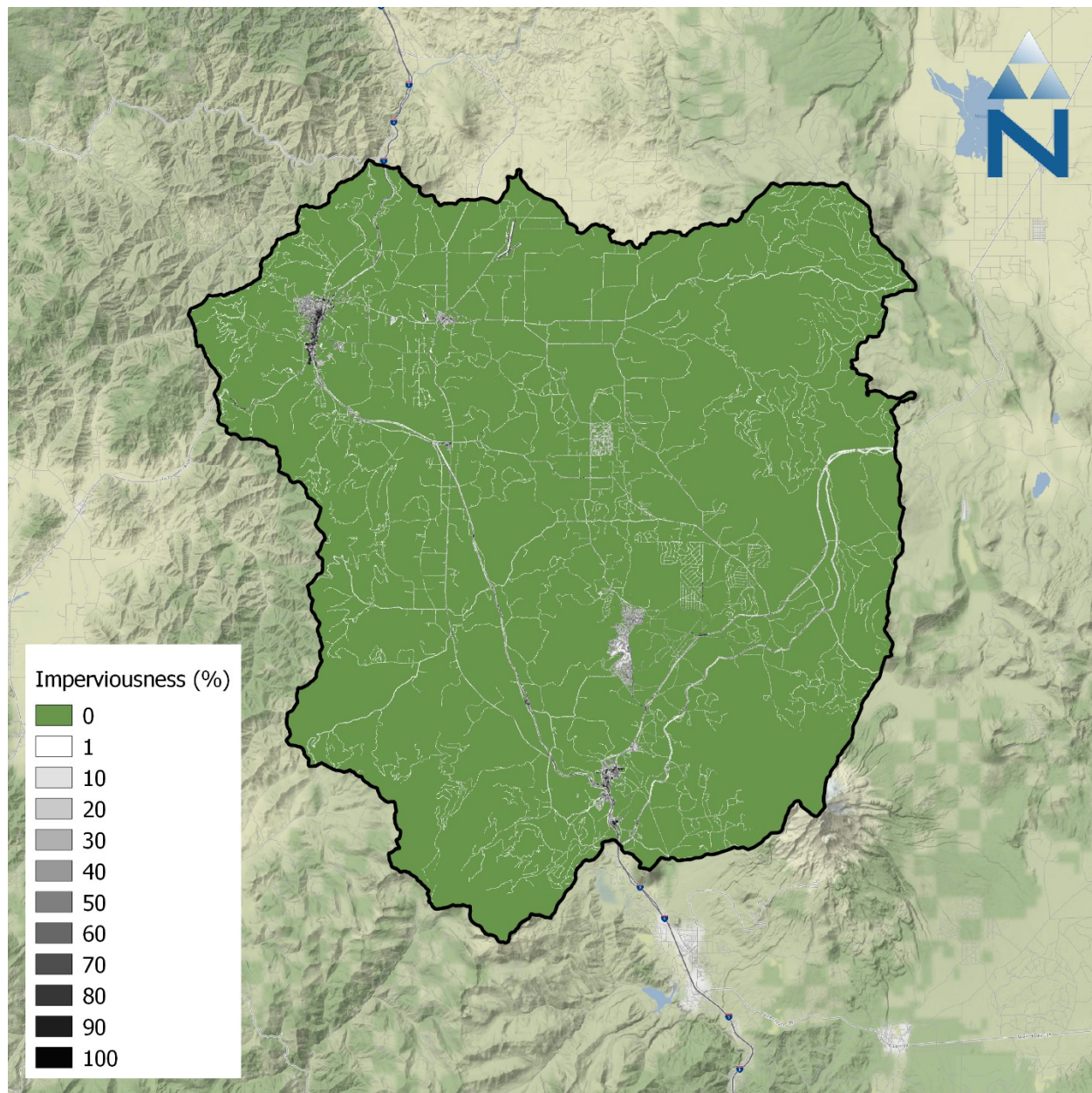


Figure 2-14. NLCD 2011 percent impervious cover in the Shasta River watershed.

2.4.4 Percent Canopy Cover

MRLC publishes a tree canopy dataset as a companion to the NLCD land cover dataset that estimates the percent of tree canopy cover spatially. The underlying data model was developed by the United States Forest Service (USFS) and is available through their partnership with the MRLC. This dataset is also provided as a raster with a 30-meter grid resolution. Like the impervious cover dataset, each raster pixel expresses the percent of the total area covered by tree canopy with values ranging from 0 to 100 percent. This layer was assessed but ultimately was not used as a basis for stratifying HRUs. Canopy coverage in the watershed is relatively sparse, especially in the valley (Figure 2-15), providing relatively little additional detail with respect to HRU development; however, when intersected with a

10-meter buffer zone around modeled stream segments, the percent canopy layer was used to inform both shading and riparian ET assumptions in proportion to canopy density within the 10-meter buffer of modeled stream segments.

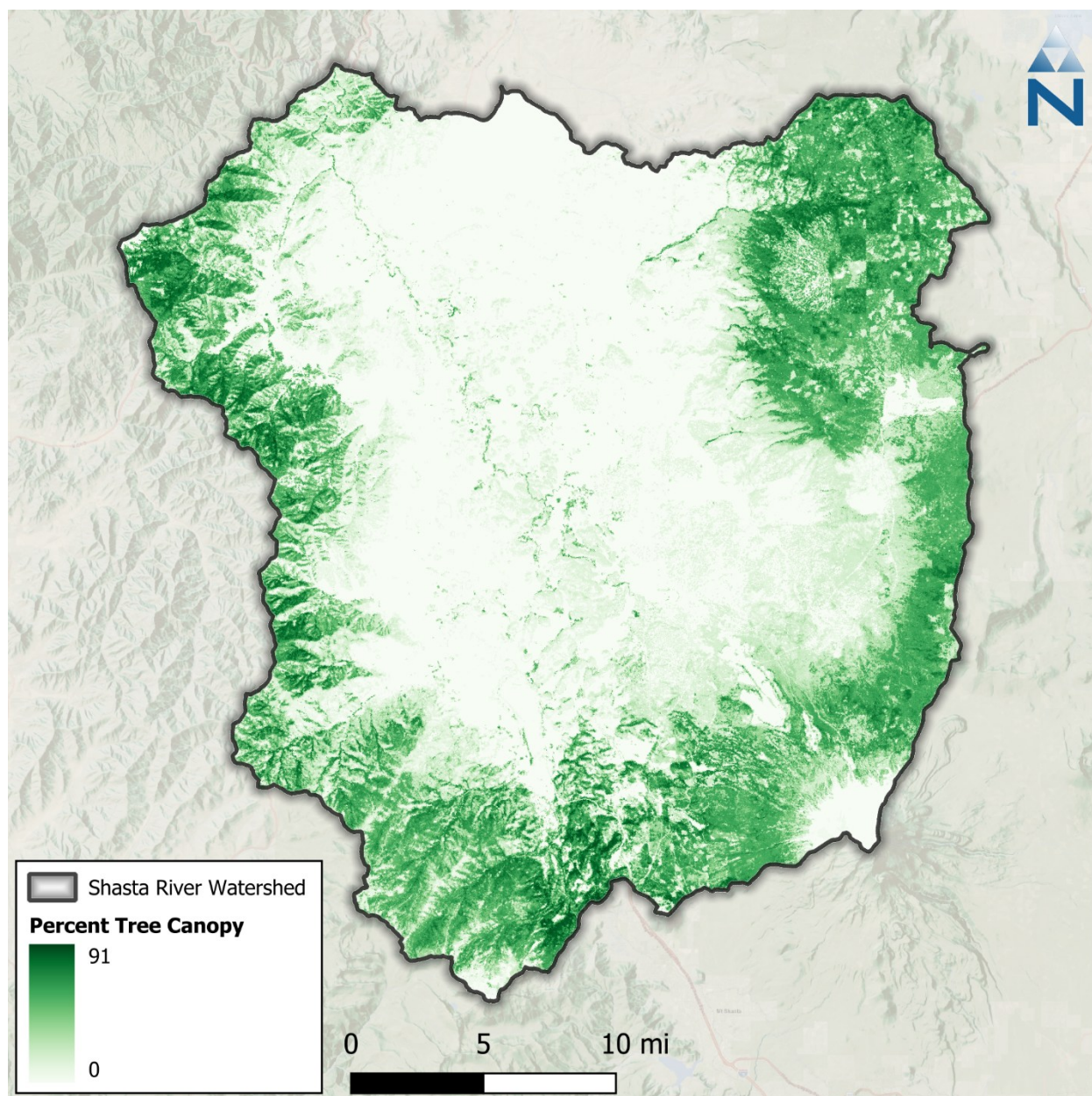


Figure 2-15. NLCD 2011 percent tree canopy cover in the Shasta River watershed.

2.4.5 Hydrologic Soil Group

Soils data for the watershed were obtained from the Soil Survey Geographic Database (SSURGO) and State Soil Geographic Database (STATSGO) both published by the Natural Resource Conservation Service (NRCS). There are four primary Hydrologic Soil Groups (HSG) used to characterize soil runoff potential (Table 2-4). Group A generally has the lowest runoff potential whereas Group D has the highest runoff potential. Both SSURGO and STATSGO soils databases are composed of a GIS polygon layer of map units and a linked database with multiple layers of soil properties.

Table 2-4. NRCS Hydrologic soil group descriptions

Hydrologic Soil Group	Description
A	Sand, Loamy Sand, or Sandy Loam
B	Silt, Silt Loam or Loam
C	Sandy Clay Loam
D	Clay Loam, Silty Clay Loam, Sandy Clay, Silty Clay, or Clay

Data Source: Natural Resource Conservation Service (NRCS), Technical Release 55 (TR-55)

Figure 2-16 presents the spatial distribution and a tabular summary of the SSURGO hydrologic soil groups for the Shasta River watershed. The dominant soil group in the watershed is Group D, containing poorly drained clays, sandy and silty clays, clay loam, and silty clay loam, silt loams, and loams. Groups A and C are the next most common soil groups and each cover approximately 23 percent of the watershed. Group A contains very well drained sand, loamy sand, or sandy loam. Group C contains sandy clay loams that are moderately to poorly drained with low infiltration rates. About 5.6% of the watershed areas had mixed soils, which were grouped with the nearest primary group as follows: B/D → C and C/D → D. Finally, approximately 12.7% of the watershed HSG area was unknown in the SSURGO database. For those areas, the corresponding HSG from the STATSGO dataset was used to supplement the data gaps.

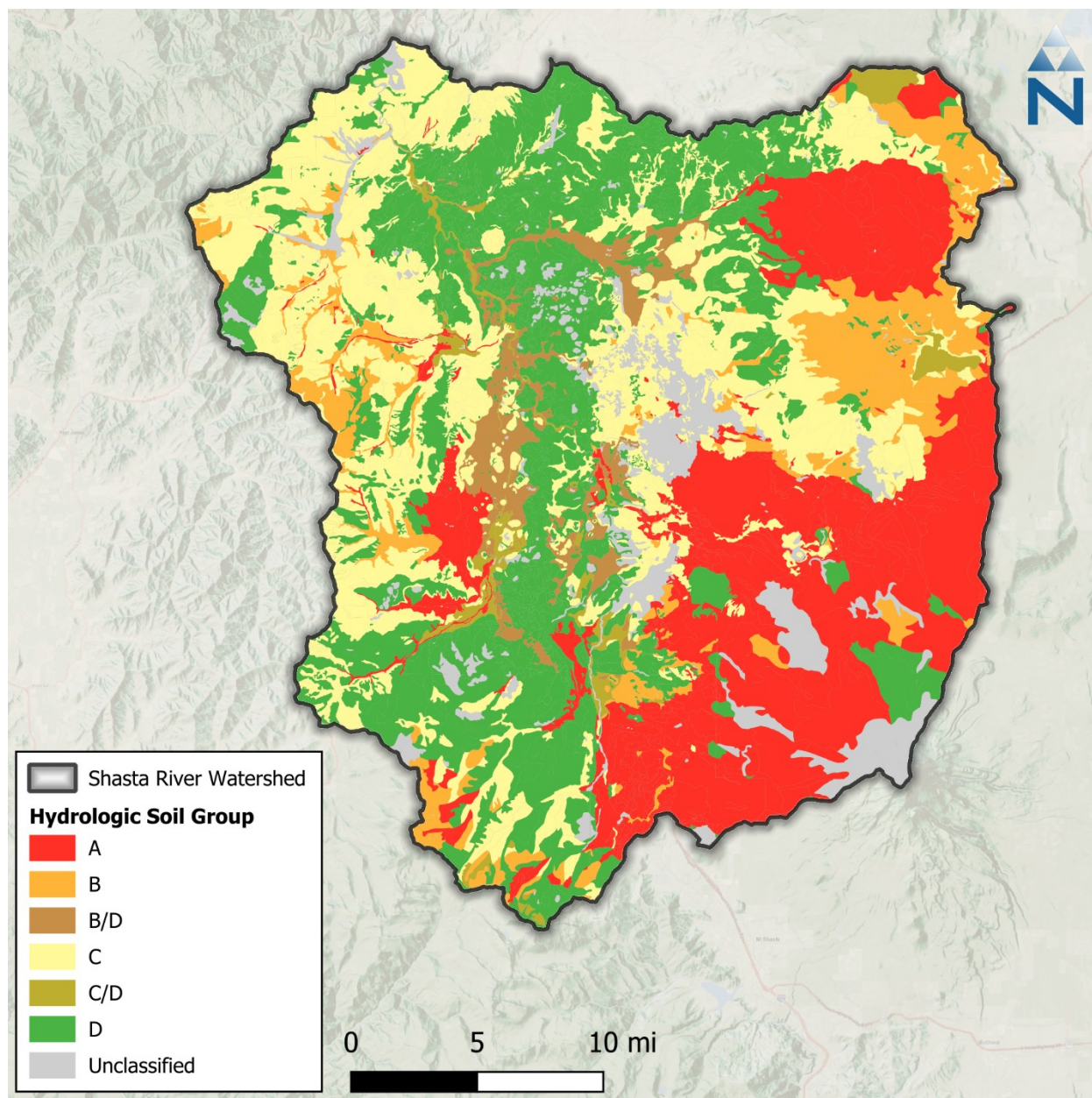


Figure 2-16. SSURGO hydrologic soil groups within the Shasta River watershed.

2.4.6 Bedrock and Hydrogeology

The Shasta River watershed is situated on the boundary between the Klamath Mountain and Cascade Range geomorphic provinces. The basin is bounded by the Scott Mountains to the west, the Siskiyou Mountains to the north, and the Cascade Range to the south and east (Figure 2-17). Geologic and hydrologic characteristics of the Shasta River watershed are highly variable and are delineated by the boundaries of the regional geomorphic provinces. Tributaries that drain the western and southwestern portions of the basin flow off the eastern slopes of the Scott Mountains and are underlain by the Paleozoic Eastern Klamath Belt terrane (Hotz, 1977; Wagner & Saucedo, 1987). Tributaries in the southeastern and eastern portions of the basin drain the western slope of the Cascade Range, which

are underlain by the Cenozoic Western Cascade and high Cascade Volcanic subprovinces (Hotz, 1977; Wagner & Saucedo, 1987). The Shasta River flows through the Shasta Valley before entering the Shasta River Canyon and eventually meets the Klamath River. The Shasta Valley is primarily underlain by various volcanic and volcanoclastic units of the High Cascades subprovince and deposits of Quaternary alluvium in the Montague vicinity. The canyon reach of the Shasta River is incised into the Western Paleozoic and Triassic Belt terrane (Hotz, 1977; Wagner & Saucedo, 1987).

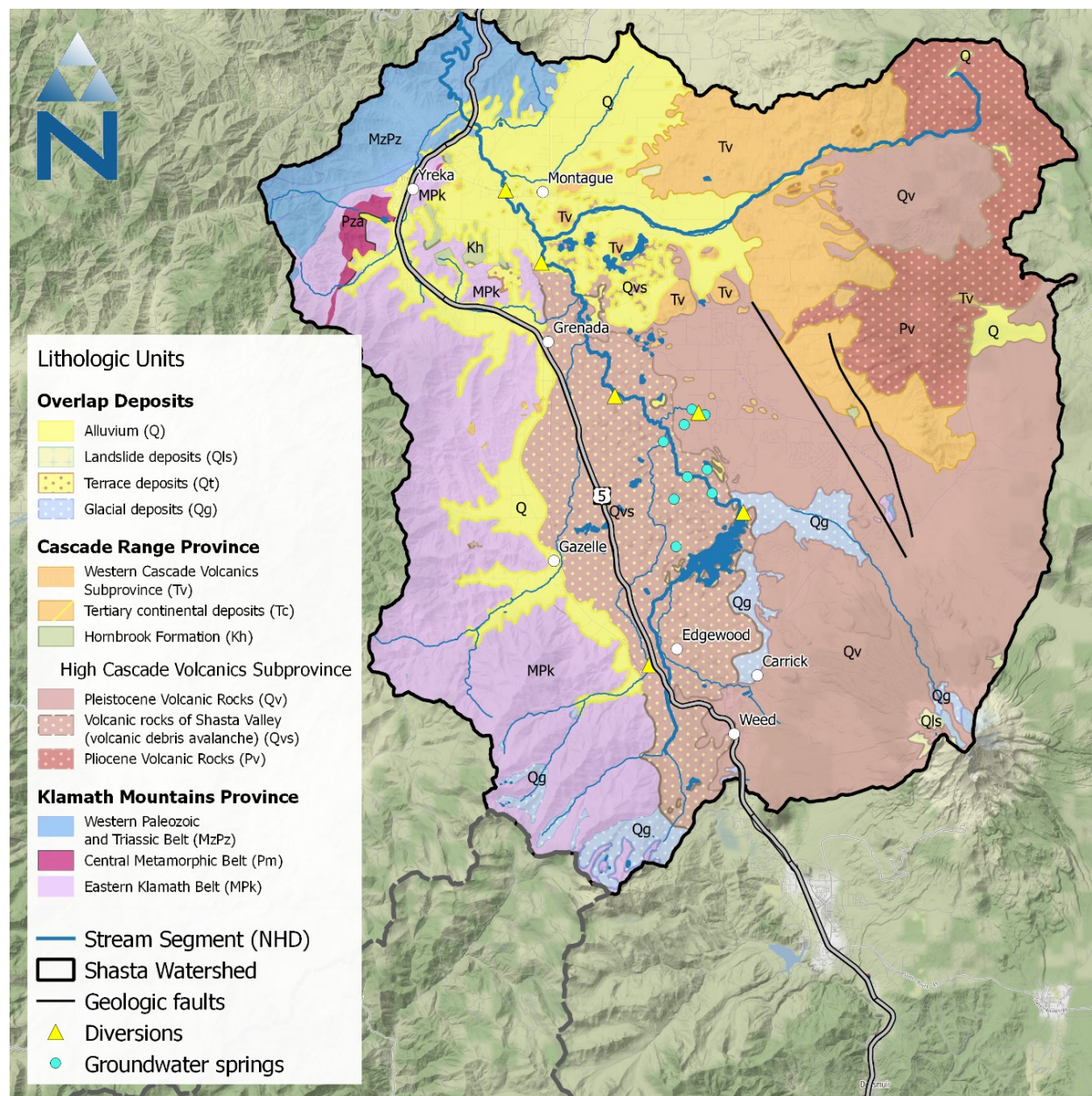


Figure 2-17. Simplified geologic map of the Shasta River watershed. Major groundwater springs and agricultural irrigation diversions are shown.

The Eastern Klamath Belt is the eastern-most terrane in the Klamath Mountains geomorphic province, which is interpreted as a structural sequence of east dipping thrust sheets, that decrease in age from east to west, formed by accretion of different oceanic and island-arc assemblages (Irwin, 1981; Saleeby et al., 1982). Paleozoic rocks of the Eastern Klamath Belt terrane in the Shasta River watershed consist of partially serpentinized peridotite, gabbro, diorite, and marine meta-sedimentary units including sandstone, shale, phyllite, chert, conglomerate, and limestone (Hotz, 1977; Mack, 1960; Wagner & Saucedo, 1987). These lithologic units compose the east face of the Scott Mountains and are dissected by a dendritic drainage pattern of Shasta River tributaries including Dale Creek, Eddy Creek, Parks Creek, Willow Creek, Julien Creek, and Yreka Creek. These stream channels flow roughly perpendicular to the northerly strike of the Eastern Klamath Belt. Hillslope mass wasting and valley bottom fluvial erosion are the dominant geomorphic processes in these tributary basins. Runoff response time is short during rainfall and snowmelt events in these areas of the Klamath Mountain terraces due to steep topography, high relief, shallow and well drained soils, and less permeable bedrock (McNab & Avers, 1994).

The Miocene-aged (i.e., erupted 50 million to 5.3 million years ago [mya]) rocks of the Western Cascade subprovince in the Shasta River watershed are primarily andesitic flows but contain an assemblage of rhyolite domes, basalt intrusions and plugs, and breccia (Hotz, 1977; Mack, 1960; Wagner & Saucedo, 1987). The Western Cascade subprovince dominates the hillslopes of the northeastern portion of the basin. These hillslopes have a moderately dissected drainage pattern and are largely devoid of perennial tributary channels, except for the Little Shasta River, which meets the Shasta River near Montague (McNab & Avers, 1994).

Conformably overlying the Western Cascade Volcanics is the Pliocene to Holocene-aged (i.e., erupted 5.3 mya to present) High Cascade Volcanics geologic province. These rocks primarily consist of the andesite and basalt that compose the uplands, volcanoes, and cones (e.g., Miller Mountain, Goosenest Mountain, Willow Creek Mountain, Ball Mountain, Deer Mountain, The Whaleback, and Mt. Shasta) forming the southern and eastern portions of the Shasta River watershed (Hotz, 1977; Mack, 1960; Wagner & Saucedo, 1987). The High Cascade Volcanics also includes more effuse basaltic flows (e.g., Pluto's Cave basalt) that dominate the eastern Shasta Valley, and the expansive pyroclastic (andesitic and volcanoclastic) deposits that cover much of the western Valley. These pyroclastic deposits represent a late Pleistocene debris avalanche originating from the northwest flank of Mount Shasta, and create the unique morphological assortment of conical hillocks, ridges, and depressions that dominate the Shasta Valley floor (Crandell, 1989; Crandell et al., 1984). This volcanic debris avalanche, which occurred between 300,000 and 380,000 years ago, covers approximately 180 square miles of valley floor and consists of a block facies and a matrix facies. The block facies that compose the hillocks and ridges is made of individual andesite blocks (ranging in size from tens to hundreds of feet in maximum dimension) and intact stratigraphic sequences of volcanoclastic materials that were transported in the same relative positions as their original deposition (Crandell, 1989; Crandell et al., 1984). The matrix facies consist of an unsorted and unstratified mixture of sediments derived from Mount Shasta and the Klamath Mountain terranes underlying the valley floor. The matrix facies embed the individual blocks and produced the lahar-like flow that transported the avalanche across the valley. Although both the block and matrix facies are considered water-bearing units, the block facies may be more permeable and transmit groundwater from both deep, confined aquifers as well as the younger, more permeable basalt flows (DWR, 2011).

The highly permeable effuse basalt flows of the High Cascade subprovince allow rainfall and snowmelt to quickly infiltrate the porous groundwater aquifer, resulting in a poorly developed surficial drainage

pattern (Mack, 1960; Tague & Grant, 2004). Numerous groundwater springs are in these young permeable volcanic units and contribute significant flow to the Shasta River and tributary creeks. The abundance and high discharge of groundwater springs indicates a well-developed subsurface drainage network exists in the southern and central extents of the Shasta Valley (Jeffres et al., 2008; Mack, 1960; A.L. Nichols et al., 2010; Nichols, 2008).

2.4.6.1 Bedrock Aquifers

2.4.6.1.1 Klamath Mountains

The Klamath Mountain terranes forming the western boundary of the Shasta River watershed generally consists of marine sediments and intrusive rocks that have experienced varying degrees of structural deformation and metamorphism during major tectonic (mountain building) episodes (approximately 500 mya to 65 mya). Extensive mineral recrystallization has reduced primary porosity in these units. Structural deformation has created secondary porosity in the form of fractures, joints, faults, and shear zones, however, these units are not important sources of groundwater within the watershed (DWR, 2011).

2.4.6.1.2 Cascade Range

The diverse Tertiary Western Cascade volcanics can be highly fractured and weathered, although they tend to have reduced porosity and permeability due to secondary infilling of fine-grained sediments. These units have shallow subsurface flow paths yielding springs and seeps on basin hillslopes – an indication of impermeable horizons that preclude vertical transmission of groundwater through the aquifer (DWR, 2011).

The younger High Cascade volcanics overlying the Western Cascade volcanics are highly vesicular and fractured rocks that store and transmit large volumes of groundwater. Many springs discharge from the contact between the Western and High Cascade subprovinces due to the discontinuity in permeability (DWR, 2011). The High Cascades volcanics includes the Holocene Pluto's Cave basalt, a highly vesicular and fractured unit that critically influences groundwater storage and recharge in the valley, contributing large volumes of water to wells and springs (DWR, 2011). Wells in the Pluto's Cave basalt yield up to 4,000 gpm, with an average of 1,300 gpm (DWR, 2011; Mack, 1960; PGS, 2001). The unit ranges in thickness from approximately 800 feet in the south near its source, to 10 feet at its distal end in the northwest (Blodgett et al., 1988). The unit is composed on multiple individual flows providing permeable contact surfaces, as well as lava tubes (including Pluto's Cave) that facilitate groundwater flow. Recharge to the aquifer occurs from direct precipitation on the ground surface, streamflows that become subsurface upon reaching the unit (e.g., Whitney Creek), irrigation ditch loss, percolation from applied irrigation water, and groundwater flow from snowmelt in the Cascade peaks to the south and east (DWR, 2011; Mack, 1960).

The hydrogeologic characteristic of these volcanic units have been shown to play a dominant role on hydrologic patterns related to peak timing and magnitude of instream flows in other Cascade Range rivers (Tague et al., 2007). The timing and shape of hydrographs and irrigation season monthly average instream flows in valley streams are related to the percentage of High Cascade volcanic units in the contributing drainage area (Tague & Grant, 2004).

2.4.6.1.3 Volcanic Debris Avalanche

The highly variable rock types within the volcanic debris avalanche, as well as the chaotic modes of transport and deposition during the event have resulted in a lack of coherent internal structure. Consequently, well yields from within the debris avalanche deposits are highly variable (DWR, 2011). Although groundwater yields are variable, the avalanche deposit exerts control on regulating and redirecting groundwater flow through the valley and to the Shasta River. The debris avalanche occurred before the eruption of the Pluto's Cave basalt and acted as the western boundary to the basalt flows. The less permeable avalanche deposits act as a barrier to groundwater flow through the more permeable Pluto's Cave basalt, resulting in multiple voluminous groundwater springs (including the Big Springs Complex) along the contact between the two formations (DWR, 2011; Mack, 1960).

2.4.6.2 Alluvial Aquifers

The Shasta Valley Groundwater Basin, as defined by DWR, consists of the Quaternary-aged (approximately 2.6 mya to present) unconsolidated alluvium located along the western and northern portions of the Shasta Valley (Table 2-5, Figure 2-18) (DWR, 2011). This aquifer unit includes stream and terrace deposits of Parks Creek, Willow Creek, Julien Creek, Yreka Creek, Shasta River, Little Shasta River, and Oregon Slough; as well as the alluvial fan deposits forming the sedimentary apron at the base of the Klamath Mountains (DWR, 2011). Holocene alluvium is primarily silt and clay interbedded with sand and gravel. Calcium derived from mafic volcanic rocks in the Little Shasta Valley has cemented the subsoil into hardpan. The alluvial western valley margin extending south past Gazelle contains no hardpan (Mack, 1960). The Holocene alluvium may be up to 150 feet thick in some locations, and well yields have previously been measured at 150 to 1,000 gpm (Mack, 1960).

The portion of the Shasta Valley Groundwater Basin north of Montague is underlain by older Pleistocene alluvium up to 100 feet thick and contains gravels derived from the Klamath Mountains. This portion of the valley contains an iron-cemented hardpan just below the ground surface. Wells within Pleistocene alluvium have previously had sufficient yields to supply domestic and stock uses (Mack, 1960). It is important to note, however, that the alluvial aquifer as defined by DWR is a much less productive aquifer and a lesser source of groundwater than the underlying volcanic aquifer. Indeed, most large wells in the valley, including those located within quaternary alluvium at the surface, produce water from the underlying basalt aquifer.

Table 2-5. Shasta Valley Groundwater Basin.

Basin	Name	Area (acres)	Groundwater Budget Type ¹
1-4	Shasta Valley Groundwater Basin	52,480	B

¹ (B) use-based estimate of groundwater extraction for the basin (DWR, 2003).

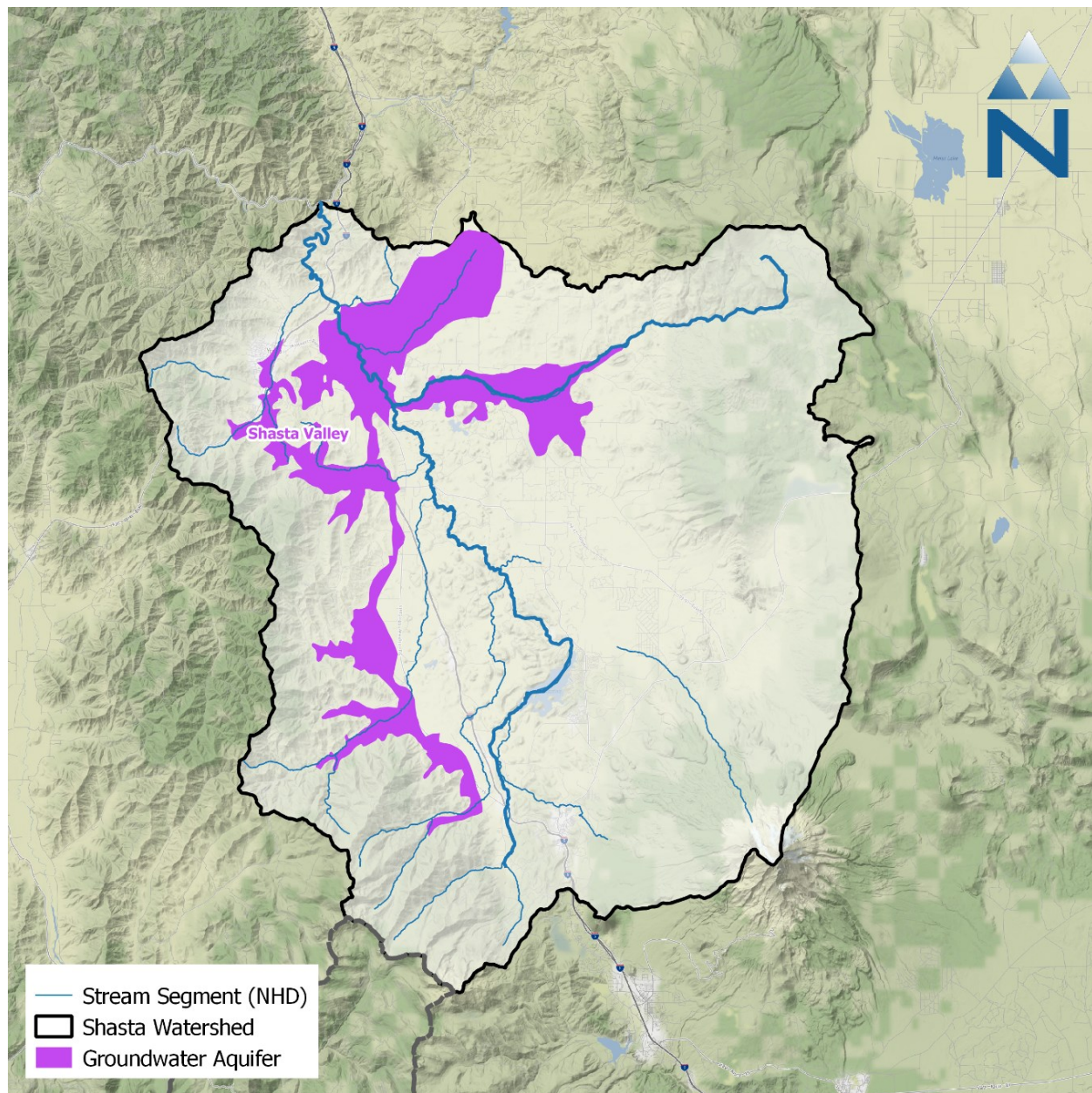


Figure 2-18. Alluvial aquifers recognized within the Shasta River watershed and water provider boundaries.

2.4.6.3 Surface Water–Groundwater Interactions

The Shasta River has a complicated seasonal and longitudinal flow regime due to complex surface water and groundwater interactions, coupled with extensive agricultural diversion and return flows (Nichols et al., 2010; Vignola & Deas, 2005). The upper Shasta River (i.e., upstream of Dwinnell Dam) originates on the eastern slope of the Scott Mountains and is characterized by a runoff-driven hydrograph derived from rainfall and snowmelt (Nichols et al., 2010). Inflows to Lake Shastina consist of the upper Shasta River, flows diverted from Parks Creek near Edgewood, and Carrick Creek originating from the northwest flank of Mt. Shasta. Lake Shastina primarily serves as a storage reservoir and diversion for agricultural irrigation water throughout the Shasta Valley. Outflow from Lake Shastina to the lower Shasta River is regulated by Dwinnell Dam, which has reduced mean

annual discharge in the reaches immediately downstream of the reservoir by up to 90% (Jeffres et al., 2008; Nichols et al., 2010; Nichols, 2008). Reservoir storage capacity in Lake Shastina is rarely achieved due to the permeable underlying volcaniclastic rocks, and therefore uncontrolled spill events at Dwinnell Dam are uncommon (Vignola & Deas, 2005). Mack (1960) reported that multiple springs along the western base of the ridge forming the western embankment of Lake Shastina increased in flow following construction of the reservoir. Seepage losses from Lake Shastina have been estimated at 6,500 to 42,000 acre-feet per year, which is very high relative to the reservoir's 50,000 acre-feet storage capacity (NCRWQCB, 2006; Paulsen, 1963).

Flows in the lower Shasta River (i.e., downstream of Dwinnell Dam) are composed of minimal releases from Lake Shastina, tributary creeks (e.g., Parks Creek, Willow Creek, Little Shasta River), multiple discrete groundwater springs (e.g., Big Springs, Little Springs, Clear Springs, Kettle Springs, Bridge Field Springs), and additional diffuse groundwater springs (Figure 2-20). The lower Shasta River currently has a spring-dominated hydrograph that is primarily sourced from Big Springs Creek (which is supplied by multiple groundwater springs in the Big Springs Complex vicinity) (Jeffres et al., 2008; Nichols et al., 2010; Nichols, 2008). Spring-fed baseflows from Big Springs Creek outside the irrigation season (i.e., October to April) are five times those of the lower Shasta River upstream of the Big Springs Creek confluence (which includes Parks Creek, see Figure 2-20) (Jeffres et al., 2009). During irrigation season (i.e., April to October), Big Springs Creek baseflows are reduced by approximately 35% from temporally variable irrigation diversion and unquantified groundwater pumping (Jeffres et al., 2009). Approximately 95% of baseflows during irrigation season in the lower Shasta River originate from the Big Springs Complex (Figure 2-19 and Figure 2-20). Following cessation of the irrigation season, instream flows downstream of the Big Springs Creek confluence quickly rebound to spring-fed baseflow conditions (Nichols et al., 2010). Buck (2013) constructed a groundwater model for a portion of the Shasta River watershed and summarized major balance components for 2008-2011.



Figure 2-19. Big Springs Complex.

The City of Yreka obtains its water supply from Fall Creek, located outside the Shasta River watershed near Iron Gate Reservoir (Pace Engineering, 2016). The City's treated wastewater, totaling 966 acre-feet in 2015, is discharged to percolation fields near Yreka Creek (Pace Engineering, 2016).

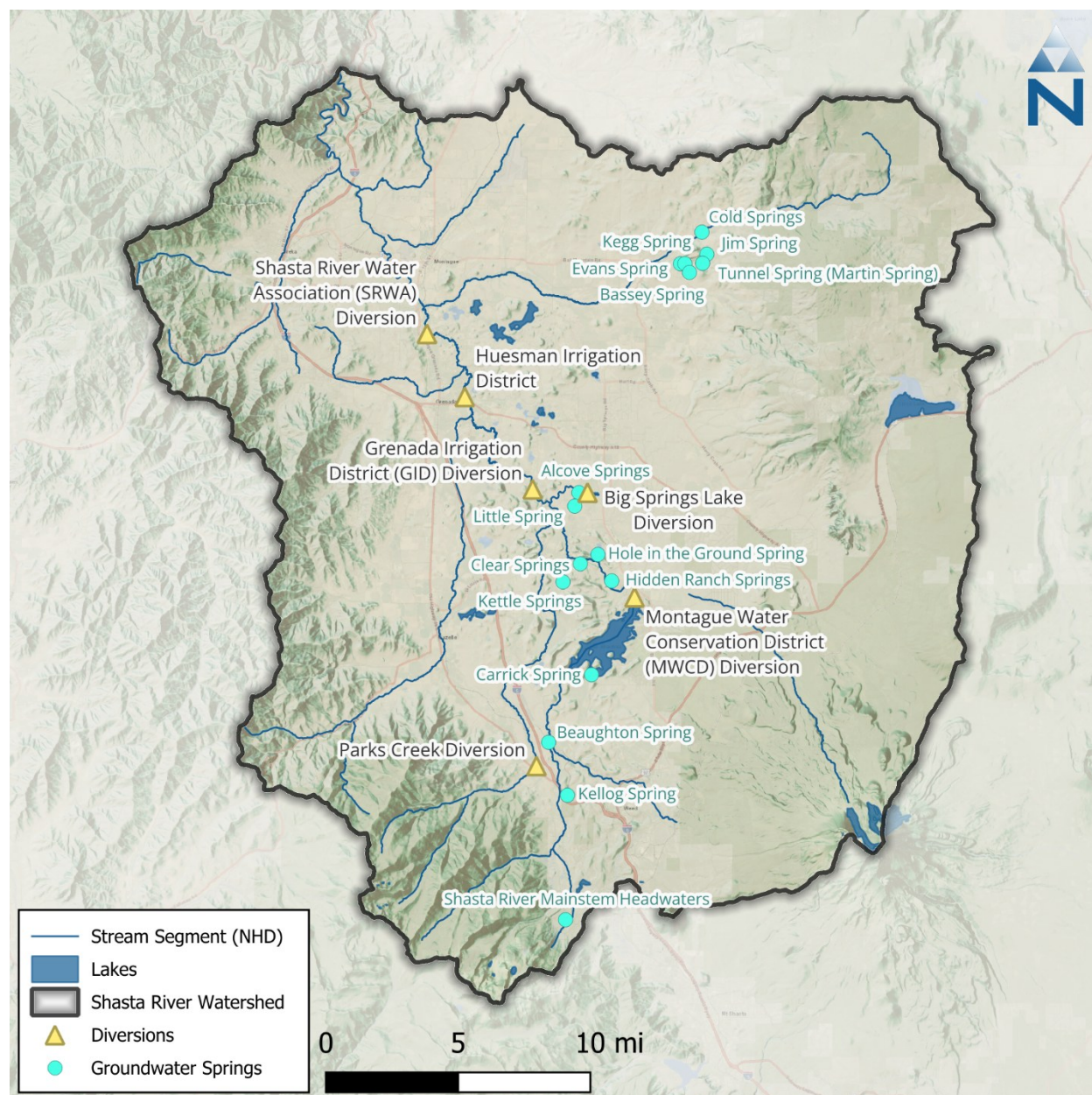


Figure 2-20. Major groundwater springs and surface water diversions of the Shasta Valley.

2.5 HRU Data Processing

Datasets discussed in the previous section were each analyzed for spatial and categorical trends with the objective of reclassifying the datasets into a smaller set of discrete categories for watershed model development. Reclassification is the mechanism for generalizing the data and identifying HRU groups to facilitate model development. Each dataset was subject to an analysis of area distributions to

support reclassification. The following sections discuss details of these analyses for slope, land cover, soils, bedrock geology, and source of irrigation water.

2.5.1 Slope Groups

The 30-meter resolution DEM grid was used to generate the percent slope raster using the slope function in QGIS software. The slope raster was then reclassified into three groups (i.e., $\leq 15\%$, 15%-35%, and $>35\%$) corresponding to *low*, *medium*, and *high* slope areas, respectively. Slope ranges were chosen to align with thresholds from local literature on forestry management and hillslope stability classifications, with 35% representing with the upper level of hydrological influence of slope (CDFFP, 2005; CDMG, 1997; NMFS, 2000). The slope category area distribution is shown in Table 2-6. The area distribution between these three groups shows that about 51% of the watershed has low sloped land, while 18% of the watershed has high slopes. *Unclassified or All* groups include wetlands and water bodies. A map showing the spatial distribution of the reclassified slope categories is presented in Figure 2-21.

Table 2-6. Slope HRU groups and area distribution for Shasta River watershed

Slope	Slope Category	HRU Group	Area (acres)	Area (%)
0-15	Low	Low	257,318	50.7%
15-35	Medium	Med	155,134	30.6%
>35	High	High	91,704	18.1%
Unclassified	Unclassified	All	3,493	0.7%

Color gradients indicate increasing **Percent Area** of slope group category.

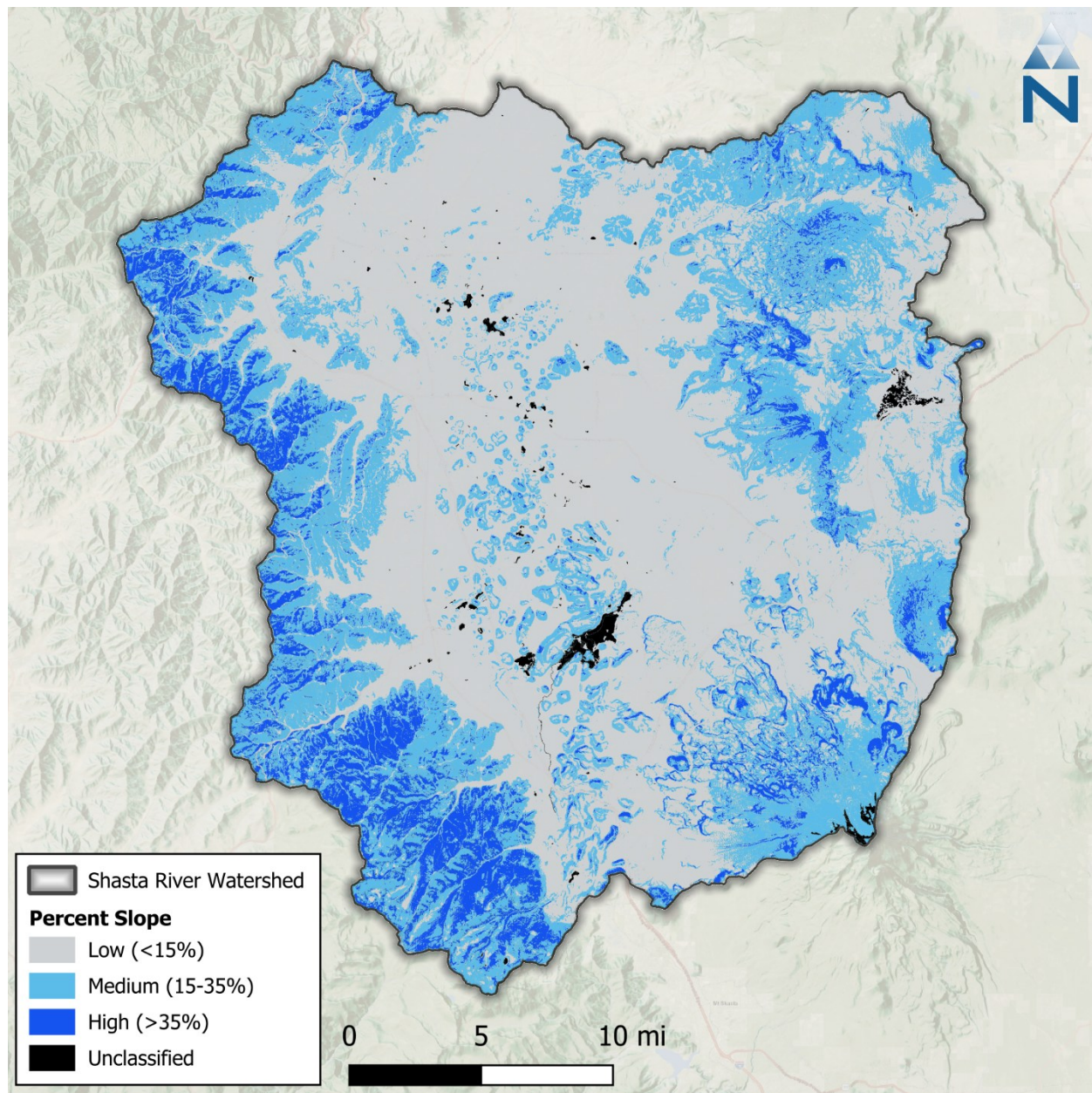


Figure 2-21. Slope Categories within the Shasta River watershed.

2.5.2 Land Cover Groups

The NLCD 2011 Land Cover dataset was used to generate a 30-meter resolution grid defining the major land cover groups. A map showing the spatial distribution of the reclassified land cover categories is presented in Figure 2-22. Table 2-7 presents the distribution of all land cover categories within the Shasta River watershed. The area distribution shows that the Forest category is dominant (35.98%) within the watershed, followed by the Grass-Shrub category (44.83%), and developed area covers approximately 3.72% of the total watershed area.

Table 2-7. Land Cover HRU groups and area distribution for Shasta River watershed

Land Cover Code	Land Cover Category	HRU Group	Area (acres)	Area (%)
11	Open Water	Water	1,687.75	0.33%
12	Perennial Ice/Snow	Water	378.74	0.07%
21	Developed, Open Space ¹	Developed	9,998.39	1.97%
22	Developed, Low Intensity ¹	Developed	6,726.97	1.32%
23	Developed, Medium Intensity ¹	Developed	1,848.32	0.36%
24	Developed, High Intensity ¹	Developed	343.60	0.07%
31	Barren Land	Grass & Shrub	17,114.10	3.37%
41	Deciduous Forest	Forest	1,490.71	0.29%
42	Evergreen Forest	Forest	180,668.84	35.57%
43	Mixed Forest	Forest	607.58	0.12%
52	Shrub/Scrub	Grass & Shrub	119,431.78	23.51%
71	Grassland/Herbaceous	Grass & Shrub	91,155.95	17.95%
81	Pasture/Hay	Pasture	21,761.03	4.28%
82	Cultivated Crops	Cultivated Crops	53,297.16	10.49%
90	Woody Wetlands	Wetland	34.25	0.01%
95	Emergent Herbaceous Wetlands	Wetland	1,393.08	0.27%

Color gradients indicate increasing **Percent Area** of land cover group category.

1: Imperviousness: Open Space (<20%); Low Intensity (20-49%); Medium Intensity (50-79%); High Intensity (≥80%).

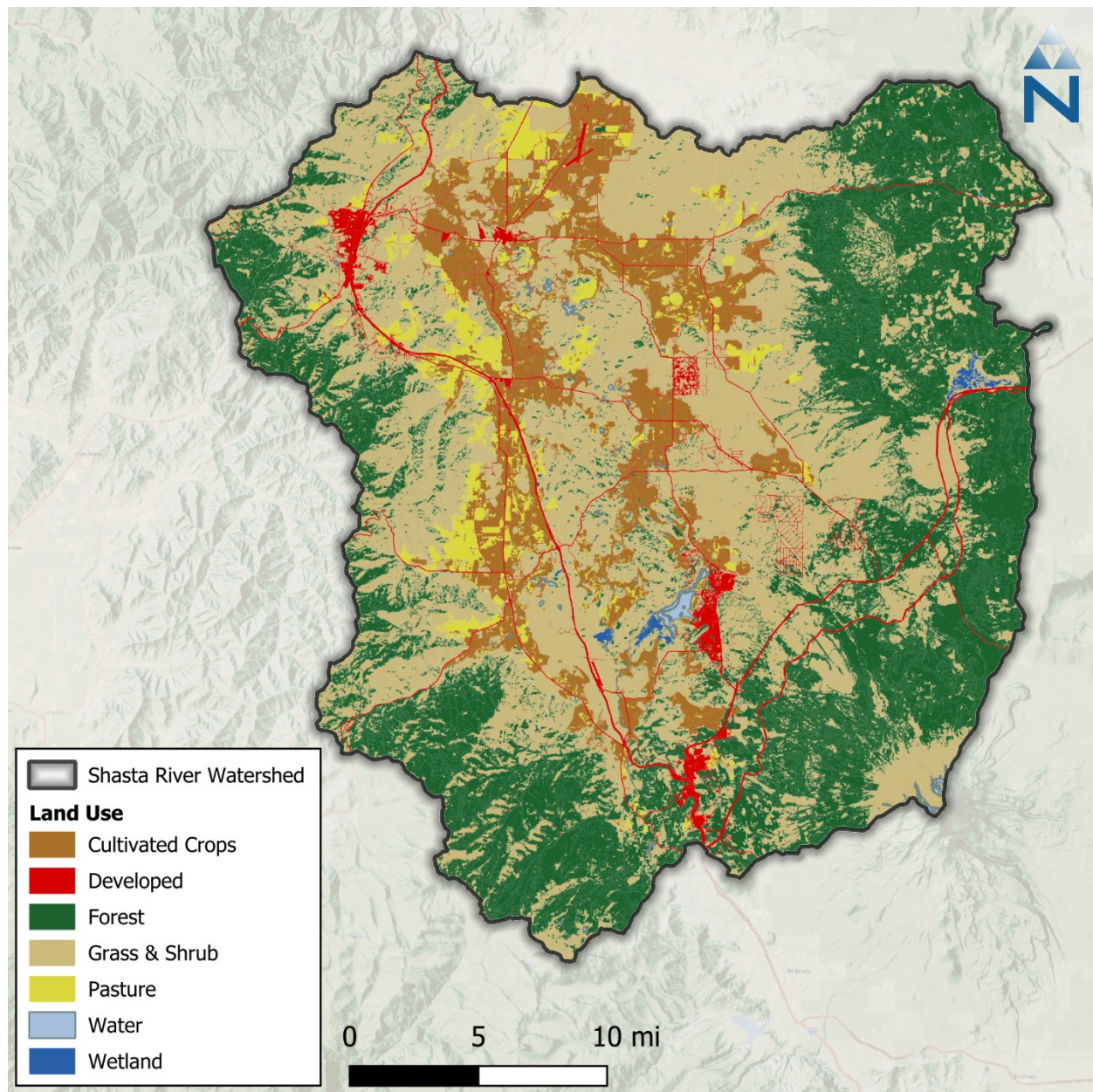


Figure 2-22. Land Use Categories within the Shasta River watershed.

2.5.3 Hydrologic Soil Groups

The SSURGO supplemental soil polygon layer was converted into a 30-meter resolution grid using the Hydrologic Soil Group (HSG) attribute value. As noted in Section 2.4.5, missing data in the SSURGO database were filled using attributes from the coarser STATSGO database, resulting in a composite SSURGO/STATSGO grid. This composite grid was overlaid with NLCD 2011 percent impervious dataset limiting the extent of the soil analysis to only pervious areas. The pervious portion of the soil area distribution was then used to define soil category HRU groups. Figure 2-23 presents the HRU soil groups. Table 2-8 presents the resulting HSG area distribution. The HSG-D and HSG-C category are dominant (32%) in the Shasta River watershed, followed by HSG-A which covers 26%,

and HSG-B, covers 8%. Less than 1% area is unclassified that covers developed impervious, wetland and water bodies.

Table 2-8. HSG category HRU groups and area distribution for Shasta River watershed

HSG	HSG Category	HRU Group	Area (acres)	Area (%)
A	Sand, Loamy Sand, or Sandy Loam	A	133,070	26.21%
B	Silt, Silt Loam or Loam	B	40,978	8.07%
C	Sandy Clay Loam	C	162,704	32.05%
D	Clay Loam, Silty Clay Loam, Sandy Clay, Silty Clay, or Clay	D	166,188	32.74%
Unclassified	Wetland or Water Bodies	All	3,493	0.69%
Unclassified	Developed Impervious	IMP	1,218	0.24%

Color gradients indicate increasing **Percent Area** of soil group category.

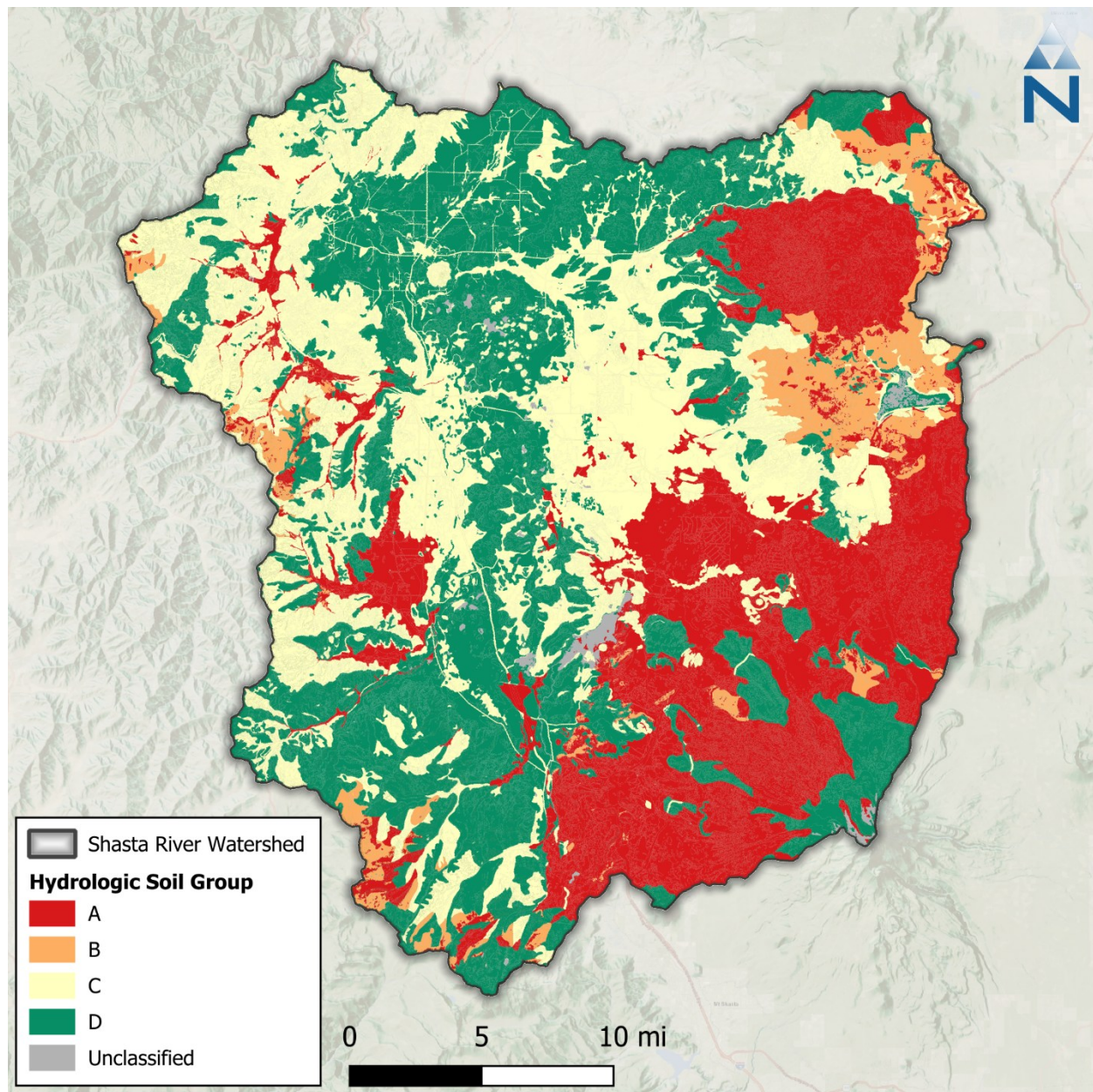


Figure 2-23. Soil Categories within the Shasta River watershed.

2.5.4 Geology Groups

The bedrock geology polygon layer was converted into a 30-meter resolution grid using the geologic feature attribute value as shown in Table 2-9. The HRU groups were defined based on geology group categories. Further analysis of area distribution shows that the Cascade category is dominant (59%) in the Shasta River watershed, whereas Klamath, and Overlap areas in this watershed cover approximately 24% and 17% respectively. A map showing the spatial distribution of reclassified geology categories is presented in Figure 2-24. It should be noted that the “Hornbrook Formation”, “Tertiary continental deposits”, and “Western Cascade Volcanics” geological features within the “Cascade” group have a different hydrologic response than other features in the “Cascade” group.

Those three geological features are geographically isolated to specific areas of the watersheds and make up 0.43%, 0.08% and 9.81% of the total subwatershed area, respectively. Instead of creating 4 unique geological classifications that would compound the number of modeled HRU combinations, the “Parameter Group” approach (described in Figure 2-10) can be used to designate an alternative set of HRUs that are applicable to the affected subwatersheds. Within those areas, the “Cascade” HRUs can be parameterized to be representative of “Hornbrook Formation”, “Tertiary continental deposits”, and “Western Cascade Volcanics” geological features, respectively. The parameter group approach can also be used to differentiate fault-impacted hydrology and shear zones.

Table 2-9. Geologic HRU groups and area distribution for Shasta River watershed

Geologic Features	Group Category	HRU Group	Area (acres)	Area (%)
Gazelle Formation	Klamath Mountains Province	Klamath	7,215.57	1.42%
Glacier	Glacier	Klamath	564.88	0.11%
Hornbrook Formation	Cascade Range Province	Cascade	2,180.35	0.43%
Plutonic Dioritic rocks	Klamath Mountains Province	Klamath	209.72	0.04%
MzPz metasedimentary rocks	Klamath Mountains Province	Klamath	3,464.90	0.68%
MzPz metavolcanic rocks	Klamath Mountains Province	Klamath	13,106.12	2.58%
MzPz metavolcaniclastic sedimentary rocks	Klamath Mountains Province	Klamath	712.11	0.14%
MzPz Stuart Fork Formation	Klamath Mountains Province	Klamath	3,096.61	0.61%
MzPz Undifferentiated	Klamath Mountains Province	Klamath	4,747.89	0.93%
Antelope Mountain Quartzite	Klamath Mountains Province	Klamath	9,770.43	1.92%
Trinity peridotite	Klamath Mountains Province	Klamath	36,555.56	7.20%
Gabbroic and dioritic rocks	Klamath Mountains Province	Klamath	4,352.25	0.86%
Pliocene Volcanic rocks	High Cascade Volcanics Subprovince	Cascade	39,125.77	7.70%
Abrams Mica Schist	Klamath Mountains Province	Klamath	2,508.38	0.49%
Alluvium	Overlap Deposits	Overlap	68,596.75	13.50%
Glacial deposits	Overlap Deposits	Overlap	15,308.04	3.01%
Landslide deposits	Overlap Deposits	Overlap	1,420.87	0.28%
Terrace deposits	Overlap Deposits	Overlap	567.10	0.11%
Pleistocene Volcanic rocks	High Cascade Volcanics Subprovince	Cascade	140,690.64	27.70%
Volcanic rocks of Shasta Valley	High Cascade Volcanics Subprovince	Cascade	67,307.09	13.25%
Moffett Creek Formation	Klamath Mountains Province	Klamath	7,679.26	1.51%
Duzel Formation	Klamath Mountains Province	Klamath	25,909.79	5.10%
Dredge and mine tailings	Dredge and mine tailings	Overlap	299.34	0.06%
Tertiary continental deposits	Cascade Range Province	Cascade	411.87	0.08%
Western Cascade Volcanics	Cascade Range Province	Cascade	49,843.16	9.81%

Color gradients indicate increasing **Percent Area** of geology group category.

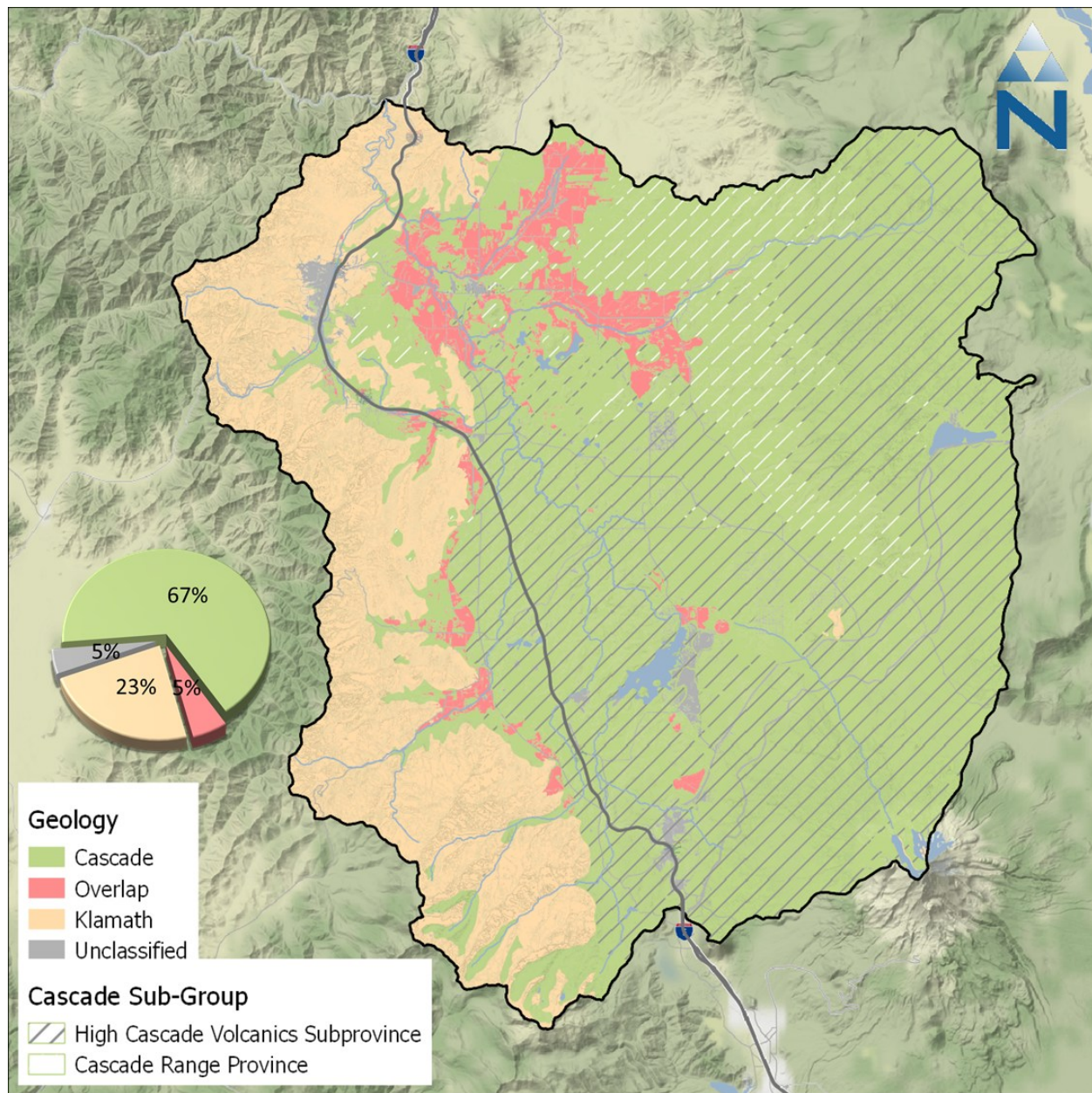


Figure 2-24. Geology groups within the Shasta River watershed. “Unclassified” represents land cover that was not stratified by geology (i.e., water, wetland, and developed area [about 5.4% of watershed area])

2.6 Hydrologic Response Units

Using the reclassified datasets discussed in the previous section, a set of representative HRUs was developed to reflect key landscape characteristics of the Shasta River watershed. These HRUs serve as the functional pervious and impervious land segment units in the watershed model.

These steps were performed to develop HRU categories:

1. Re-project all GIS layers into USA Contiguous Albers Equal Area Conic projected coordinate system (EPSG-102003) to ensure proper overlay and accurate area calculations
2. Clip all GIS layers to watershed extent to ensure data overlay to the same spatial extent
3. Convert all vector GIS layers into raster grids, resampled to a 30-meter resolution (i.e., 30-meter pixel width by 30-meter pixel height)
4. Intersect all input spatial layers and tabulate area distribution for each of the unique combinations of “primary attributes,” including land cover, soil, slope, bedrock geology, and irrigation source group categories
5. Using the final set of HRUs, summarize “secondary attributes” by HRU. Secondary attributes include characteristics such as canopy cover and imperviousness, which can be used to inform the parameterization of model processes.

Table 2-10 summarizes the percent area by soil, slope, and geology HRU groups by each land cover HRU category. Combining the 11 land cover groups, 4 soil groups, 3 slope groups and 3 geology groups results in 396 unique HRU combinations; however, the amount of area that each combination ultimately represents influences whether there is a need to further stratify the land cover category. For example, “Cultivated Crops” accounts for 0.4% of soil class B, none of which is on medium- or high-sloped areas of within the Klamath geology group. That leaves six (6) potentially meaningful combinations out of 36 for Crop land cover combinations for HRU consideration (i.e., “soil class A, low slope, and cascade geology”, “soil class A, low slope, and overlap geology”, “soil class C, low slope, and cascade geology”, “soil class C, low slope, and overlap geology”, “soil class D, low slope, and cascade geology”, and “soil class D, low slope, and overlap geology”). A single-digit code assigned to each HRU subcategory (as shown in Table 2-10) was used as a raster attribute to perform HRU raster analyses. Combining four HRU category layers generates a 4-digit code representing the unique combination of each layer’s attribute value. Figure 2-25 shows the spatial map and area distribution of the selected 89 HRUs with unique 4-digit HRU codes (from left: first digit represents the land cover, second digit represents the soil, third digit represents the slope, and fourth digit represents the geology). For example, the most common HRU code is “1121,” which represents “Forest-A-Medium-Cascade” areas—8% of the entire watershed area falls into this category.

Table 2-10. Percent land cover distribution by HRU category for the Shasta River watershed

HRU Land Cover*	Percent of Watershed Area	HRU Soil					HRU Slope				HRU Geology			
		All/Imp	A	B	C	D	ALL	0-15	15-35	>35	ALL	Cascade	Overlap	Klamath
		0	1	2	3	4	0	1	2	3	0	1	2	3
Forest	36.0%	0.0%	14.6%	5.6%	7.8%	8.0%	0.0%	9.0%	17.1%	9.8%	0.0%	25.8%	0.0%	10.2%
Grass & Shrub	42.0%	0.0%	7.4%	2.5%	14.9%	17.3%	0.0%	20.4%	13.4%	8.2%	0.0%	30.0%	0.0%	12.0%
Cultivated Crop, NI	6.4%	0.0%	0.8%	0.0%	2.8%	2.8%	0.0%	6.4%	0.0%	0.0%	0.0%	3.1%	3.4%	0.0%
Cultivated Crop, SW	3.4%	0.0%	0.3%	0.0%	1.5%	1.6%	0.0%	3.4%	0.0%	0.0%	0.0%	1.6%	1.8%	0.0%
Cultivated Crop, GW	0.7%	0.0%	0.2%	0.0%	0.4%	0.1%	0.0%	0.7%	0.0%	0.0%	0.0%	0.5%	0.2%	0.0%
Pasture, NI	5.4%	0.0%	1.0%	0.0%	2.3%	2.0%	0.0%	5.4%	0.0%	0.0%	0.0%	3.0%	2.4%	0.0%
Pasture, SW	1.8%	0.0%	0.3%	0.0%	0.7%	0.8%	0.0%	1.8%	0.0%	0.0%	0.0%	1.4%	0.4%	0.0%
Pasture, GW	0.4%	0.0%	0.2%	0.0%	0.2%	0.1%	0.0%	0.4%	0.0%	0.0%	0.0%	0.3%	0.2%	0.0%
Developed	3.2%	0.2%	1.4%	0.0%	1.5%	0.0%	0.0%	3.2%	0.0%	0.0%	3.2%	0.0%	0.0%	0.0%
Wetland	0.3%	0.3%	0.0%	0.0%	0.0%	0.0%	0.3%	0.0%	0.0%	0.0%	0.3%	0.0%	0.0%	0.0%
Water	0.4%	0.4%	0.0%	0.0%	0.0%	0.0%	0.4%	0.0%	0.0%	0.0%	0.4%	0.0%	0.0%	0.0%

Color gradients indicate more Watershed Area and increasing percentage of Soil, Slope, and Geology, respectively.

* NI = No Irrigation, SW = Surface water irrigation, GW = Groundwater irrigation

-- Represents land cover that was not further stratified by the corresponding HRU category.

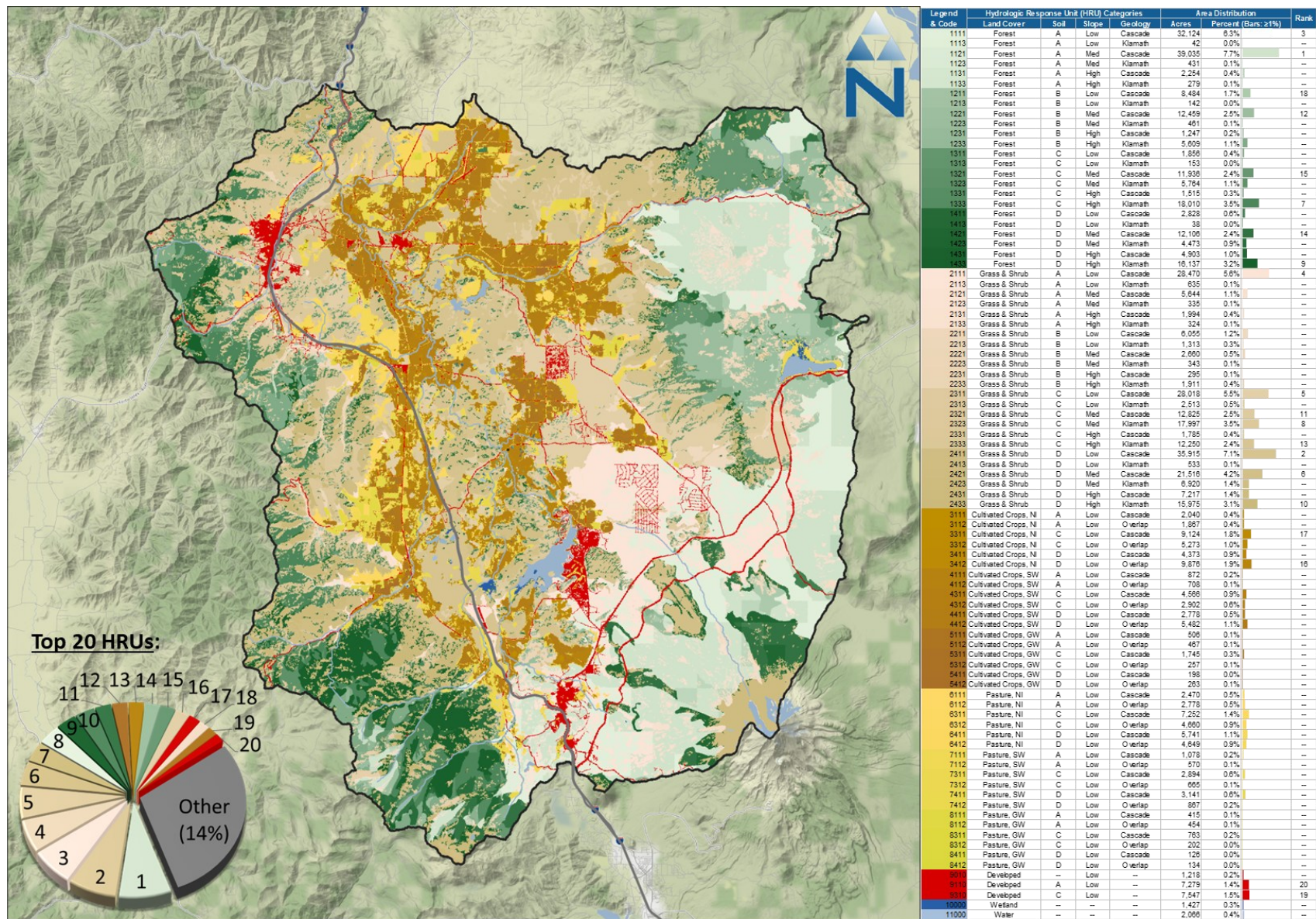


Figure 2-25. HRU categories map of the Shasta River watershed.

2.6.1 Directly Connected Impervious Area

The HRU approach not only highlights the predominant composition of area within the watershed, but also provides additional texture and physical basis for parameterizing and representing natural processes. Within a given modeled subwatershed, HRU segments are modeled as being parallel to one another. Each segment flows directly to the routing segment without any interaction with neighboring segments. However, in the physical environment, sometimes the lines between impervious and pervious land are not as clearly distinguished—impervious land may flow downhill over pervious land on route to a storm drain or watercourse.

For modeling purposes, Effective Impervious Area (EIA) represents the portion of total, or Mapped Impervious Area (MIA), that routes directly to the stream segments. It is derived as a function of Directly Connected Impervious Area (DCIA), with other adjustments as needed to account for other structural and non-structural management practices in the flow network. Figure 2-26 illustrates the transitional sequence from MIA to DCIA. Impervious areas that are not connected to the drainage network can flow onto pervious surfaces, infiltrate, and become part of pervious subsurface and overland flow. Because segments are modeled as being parallel to one another in watershed models (i.e., LSPC), this process can be approximated using a conversion of a portion of impervious land to pervious land. On the open landscape, runoff from disconnected impervious surfaces can overwhelm the infiltration capacity of adjacent pervious surfaces during large rainfall/runoff events creating sheet flow over the landscape—therefore, the MIA→EIA translation is not actually a direct linear conversion. Finding the right balance between MIA and EIA can be an important part of the hydrology calibration effort. EIA can be further refined to represent features such as rooftops, driveways, and sidewalks, for example. Because developed area represents only 3.7% of the Shasta River watershed area, this additional refinement is unlikely to provide a meaningful improvement in this case.

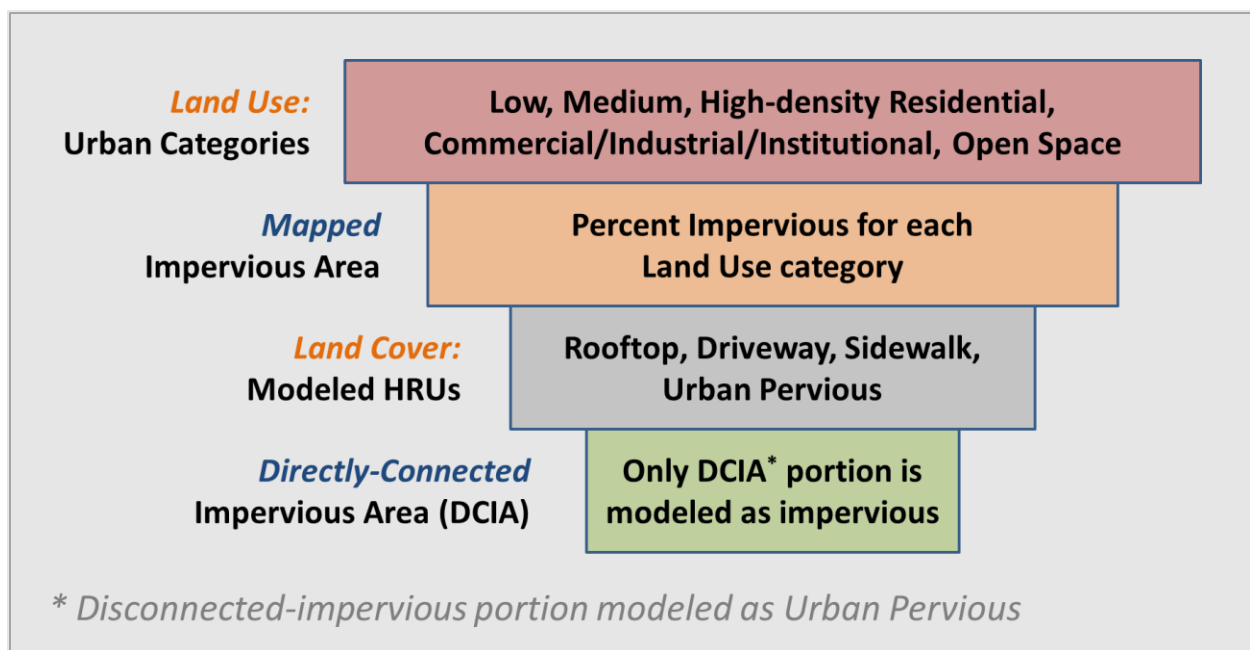


Figure 2-26. Translation Sequence from MIA to DCIA.

Empirical relationships like the Sutherland Equations (Sutherland, 2000) presented in Figure 2-27 show a strong correlation between the *density* of developed area and DCIA. The curve for high-density developed land trends closer to the line of equal value than the curve for less developed areas. Similarly, as the density of mapped impervious area approaches 1, the translation to DCIA also approaches 1. An initial estimate of EIA is equal to $MIA \times DCIA$. This empirical approximation can be further refined during model calibration to account for other flow disconnections resulting from structural or non-structural BMP practices or other inline hydraulic routing features.

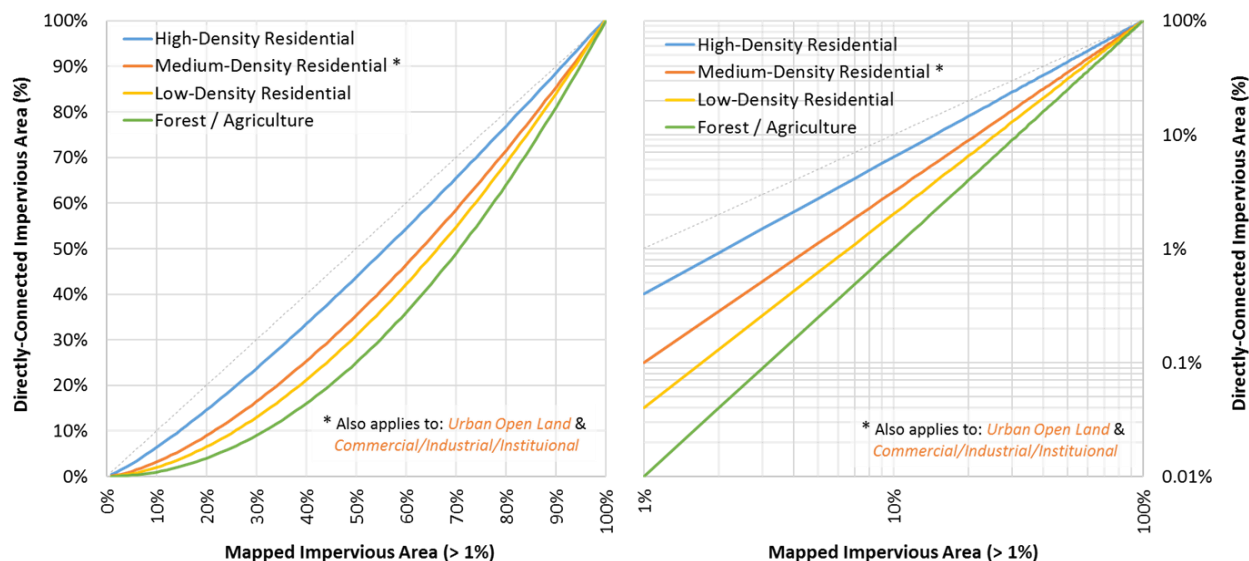


Figure 2-27. Mapped and directly connected impervious area relationships (Sutherland, 2000).

After incorporating irrigation consumptive uses (as further described in Section 5.2.1), 89 HRU categories ultimately represented the basic building blocks used in LSPC to capture hydrologic responses from land units in watershed. The four HRU subcategories (i.e., land use, soil, slope, and geology) represent the dominant primary bins that influence hydrology. Impervious cover is a secondary attribute that can be summarized per each of the primary HRU bins. The HRU layer was intersected with the percent impervious layer to identify the pervious and impervious portions of each HRU. The MIA, which is the impervious portion of each grid, was converted to EIA areas using the numerical relationship shown in Figure 2-27. Sutherland (2000) notes that areas with less than 1% MIA effectively behave like 100% pervious areas; therefore, EIA adjustments were only applicable for “Developed” areas. Table 2-11 is a summary of resampled MIA and calculated EIA by the original Land Cover Category, prior to incorporating irrigation HRUs. Although the model includes one aggregated “Developed” category, the final EIA estimates within each subwatershed are aggregated from the finer-resolution urban land cover classifications.

Table 2-11. Mapped Impervious Area compared with Effective Impervious Area.

NLCD Code	Land Use Category	HRU Land Cover Group	Area Total (acres)	Area (%)	Impervious (%)	
					MIA ¹	EIA ²
11	Open Water	Water	1,687.75	0.33%	0.2%	0.0%
12	Perennial Ice/Snow	Water	378.74	0.07%	0.0%	0.0%
21	Developed Open Space	Developed	9,998.39	1.97%	7.6%	2.5%
22	Developed Low Intensity	Developed	6,726.97	1.32%	19.0%	6.9%
23	Developed Medium Intensity	Developed	1,848.32	0.36%	34.0%	21.0%
24	Developed High Intensity	Developed	343.60	0.07%	51.6%	46.1%
31	Barren Land	Grass & Shrub	17,114.10	3.37%	0.2%	0.0%
41	Deciduous Forest	Forest	1,490.71	0.29%	0.5%	0.0%
42	Evergreen Forest	Forest	180,113.75	35.46%	0.4%	0.0%
43	Mixed Forest	Forest	607.58	0.12%	0.6%	0.0%
51	Dwarf Scrub	Grass & Shrub	0.00	0.00%	0.0%	0.0%
52	Shrub/Scrub	Grass & Shrub	119,431.78	23.51%	0.7%	0.0%
71	Grassland/Herbaceous	Grass & Shrub	91,155.95	17.95%	0.6%	0.0%
81	Pasture/Hay	Pasture	21,761.03	4.28%	0.4%	0.0%
82	Cultivated Crops	Cultivated Crops	53,297.16	10.49%	0.7%	0.0%
90	Woody Wetlands	Wetland	34.25	0.01%	0.0%	0.0%
95	Emergent Herbaceous Wetlands	Wetland	1,393.08	0.27%	0.1%	0.0%
99	No Data	Forest	555.10	0.11%	0.3%	0.0%

Data Source: 2011 National Land Cover Database, NLCD (Homer et al. 2015)

1: MIA = Mapped Impervious Area

2: EIA = Effective Impervious Area (derived using Sutherland 2000 methodology)

Color gradients indicate increasing **Percent Area** and **Percent Impervious**, respectively.

2.6.2 Secondary HRU Attributes

Two other secondary attributes not physically mapped by HRU category are percent slope and percent canopy cover. Although slope was a primary HRU component, resampling average slope within each of the final HRU categories provides additional precision for the slope estimate for the model. The final HRU layer was intersected with both the percent slope and percent tree canopy layers to identify the average slope and average tree canopy within each HRU category, respectively. Percent canopy estimates provide guidance for parameters such as interception storage and lower zone evapotranspiration rate and are highly correlated to percent canopy cover. Appendix C provides a summary of area distribution, average percent slope, and average percent canopy cover for the selected HRU categories in the Shasta River watershed.

As previously shown in Table 2-11, most of the forest area in the Shasta River watershed is classified as evergreen which includes conifers and broadleaf species. The most common conifers are Douglas-fir (*Pseudotsuga menziesii*) and coast redwood (*Sequoia sempervirens*). Broadleaf evergreen species include tanoak (*Notholithocarpus densiflorus*), interior live oak (*Quercus wislizeni*), Pacific madrone (*Arbutus*

menziesii), and California bay (*Umbellularia californica*). Common deciduous trees in riparian zones and moist sites include alders (*Alnus* spp.), willows (*Salix* spp.), cottonwood (*Populus* spp.), and big-leaf maple (*Acer macrophyllum*). Alder establishes well after disturbance such as timber harvest (Deal & Harrington, 2006). Outside riparian zones, the most common deciduous trees are Oregon white oak (*Quercus garryana*) and California black oak (*Quercus kelloggii*). Fire suppression and lack of prescribed fire has reduced wildfire frequency since the 1860s, leading to encroachment of Douglas-fir into grasslands and oak woodlands, except where soil conditions are unsuitable (e.g., too poorly drained, dry, or shallow) for supporting conifers (Keter & Busam, 1997; Murphy, 2008).

The effect of conifer encroachment on streamflow has not been well-studied, but mechanical removal of Douglas-fir was shown to decrease interception of precipitation and increased shallow soil moisture in oak woodlands (Devine & Harrington, 2007). In addition, rainfall interception is lower in oak forests than conifer forests, likely due to oak's lower leaf surface area (Devine & Harrington, 2007; Fenn & Bytnerowicz, 1997; Silva & Rodriguez, 2001) as well as lack of leaves during the winter in many oak species. Douglas fir transpiration occurs throughout the winter, peaks in the spring, and declines sharply in summer (Link et al., 2014; Stubblefield et al., 2012). Conversely, the transpiration rate of madrones, and to a lesser extent other broadleaf evergreen species, is highest in the summer (Link et al., 2014). Transpiration of Oregon white oaks also peaks in the summer (Phillips et al., 2003).

The primary HRU categories stratify the Forest category by geology and slope, which yields bins that reflect the additional resolution of vegetation growth regions described above. The summary table presented Table 2-12 suggests that soil, slope and geological properties are good predictors of the prevalent forest vegetation type.

Table 2-12. Summary of Forest Land Cover Classification by Forest HRU category

HRU Code	Hydrologic Response Unit (HRU) Categories				Percent Area (Forest)	NLCD Forest Classification		
	Land Use	Soil	Slope	Geology		Deciduous	Evergreen	Mixed
1111	Forest	A	Low	Cascade	17.65%	0%	99%	0%
1113	Forest	A	Low	Klamath	0.02%	3%	97%	0%
1121	Forest	A	Med	Cascade	21.39%	1%	99%	1%
1123	Forest	A	Med	Klamath	0.24%	1%	99%	0%
1131	Forest	A	High	Cascade	1.25%	0%	100%	0%
1133	Forest	A	High	Klamath	0.15%	1%	99%	0%
1211	Forest	B	Low	Cascade	4.64%	0%	100%	0%
1213	Forest	B	Low	Klamath	0.08%	1%	99%	0%
1221	Forest	B	Med	Cascade	6.82%	0%	100%	0%
1223	Forest	B	Med	Klamath	0.25%	0%	100%	0%
1231	Forest	B	High	Cascade	0.68%	2%	98%	0%
1233	Forest	B	High	Klamath	3.07%	0%	100%	0%
1311	Forest	C	Low	Cascade	1.02%	6%	93%	1%
1313	Forest	C	Low	Klamath	0.08%	3%	93%	3%
1321	Forest	C	Med	Cascade	6.53%	1%	99%	0%
1323	Forest	C	Med	Klamath	3.28%	1%	98%	0%
1331	Forest	C	High	Cascade	0.83%	2%	98%	0%
1333	Forest	C	High	Klamath	9.85%	3%	96%	1%
1411	Forest	D	Low	Cascade	1.55%	2%	98%	0%
1413	Forest	D	Low	Klamath	0.02%	11%	86%	3%
1421	Forest	D	Med	Cascade	6.63%	0%	100%	0%
1423	Forest	D	Med	Klamath	2.45%	1%	99%	0%
1431	Forest	D	High	Cascade	2.68%	0%	100%	0%
1433	Forest	D	High	Klamath	8.83%	1%	99%	0%
				Total	100%	0.82%	98.85%	0.33%

Data Source: 2011 National Land Cover Database, NLCD (Homer et al. 2015)

Color gradients indicate increasing **Percent of Forest Area**, and **Forest Vegetation Type**, respectively.

3 METEOROLOGICAL BOUNDARY CONDITIONS

Meteorological boundary conditions for LSPC were generated based on best available observed monitoring data. Several sources were reviewed and summarized as candidates for consideration. Among the primary sources of observed data were the Global Historical Climatology Network (GHCN), Remote Automated Weather Stations (RAWS), and the California Data Exchange Center (CDEC). The Parameter-elevation Regressions on Independent Slopes Model (PRISM) was also proposed as a secondary data product. PRISM provides daily or monthly timeseries of meteorological

conditions at a 4-km spatial resolution across the conterminous United States (Daly et al., 1994, 2008, 1997; Gibson et al., 2002). Additionally, the North American Land Data Assimilation System (NLDAS)—a product of the National Aeronautics and Space Administration (NASA), was also evaluated for consideration. NLDAS is a quality-controlled land surface model (LSM) dataset of meteorological data designed specifically to support continuous simulation modeling activities (Cosgrove et al., 2003; Mitchell et al., 2004). NLDAS provides real-time hourly predictions of meteorological data required for LSPC at a $1/8^{\text{th}}$ degree spatial resolution (about 8.625-mile [13.88 km] intervals) for North America, with retrospective simulations beginning in January 1979. NLDAS has undergone rounds of refinement, extensive peer review, and performance validation through case study applications, all of which have demonstrated it to be a more robust predictor of variable meteorological conditions for continuous simulation modeling than using individual gages (Xia et al., 2012; Xia et al., 2012).

Because hydrologic models are highly dependent on the quantity and quality of meteorological forcing data, challenges can arise when trying to associate point-sampled weather gage data over complex terrain (Henn et al., 2018). The development and application of high-resolution gridded data products to support continuous-simulation modeling and other geophysical applications has increased with advancements in computing capability and resources. Research related to those products focuses on methodology refinements, assessment of differences between products, and identification of primary drivers and geophysical conditions that affect the robustness of their application in different settings (Behnke et al., 2016; Henn et al., 2018). All seven of the gridded products reviewed by Benke et al. (2016) use the PRISM methodology to interpolate spatially because it considers orographic influence on rainfall variability.

The use of products like NLDAS and PRISM also helps to overcome some of the common issues encountered when working with rainfall gage data, which sometimes contain impaired intervals of missing, deleted, or accumulated data. Missing or deleted intervals are periods during which either the gage malfunctioned, or the data records were lost. Accumulated intervals contain cumulative precipitation reported over several hours or days, but the exact temporal distribution of the data is unknown due to a gage malfunction. The LSM uses observed gage data to guide the meteorological data extrapolation at fixed spatial intervals. LSM extrapolation considers orographic influence, which is an important consideration in the Shasta River watershed. Topographic properties like elevation, aspect, and the windward/leeward location of the prediction point are considered when modeling rainfall variability (both timing and volume) across the landscape. As a result, LSMs extrapolate conditions for 52 ungaged areas and interpolate spatial variability between gaged areas in a non-linear way. LSM approaches can capture localized impacts such as rain shadow over the landscape. The quality-control and increased spatiotemporal resolution of meteorological boundary conditions improves the predictions of continuous simulation watershed models and benefits water balance calculations in large-scale continuous-simulation applications. NLDAS and PRISM are also updated in real-time in a consistent format, making it easier to periodically update boundary conditions for the watershed model as new information becomes available.

Table 3-1 is a summary of available meteorological data by source that were reviewed as part of the Shasta River hydrology model development. Table icons indicate the temporal resolution of the data by source. NLDAS also includes the full suite of hourly meteorological timeseries that the model uses, except for dewpoint temperature; however, dewpoint temperature, which is a function of air temperature, station pressure, and specific humidity, was computed from those NLDAS timeseries. To leverage both NLDAS and PRISM datasets, the NLDAS hourly rainfall timeseries distributions were used to disaggregate monthly PRISM timeseries on hourly scale. A minimum hourly rainfall

depth of 0.01 inches, which is the threshold for trace rainfall among the observed gages, was applied to the hourly PRISM timeseries to remove numeric “noise” from it. The resulting dataset is an hourly 4-km spatial distribution of PRISM timeseries (based on NLDAS rainfall distributions). In other words, the relative hourly rainfall distributions follow the NLDAS rainfall patterns, while the monthly totals are equal to the monthly PRISM totals. For the Shasta River watershed, there are 135 unique sets of meteorological timeseries available for assignment to the modeled subwatersheds.

Table 3-1. Climate parameters evaluated during the initial inventory.

Meteorological Data	Temporal Resolution of Meteorological Data by Source						
	(Timestep: ● Hourly, ○ Daily, □ Monthly)						
	(a)	(b)	(c)	(d)	(e)	(f)	(g)
	GHCN	LCD	CDEC	RAWS	DRI	PRISM-M	NLDAS
Precipitation	○	●	●	●	○	□	●
Potential Evapotranspiration	--	--	--	--	--	--	●
Daily Air Temperature (Min/Max)	○	--	--	--	--	□	--
Hourly Air Temperature	--	●	--	●	--	--	●
Solar Radiation	--	●	--	●	--	--	●
Cloud Cover	--	●	--	●	--	--	●
Wind Speed	--	●	--	●	--	--	●
Wind Direction	--	●	--	●	--	--	●
Station Pressure	--	--	--	--	--	--	●
Specific Humidity	--	--	--	--	--	--	● ¹
Dewpoint Temperature	--	●	--	●	--	--	● ²

Acronyms: (a) Global Historical Climatology Network, (b) Local Climatic Data, (c) California Data Exchange Center, (d) Remote Automated Weather Stats, (e) Desert Research Institute, (f) Parameter-elevation Regressions on Independent Slopes Model-Monthly aggregated timeseries, (g) North American Land Data Assimilation System.

1: Specific Humidity converted to Relative Humidity as a function of Air Temperature and Station Pressure
 2: Dewpoint Temperature calculated as a function of Air Temperature, Station Pressure and Relative Humidity

3.1 Subwatershed Gage Assignment

In the Shasta River LSPC model, one set of meteorological timeseries are assigned to each of the 261 delineated model subwatersheds—it is also assumed that the associated rainfall falls uniformly within each subwatershed. To better manage the rigidity of that assumption, subwatersheds were delineated at a finer resolution in portions of the watershed where rainfall variability was relatively high over short distances. Data analysis from other modeling studies at times shows notable differences in observed rainfall data collected at different locations at the same facility (e.g., opposite ends of an airport runway). Henn et al. (2018) also describe paired comparisons of observed rainfall gages located within the extent of a single LSM grid, which report different rainfall volumes and distributions. Ultimately, the predicted hydrologic response of higher-resolution meteorological boundary

conditions validates how representative they are of weather conditions upstream of the modeled assessment point.

Figure 3-1 shows the regional distribution of annual average summaries of PRISM rainfall overlaid with modeled subwatersheds, and NLDAS data centroids. Meteorological boundary conditions were associated with subwatersheds by assigning the grid that covered most of the subwatershed area. Figure 3-2 shows average annual rainfall summaries of the hourly PRISM-NLDAS timeseries that were assigned to model subwatersheds. Hourly data were used for model simulation.

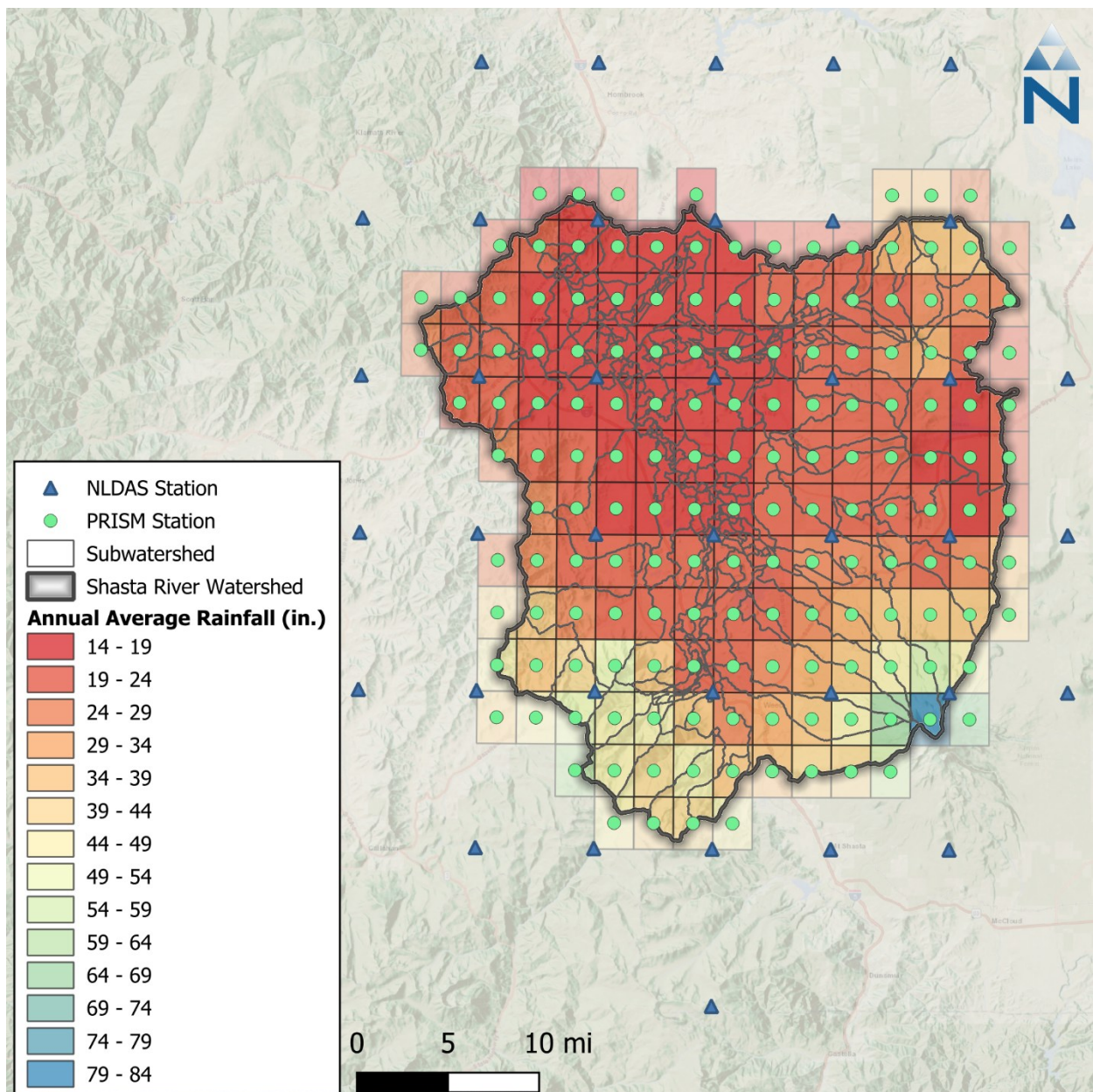


Figure 3-1. Annual average PRISM rainfall depths with NLDAS and PRISM centroids.

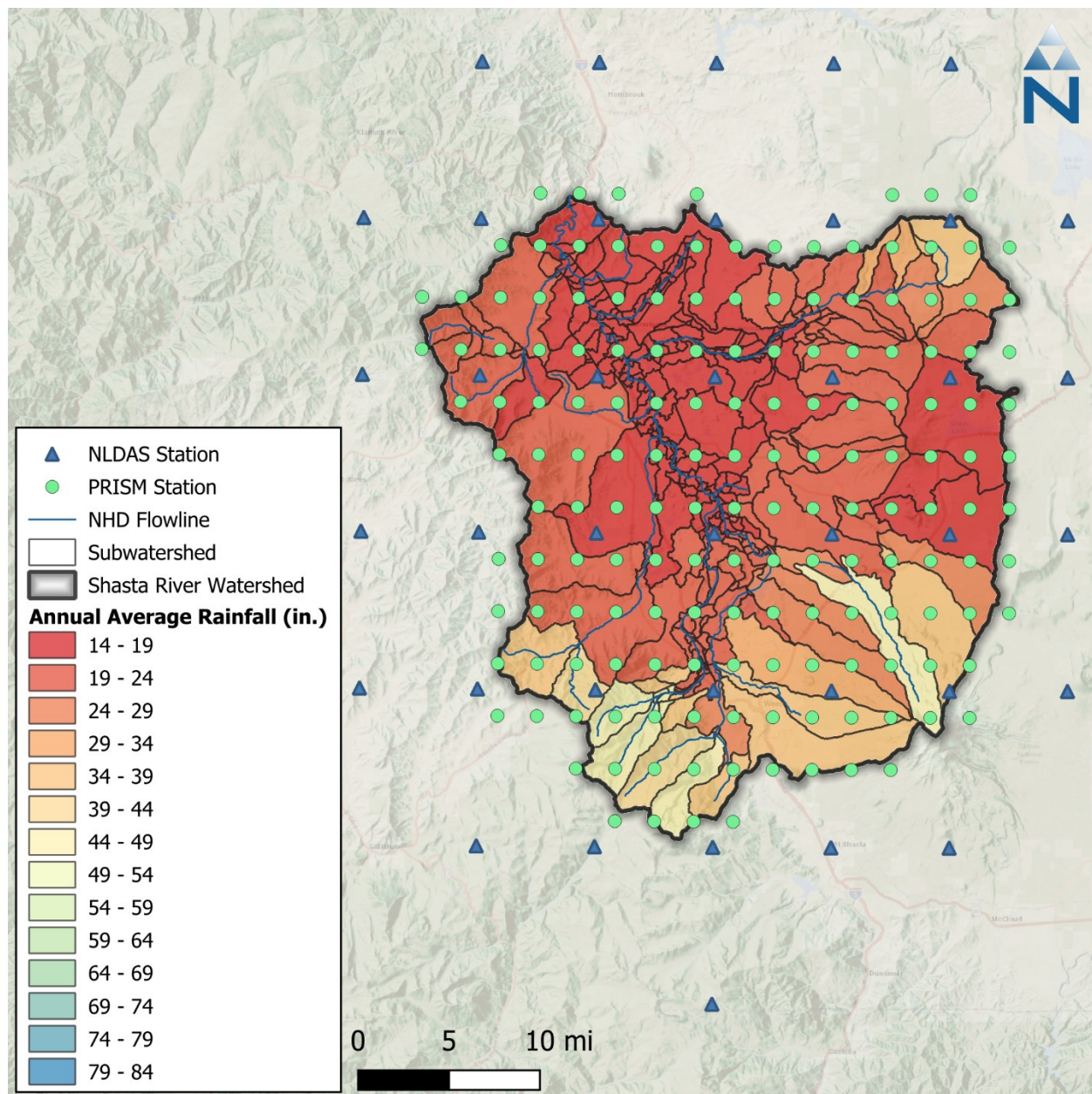


Figure 3-2. Annual average rainfall by subwatershed (from PRISM and NLDAS gridded data).

3.1.1 Elevation and Aspect Analysis

The PRISM data were analyzed with respect to topographic data to better understand the implications of orographic influences reflected in the PRISM annual average rainfall totals. The elevation of each PRISM centroid was extracted from an overlay with NED DEM. Hillslope aspect was also derived from the DEM and extracted for each PRISM centroid. Aspect was categorized into north-, east-, south-, and west-facing quadrants using the degrees scale shown in the legend of Figure 3-3. Of the 162 available PRISM grid centroids, 124 centroids were within the clipped NED-watershed boundary.

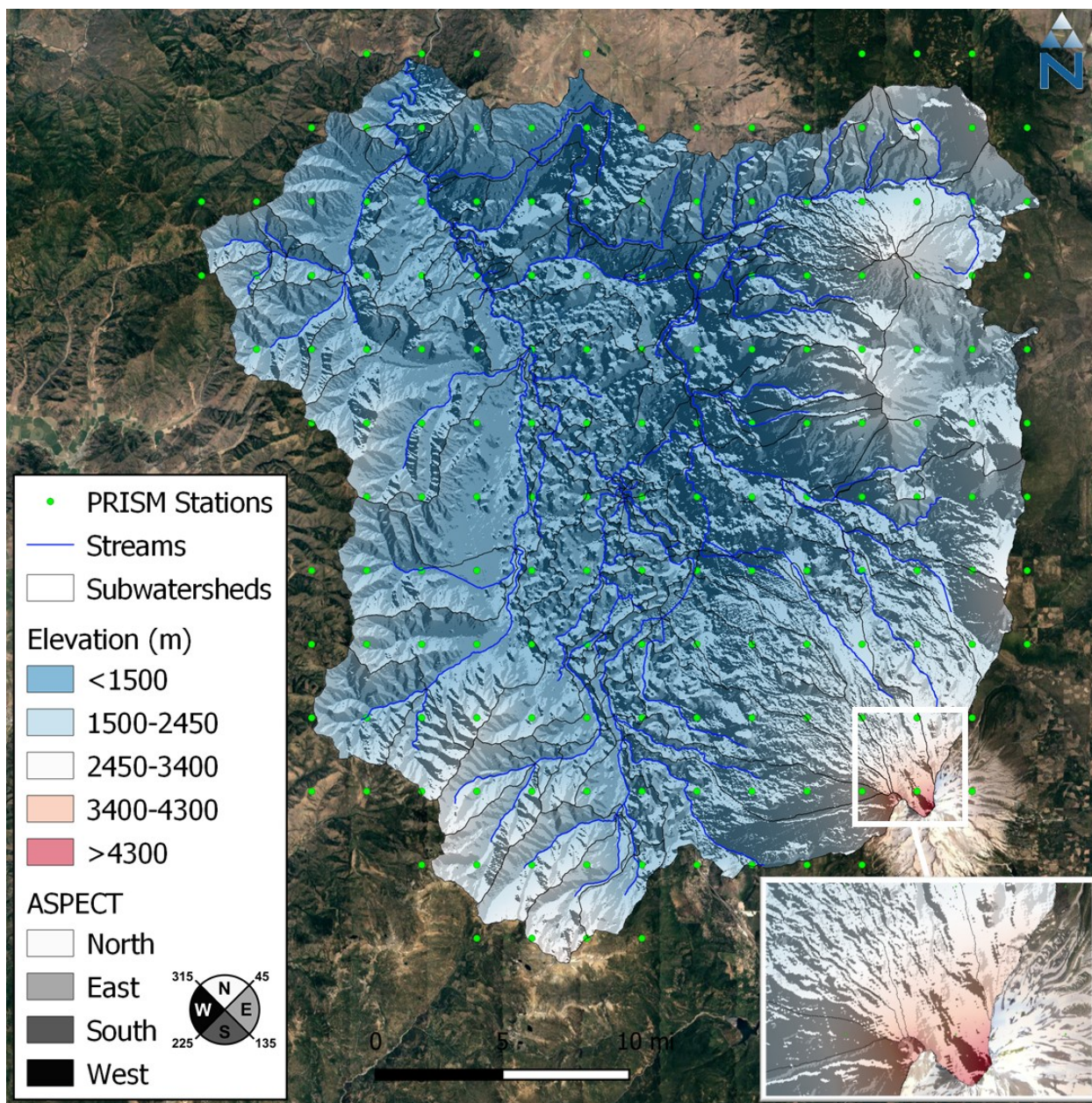


Figure 3-3. Overlay of PRISM centroids with NED-derived elevation and aspect.

To assess the influence of elevation, PRISM centroids were sorted by increasing elevation and associated average annual rainfall was plotted. The data were grouped into 5 equal elevation bins for analysis (low, medium-low, medium, medium-high, and high)—the median elevation of each bin was plotted for reference, as shown in Figure 3-4. The graph shows a gradual increase in rainfall with elevation; however, the variability suggests that other factors besides elevation also have an influence on annual average rainfall. The data were also binned and analyzed by aspect. Figure 3-5 shows how average rainfall varies by both elevation and aspect.

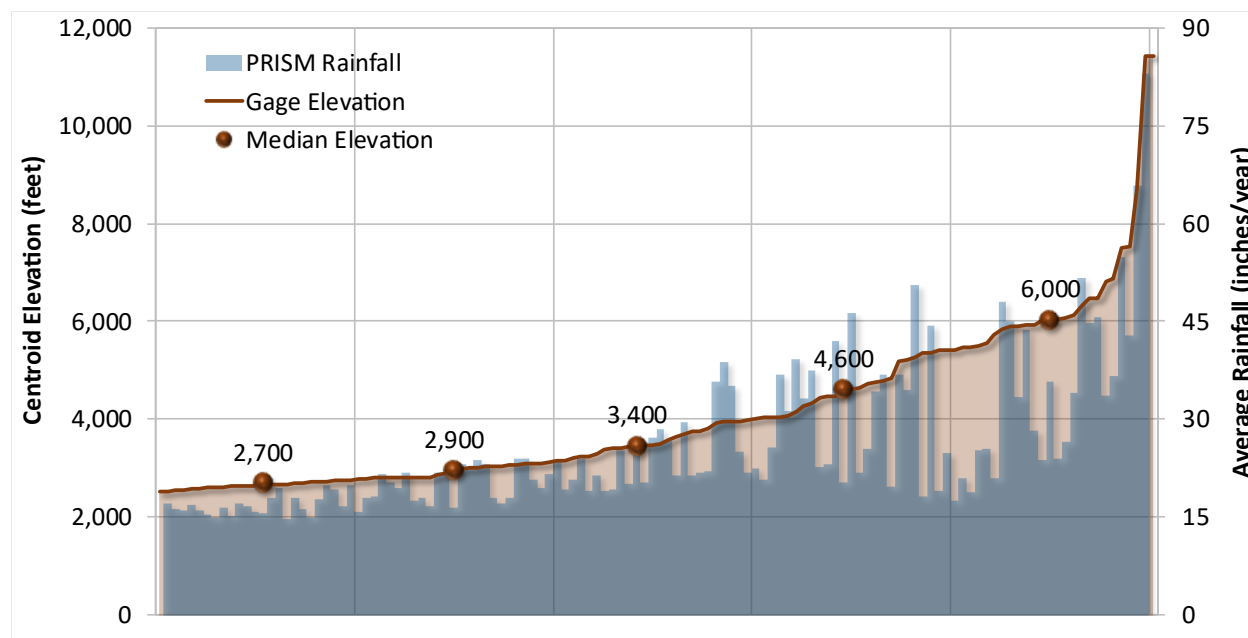


Figure 3-4. Average annual PRISM rainfall vs. centroid elevation (with median elevation).

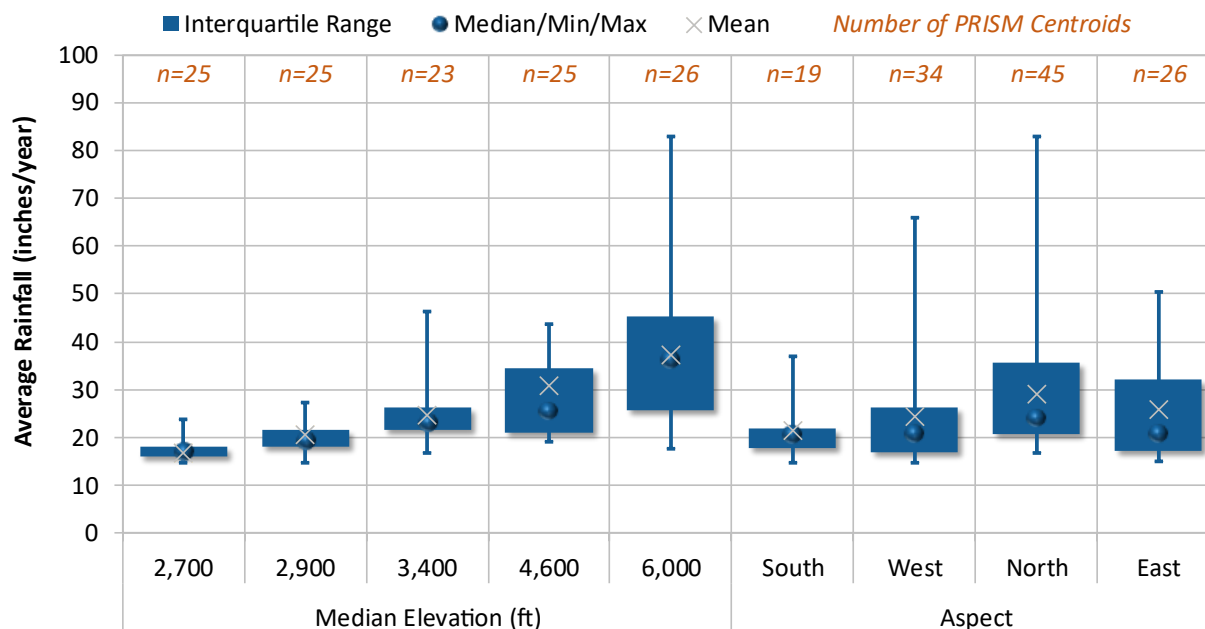


Figure 3-5. Box plots of average annual rainfall variability by elevation and aspect.

To assess the combined impact of elevation and aspect in the Shasta River PRISM average annual rainfall, the 124 centroids were grouped into 20 bins of elevation and aspect (5 elevation \times 4 aspect groups). On average, there were 6 centroids within each of the 20 bins, and the median rainfall was calculated for each bin, as summarized in Table 3-2. Figure 3-6 is a surface plot of the median rainfall (vertical axis) vs. elevation and aspect (horizontal plane)—the surface illustrates the central tendency of the combined impact of elevation and aspect on average annual rainfall. The right panel of Figure 3-6 is the birds-eye view from the top of the surface shown in the left panel—it shows horizontal and vertical surface transects for aspect and elevation, respectively.

Table 3-2. Median rainfall (and distribution of PRISM centroids) by elevation and aspect

Elevation		Hillslope Aspect (Number of Centroids)				Total
Bin	Median (feet)	East	South	West	North	
1	2,700	4	7	9	5	25
2	2,900	4	7	9	5	25
3	3,400	3	6	9	5	23
4	4,600	4	7	9	5	25
5	6,000	4	7	9	6	26
Total		19	34	45	26	124
Elevation		Hillslope Aspect (Median Rainfall, inches/year)				Median
Bin	Median (feet)	East	South	West	North	
1	2,700	16	16	19	17	16
2	2,900	19	17	21	19	21
3	3,400	21	23	25	22	22
4	4,600	22	21	28	33	31
5	6,000	30	33	45	44	34
Median		20	21	24	21	22

Color gradient shows **relative rainfall depth**. Darker is higher.

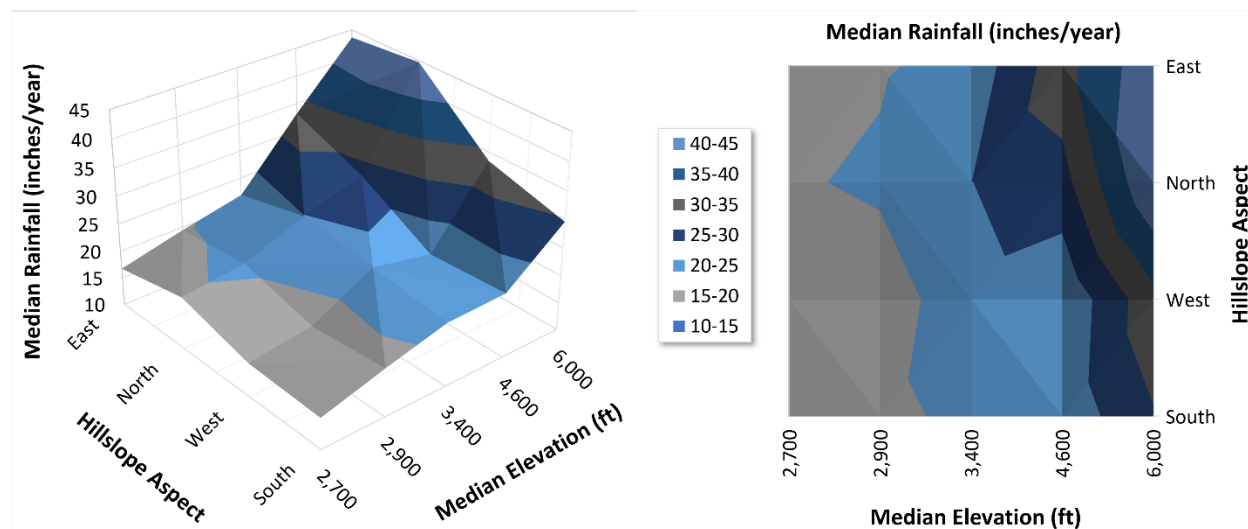
**Figure 3-6. Median rainfall (vertical axis) vs. elevation and aspect (horizontal plane).**

Figure 3-6 shows that the driest areas of the Shasta River watershed were the lowest-elevation south-, southwest-, and east-facing slopes, while the wettest were highest-elevation east and north-facing slopes. The 2,700 foot elevation transect had the least variability in median rainfall, while the 6,000 foot elevation transect had the greatest. Along the aspect transects, north- and west-facing slopes had the highest median rainfall across the range of elevations. South- and west-facing slopes had the least variability (i.e., four or five color changes) across the range of elevations. PRISM centroids were assigned to subwatersheds based on proximity alone, no additional refinement based on elevation or aspect was necessary.

4 INTEGRATED GROUNDWATER MODEL

LSPC served as the aggregation platform for the integrated surface-groundwater model for the Shasta River watershed. As described in Sections 2 and 3, detailed land use, soils/geology, and topographical (elevation/slope) were used to configure HRUs, while high-resolution gridded weather data were used to represent meteorological boundary conditions. This section describes how other assumptions related to surface water withdrawals, diversions, and groundwater pumping were incorporated into the models for model calibration. Finally, the coupled modeling system was used to represent existing instream flows (baseline). Unimpaired flows can also be estimated by turning off withdrawal, diversions, and groundwater pumping in the integrated model. Figure 4-1. shows generalized interaction of model inputs, connections and outputs for coupled model calibration.

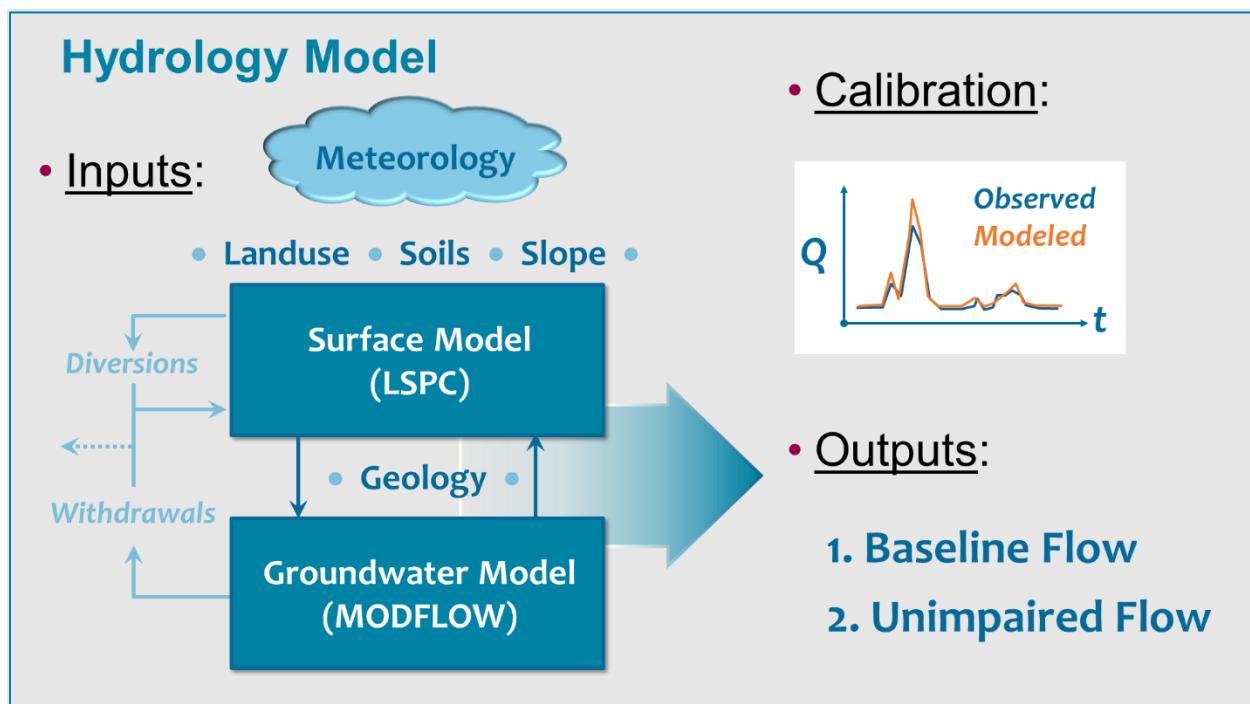


Figure 4-1. Schematic of coupled hydrology model components, interactions, and application.

Figure 4-2 is a more detailed schematic of the processes and associated parameters and timeseries used in LSPC. The schematic represents land-based processes for a single land unit in the model, all of which collectively discharge to a stream transport segment. The shaded box with a dotted outline at the bottom of the schematic represents the default groundwater module within LSPC. In LSPC, the water balance is computed independently for each land unit within the model. Water moves in the direction of the arrows as illustrated in the schematic, and neighboring HRUs are not connected in the subsurface layer. The default groundwater formulation in LSPC has limitations for representing the complex geology in the Shasta River watershed and lateral groundwater movements that are important for characterizing watershed hydrology. LSPC was used to predict groundwater inflow (GWI) to MODFLOW. In return, MODFLOW outputs, which are highly variable spatially and vertically, were used to update the LSPC-predicted groundwater outflow (AGWO).

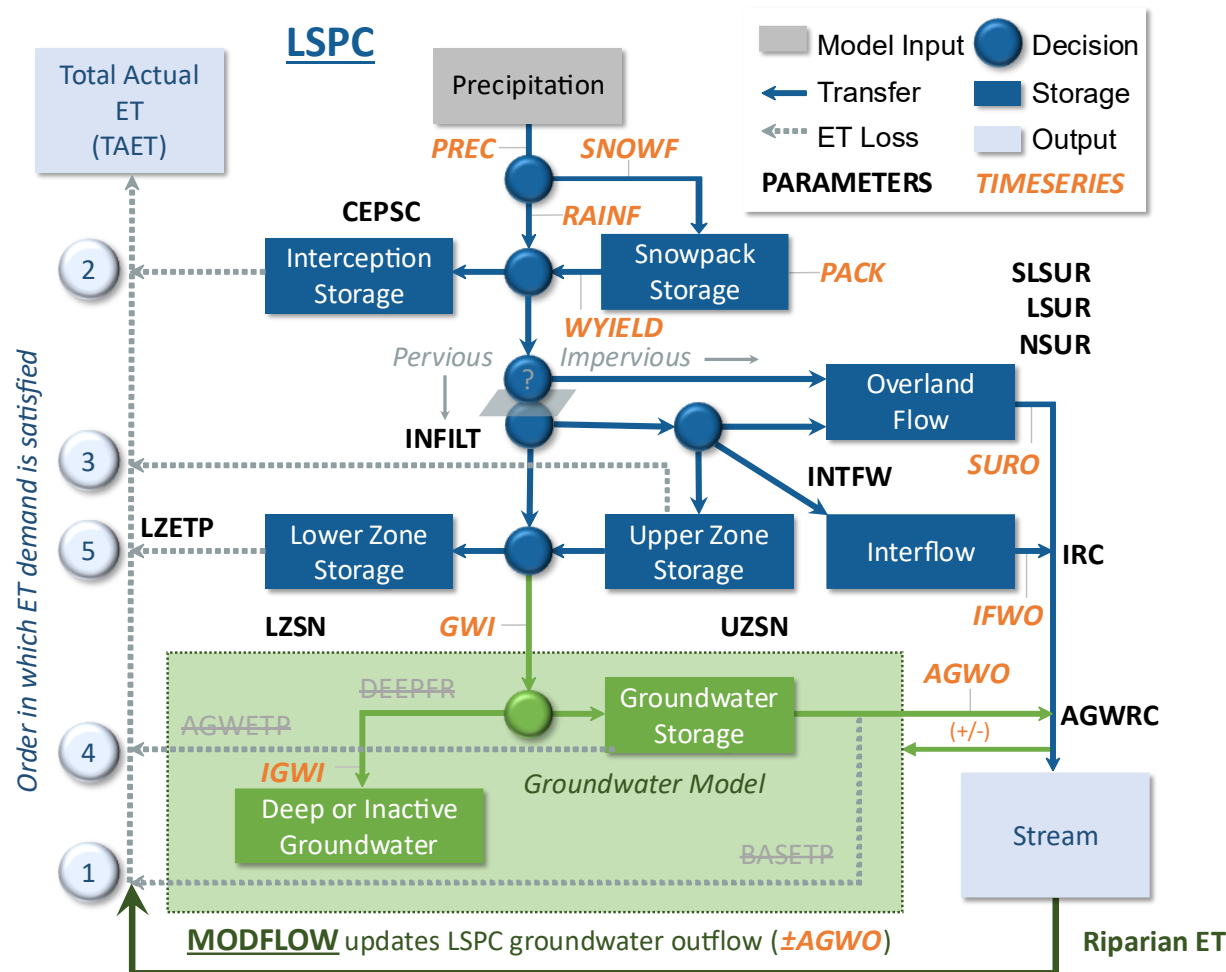


Figure 4-2. LSPC hydrology model processes, parameters, and timeseries.

Figure 4-3 provides a general overview of key model components for the coupled LSPC-MODFLOW hydrology model. Each subwatershed in LSPC was associated with meteorological boundary conditions and a distribution of HRUs (See Report Sections 3 and 2.4, respectively, for additional information). The HRUs within each subwatershed were linked to the underlying MODFLOW grid to provide GWI. Conceptually, the primary source of water to the groundwater system is groundwater recharge, and water leaves the groundwater system via streams as baseflow and spring flow and via pumping wells.

The groundwater model developed by Siskiyou County GSA (2021) was the starting point for the development of the MODFLOW model providing the framework for spatial discretization, geologic zonation, and the simulation period. Several changes were made to the model as discussed in the following sections. MODFLOW-NWT (Niswonger et al., 2011) was used as the underlying numerical simulation code for the coupled LSPC-MODFLOW model because it provides a robust solution for models involving drying and rewetting nonlinearities of the unconfined groundwater-flow equation.

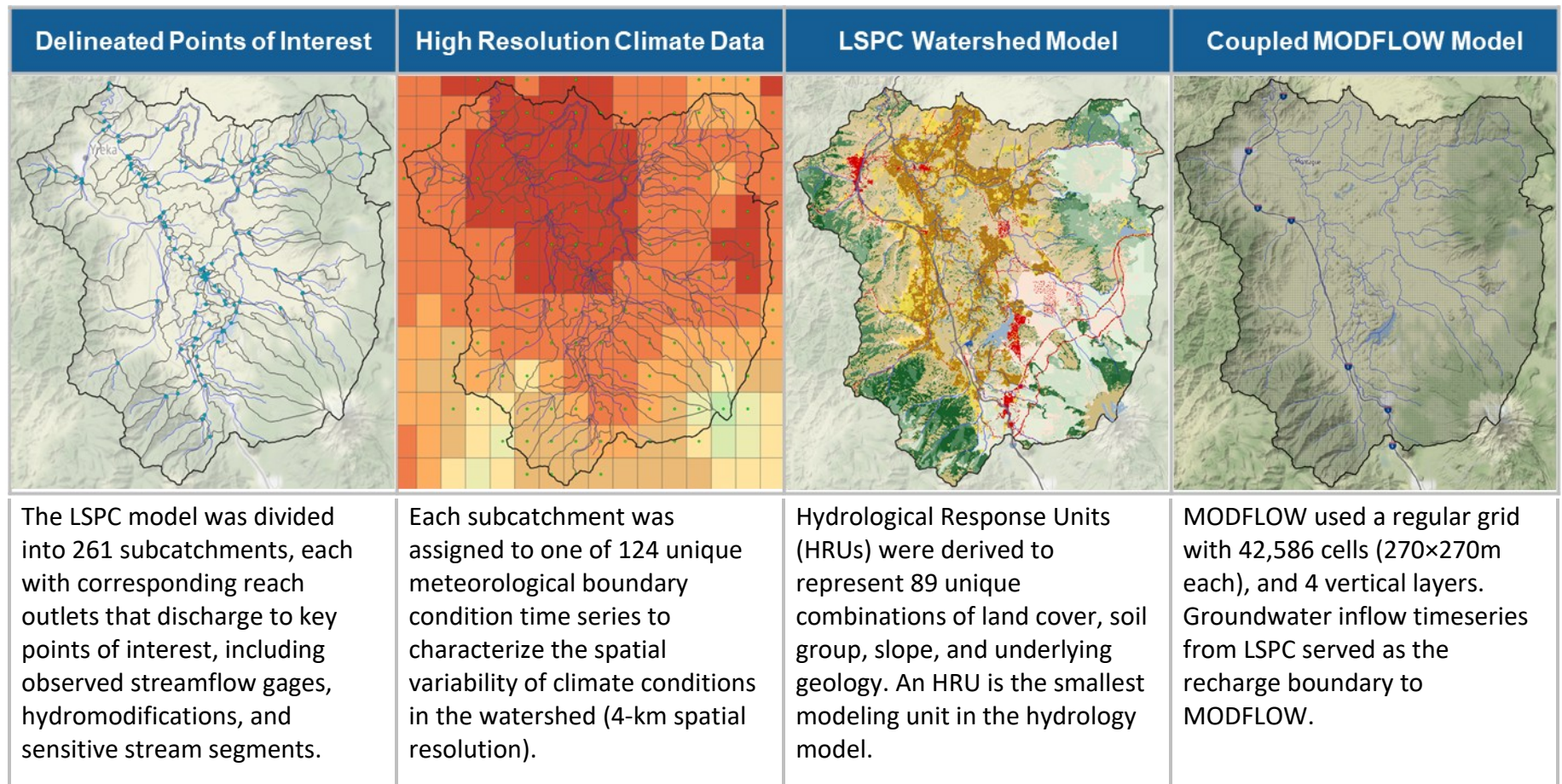


Figure 4-3. Overview of key model development components for LSPC and MODFLOW.

4.1 Domain and Discretization

The groundwater model domain was assumed to coincide with the watershed boundary. The spatial domain was discretized horizontally into a regular square grid consisting of 42,586 cells, each 270 × 270 m in size (Figure 4-3). The model was discretized vertically into four layers. The top elevation of the upper model layer was defined by averaging the digital elevation model (DEM, Figure 4-4) over each model cell.

MODFLOW layering was defined by smoothing the surfaces that represent the bottom elevations of each model layer to ensure that layer thicknesses capture the major geologic groups while maintaining numerical stability. Left panels of Figure 4-5 through Figure 4-8 shows bottom elevations for the four model layers. These figures illustrate that the top three layers conform to the watershed domain, whereas Layer 4 conforms to the basin boundary as delineated in Bulletin 118. The spatial domain and discretization are consistent with the groundwater model developed by the Siskiyou County GSA (2021).

The bottom elevation of Layer 4 was assigned a uniform elevation of 145 m, selected to maintain a minimum Layer 4 thickness of approximately 350 m, consistent with the original GSA model. Although the elevations and thicknesses of the model layers are approximate, they generally represent the geologic cross sections described by Ward & Eaves (2011) and referenced by the Siskiyou County GSA (2021).

4.2 Simulation Period

The simulation period for the coupled model was from water year 1991 (October 1990) through 2023 (September 2023). LSPC was run at an hourly timestep over the simulation period while MODFLOW was run at a monthly timestep. In contrast with surface water, groundwater movement occurs gradually within slower temporal regimes where impacts are realized over months and years rather than hours or days. MODFLOW was discretized into monthly “stress periods” over the simulation period. Timeseries of aggregated monthly GWI from LSPC were used as inflows from surface to groundwater in each grid cell for each stress period. The first stress period was simulated as steady-state to obtain reasonable initial conditions throughout the system representing initial conditions for October 1990. A total of 397 stress periods were simulated. Averaged boundary conditions (recharge, pumping, and others) were used for the first stress period.

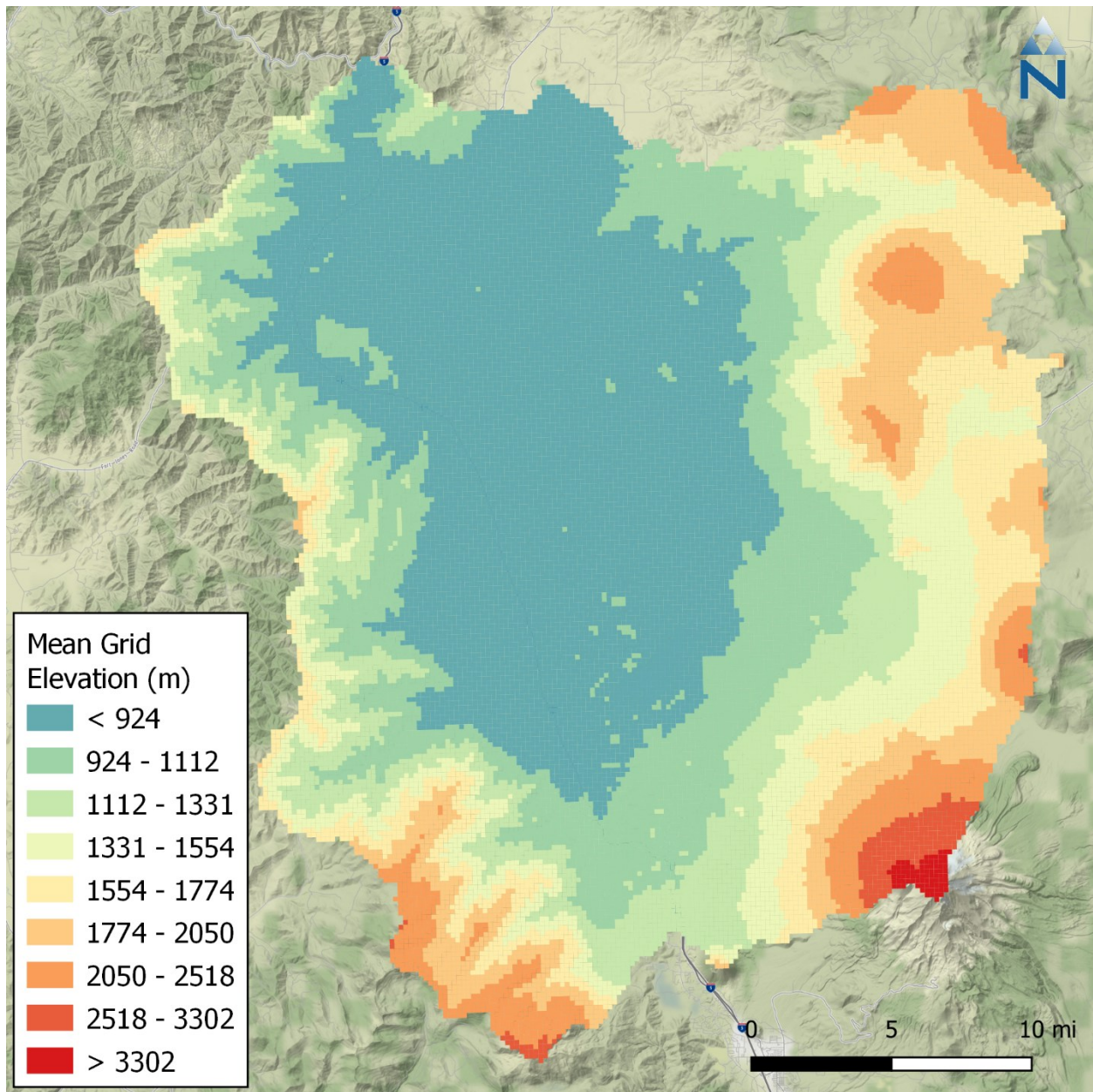


Figure 4-4. Top elevations of the Shasta River watershed MODFLOW model.

4.3 Aquifer Properties

The following aquifer system groups were incorporated in the groundwater model:

1. Klamath Mountains
2. Hornbrook Formation
3. Western Cascades Pliocene Volcanic
4. Alluvium
5. Glacial Deposits
6. Pleistocene Volcanic
7. Shasta Valley Volcanic
8. Western Cascades Volcanic
9. Pluto's Cave Basalt/Lava Tubes

Right panels of Figure 4-5, Figure 4-6, Figure 4-7, and Figure 4-8 show the spatial distribution of these aquifer groups within the model layers. Each group was assigned a unique set of hydraulic properties, including horizontal and vertical hydraulic conductivity, specific yield, and specific storage. These parameters were estimated and adjusted within plausible ranges as part of the model calibration process.

The first eight aquifer groups listed above are consistent with the groundwater model developed by the Siskiyou County GSA (2021). The ninth group, Pluto's Cave Basalt, was incorporated based on the Pluto's Cave Basalt delineation provided by LWA (Qb basalt flow lines) and was further refined through review of airborne electromagnetic (AEM) survey data and local well log information. The presence of lava tubes/flows within the Pluto's Cave Basalt formation has been documented and discussed in several studies, including Mack (1960), Blodgett et al. (1988), and Buck (2013). These studies indicate the potential for high-conductivity flow paths supported by multiple lines of empirical evidence. Accordingly, the Pluto's Cave Basalt unit was assigned relatively high hydraulic conductivity. This unit was implemented in Layer 2 of the model, consistent with the interpreted depth of the formation.

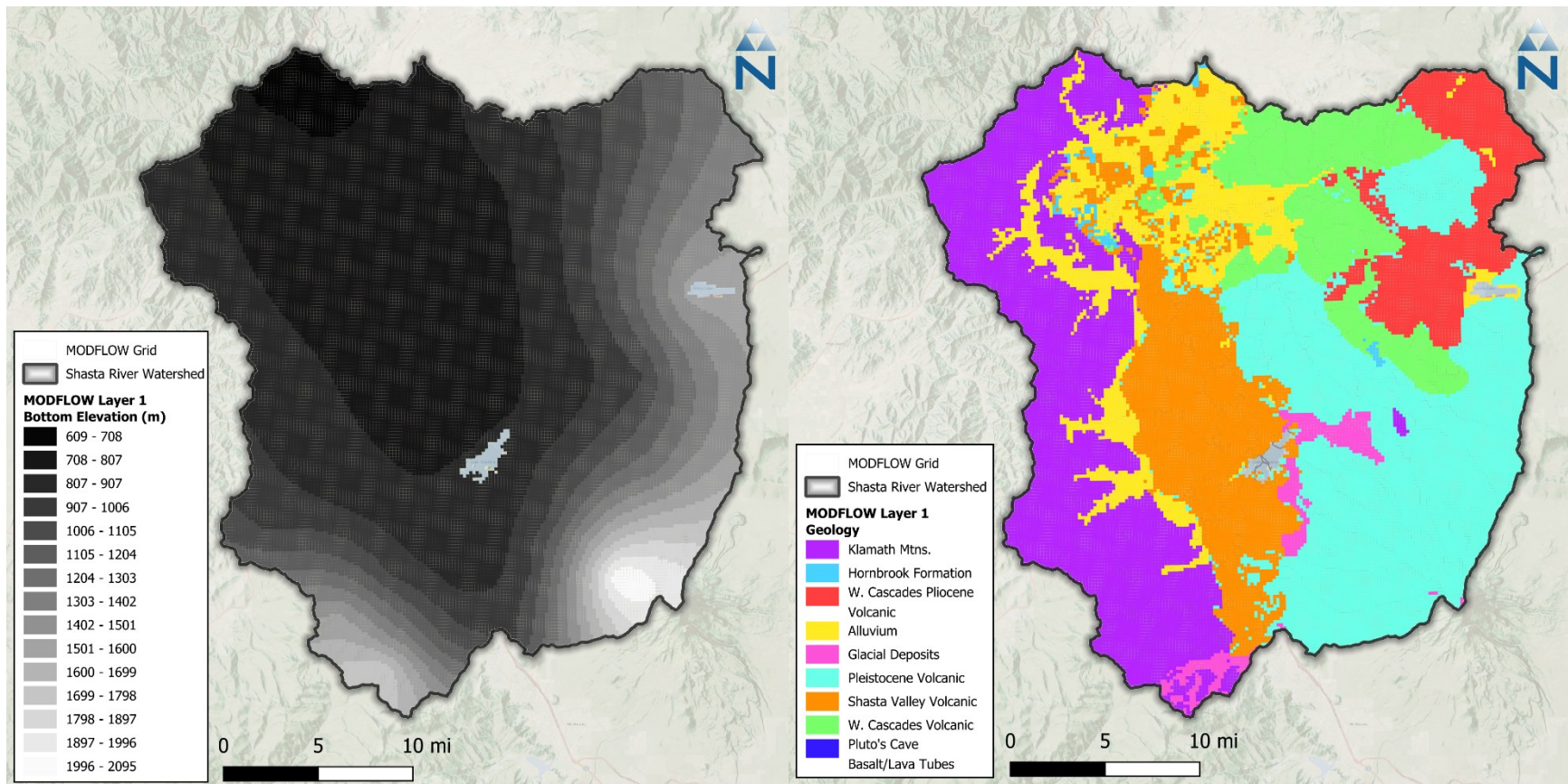


Figure 4-5. Bottom elevation and geological attributes for MODFLOW layer 1 in the Shasta River watershed.

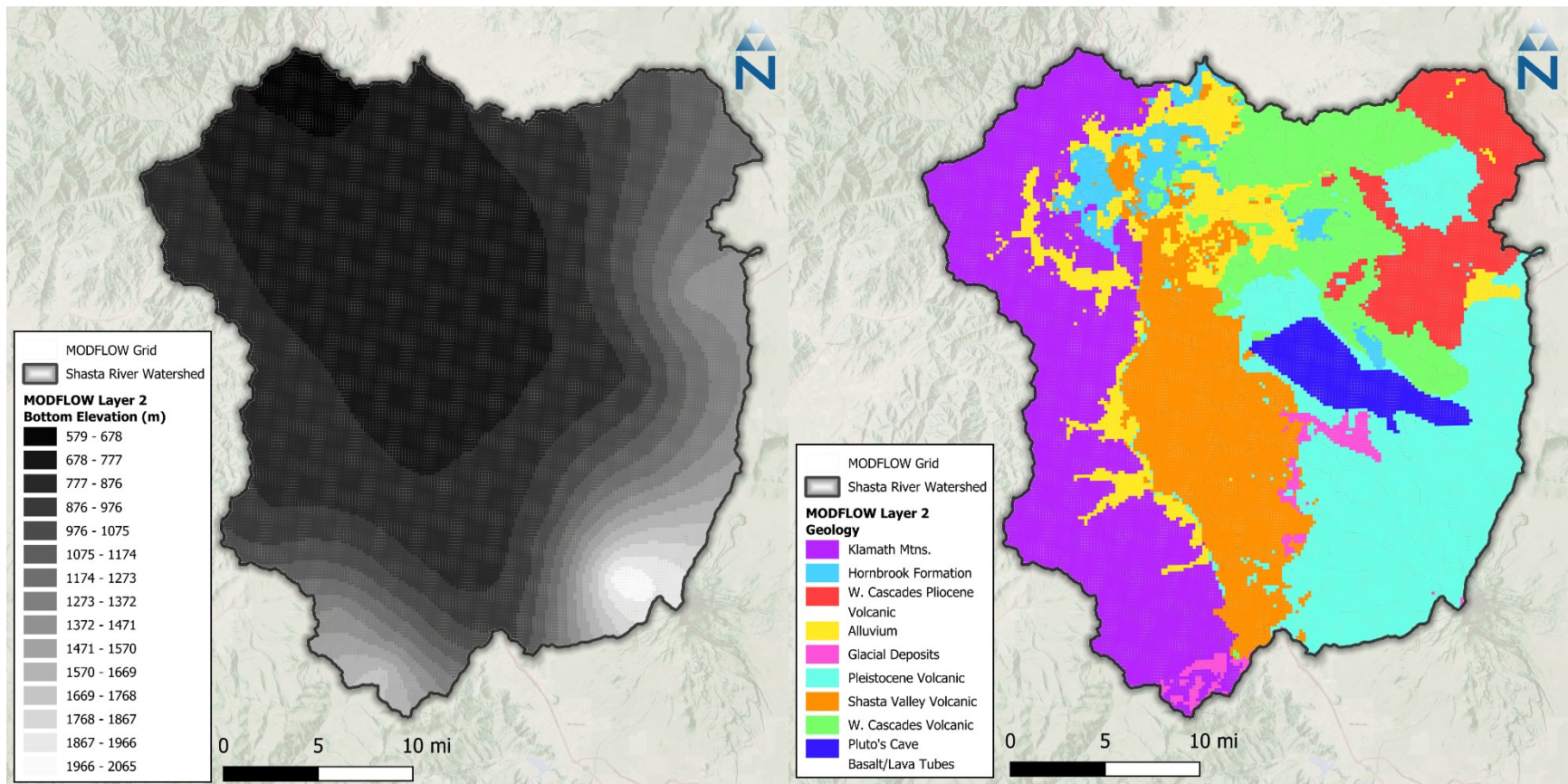


Figure 4-6. Bottom elevation and geological attributes for MODFLOW layer 2 in the Shasta River watershed.

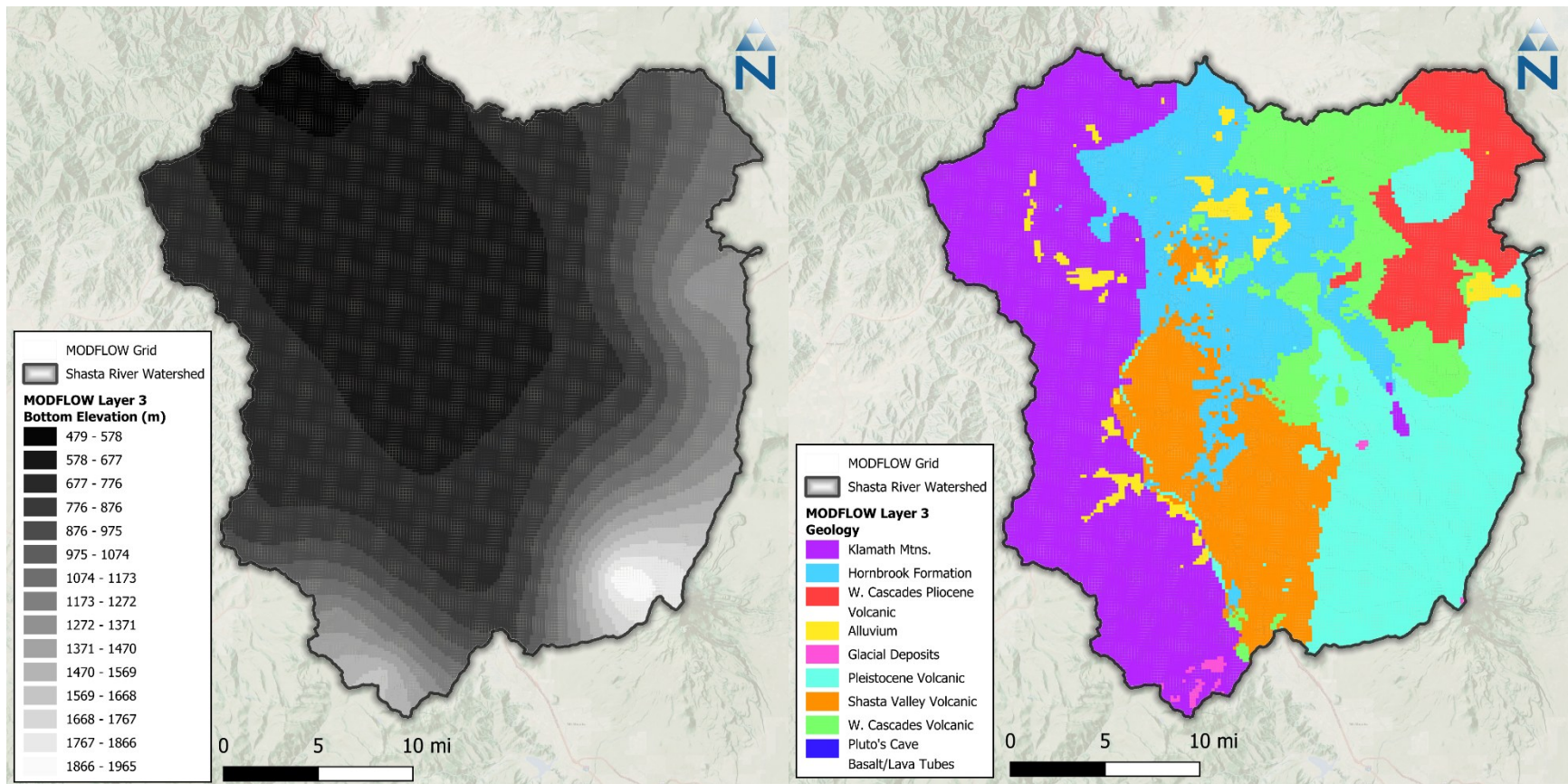


Figure 4-7. Bottom elevation and geological attributes for MODFLOW layer 3 in the Shasta River watershed.

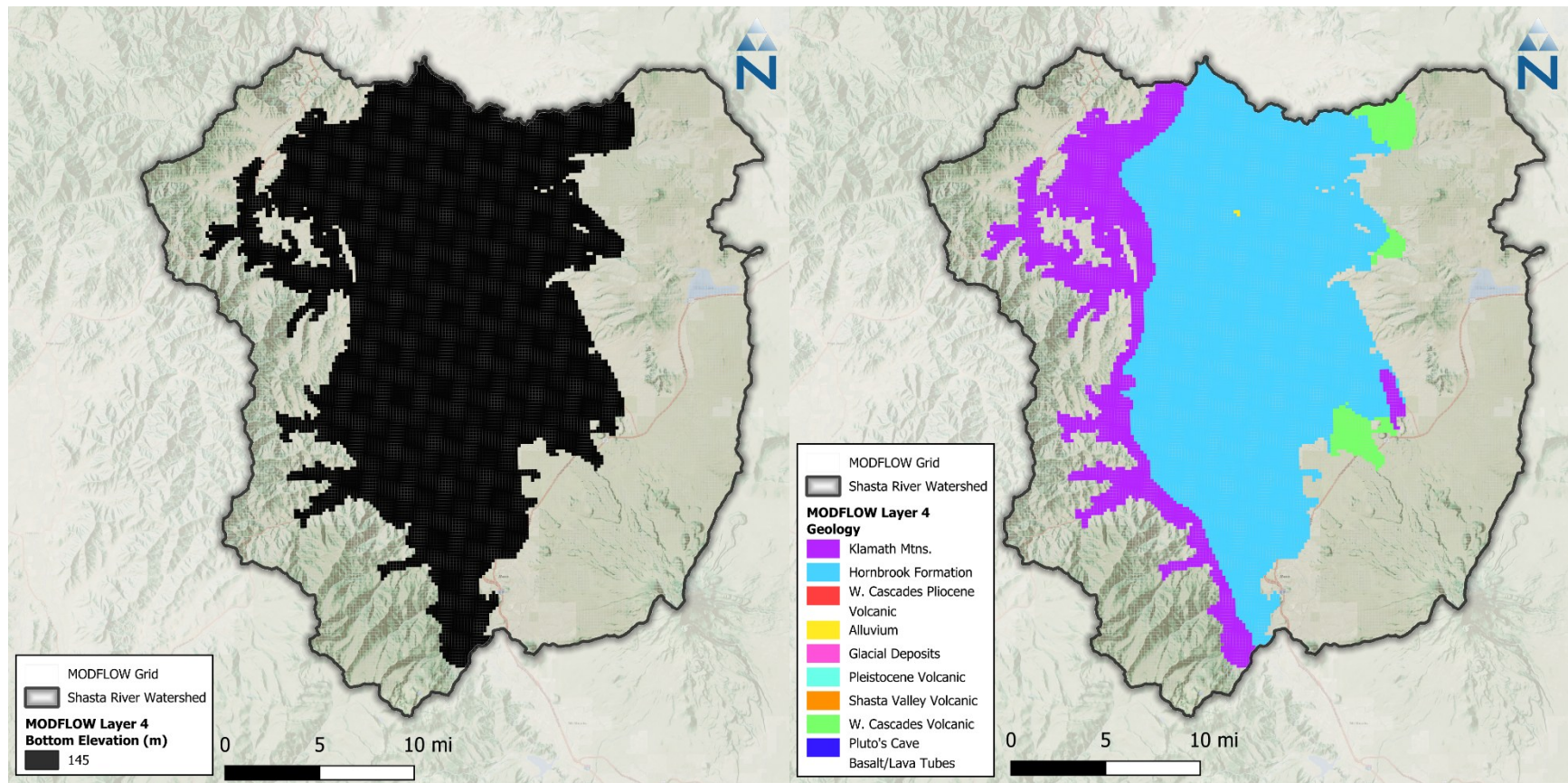


Figure 4-8. Bottom elevation and geological attributes for MODFLOW layer 4 in the Shasta River watershed.

4.4 Recharge

Recharge to the groundwater system was provided by the LSPC surface water model. The GWI term shown in the schematic in Figure 4-2 represents the total volume of water that percolates into the ground. The spatially and temporally varying cell-by-cell monthly volumes of recharge were input into MODFLOW as a recharge (RCH) boundary.

The spatial variability was captured by a combination of land use/land cover, hydrological soil group, slope, and geology (89 HRU types) in addition to the spatial variability of climate (124 unique sets) and orographic influences (elevation, slope) assigned to each of the 261 subcatchments. These combinations created a unique spatially variable recharge value for each groundwater model cell. Furthermore, other site-specific information like applied water for irrigation added even more texture beyond the variability represented by HRU types and meteorological data alone. The same HRU type in different subcatchments with different weather (and different irrigation demand, where applicable) produced very different modeled responses. The HRUs were spatially resampled for each MODFLOW grid cell. For each model cell, the temporal variability of GWI generated by LSPC on a hourly timescale was temporally rolled up as monthly volumes for each MODFLOW grid to match the monthly stress period duration used by the MODFLOW model.

Figure 4-9. shows average annual recharge (GWI) for each MODFLOW grid cell and Figure 4-10 shows the ratio of GWI to PREC for each MODFLOW grid cell. The maps highlight that irrigated areas have ratios up to 2.8, indicating that recharge in those areas is up to 2.8 times average precipitation volume.

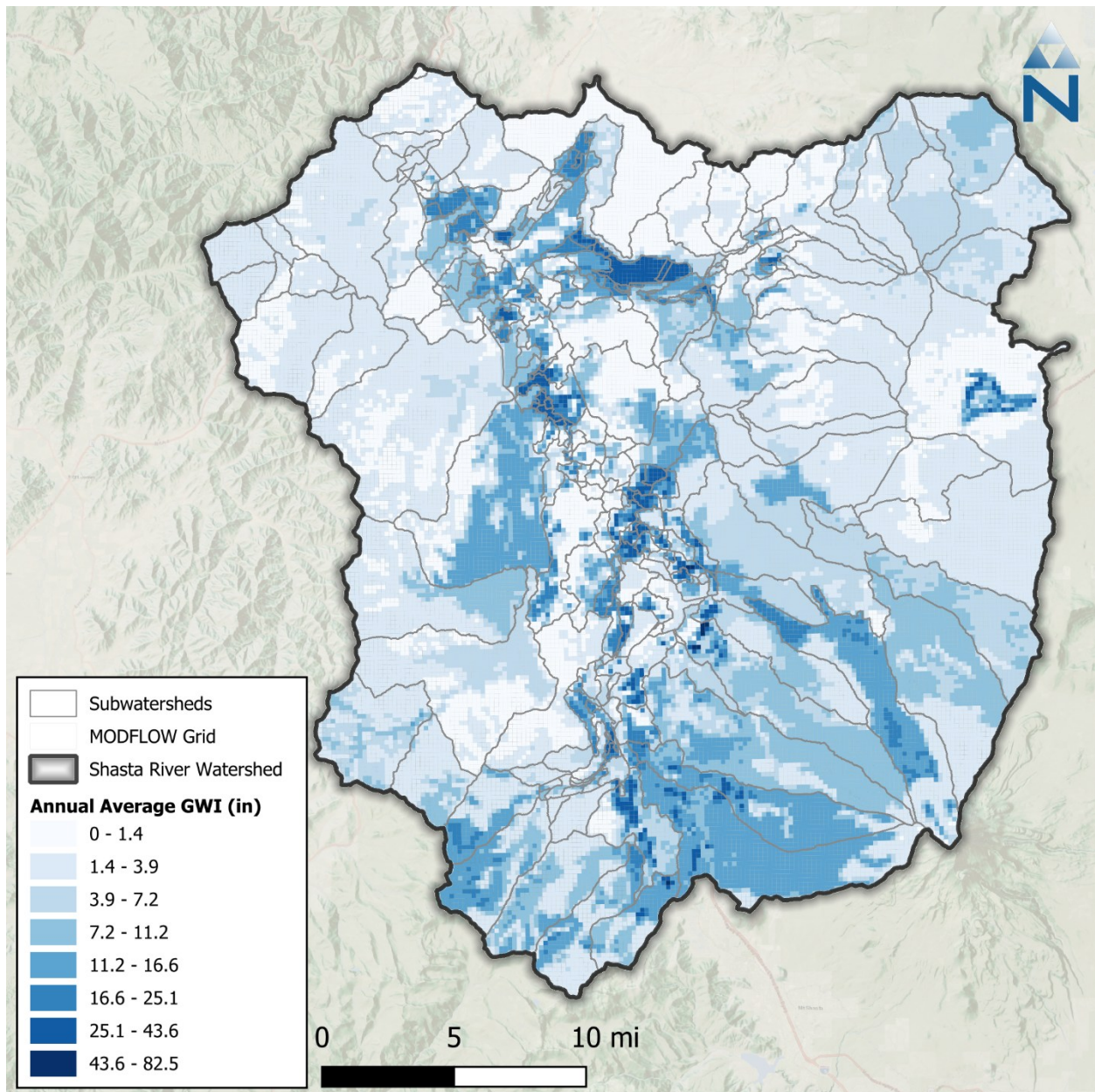


Figure 4-9. Annual average recharge (GWI) sent from LSPC to MODFLOW grids.

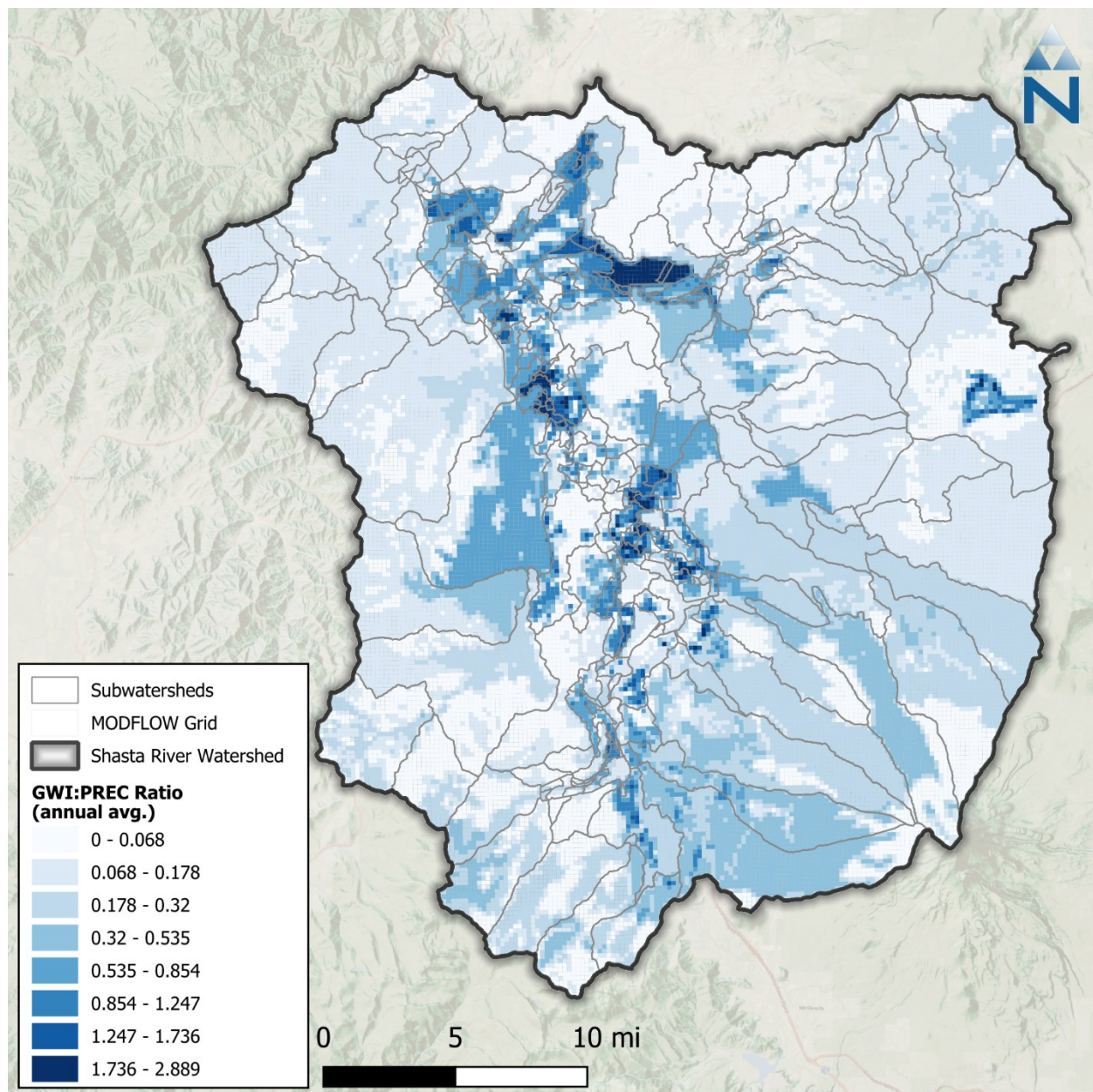


Figure 4-10. Ratio of annual average GWI to PREC for MODFLOW grid cells.

4.5 Lake Shastina

Lake Shastina (also known as the Dwinell Reservoir) was simulated explicitly using the lake (LAK) package of the MODFLOW model. Inflows to the lake included streamflow feeding the lake, groundwater seeping into the lake, precipitation, surface runoff (SURO) and interflow (IFWO) generated by LSPC, and outflows from the lake included lake outflow to Shasta River via reservoir releases, lake leakage from the dam, and environmental releases, seepage to groundwater, lake evaporation, and diversion from the lake. The stream network, discussed in the next section, encompassed Lake Shastina by simulating the lake inflow from the Upper Shasta River (which includes a MWCD diversion from Parks Creek), Carrick Creek, and outflows to the Lower Shasta

River and irrigation diversions from the Lake to the MWCD canal. Lake boundary was defined within the first layer of the MODFLOW model.

Lake level changes and associated volume changes were also calculated in MODFLOW in parallel with LSPC. Lake bathymetry information was provided as the relation between lake stage, volume, and area and was based on Willis and Deas (2009; Figure 12 of the report). Lake precipitation and evaporation were obtained from the LSPC model. Simulated lake volumes were compared to observed lake volumes to assess the performance of the model.

4.6 Streams and Springs

Although surface water flow was handled primarily by LSPC in the integrated model, streams were needed in the groundwater model to account for all the intricate water movement within the integrated system. The purpose of including streams within MODFLOW was to obtain flow occurring between groundwater and streams (AGWO); primarily baseflow and spring flow.

Streams in the groundwater model were represented as a head-dependent flux boundary using the streamflow routing (SFR) package of MODFLOW. The Shasta River and its major tributaries were delineated in the model based on the flowlines in the National Hydrograph Dataset (NHD) within the model domain. The SFR stream network was delineated into 180 segments and 1529 reaches. The segment numbers were subsequently assigned from upstream to downstream. Flow along the stream channels was simulated using Manning's equation, which relates stream depth and stream hydraulic head to flow; a Manning's roughness coefficient of 0.0286 was specified. The streambed elevations were estimated at the midpoint of each stream reach using the 1/3 arc-second (approximately 10m) DEM data. Adjustment has been made to maintain the streambed elevation decrease monotonically downstream and also to ensure that streambed elevations are consistent with the top elevation of the model grid. All streams are connected to the aquifer in Model Layer 1. The stream-aquifer exchange flux is computed in MODFLOW as the product of the difference between stream stages and groundwater levels (or streambed elevation if groundwater levels are below streambed elevation in case of disconnected streams) and the streambed conductance which was adjusted during the model calibration process.

Headwater inflows, surface runoff, and interflow to tributaries and mainstream branches are provided by LSPC through the SURO and IFWO terms. Additional inflows to the stream network include reservoir releases, dam leakage, and environmental flows from Lake Shastina (as discussed in the previous section), as well as instream flows from the Flying L pumping wells (discussed in a later section) that are used for temperature control. Diversions from Parks Creek to the upper Shasta River reroute water within the stream network, acting as an outflow from one stream segment and a corresponding inflow to another. Other outflow terms include stream diversions (represented by the IRWD term in LSPC), riparian evapotranspiration losses (simulated by LSPC), non-irrigation consumptive use (also simulated by LSPC), and terminal outflow from the stream network at the northern model boundary as calculated by MODFLOW.

There are several springs within the modeling domain. Big Springs is one of the most prominent springs in the area for which measured flow rates are available, which were used for model calibration purposes. There are several other springs for which flow estimates are available only at specific times or as estimated averages. These spring flow estimates were not used for calibration purposes but were used to assess the model performance at these spring flow sites; to identify the areas that reproduce estimated spring flows within a reasonable range and the model areas that are deficient in reproducing

stream flows. If spring flows were located close to delineated stream segments in the model, then simulated spring flows were obtained by monitoring stream flow within the stream reach that is representative of the spring located in its proximity. For springs that were located away from stream reaches, a drain (DRN) boundary of MODFLOW was assigned to evaluate the expected stream flow at that location. The drain elevation was set equal to the land surface elevation used in the model. The DRN boundary is a sink boundary and water entering the DRN boundary is not routed within the model. Average simulated flow within the stream or the drain boundaries associated with springs were compared to estimated values.

Flow between the aquifer and the streams was calculated from both the SFR and the DRN boundary in the groundwater model. Those terms represent the *net* upward flux of water from the ground to the surface. The calculated flow represents the active groundwater outflow (AGWO)' term in the LSPC model that was provided to the LSPC model in the feedback loop of the model integration process as shown in Figure 4-2.

To preserve the temporal variability of LSPC, coupling was performed by superimposing the relative difference in simulated AGWO from MODFLOW on the LSPC AGWO timeseries. In other words, the hourly AGWO timeseries from LSPC were scaled and adjusted to match the monthly predicted totals from MODFLOW. The coupling is bidirectional by month over the simulation period—the adjusted values can be either positive or negative from month to month. Although pumping rates in MODFLOW were applied at the same pattern of monthly variable rates each year, predicted AGWO varied more with year-to-year changes in GWI. This methodology conserves the water balance of the integrated surface water – groundwater system (Figure 4-2).

4.7 Shallow Groundwater Discharge

In addition to the major and minor spring flow monitored within the basin, there are other areas where shallow groundwater is discharged to the land surface. Shallow groundwater discharge occurs where groundwater levels rise above the land-surface elevation. These areas are most pronounced in the vicinity of the Little Shasta River, where shallow groundwater conditions and geologic controls on the valley floor give rise to springs, seeps, and small ponds (Mack, 1960). These discharge features are represented in the MODFLOW model and are separate from the major and minor spring flow discussed in the previous section.

This discharge process is simulated using a drain (DRN) boundary imposed at the land surface in the MODFLOW model. The simulated discharge represents a minor component of the overall water budget; however, to fully account for all water in the system, this water is routed to the closest stream within the subcatchment. The average rate of shallow groundwater discharge by MODFLOW grid cell is shown in Figure 4-11. In June of 2025, the Environmental Protection Information Center (EPIC) joined EcoFlight, a non-profit environmental organization on an aerial tour of the Shasta River watershed. Figure 4-12 is an aerial photograph of the Shasta Valley. Surface ponds are visible on the landscape in the vicinity of modeled shallow groundwater discharges shown in Figure 4-11.

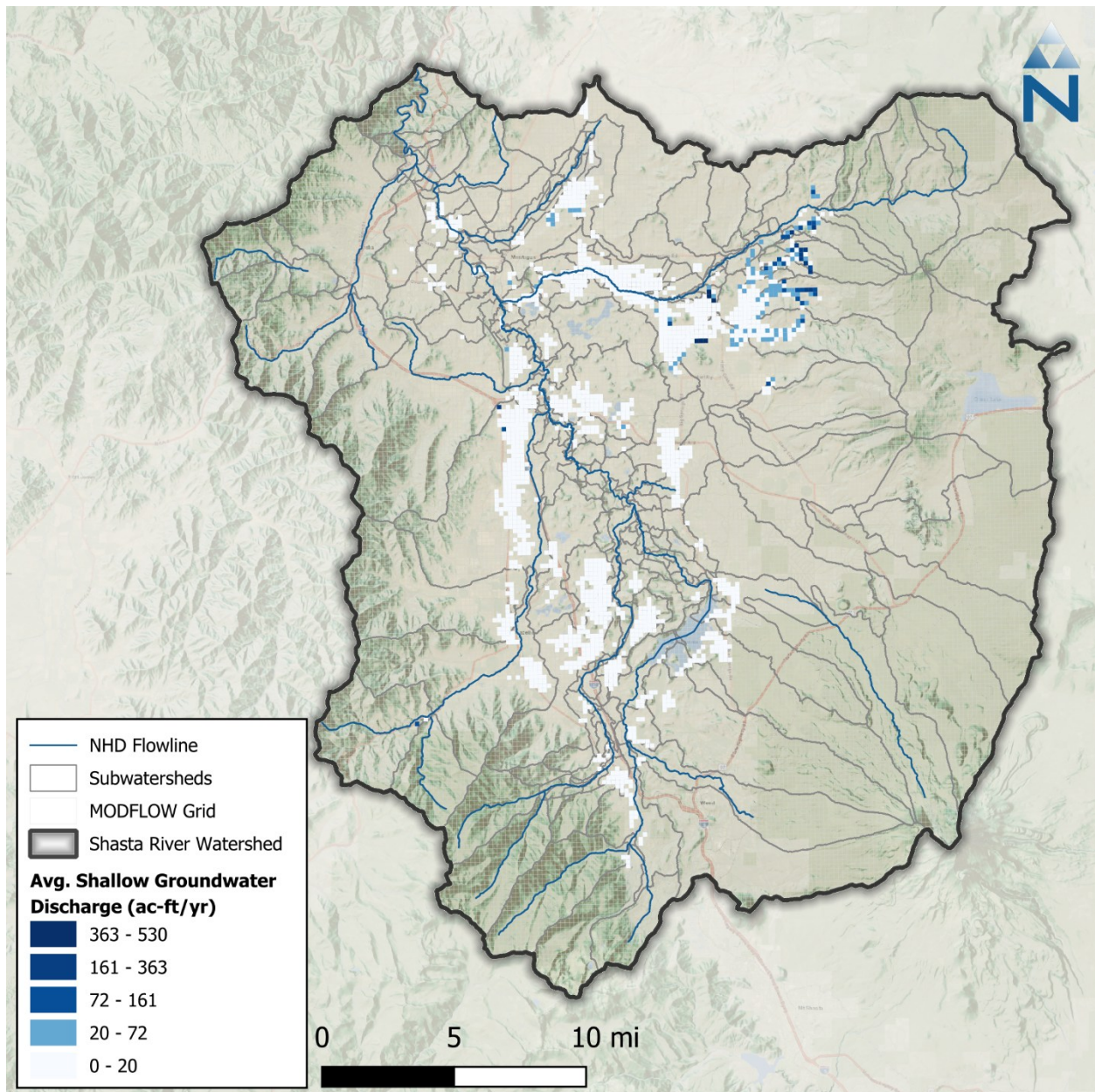


Figure 4-11. Average shallow groundwater discharge per MODFLOW grid cell.



Photo Credit: Environmental Protection Information Center, 2025

<https://www.wildcalifornia.org/post/seeing-the-scott-and-shasta-rivers-from-the-sky-a-tour-with-ecoflight>

Figure 4-12. Shasta Valley surface ponds in the vicinity of modeled shallow groundwater discharges.

4.8 Groundwater Pumping

Groundwater pumping was implemented in the model as a specified flow boundary using the Well (WEL) package of MODFLOW. Groundwater withdrawal estimates were based on agricultural water demands that were satisfied by groundwater supply. In LSPC, irrigation demand from groundwater-sourced areas were assumed to be satisfied from an unlimited water source. The applied irrigation volumes were aggregated as monthly time series by subwatershed for linkage to MODFLOW. Because pumping locations were unknown in some areas, withdrawals were implemented across the entire footprint of the agricultural areas served by groundwater supply. Water demand for these agricultural areas was divided equally among all model cells underlying the agricultural area where exact pumping-well locations were unknown. For known pumping-well locations, withdrawals associated with the service areas were aggregated and assigned to specific well locations. These include the Big Springs Irrigation District (BSID) pumping wells operated by BSID, Pacey wells that serve MWCD irrigation, and the Flying L wells, which are also operated by MWCD for instream benefits.

Three Pacey wells are operated by MWCD (SG005910, SG005911, and SG005438) to augment water supply during dry periods (see Section 5.2.1.1.2. for more details), whereas the Flying L pumps are a set of three groundwater wells (SG005439, SG005440, and SG005441) that pump cold groundwater

near Lake Shastina and convey water through the Flying L pipeline to the Shasta River. This operation is intended to reduce river temperatures and create favorable conditions for species such as coho salmon and other salmonids. The Flying L pumps are capable of delivering up to 5.5 cubic feet per second (cfs) of cold water to the Shasta River (MWCD, 2021). In the absence of detailed pumping records, and given that the pumps are operated during hot periods, Flying L pumping was assumed to occur during July and August at a total rate of 5.5 cfs. The Flying L pumping was represented using a single model cell.

Figure 4-13 and Figure 4-14 shows all pumping locations and associated withdrawals volume and rates.

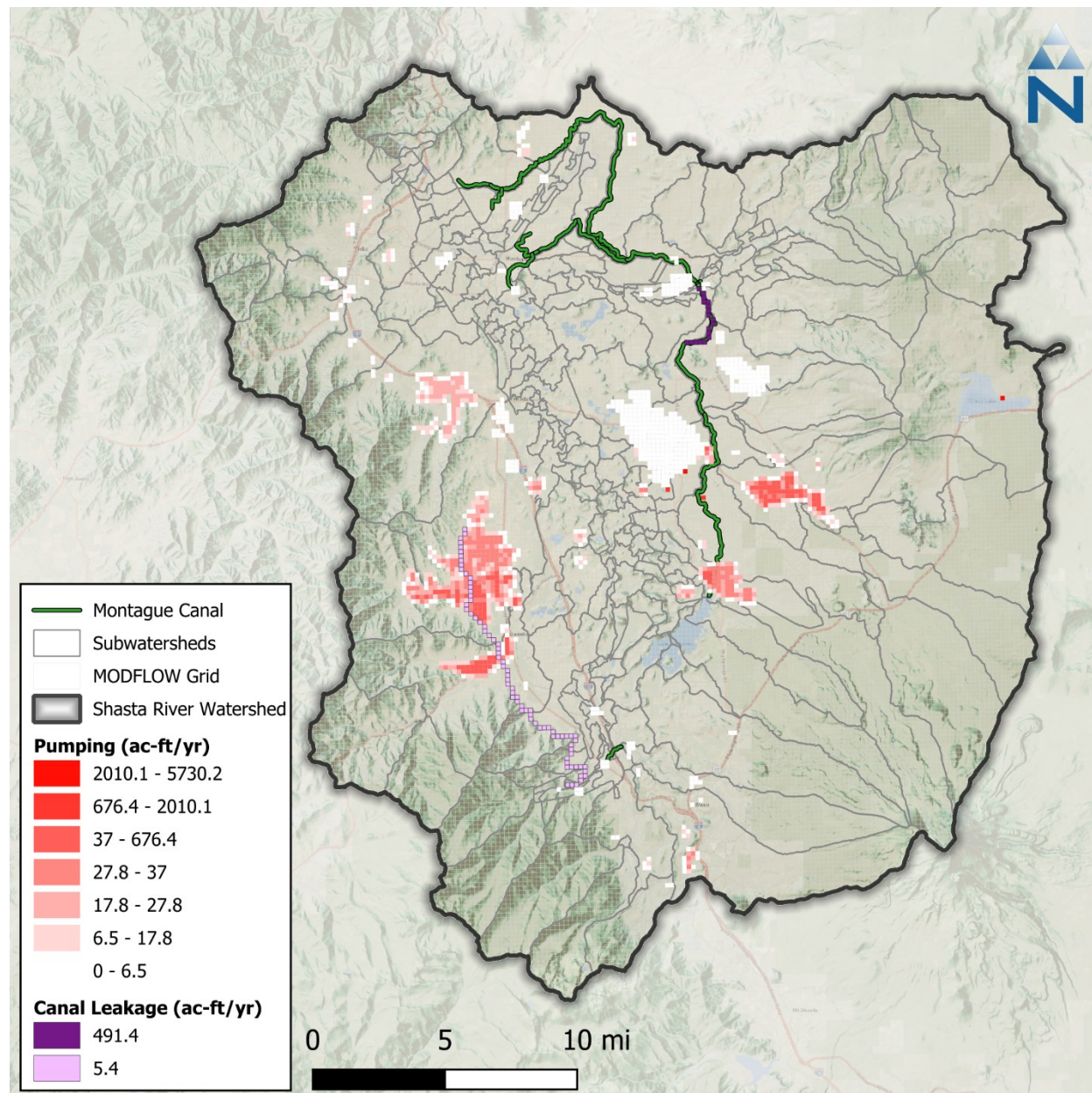


Figure 4-13. Annual average volumes of groundwater pumping and recharge (due to canal leakage) within the Shasta River watershed.

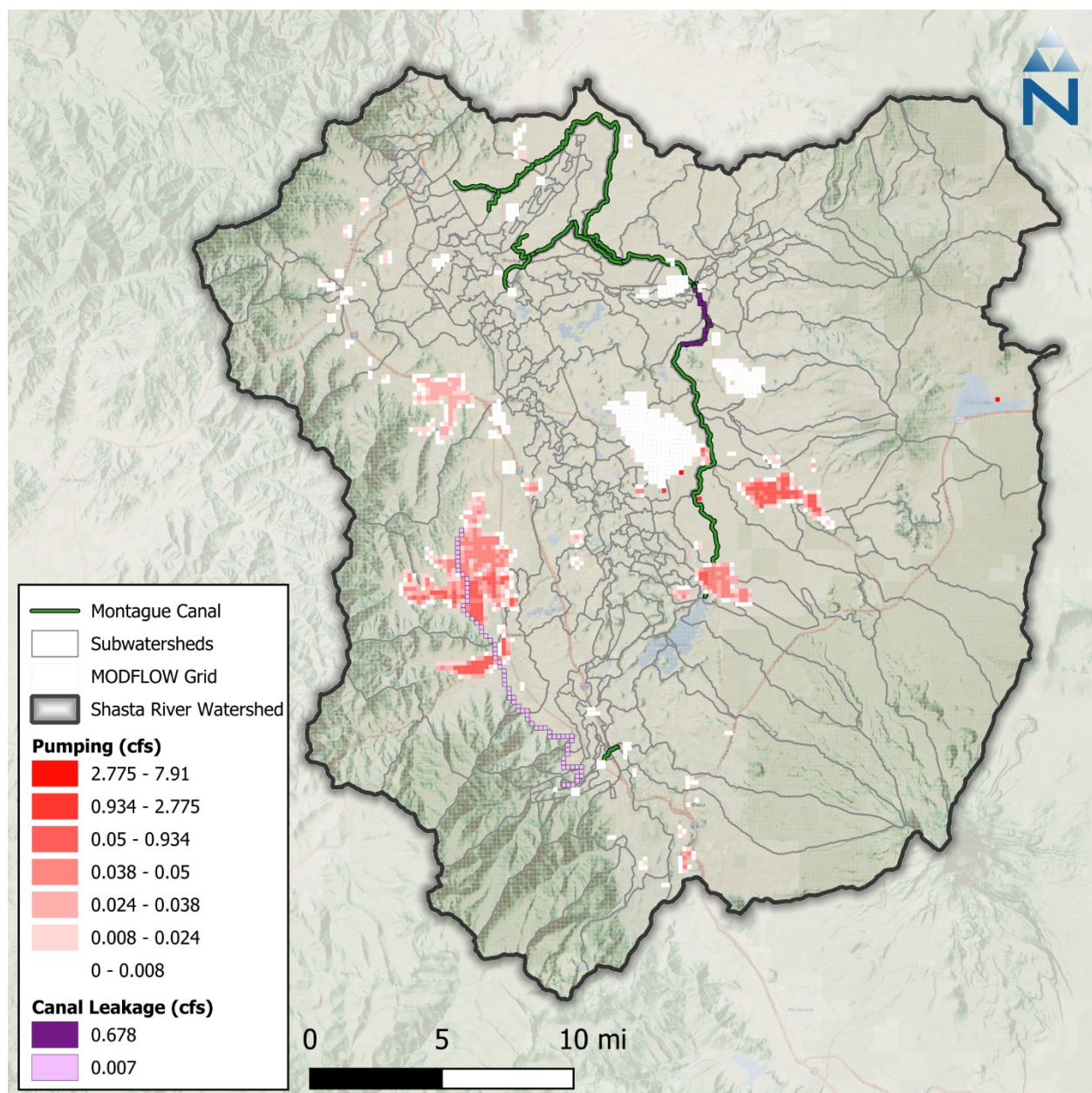


Figure 4-14. Annual average rates of groundwater pumping and recharge due to canal leakage within the Shasta River watershed.

4.9 Canal Leakage

Canal leakage occurs during the conveyance of diverted surface water to irrigated areas. Leakage along canals reduces delivery efficiency but also contributes to localized groundwater recharge along the conveyance route. In general, longer conveyance systems present greater opportunities for leakage to occur. To represent this process in the model, canal leakage was explicitly simulated for the two longest canal systems in the study area: (1) the Edson Foulke Yreka Ditch, which conveys water from

Parks Creek, and (2) the Montague Canal, which diverts water from Lake Shastina (Dwinnell Reservoir).

Leakage from shorter canals was not explicitly simulated because of the relatively short distances between diversion points and irrigated fields, which limit both the magnitude and spatial extent of conveyance losses. For these shorter canals, irrigation application rates were assumed to already incorporate any minor conveyance losses.

For the Edson Foulke Yreka Ditch and the Montague Canal, a leakage rate equal to 25% and 33% of conveyed flow was assumed respectively. Canal leakage was applied spatially along the canal alignments, and the locations where leakage was represented in the model are shown in Figure 4-14.

Canal leakage was implemented in the groundwater model as specified-flux boundaries using the Well (WEL) package of MODFLOW, allowing the leaked water to be introduced directly to the groundwater system as recharge along the canal corridors.

4.10 Additional Boundary Conditions

In addition to Lake Shastina, a second lake (Grass Lake) is explicitly incorporated into the groundwater model, consistent with the conceptualization used in the GSA model. Grass Lake is conceptualized as a surface-water feature that accumulates local runoff and surface flows and provides recharge to the underlying groundwater system through percolation. While this process is represented in the model to maintain consistency with the conceptual hydrogeologic framework, the contribution of Grass Lake to the overall basin water budget is negligible. Accordingly, Grass Lake is not reported as a separate water-budget component in the same manner as Lake Shastina.

To account for potential groundwater underflow exiting the basin at its northern extent beneath the Shasta River, a head-dependent flux boundary was implemented using the General-Head Boundary (GHB) package in MODFLOW. This boundary allows groundwater to flow out of the modeled domain in response to simulated hydraulic gradients and provides a mechanism to represent possible subsurface discharge beyond the model boundary. Although this boundary condition is included to ensure conceptual and numerical completeness of the model, its contribution to the basin-wide groundwater budget is negligible.

5 MODEL APPROACH & PERFORMANCE

5.1 Model Approach

The modeling approach is designed to follow internationally recognized modeling protocols and conventions. For example, the EPA guidance for Quality Assurance Project Plans (QAPP) for modeling refers to calibration as the configuration and refinement of the analytical instruments that will be used to generate analytical data (EPA, 2002). The “instrument” is the predictive tool (i.e., the model) that is to be developed and/or applied. Figure 5-1 is a schematic describing a process for model calibration that aims to minimize the propagation of uncertainty. Through development of the Model Study Plan, the analysis of weather data was initiated and discussed in Section 3. The discussion below includes details on calibrating snow depths as well as surface and ground water hydrology. Figure 5-1 provides a conceptual model of the calibration sequence.

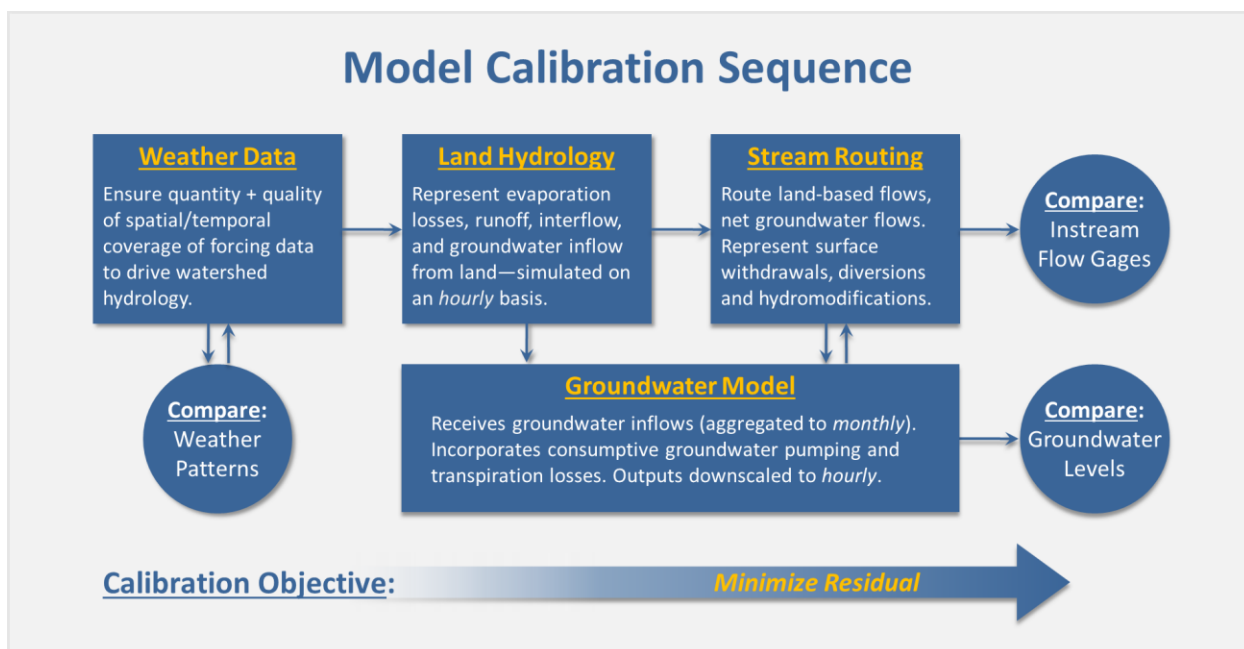


Figure 5-1. Process for model calibration to minimize propagation of uncertainty.

After weather data and meteorological boundary conditions were well established, a top-down weight of evidence approach to calibration progressed as follows:

1. Use the Parameter Estimation tool (PEST) to calibrate LSPC surface flow with an objective of reducing the difference between observed and predicted flows as much as possible. This calibration accounts for surface water consumptive use estimates.
2. Couple LSPC and MODFLOW using LSPC groundwater inflow (GWI) output as MODFLOW input (Figure 4-1)
3. In MODFLOW, further adjust aquifer configuration/parameters and add groundwater pumping consumptive use estimates to improve agreement between predicted groundwater outflow (AGWO) and observed baseflows/spring flows
4. Link MODFLOW back to LSPC by creating point source timeseries to represent the required additions or depletions to adjust the LSPC-predicted AGWO to match MODFLOW.
5. If needed, further adjust LSPC in-stream gains or losses (e.g., riparian evapotranspiration) and further investigate the influence of various pumping and diversion scenarios on coupled model results to improve prediction, repeat steps (2) through (4) as necessary. This iterative calibration process guides all components of the integrated hydrologic system to collectively work towards an integrated water budget by providing constraints on parameters and boundary conditions on the land use, surface water, and groundwater regimes.

5.2 Additional Model Configuration

5.2.1 Consumptive Use Assumptions

The consumptive use of water within the Shasta River watershed includes two main components: irrigation use (i.e., agricultural) and non-irrigation use. This section summarizes the assumptions and estimates for both types of consumptive use.

5.2.1.1 Irrigation Water

The spatial and temporal distribution of irrigation water volume was estimated based on modeled crop demand estimates compiled by SEI, which were derived from greenness surveys conducted by Davids Engineering (Davids Engineering, 2020). Those data represented ET over the irrigated areas shown in Figure 5-4. Areas with recycled and mixed surface water/groundwater only represented 0.76% and 0.47% of total irrigated area, respectively, and were reclassified as either surface water or groundwater source areas. After reclassification, surface-water-irrigated area represented about 83% of total irrigated area and total estimated irrigation demand volume. Groundwater-irrigated area makes up the remaining 17% of irrigated area and total irrigation demand volume.

Irrigation demand follows seasonal agricultural cycles where the warmer/drier summer growing months have greater ET demand, and therefore more water consumption, while the winter months have less. The estimated monthly average surface water withdrawals and groundwater pumping volumes are shown in Figure 5-2. These trends are further stratified by examining the distribution of irrigation across both groundwater and surface-water-sourced land for both crop and pasture HRUs (Figure 5-3).

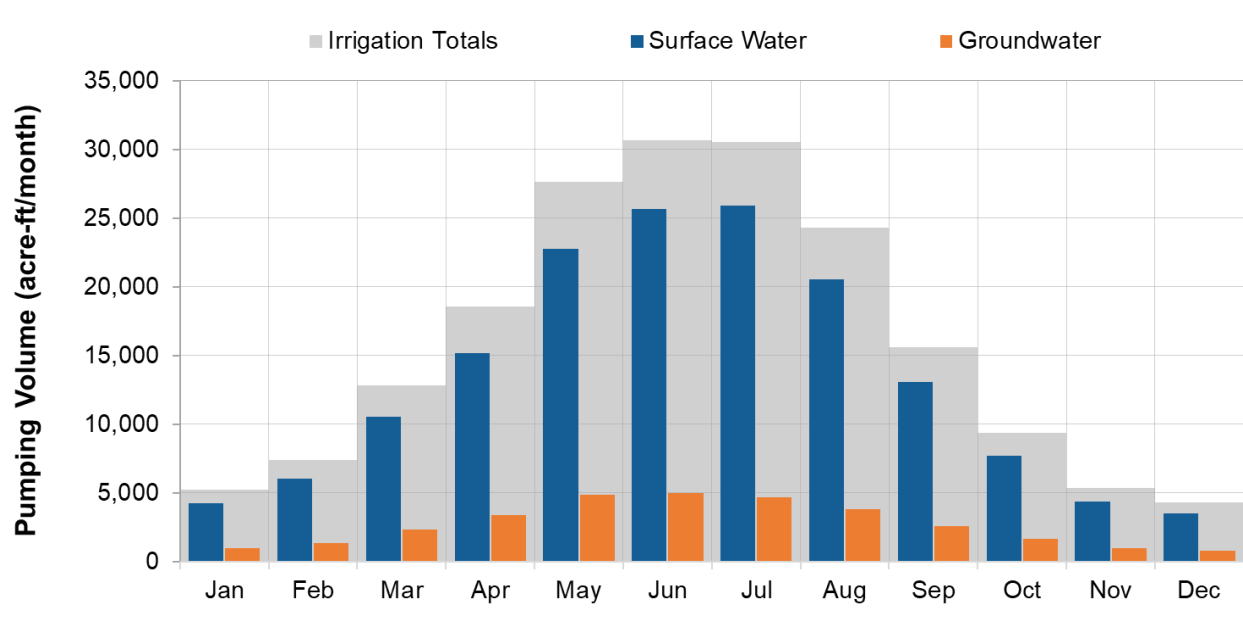


Figure 5-2. Monthly average surface water, groundwater, and total volumes pumped for irrigation within the Shasta River watershed.

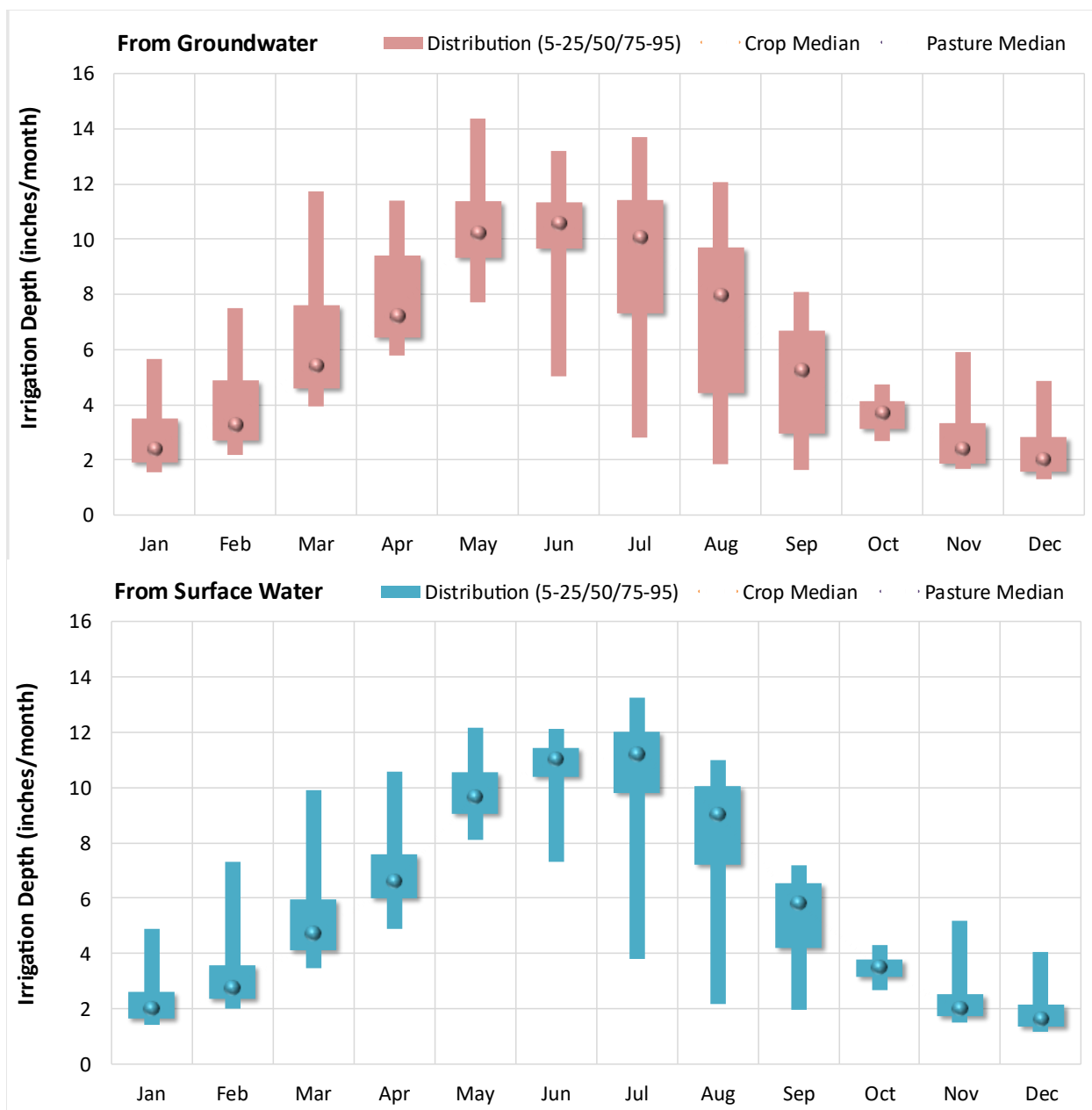


Figure 5-3. Monthly groundwater (top) and surface water (bottom) irrigation depth distributions, with crop and pasture medians, across irrigated subwatersheds.

In LSPC irrigation demand is calculated as a function of the potential ET boundary conditions associated with the subwatershed. Two sets of twelve-monthly ET coefficients were applied for irrigated HRUs in the model to scale potential ET to match the irrigation demand. Those two sets of coefficients were derived for both groundwater and surface-water sourced HRUs as the average ratio of irrigated demand to the average observed potential evapotranspiration timeseries.

Within LSPC, irrigation water is applied using an even 50-50% split between sprinkler and flood type irrigation. Sprinkler irrigation water, which conceptually behaves like precipitation, is applied over the vegetation canopy and is therefore subject to interception storage and additional evaporation. Flood irrigation, which is applied directly to the soil surface below vegetation canopy, is only subject

to surface ponding. Irrigation water, like rainfall and snowmelt, is subject to the same processes downstream of their points of application, and exit the surface layer through ET, surface runoff, and groundwater recharge via infiltration.

Return flows are calculated through the model's hydrologic processes rather than being prescribed as a fixed percentage. Because irrigation water is applied in addition to natural precipitation, it enters the simulated hydrologic cycle for each irrigated HRU in the same way as precipitation and is subject to the same interception, storage/ponding, and surface/subsurface transport processes. Therefore, for a given HRU, irrigation return flows represent the change in surface, interflow, and groundwater outflow relative to the non-irrigated HRU counterpart. Achieving a representative balance between these pathways for return flows becomes especially important when simulating temperature because surface water temperature will generally be higher than baseflow.

5.2.1.1.1 Irrigation Districts Representation

Within the Shasta River watershed, there are five main irrigation districts (i.e., Big Springs, Grenada, Huesman, Montague, and the Shasta Water Association), as well as other major water rights holders such as those within the Edson Foulke-Yreka Ditch service area. Each irrigation district operates canals and ditches to deliver water to its point of use (Figure 5-4). The mapped districts move the most water the farthest; other irrigated land are assumed to source their water from the respective stream segment associated with the subwatershed. Observed data at two long-term USGS streamflow gages on the Shasta River mainstem, located at Montague and Yreka, provide a measure of impact of consumptive use diversions and return flows, respectively. All the major diversions occur just upstream of the Montague gage. The Yreka gage at the outlet of the watershed is downstream of all places of use and is reflective of (1) natural hydrology and (2) surface withdrawals and diversions, (3) groundwater pumping, (4) irrigation and non-irrigation consumptive uses, and (5) all return flows to streams in the Shasta River watershed. Figure 5-5 is a schematic of major water features and consumptive uses represented in the model. All other withdrawals, diversions, and return flows occur at the place of use. The five major irrigation districts are described below:

- ▼ The Big Springs irrigation canals are serviced by groundwater pumps located south of the district boundary. Several major water right holders also withdraw surface water from nearby Big Springs Lake. The remaining mapped irrigation districts primarily use surface water.
- ▼ The Montague Water Conservation District (MWCD) operates one of the longest canal networks, which routes water from Parks Creek to Lake Shastina in the central portion of the watershed, and from the Lake to irrigation fields in the Little Shasta drainage area to the north.
- ▼ The Shasta Water Association, Huesman, and Granada Districts divert water from the mainstem Shasta River upstream of the Montague streamflow gage and transport that water through their respective irrigation canal networks to the places of use to the north and west of the point of diversion. Return flows from much of that area ultimately drain to points downstream of both the point of diversion and the Montague gage. During model development, adding those diversion points improved flow predictions at the Montague gage by reducing streamflow.

In the LSPC model, surface water diversions are sourced from the reach that corresponds to the point of diversion for the respective irrigation district canal, e.g., from Lake Shastina for the MWCD service area. Diverted water is applied to irrigated surface water HRUs within those subwatersheds and exits as return flows to the closest stream, groundwater recharge, or evapotranspiration. Water movement through the canals is not explicitly modeled in LSPC. Instead, surface water diversions for irrigation are sourced from the reach that corresponds to the point of diversion. The Figure 5-5 maps the MWCD

infrastructure, which includes a diversion channel from Parks Creek to Lake Shastina and the Montague Canal, which send water from Lake Shastina to the MWCD irrigation service areas to the north. Figure 5-6 shows the mapped location and Google Street View image of the MWCD Parks Creek diversion channel from I-5.

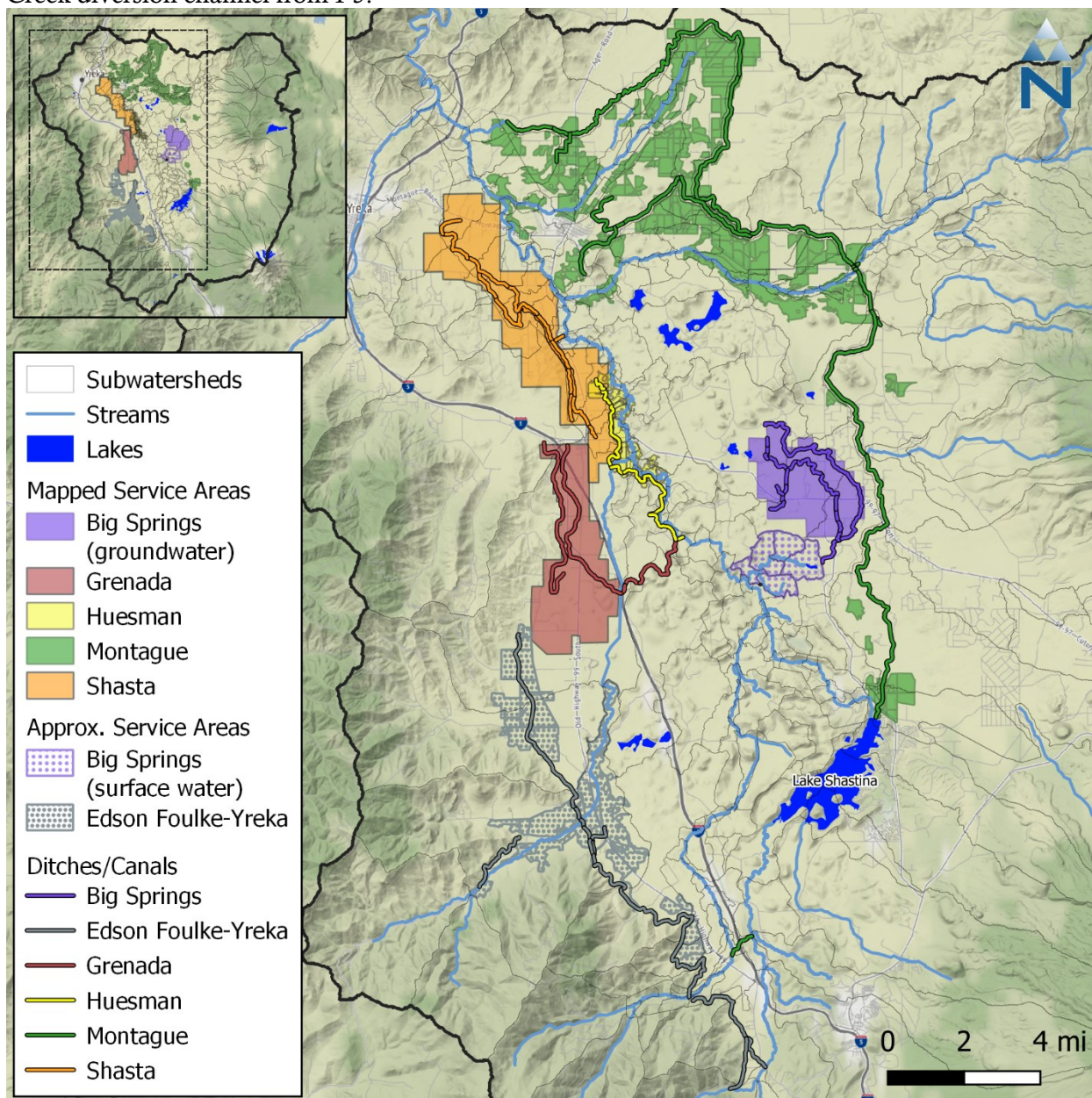


Figure 5-4. Irrigation districts, service areas, canals, and ditches within the Shasta River watershed.

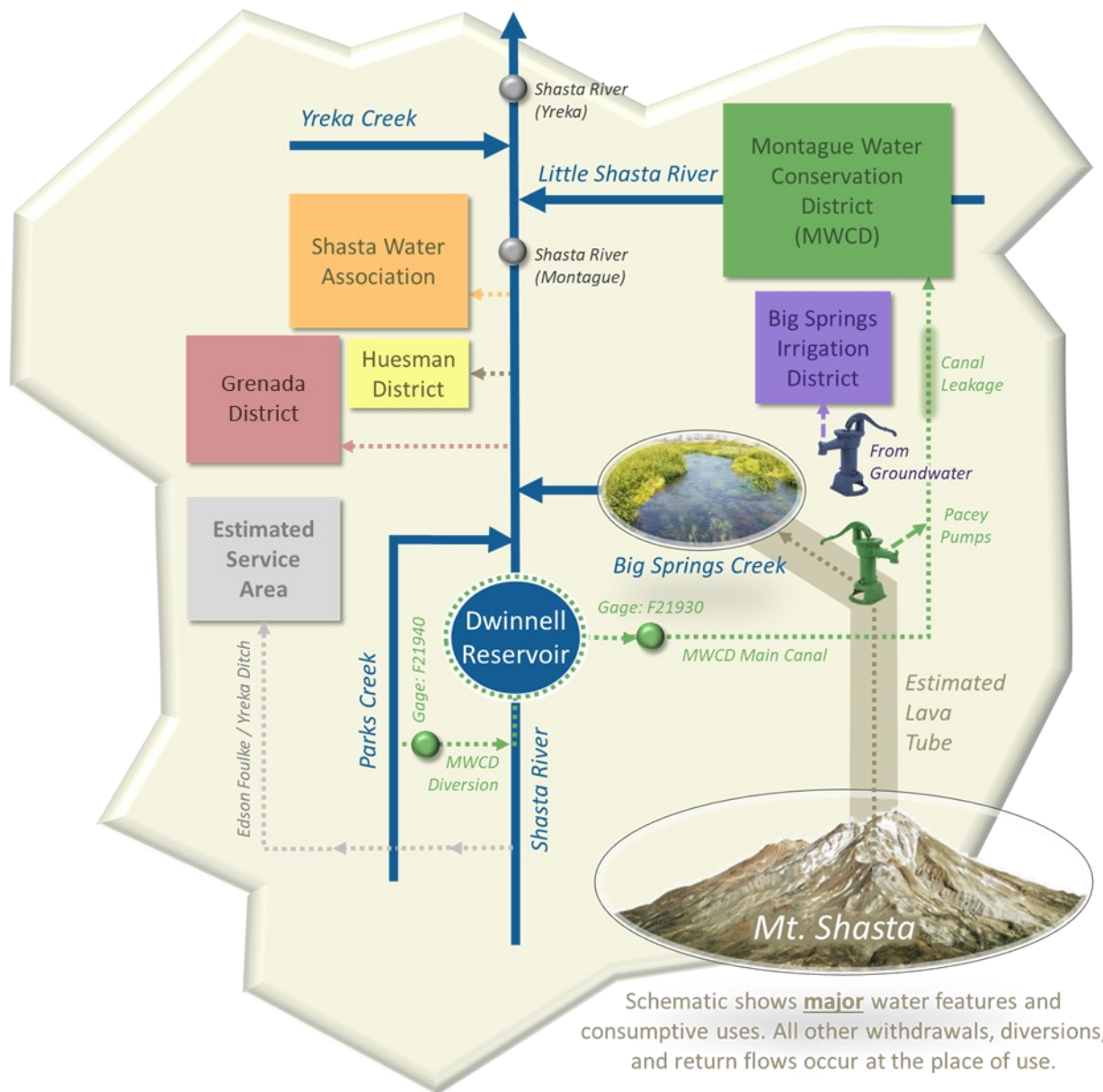


Figure 5-5. Schematic of major water features and consumptive uses in the Shasta River watershed.

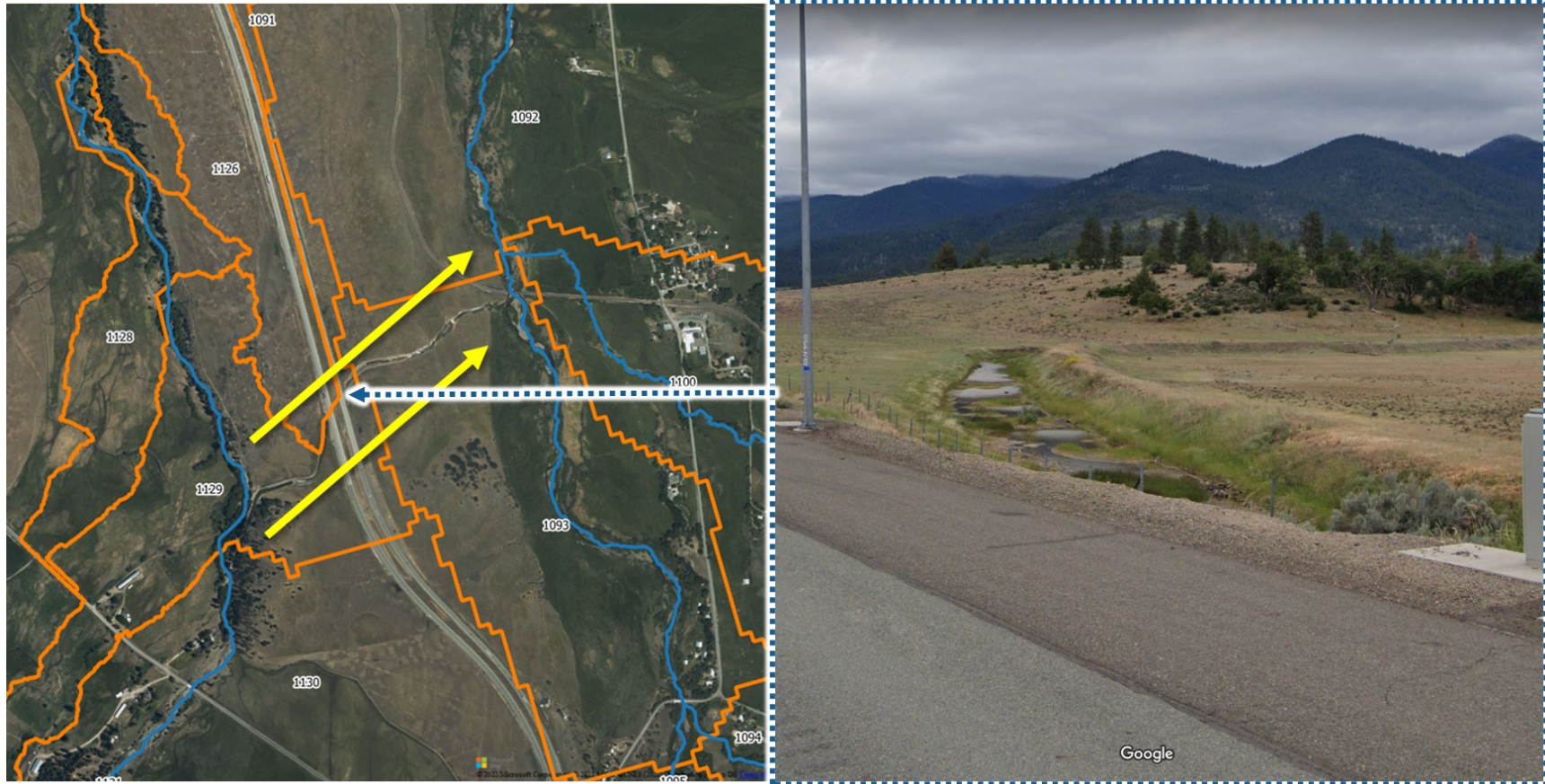


Figure 5-6. MWCD Parks Creek diversion channel.

According to the MWCD Site Plan Agreement (MWCD, 2020), the diversion from Parks Creek to storage in the Dwinnell Reservoir has three general conditions:

1. Water can be diverted only between 10/1 and 6/15
2. From 10/1 to 2/28, instream flow in Parks Creek below the diversion should be ≥ 6 cfs
3. From 3/1 to 9/30, instream flow in Parks Creek below the diversion should be ≥ 16 cfs

This diversion was represented in the model as a point withdrawal from segment 1130 to segment 1093, which flows down to the Dwinnell Reservoir. Those conditions of the permit were applied directly to the modeled flow to represent the diversion from Parks Creek to Dwinnell Reservoir. Observed data in the Parks Creek Diversion Channel (F21940) were available between 12/15/2004 and 10/1/2017 for comparison against the estimated diversion volumes. The rules above were applied to the modeled flow in Parks Creek at the point of diversion to estimate a diversion timeseries, which are labeled as “Rules” in Figure 5-7. Because the actual diversion is human operated; it will not exactly follow the timeseries generated by applying the rules. Furthermore, because the model generally underpredicts flow in Parks Creek; using the observed timeseries in the diversion canal risks diverting the entire flow from Parks Creek. For this reason, the minimum flow requirements of the permit were used to calculate the diversion as a function of modeled flow upstream of the point of diversion. Future model refinements should consider revisiting snow and water balance predictions in Parks Creek.

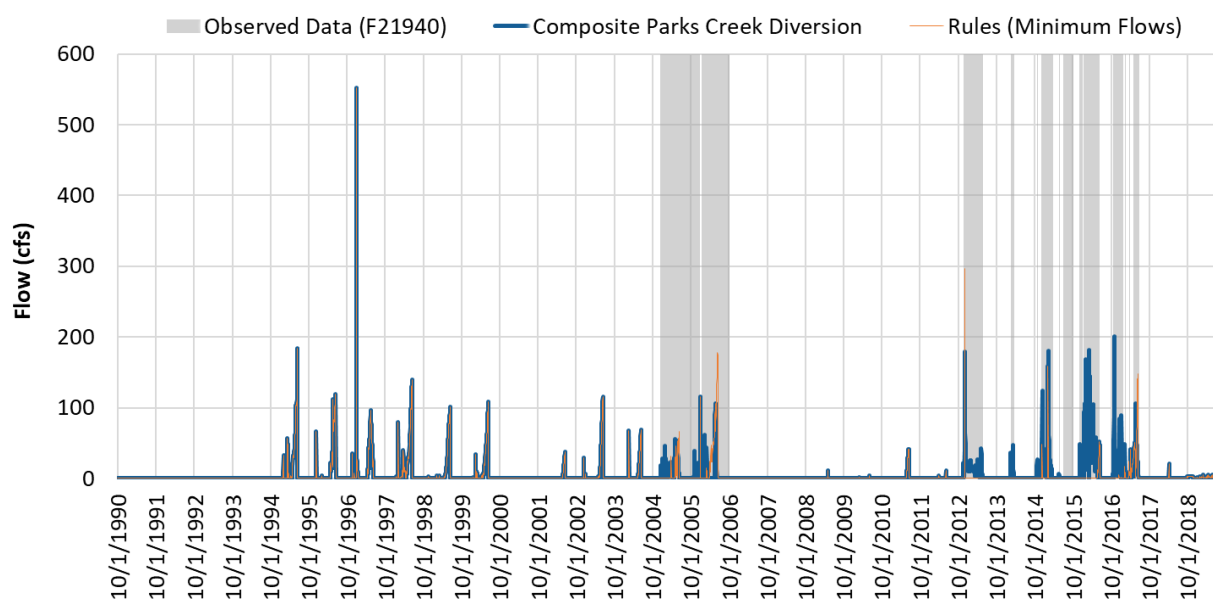


Figure 5-7. Validation of flow and diversion volumes in the MWCD Parks Creek diversion channel.

Another feature of the MWCD infrastructure is the diversion to the Main Canal from the Dwinell Reservoir. Observed flow data in the MWCD Main Canal (F21930) was available between November 15, 2012 through the end of the MODFLOW calibration period, September 30, 2018. Diverted water from Dwinell Dam was estimated from the irrigation demand of the MWCD service area of the Canal—this ensured a dynamic linkage between modeled irrigation activity and the withdrawal from the Reservoir. A study of conveyance efficiency of the MWCD Main Canal suggests that 33% of the flow is lost between the top of the canal at Dwinnell Dam and the end of the Main Canal at the B/C canal split (Willis & Deas, 2010). The study further noted that the highest losses primarily occur at two locations: (1) the partially lined reach from Louie Rd. to Pacey pump #3 (18.5%) and (2) the reach between the north side of Rabbit Hill and the Little Shasta River (15.6%). In addition to MWCD canal

leakage, Edson-Foulke Yreka Ditch canal also reported to lose 25% of flow as canal leakage and thus both canal leakages were dynamically simulated in LSPC as function of amount of surface water withdrawn for irrigation from the areas served by these two canals.



Figure 5-8. Montague Canal and nearby irrigated fields.

As currently configured, Irrigation demand in LSPC is expressed as a function of the potential ET boundary condition. During early model calibration, before irrigation withdrawals were applied in the model, the severe drought period in water years 2014-2015 consistently showed closer agreement at the Montague Gage (Figure 5-9). Drought restrictions during that period most likely minimized the volume of water being diverted for irrigation by all Districts, making it possible for a model without those activities to reasonably predict flow at the Montague Gage. The current configuration does not allow a user to “turn off” irrigation demand only for specific years because the footprint of irrigated area is static over the whole simulation. Future model refinements should consider increasing model flexibility to represent variation in water management for irrigation.

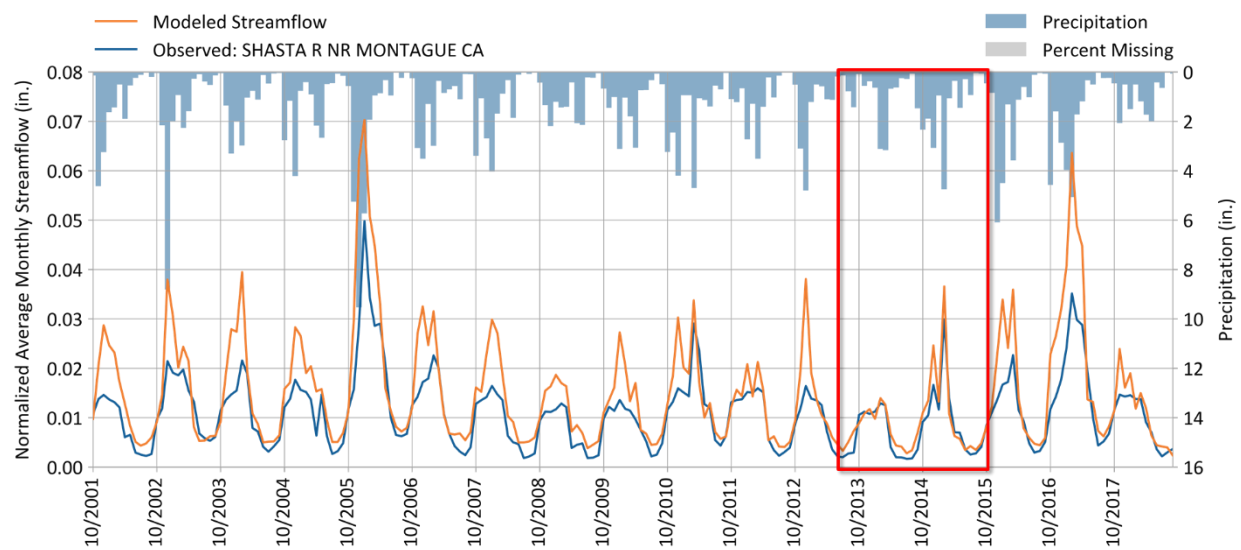


Figure 5-9. Early model calibration comparison, prior to MODFLOW and consumptive uses (irrigation withdrawals, groundwater pumping, and diversions), showed close agreement at the Montague Gage during the 2014-2015 drought period.

5.2.1.1.2 Pacey Pumps

Pacey Pumps are documented to supply irrigation water downstream of the Dwinnell reservoir; however, the exact volume they supply was not available as input to the model. Pacey Pumps are occasionally used to offset deficits in surface water irrigation demands for MWCD. The following operational guidelines were applied in the modeling and estimation of Pacey Pumps' contributions:

1. Pacey Pumps are not operated during wet water years.
2. The maximum allowable pumping rate is limited to 30 cubic feet per second (cfs).
3. In dry water years, pacey pumps are operated up to the maximum rate to offset irrigation deficit as needed. During normal years, they are assumed to provide up to half of the deficit, always adhering to the 30 cfs maximum rate. If, in any given instance, the irrigation deficit exceeds what can be delivered at this maximum rate, the pumping volume is capped at 30 cfs.

The irrigation deficit was determined by subtracting the actual surface irrigation withdrawals from the maximum potential irrigation applied to MWCD during the same period. Based on the guidelines above, a monthly pumping rate time series was developed by categorizing water years as dry, normal, or wet, using annual precipitation data. Figure 5-10 shows the resulting estimated Pacey Pumping volumes alongside irrigation demand and surface water diversion volumes. As expected, results show that Pacey Pumps contributed higher pumping volumes during dry years compared to normal years. On average, for the period from water years 1991 to 2023, Pacey Pumps supplied approximately 5,948 acre-feet per year (ac-ft/year) during dry years, and 413 ac-ft/year during normal years.

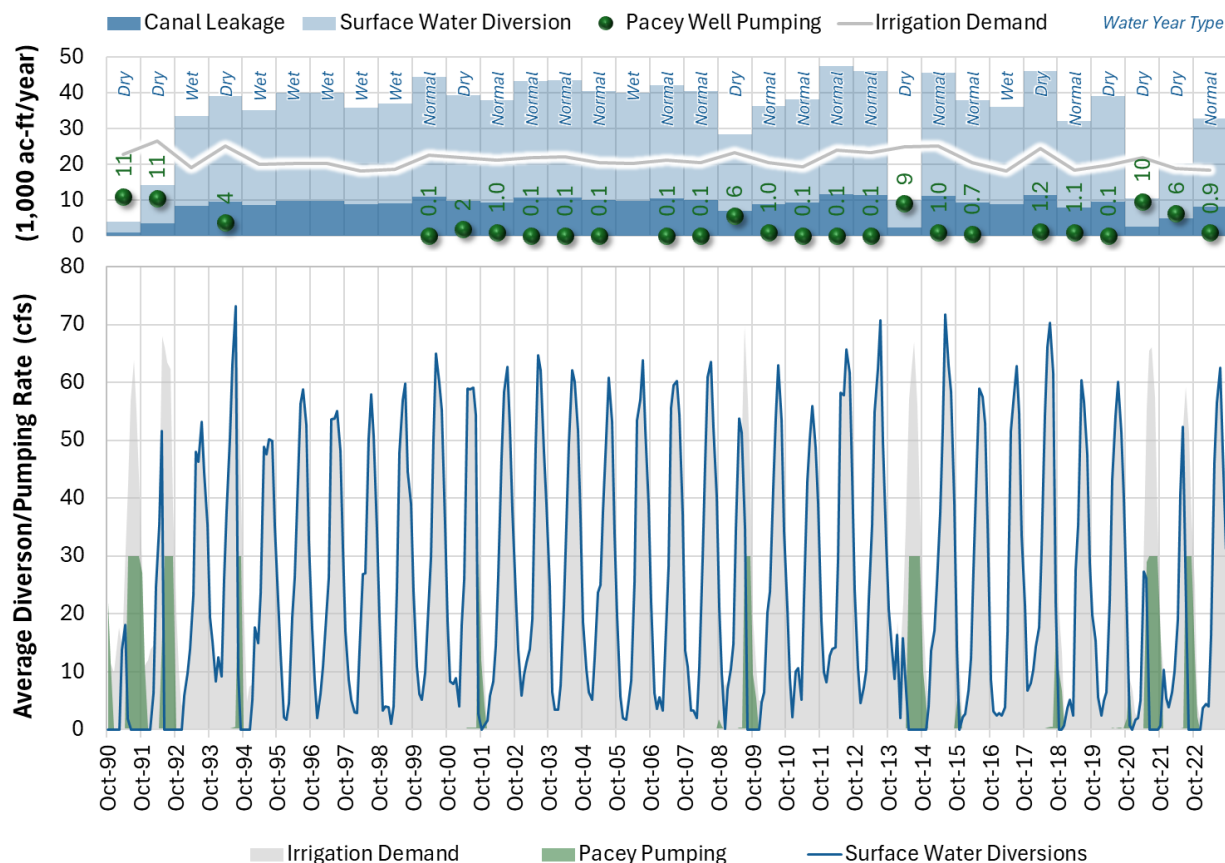


Figure 5-10. Pacey pumping and canal leakage losses within Shasta River watershed.

5.2.1.1.3 Irrigated HRU Area Adjustment

To match irrigation rates within LSPC with the minimum irrigation withdrawal volumes (SEI ET data) the footprint of irrigated and non-irrigated Crop and Pasture HRUs within each subwatershed had to be adjusted. Because the LSPC irrigation module assigns one representative irrigation distribution/profile per HRU, the footprint of irrigated land can be adjusted to match the volume of irrigation water required for each subwatershed.

The first step in the irrigated area adjustment process was an examination of the irrigation rate by water source type and area (Figure 5-11). Then, using the 97th percentile, which corresponds to a maximum irrigation rate of $69.38 \text{ in} \cdot \text{ac}^{-1} \cdot \text{yr}^{-1}$ (Figure 5-11), as an upper bound, the surface water and groundwater irrigated areas within each watershed are adjusted such that their maximum rate equals $69.38 \text{ in} \cdot \text{ac}^{-1} \cdot \text{yr}^{-1}$. The total crop or pasture HRU area within each subwatershed is preserved during this process because area is simply shifted between the irrigated and non-irrigated HRU counterparts of surface-water or groundwater-sourced irrigation HRUs.

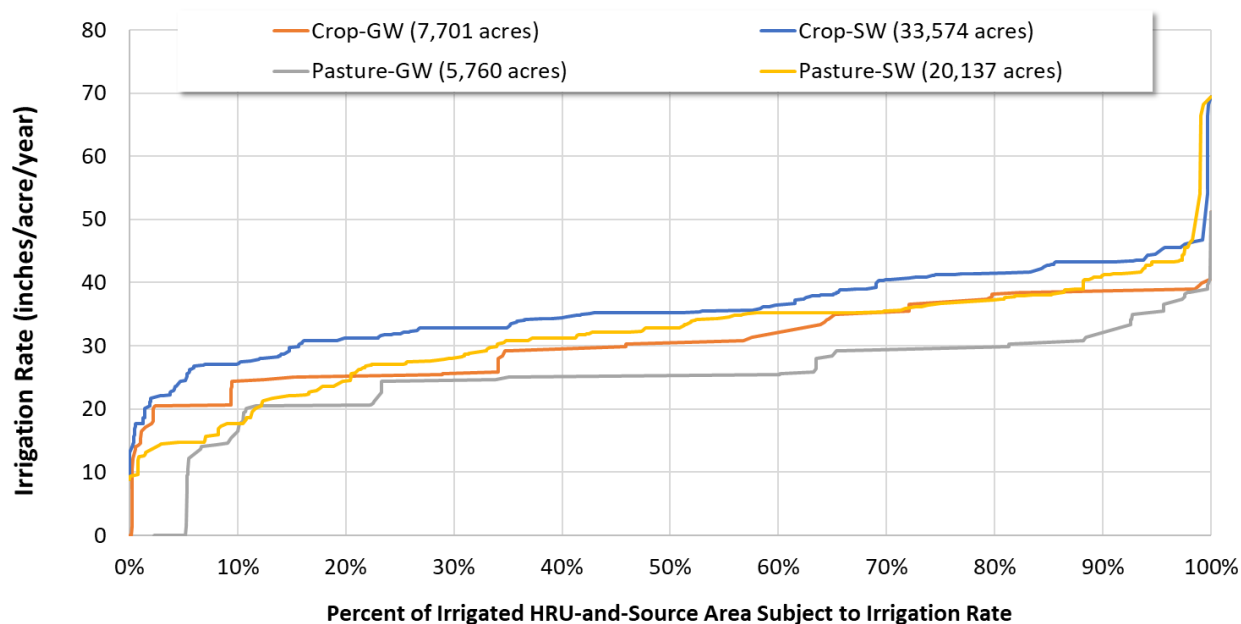


Figure 5-11. Percent of irrigated HRU area subject to an irrigation rate by water source type. The unadjusted Crop and Pasture irrigated areas are shown in the legend.

5.2.1.2 Non-Irrigation Water Use

For non-irrigation demands, observed and permitted surface water diversions were summarized from the Electronic Water Rights Information Management System (eWRIMS) and expressed as average monthly diversion totals. SEI provided estimates of withdrawals and return flows from all surface water consumptive use at the subwatershed level. Figure 5-12 is a summary of diversion, consumption and returns aggregated over the entire Shasta watershed. Consumption estimates ranged from 10-80% of diversions; returns were calculated as diversions minus consumption.

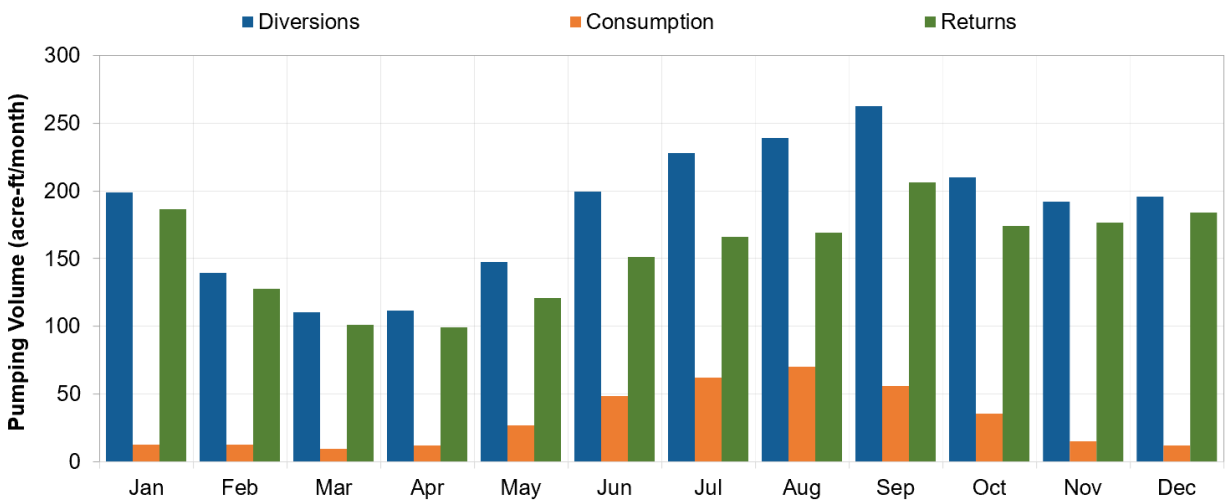


Figure 5-12. Summary of non-irrigation surface water diversions used in the LSPC model.

5.2.2 Riparian Evapotranspiration

Evapotranspiration (ET) represents various processes and pathways by which water leaves the surface water and groundwater systems to the atmosphere. Most of the evapotranspiration processes (i.e., evaporation and partially transpiration) are accounted for by the LSPC model. Riparian ET losses were estimated during calibration to account for the losses that occur from the shallow soil and primarily the transpiration that occurs within the root zone along the riparian corridor.

The estimation of riparian evapotranspiration (ET) within the LSPC model is based on a combination of potential evapotranspiration and the vegetation cover present along riparian corridors. Due to the significant variability in vegetation within the stream corridor across the watershed, a tailored approach is applied for each stream segment. Specifically, the total riparian ET for each modeled stream segment is determined in proportion to the percent canopy found within a 5-meter radial buffer surrounding that segment (Figure 5-13). This method ensures that the effects of local vegetation density are reflected in the riparian ET estimates. In addition, monthly adjustment factors are calibrated to ensure that the riparian ET matches the area-proportioned actual evapotranspiration reported from forest HRUs. Figure 5-14 shows the distribution of monthly Forest TAET for all modeled subwatersheds, which was used to model riparian ET within the associated stream corridor. This calibration process further refines the model, enhancing its accuracy in representing evapotranspiration dynamics along riparian zones.

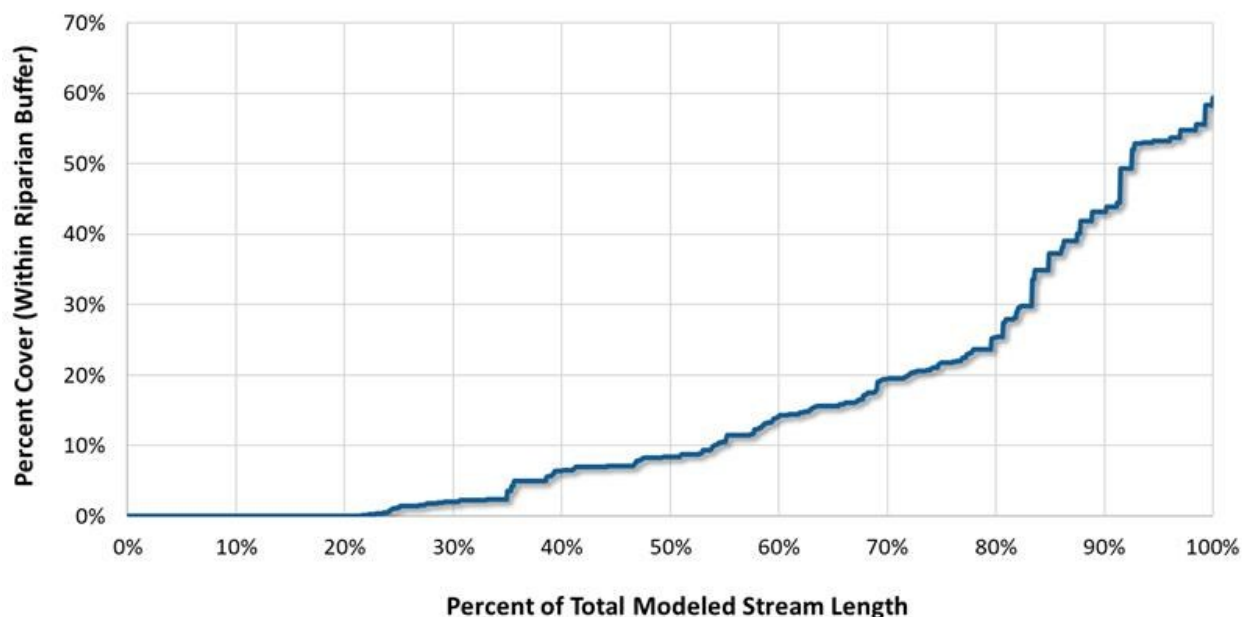


Figure 5-13. Cumulative distribution of average percent canopy within a 10-m stream buffer.

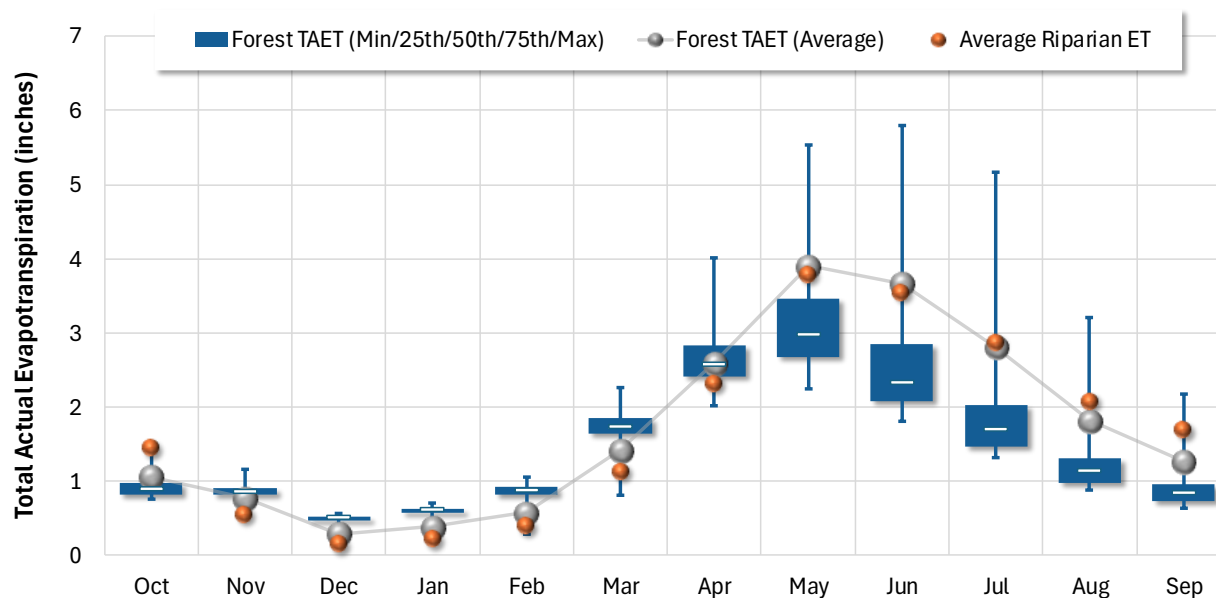


Figure 5-14. Distribution of monthly Forest TAET for all modeled subwatersheds vs. average Riparian ET.

5.3 Metrics for Model Evaluation

The demonstration of model calibration is key to the model development process, as it forms the basis for establishing the degree of uncertainty in model predictions and the reliability of the model to base management decisions. Calibration was assessed using a combination of visual assessments and computed statistical evaluation metrics. Visual assessment involved reviewing panels of simulated vs observed graphical outputs, which are presented in the following sections. For statistical assessment of model performance, agreement between LPSC outputs and observed data was assessed using performance metrics based on those recommended by (Moriassi et al., 2015). These performance metrics are considered highly conservative, and it is very rare to receive “Very Good” evaluations across all metrics – “Satisfactory” is a significant outcome. The metrics are used as a weight of evidence approach to evaluate whether model performance is reasonable.

For MODFLOW, statistics were calculated to assess the ability of the model to reproduce groundwater elevations. Two different metrics were used to quantify the ‘goodness-of-fit’ of the modeled data as compared to the observed groundwater elevation data. The statistics follow methods presented by Legates and McCabe (1999): the coefficient of efficiency, R^2 , and the index of agreement, d , were calculated to assess the agreement between modeled and observed values.

LPSC performance targets for simulation of the water balance components are summarized in Table 5-1. The relative error is the ratio of the absolute mean error to the mean of the observations and is expressed as a percent. Model performance will be deemed fully acceptable where a performance evaluation of “Good” or “Very Good” is attained. Nevertheless, every calibration outcome will be explained, with some insights and rationale provided for both “Very Good” to “Unsatisfactory” calibration metrics considering the top-down weight-of-evidence approach described above. If these levels are not attained, an analysis of sources of uncertainty and implications for model usability will be conducted.

The performance metrics are based on the following statistics as follows:

- ▼ The percent bias (PBIAS) quantifies systematic overprediction or underprediction of observations. A bias towards underestimation is reflected in positive values of PBIAS while a bias towards overestimation is reflected in negative values. Low magnitude values of PBIAS indicate better fit, with a value of 0 being optimal. PBIAS is expressed as:

$$PBIAS = 100 \times \frac{\sum_{i=1}^n (Q_{obs,i} - Q_{sim,i})}{\sum_{i=1}^n Q_{obs,i}}$$

where, $Q_{obs,i}$ = observed value at time step i
 $Q_{sim,i}$ = simulated value at time step i
 n = number of observations

- ▼ The coefficient of determination (R^2) describes the degree of collinearity between simulated and measured data and is calculated as the square of the Pearson's correlation coefficient ($R^2 = r^2$, where r is the Pearson's coefficient). The correlation coefficient is an index that is used to investigate the degree of linear relationship between observed and simulated data. R^2 describes the proportion of the variance in observed data that is explained by a model. Values for R^2 range from 0 to 1, with 1 indicating a perfect fit. Values greater than 0.70 indicate acceptable model performance (Donigian, 2000). Pearson's coefficient r is calculated using the equation below:

$$r = \frac{n(\sum Q_{obs,i} Q_{sim,i}) - (\sum Q_{obs,i})(\sum Q_{sim,i})}{\sqrt{n \sum Q_{obs,i}^2 - (\sum Q_{obs,i})^2} \sqrt{n \sum Q_{sim,i}^2 - (\sum Q_{sim,i})^2}}$$

where, $Q_{obs,i}$ = observed value at time step i
 $Q_{sim,i}$ = simulated value at time step i
 n = number of observations

- ▼ The Nash-Sutcliffe efficiency (NSE) is a normalized statistic that determines the relative magnitude of the residual variance ("noise") compared to the measured data variance ("information" (Nash & Sutcliffe, 1970)). NSE indicates how well the plot of observed versus simulated data fits the 1:1 line. Values for NSE can range between $-\infty$ and 1, with NSE = 1 indicating a perfect fit. NSE is defined as:

$$NSE = 1 - \frac{\sum_{i=1}^n (Q_{obs,i} - Q_{sim,i})^2}{\sum_{i=1}^n (Q_{obs,i} - \bar{Q}_{obs})^2}$$

where, $Q_{obs,i}$ = observed value at time step i
 $Q_{sim,i}$ = simulated value at time step i
 \bar{Q}_{obs} = mean of observed values
 n = number of observations

- ▼ The index of agreement, d , is a relative goodness-of-fit metric that informs how well the model reproduces observed variability, but not necessarily whether it is unbiased. It is bounded between 0 and 1 with higher values indicating greater agreement between the modeled and observed variability. The index of agreement, d , is defined as:

$$d = 1 - \frac{\sum_{i=1}^n (Q_{obs,i} - Q_{sim,i})^2}{\sum_{i=1}^n (|Q_{sim,i} - \bar{Q}_{obs}| + |Q_{obs,i} - \bar{Q}_{obs}|)^2}$$

where,
 $Q_{obs,i}$ = observed value at time step i
 $Q_{sim,i}$ = simulated value at time step i
 \bar{Q}_{obs} = mean of observed values
 n = number of observations

- ▼ The ratio of the root-mean-square error to the standard deviation of measured data (RSR) provides a measure of error based on the root-mean-square error (RMSE), which indicates error results in the same units as the simulated and observed data but normalized based on the standard deviation of observed data. Values for RSR can be greater than or equal to 0, with a value of 0 indicating perfect fit. RSR is defined as:

$$RSR = \frac{RMSE}{\sigma_o}$$

where RMSE is the root mean square error and σ_o is the standard deviation of the observed population.

Table 5-1. Summary of performance metrics used to evaluate hydrology calibration

Calibration Metrics (10/01/2012 - 09/30/2018)	Recommended Error Criteria				Reference
	Very Good	Good	Fair	Poor	
PBIAS (All Conditions)	<5%	5% - 10%	10% - 15%	>15%	Based on HSPF experience by A.A. Donigian, Jr., prepared for USEPA (2000); Moriasi et al. (2015)
PBIAS (Seasonal Flows)	<10%	10% - 15%	15% - 25%	>25%	
R ² (All Conditions)	>0.85	0.75 - 0.85	0.60 - 0.75	≤0.60	
R ² (Seasonal Flows)	>0.75	0.60 - 0.75	0.50 - 0.60	≤0.50	
NSE (All Conditions)	>0.80	0.70 - 0.80	0.50 - 0.70	≤0.50	
NSE (Seasonal Flows)	>0.70	0.50 - 0.70	0.40 - 0.50	≤0.40	
RSR (All Conditions)	≤0.50	0.50 - 0.60	0.60 - 0.70	>0.70	
RSR (Seasonal Flows)	≤0.60	0.60 - 0.70	0.70 - 0.80	>0.80	

6 MODEL CALIBRATION & VALIDATION

This section described the results of the model calibration and performance assessment using some of the performance metrics presented in Section 5. Observed snow data included measurements of snowpack collected by automated telemetry (SNOTEL) and manual observations (CDEC). The continuous daily snowpack available through the SNOTEL network was used to perform LSPC snow module calibration and the CDEC snow survey data was used to validate the parameters developed against the SNOTEL data. Additionally, a comparison between the LSPC snow results extrapolated across the Shasta River watershed was made to the UCSB Snow Lab model.

6.1 Observed Snowpack

Snowfall and snowmelt play an important role in the water balance of the Shasta River watershed. From a modeling perspective, snowpack acts like a reservoir that stores water based on a set of temperature-based rules that govern when precipitation arrives as snowfall, and releases water based on another set of climate-based rules that govern when snowmelt occurs.

The Natural Resources Conservation Service (NRCS) maintains a network of snowfall telemetry gages (SNOTEL) that report valuable information for informing and calibrating snow in watershed models. Daily snow water equivalent data (SWE) track water content in the snowpack. SWE can be used directly as observed snowpack data for calibrating the LSPC SNOW module. Daily minimum and maximum temperatures are also reported at each site. When disaggregated to an hourly basis, those data improve the precision of temperature for informing the model as to when to consider precipitation as snowfall. While there are no primary SNOTEL gages in the Shasta River watershed, data from other SNOTEL sites in the Klamath River watershed can be used to calibrate snowfall/snowmelt processes. The station at Big Red Mountain SNOTEL site is the nearest to the Shasta River watershed and is located approximately 50 miles northwest of Yreka.

CDEC also maintains a cooperative snow survey data set which includes observation at several locations within the Shasta River watershed. These data are collected monthly in the field through site visits when snowpack is present. A subset of these stations also uses automated sensors; however, all the locations in the Shasta River watershed are manually collected. While these data are at a lower temporal resolution (i.e., monthly instead of daily), they provide an important point of comparison within the watershed boundary.

Table 6-1 presents a summary of the locations with available snowpack data and Figure 6-1 shows a map of these locations in relation to the Shasta River watershed.

Table 6-1. Summary of observed snowpack data reviewed for the Shasta River watershed

Site Name	Site ID	Latitude	Longitude	Elevation (ft.)	Start Date	End Date
PARKS CREEK ¹	PRK	41.367	-122.550	6,700	2/1/1990	9/30/2023
SWEETWATER ¹	SWT	41.382	-122.535	5,850	2/1/1990	9/30/2023
LITTLE SHASTA ¹	LSH	41.808	-122.195	6,200	4/1/1990	9/30/2023
SAND FLAT ¹	SFT	41.353	-122.247	6,800	2/1/1990	9/30/2023
MOUNT SHASTA ¹	MSH	41.372	-122.230	7,900	2/1/1990	9/30/2023
BREWER CREEK ¹	BWR	41.435	-122.100	6,250	2/1/1990	9/30/2023
GOOSENEST ¹	SVG	41.727	-122.218	7300	8/1/2020	9/30/2023
BOLAM ¹	SVB	41.476	-122.207	6800	8/1/2020	9/30/2023
BIG RED MOUNTAIN ²	BRM	42.050	-122.850	6,050	10/1/1980	9/30/2023

1. California Cooperative Snow Survey site.

2. NRCS SNOTEL site.

Several gridded model data sets were also catalogued and evaluated for use in comparison to model results. These data sets include gridded models developed by the National Oceanic and Atmospheric Association (NOAA) National Snow and Ice Data Center (NSIDC) and University of California at Santa Barbara (UCSB) Snow Lab. While these model data sets cover the spatial gaps left by observations from individual sites, they also include elements of model uncertainty. Therefore, they may be used for qualitative comparisons while primary calibration and validation continue to rely on observed data. The Snow Data Assimilation System (SNODAS) developed by the NSIDC provides precipitation, snow depth, and snow melt data from September 2003 through the present at a 1 km spatial resolution (NSIDC, 2021); however, upon review and comparison to other available sources, that dataset was ultimately not used. The UCSB model data received provided estimates of snow-water equivalent from Water Year 2001 through Water Year 2019 for the Sierra Nevada mountains plus other parts of the Cascades up to approximately 42.43° latitude, including the Shasta River watershed (Cab Esposito, personal communication, July 8, 2020).



Figure 6-1. SNOTEL and CDEC stations in the vicinity of the Shasta River watershed.

6.2 Snow Calibration

The LSPC SNOW module has mechanisms for adjusting calibrated parameters from one location to represent processes at another location. Temperature lapse rate, the rate at which temperature decreases with increasing elevation, is one mechanism that can significantly influence snowfall prediction, especially when extrapolating snow behavior to subwatersheds without gages. The snow calibration builds upon insights gained about the watershed during model segmentation. Analyzing the observed snowpack datasets (Section 6.1) against elevation often reveals inherent trends in the data to refine the modeled temperature lapse rate assumptions.

To calibrate snowpack, a unit-area model was configured to the Big Red Mountain SNOTEL site. Observed precipitation and temperature data at the SNOTEL site, along with other energy balance meteorological timeseries at the nearest NLDAS grid cell, were used to drive the unit-area model. The model was run for the 16 Water Years between 10/1/2003 and 9/30/2019 as a common period across the six additional CDEC snow survey sites (i.e. except SVG and SVB) (see Section 6.1). SVG and SVB were two recently installed CDEC stations with data coverage starting August 2020 and were used as additional validation stations. The EPA parameter estimation package (PEST) was used to optimize snowpack goodness of fit by varying snow parameters between the typical min/max range (Doherty, 2009). Table 6-2 lists the key model parameters computed prior to or adjusted during model calibration, along with typical and possible ranges for those values as outlined in BASINS Technical Note 6 (EPA, 2000). Table 6-3 shows the final calibrated snow parameters for the Shasta River LSPC model.

Table 6-2. Typical and possible parameter values for snow calibration (Source: EPA 2000).

Parameter	Description	Unit	Typical		Possible	
			Min	Max	Min	Max
FOREST	Fraction of LAND covered by Forest (winter transpiration)	none	0	0.5	0	0.95
ELDAT ¹	Difference between temperature station and mean watershed elevation	ft	-1,000	1,000	none	none
LAT	Latitude of the pervious land segment (PLS)	Dec-deg.	30	50	-90	90
MELEV ¹	Mean elevation of LAND above sea level	ft	50	3,000	0	7,000
SHADE	Fraction of LAND shaded from solar radiation (i.e. by trees)	none	0.1	0.5	0	0.8
SNOWCF	Precipitation-to-snow multiplier (accounts for poor gage-catch efficiency during snow)	none	1.1	1.5	1	2
COVIND	Maximum snowpack (water equivalent) at which the entire LAND is covered with snow	in.	1	3	0.1	10
RDSCN	Density of cold, new snow relative to water	none	0.1	0.2	0.05	0.3
TSNOW	Air temperature below which precipitation will be snow, under saturated conditions	°F	31	33	30	40
SNOEVP	Adapts sublimation equation to field conditions	none	0.1	0.15	0	0.5
CCFACT	Adapts snow condensation/convection melt equation to field conditions	none	1	2	0.5	8
MWATER	Maximum water content of the snowpack	in./in.	0.01	0.05	0.005	0.2
MGMELT	Maximum rate of snowmelt by ground heat	in./day	0.01	0.03	0	0.1

1: Not calibrated. These values were computed from spatial data as physical watershed characteristics.

Table 6-3. Calibrated snow parameter ranges by land use group and soil type.

Parameter	Unit	Final Values (PEST)	Basin wide Extrapolation (LSPC)
FOREST	none	0.75	0.75
ELDAT ¹	ft.	0	Varies
LAT	Dec-deg.	40	40
MELEV ¹	ft	Varies	Varies
SHADE	none	0.75	0.75
SNOWCF ²	none	1.2	1.0
COVIND	in.	1.5	1.5
RDSCN	none	0.2	0.2
TSNOW	°F	35	35
SNOEVP	none	0.15	0.15
CCFACT	none	0.08	0.08
MWATER ²	in./in.	0.03	0.1
MGMELT	in./ day	0.01	0.01

1: Not calibrated. These values were computed from spatial data as physical watershed characteristics.

2: These parameters were adjusted from the calibrated SNOTEL PEST values after basin-wide extrapolation

ELDAT, which is the difference between temperature station and mean watershed elevation, is one of the most sensitive “parameters” for snow simulation because the lapse rate adjustment of temperature timeseries, together with the specified value of TSNOW (air temperature below which precipitation will be snow under saturated conditions), combine to trigger snowfall. Because timeseries of observed temperature data at the SNOTEL site was used directly, ELDAT was set to a value of 0 in the unit-area model. Although ELDAT is traditionally considered as a model parameter, LSPC considers it as a physical watershed characteristic that is computed directly from spatial data. Because of the rapidly changing terrain at higher elevations, ELDAT trends higher for about 50% of the study area temperature gage locations at higher elevations. Higher ELDAT in the lapse rate equation adjusts temperature lower than reported values at higher elevations, which lowers the threshold for snow.

Figure 6-2 show a daily timeseries of modeled vs. observed snow-water equivalent snowpack depth at the three selected calibration locations. Figure 6-3 shows the same data as annualized average snowpack for each calendar day.

Table 6-4 shows annual PBIAS, r-Squared, and NSE calibration statistics of modeled vs. observed snowpack at the calibration stations along with temperature summary statistics for each year.

Table 6-4. Snowpack simulation Nash-Sutcliffe (NSE), PBIAS (percent bias), and R-squared value for modeled vs. observed snowpack at the Big Red Mountain SNOTEL location.

Water Year	NSE	PBIAS	R ²	Mean Temperature (°F)	Median Temperature (°F)
2004	0.86	3%	0.87	36	34
2005	0.62	24%	0.68	36	36
2006	0.94	-13%	0.96	35	33
2007	0.60	39%	0.76	36	35
2008	0.97	-1%	0.97	34	33
2009	0.76	33%	0.90	36	35
2010	0.96	-8%	0.97	34	32
2011	0.95	-9%	0.96	33	32
2012	0.89	-26%	0.94	35	35
2013	0.83	14%	0.85	35	35
2014	0.04	75%	0.34	37	37
2015	0.43	45%	0.53	39	39
2016	0.84	-30%	0.98	36	35
2017	0.66	-47%	0.94	33	33
2018	0.71	32%	0.78	36	35
2019	0.97	-13%	0.99	35	34

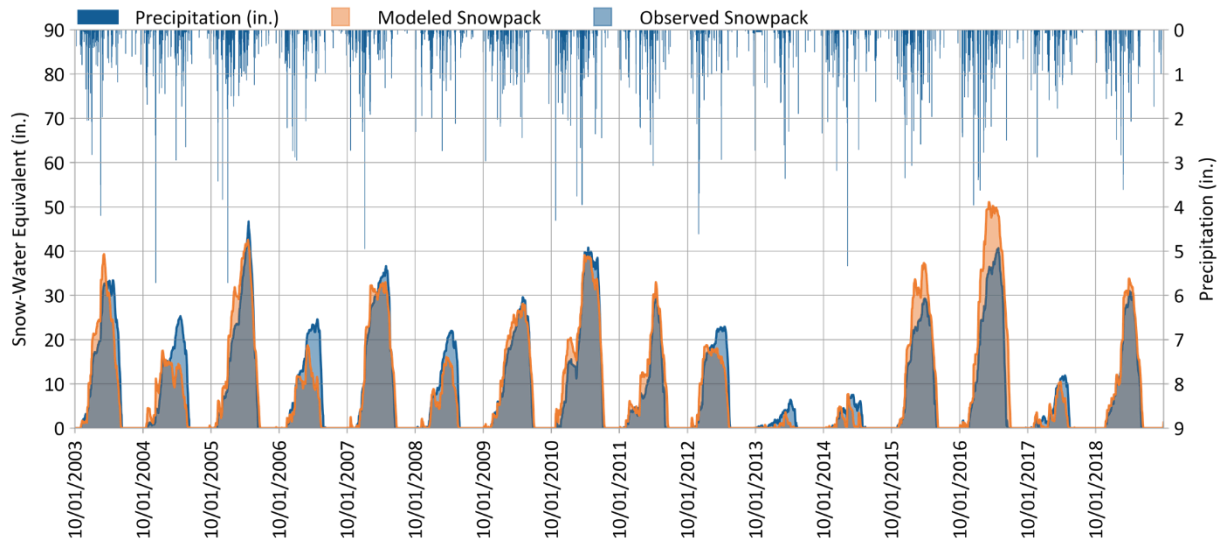


Figure 6-2. Modeled and observed snowpack time series for Big Red Mountain (Station ID: BRM).

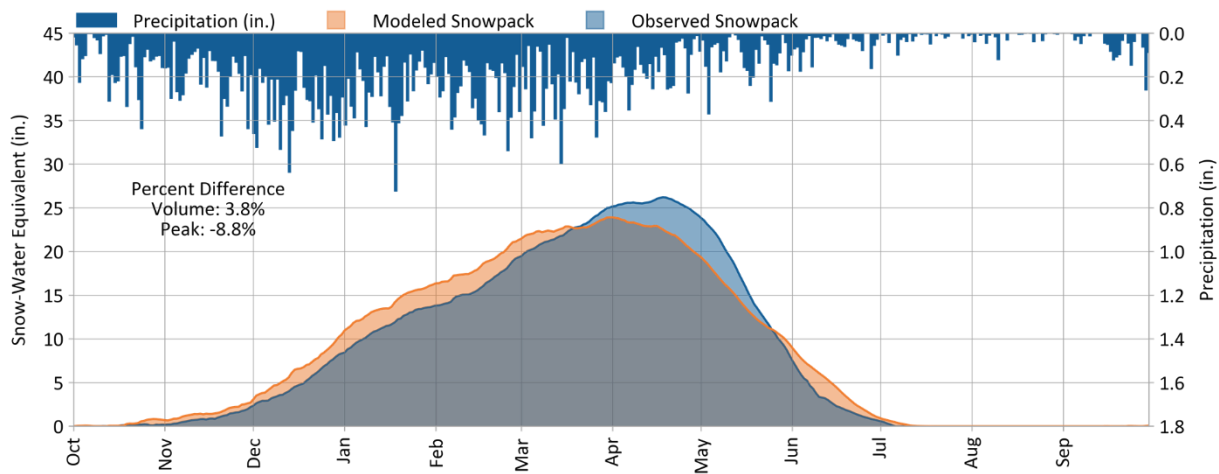


Figure 6-3. Modeled and observed average monthly snowpack values for Big Red Mountain (Station ID: BRM).

6.3 Snow Validation

The calibrated snow parameters developed through unit-area model calibration using the Big Red Mountain SNOTEL site (Section 6.2) were also applied to unit-area models representing the eight CDEC snow survey sites. These data were more synoptic with monthly snowpack samples year over year during the period when snowpack is present. Therefore, while the SNOTEL data provided a basis for quantifying Water Year performance metrics, the snow survey data provided a good foundation for testing and evaluating the long-term trend on model predictions independently at locations across the Shasta River watershed to verify model calibration from the SNOTEL site.

Results for these sites were evaluated through visual means by plotting year by year simulated snowpack against the monthly snowpack observations. Examples showing daily timeseries of modeled vs. observed snow-water equivalent snowpack depth at the Parks Creek (PRK) and Mount Shasta (MSH) snow survey sites are presented as Figure 6-4 and Figure 6-5. Figure 6-6 and Figure 6-7 show the same data as annualized average snowpack for each calendar day. A full set of snow calibration plots for all nine locations, one SNOTEL and eight CDEC snow survey sites, is presented as Appendix E. Along with the original calibration-validation period (WY 2003–2019), Appendix E also contains snow exhibits covering an extended timeframe through the end of the simulation period (up to WY 2023) for SNOTEL and subset of CDEC snow survey sites.

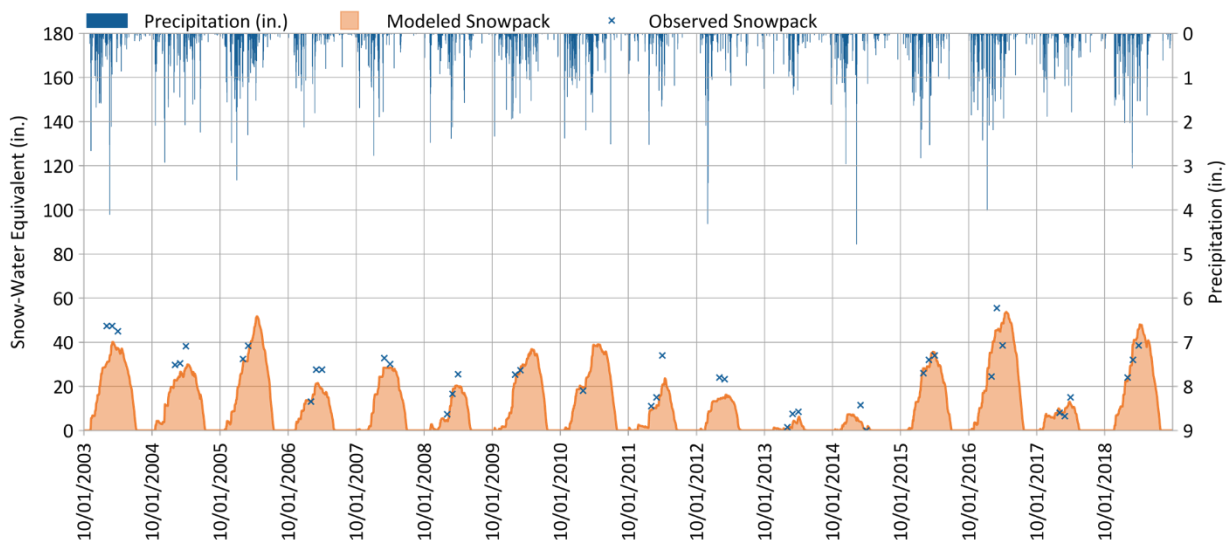


Figure 6-4. Modeled and observed snowpack time series for CDEC snow survey data at Parks Creek.

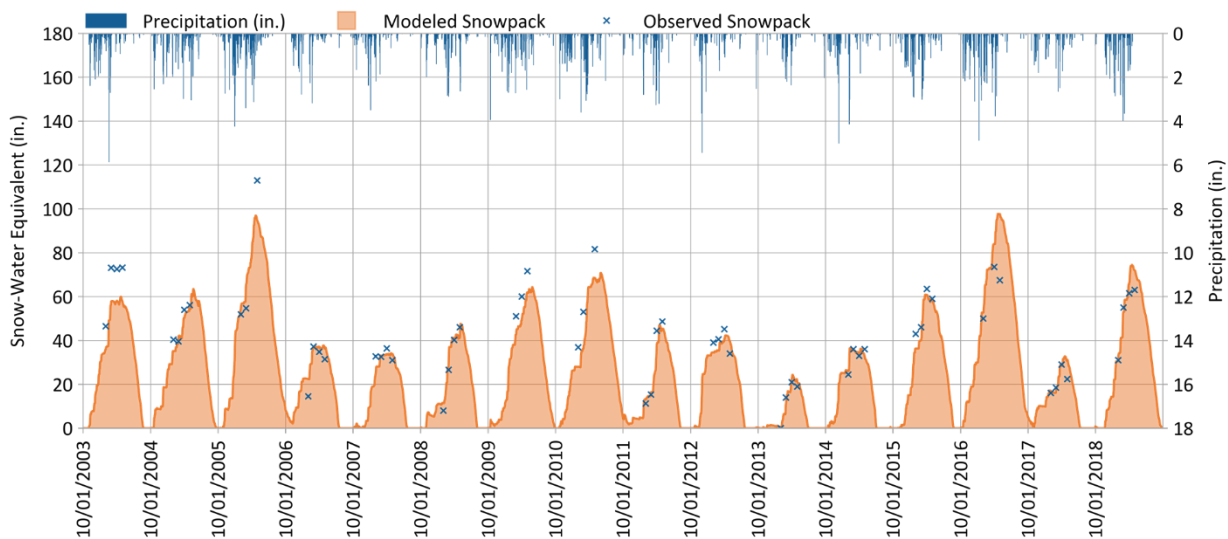


Figure 6-5. Modeled and observed snowpack time series for CDEC snow survey data at Mt. Shasta.

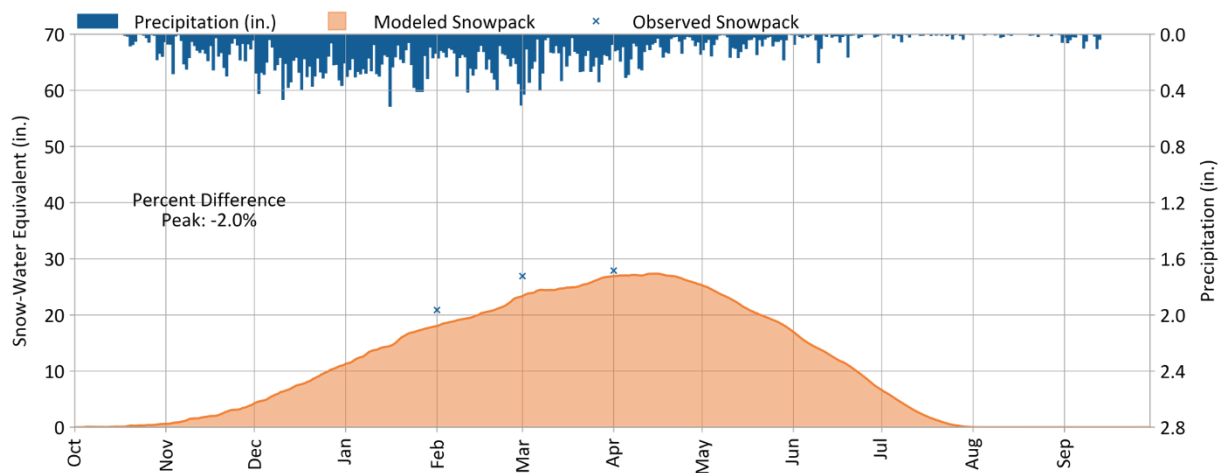


Figure 6-6. Modeled and observed average monthly snowpack values for CDEC snow survey data at Parks Creek.

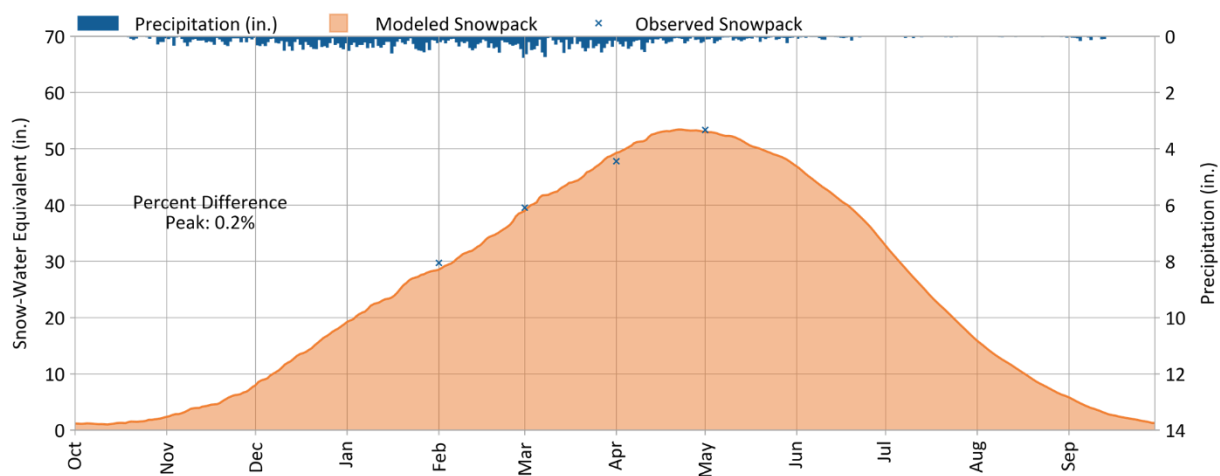


Figure 6-7. Modeled and observed average monthly snowpack values for CDEC snow survey data at Mt. Shasta.

An additional spatial validation against independently modeled snowpack provided by the UCSB Snow Lab was performed. The UCSB model has a 500-m resolution and represents water years 2001-2019. Average annual snowpack from the LSPC model was calculated by resampling both LSPC HRUs and the 500-m UCSB snowpack model outputs to an earlier 8-mile quadrilinear MODFLOW grid that was being used at the time snow was being calibrated. Figure 6-8 presents a cumulative distribution function (CDF) of average annual snowpack depth over the Shasta River watershed area that was modeled by the UCSB Snow Lab. Eight points along the CDF were sampled for detailed comparison against corresponding LSPC snow predictions. The rate of change in average snowpack was sharper in the upper half of sampled grid than the lower half; therefore, 3 points at 20% intervals were sampled in the lower half while 5 points at 10% intervals were sampled in the upper half of area.

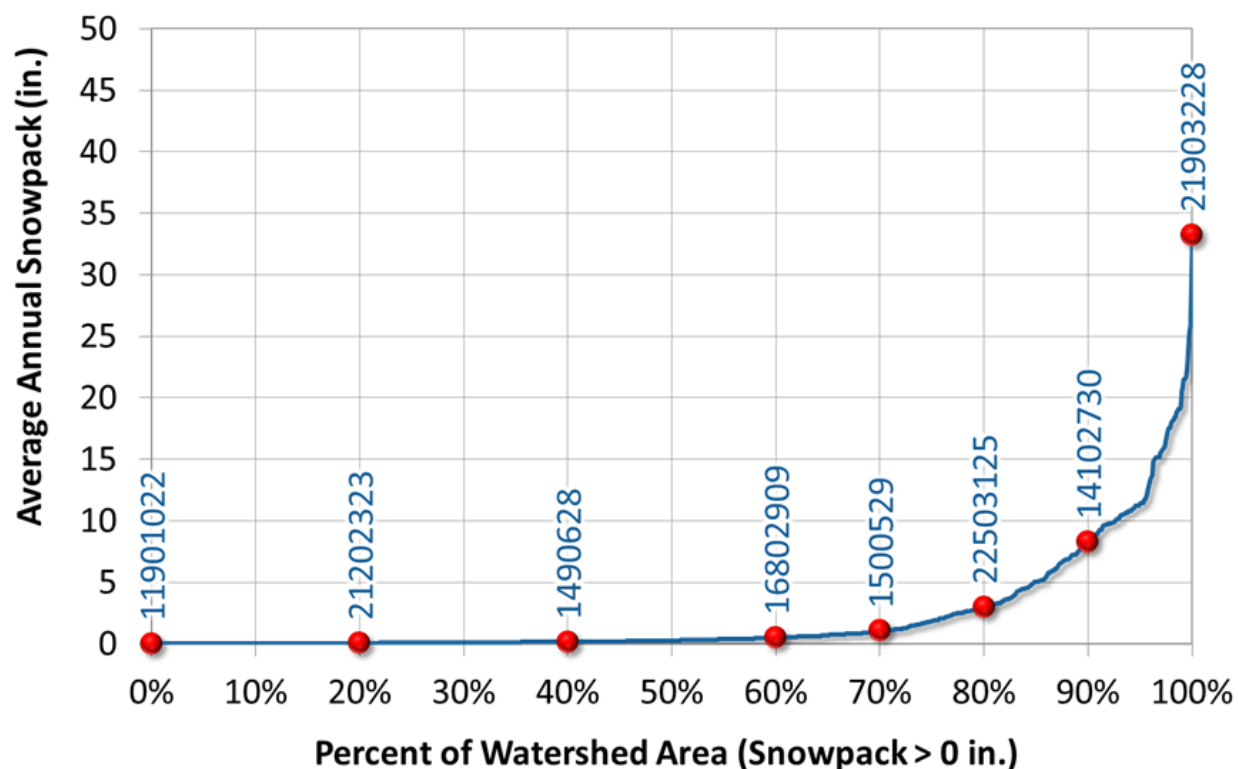


Figure 6-8. CDF comparing annual average snow depth by percent of watershed area.

Figure 6-9 presents a map of the 8 points selected from the CDF for comparison with the UCSB Snow Lab model predictions. This map provides a visual validation of broad spatial patterns across the watershed ranging from the highest average snow depth in the southeastern portion of the watershed near Mt. Shasta to little-or-no accumulation in the valley. Figure 6-10 and Figure 6-11 presents daily snowpack depth comparisons for the 90th and 100th percentile points on the CDF. The 90th percentile point represents about 8 inches of snowpack on average, where 90% of the watershed receives less snow on average than 8 inches per year. The LSPC modeled snow predictions were consistent in magnitude and duration at nearly all sampled points of the UCSB Snow Lab model domain. Detailed comparisons at all 8 points are included in Appendix E.

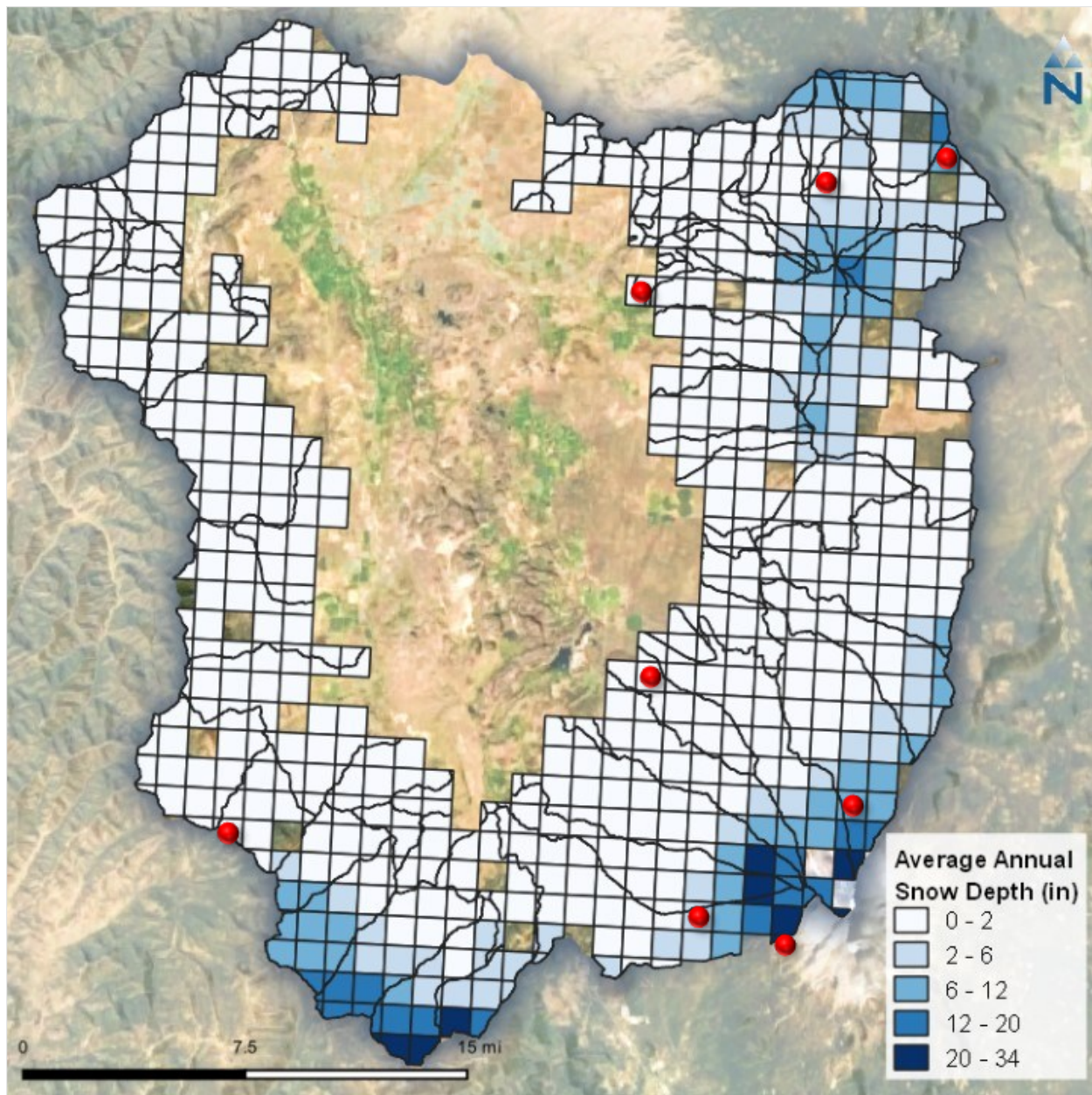


Figure 6-9. Modeled average annual snowpack in the Shasta River watershed. Red dots represent grid cells selected for comparison with the UCSB snow model.

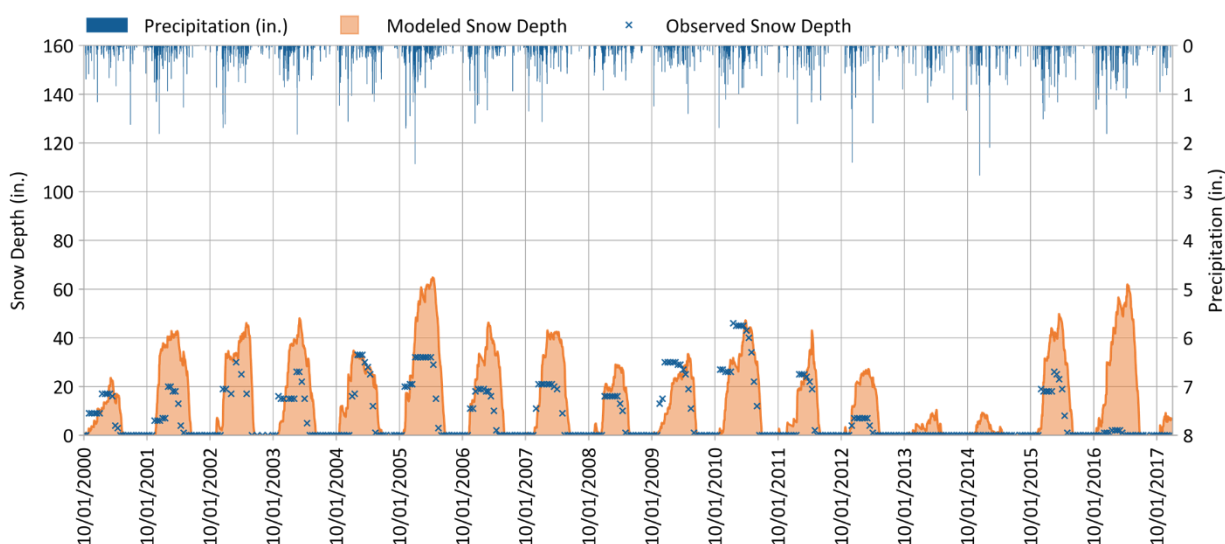


Figure 6-10. Modeled LSPC vs. USCB daily snowpack depth (GRID 15201029).

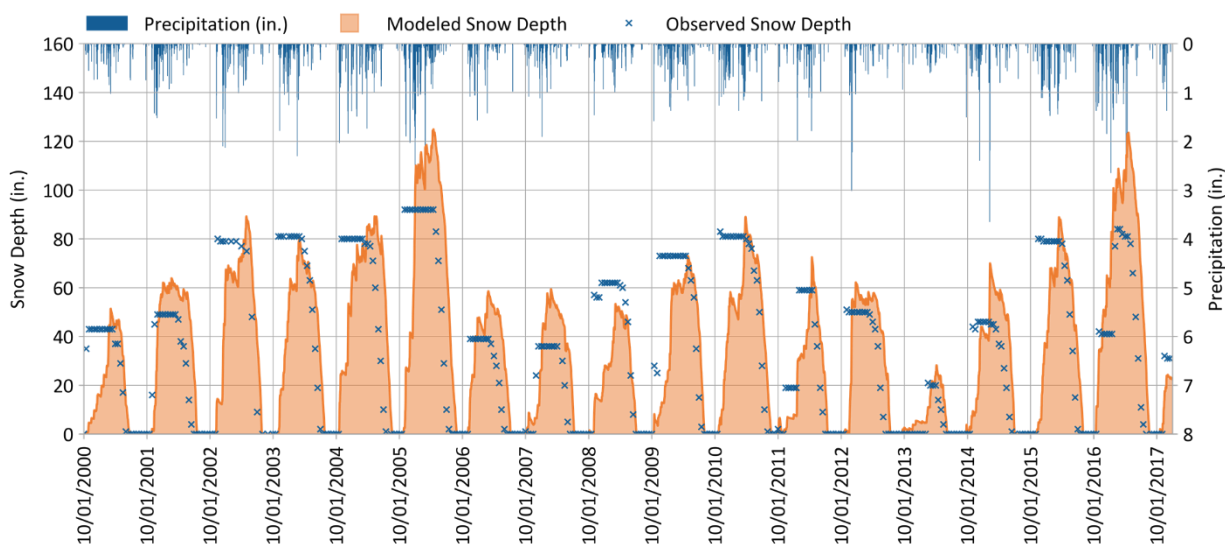


Figure 6-11. Modeled LSPC vs. USCB daily snowpack depth (GRID 21903228).

6.4 Observed Streamflow

Eight streamflow stations with varying data quality and quantity were available within the Shasta River watershed (Figure 6-12, Appendix D). The USGS streamflow stations at Yreka (11517500) and Montague (11517000) are mainstem gages with high-quality long-term records. The other gages provide additional information at intermediate points in the network (e.g., Shasta River at Grenada, Shasta River at Edgewood), points of interest representing spring flow (e.g., Big Springs Creek Water Wheel). Other observed timeseries of diversions (e.g., MWCD Parks Creek Diversion and Main Canal) were useful for validating water movements for consumptive uses. Table 6-5 summarizes

upstream drainage area characteristics for a selection of these stations which are most useful for assessing model performance during and after calibration.

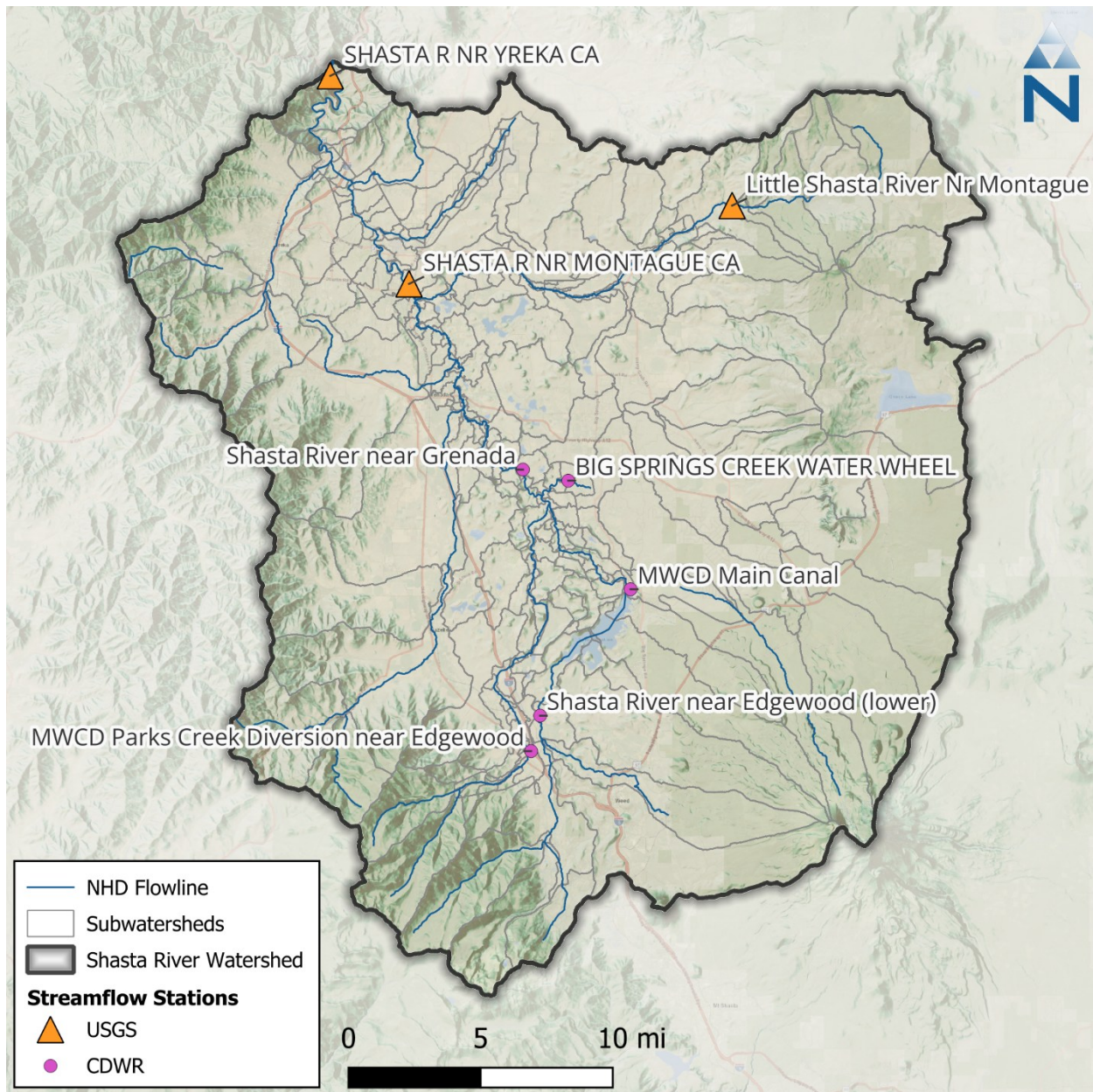


Figure 6-12. Streamflow stations within the Shasta River watershed by agency.

Table 6-5. Upstream drainage area characteristics for selected streamflow stations

USGS Gage:		Shasta River near Yreka (11517500)	Shasta River near Montague (11517000)	Shasta River near Grenada (F21370)	Big Springs Creek Water Wheel (105SRBSWW)	Shasta River near Edgewood (F21675)
Model Outlet ID:		1002	1025	1044	1151	1091
Drainage Area (mi ²):		793	673	305	4.4	74
HRU Characteristics						
Land Use	Ag/Crop	15.52%	17.50%	15.54%	32.39%	3.13%
	Developed	3.93%	3.51%	4.12%	7.19%	5.04%
	Forest	34.23%	36.05%	36.73%	4.59%	59.98%
	Grass	46.33%	42.94%	43.61%	55.83%	31.86%
Slope	High (>35%)	19.28%	21.29%	26.93%	0.00%	27.93%
	Med (15-35%)	29.02%	30.73%	28.58%	0.00%	34.83%
	Low (<15%)	51.09%	47.15%	43.49%	100.00%	36.88%
Hydrologic Soil Group	A	24.75%	23.38%	26.99%	4.39%	50.41%
	B	7.33%	7.67%	5.58%	4.98%	6.72%
	C	33.06%	29.57%	26.79%	87.14%	10.24%
	D	33.98%	38.35%	39.37%	2.54%	31.68%
	Impervious	0.88%	1.03%	1.28%	0.95%	0.94%
Geology	Cascade	62.66%	61.48%	59.33%	91.96%	72.22%
	Overlap	8.76%	8.21%	4.46%	0.00%	0.00%
	Klamath	24.08%	26.01%	31.14%	0.00%	22.40%
	Unclassified	4.51%	4.30%	5.07%	8.04%	5.39%

Color gradient shows relative area distribution. Darker is higher.

6.5 LSPC Initial Streamflow Calibration

Initial LSPC hydrology parameter were calibrated against the surface water discharge in LSPC was facilitated using the PEST parameter estimation software (Doherty, 2009) to automatically adjust parameters to improve agreement between predicted and observed streamflow. Since the Shasta River watershed is a relatively unurbanized system, initial calibration focused on evaluating model terms that govern the overall system water budget and impact the groundwater inflow (GWI) term linking to MODFLOW.

Table 6-6 presents the parameters that were initially used in the PEST calibration. Three parameters were tested using PEST which included the Lower Zone Nominal Storage (LZSN), Index to Infiltration Capacity (INFILT), and Upper Zone Nominal Storage (UZSN) parameters described below. Initial model parameters were derived by soil type with guidance from BASINS Technical Note 6 (EPA, 2000).

Table 6-6. Parameters and ranges used in automated calibration

Parameter	Description	Units	Soil Group			
			A	B	C	D
INFILT	Index to Mean Soil Infiltration	in./hr	0.4 - 1.0	0.1 - 0.4	0.05 - 0.1	0.01 - 0.05
LZSN	Lower Zone Nominal Soil Moisture Storage	in.	7.0 - 15.0	7.0 - 15.0	7.0 - 12.0	7.0 - 10.0
UZSN	Upper Zone Nominal Soil Moisture Storage	in.	6-14% of LZSN based on Slope			

As shown in Table 6-7, BASINS Technical Note 6 (EPA, 2000) was used as a guide to select typical values for other key hydrology parameters for the initial calibration. AGWRC: The value of AGWRC was set at the maximum value of 0.999. This parameter controls the release rate of active groundwater outflow which is controlled by MODFLOW. Therefore, this parameter does not affect the simulation results when LSPC is coupled with MODFLOW.

During the calibration these parameters, values other than INFILT and LZSN were not adjusted to improve agreement between observed and simulated flows. Parameters related to riparian evapotranspiration (e.g., BASETP, AGWETP) and groundwater losses (e.g., DEEPFR) were set to zero as these parameters related to processes that need evaluation during or after the linkage to MODFLOW. Conceptually, it is more appropriate to apply riparian ET at the edge-of-field along the stream corridor (as a function of vegetation density) downstream all AGWO than individually at the HRU level. Linkage to MODFLOW further improves the prediction of available water in the stream corridor.

While some parameter values can vary monthly, such as USZN and LZETP, no monthly variation was set for the Shasta River watershed as no streamflow gages were available to isolate and test monthly variation without the influent of diversion and springs, which tend to have a bigger impact on the system. The decision to keep constant parameter values instead of varying by month was made to limit the amount of uncertainty introduced through assumptions were could not be explicitly tested. Final calibrated LSPC parameters are presented in Appendix F.

Table 6-7. Typical and possible parameter values for hydrology calibration (Source: EPA 2000)

Parameter	Description	Unit	Typical		LSPC Calibrated Value
			Min	Max	
LZSN	Lower Zone Nominal Soil Moisture Storage	in.	3	8	9 - 15
INFILT	Index to Infiltration Capacity	in./hr	0.01	0.25	0 - 1.5
KVARY	Variable groundwater recession	1/in.	0	3	0.0
AGWRC	Base groundwater recession	none	0.92	0.99	0.85 - 0.999
DEEPFR	Fraction of GW inflow to deep recharge	none	0	0.2	0
BASETP	Fraction of remaining ET from baseflow	none	0	0.05	0
CEPSC	Interception storage capacity	in.	0.03	0.2	0.05 - 0.3125
UZSN	Upper zone nominal soil moisture storage	in.	0.1	1	0.6 - 3.15
NSUR	Manning's n (roughness) for overland flow	none	0.15	0.35	0.1 - 0.45
INTFW	Interflow inflow parameter	none	1	3	2 - 3
IRC	Interflow recession parameter	none	0.5	0.7	0.3 - 0.8
LZETP	Lower zone ET parameter	none	0.2	0.7	0.4 - 0.8
PETMAX	Temp below which ET is reduced	°F	35	45	45
PETMIN	Temp below which ET is set to zero	°F	30	35	35
INFEXP	Exponent in infiltration equation	none	2	2	2
INFILD	Ratio of max/mean infiltration capacities	none	2	2	2
AGWETP	Fraction of remaining ET from active GW	none	0	0.05	0

Performance metric results for LSPC streamflow predictions at the Shasta River near Yreka CA (USGS 11517500) gage prior to MODFLOW coupling is presented in Figure 6-13 through Figure 6-16. The intention of this comparison at this stage in the calibration process is not necessarily to match streamflows, but rather to ensure that enough water is available in the system for other processes such as consumptive use withdrawals, diversions, and groundwater pumping. Some notable observations include:

- ▼ In general, the LSPC watershed model overpredicts the annual water budget at the Shasta River near Yreka CA (USGS 11517500) streamflow gage. The delayed release of groundwater, which will be represented by the MODFLOW model are likely causes of this initial overprediction.
- ▼ The trends evident in the aggregate monthly summary plots of modeled vs. observed streamflow is the overprediction of flows in the wet season and underprediction of flows in the dry season. This points to the limitation of LSPC alone to represent the lag in groundwater inflows and the absence of critical springs contributing to the system.

Based on these results, the modeling effort proceeded with coupling LSPC and MODFLOW to better represent dry season low flows, springs, and the effect of pumping on the system.

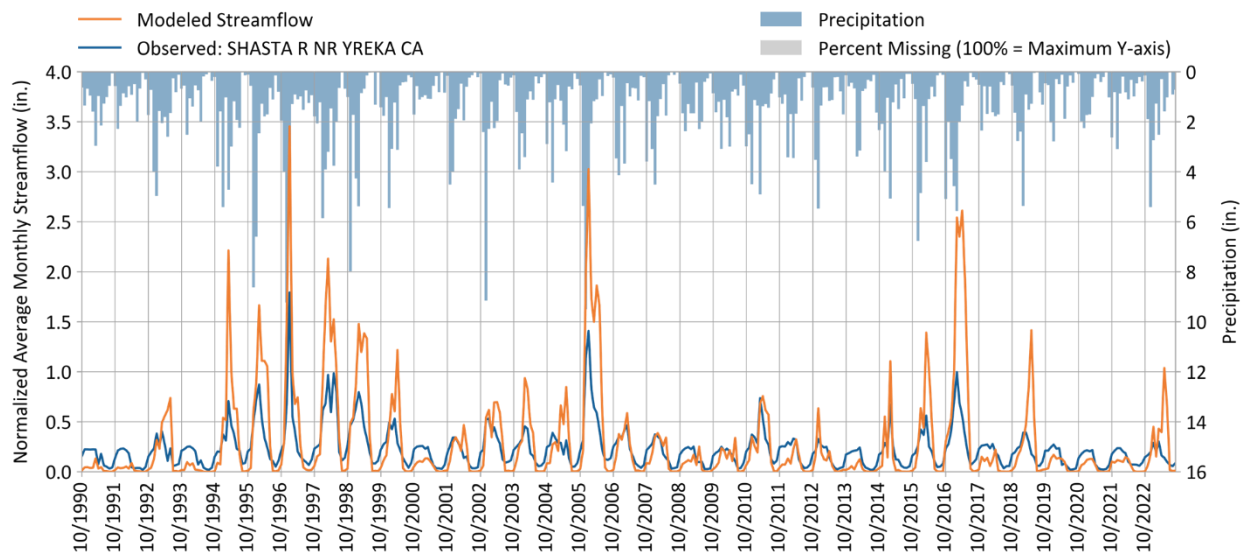


Figure 6-13. SHASTA R NR YREKA CA (11517500) - Hydrology calibration: Simulated vs. observed normalized monthly streamflow.

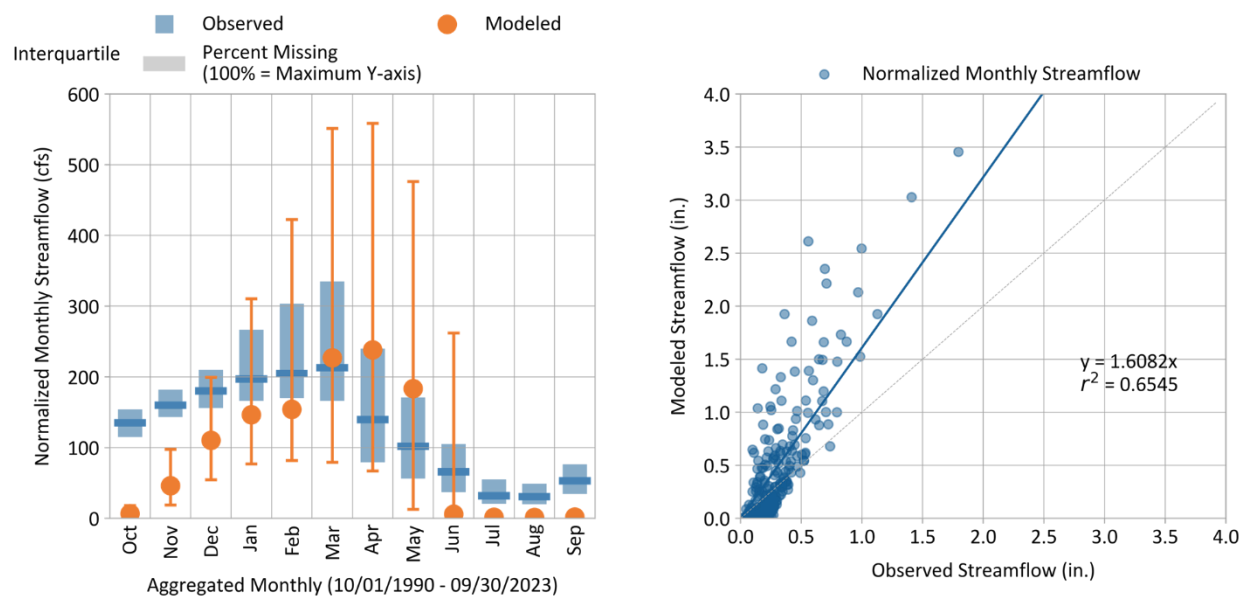


Figure 6-14. SHASTA R NR YREKA CA (11517500) - Hydrology calibration: Simulated vs. observed normalized monthly streamflow.

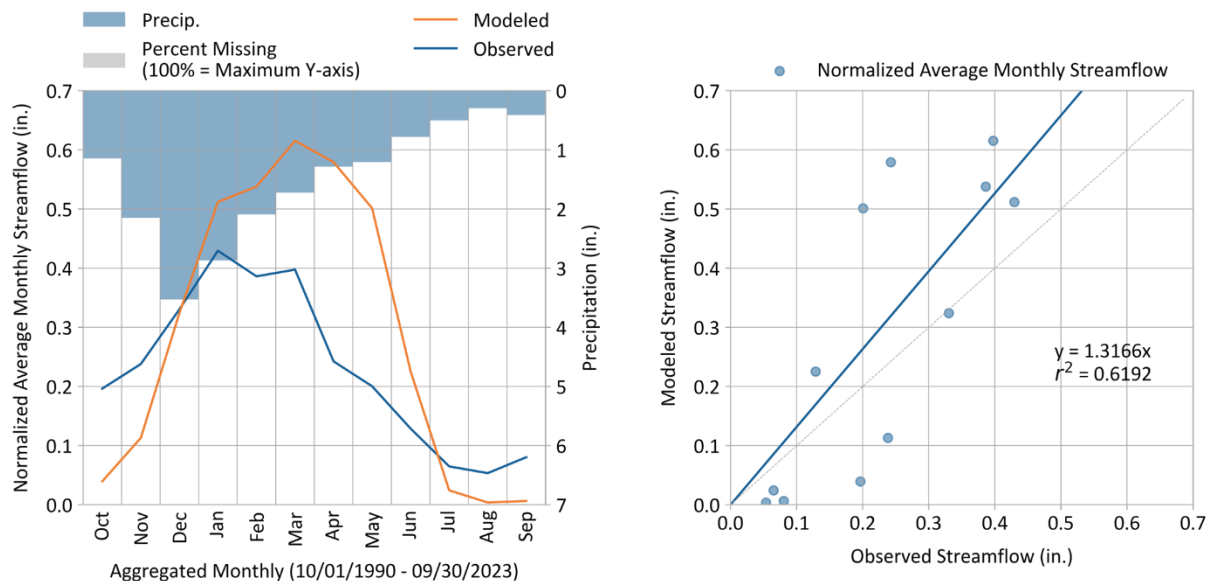


Figure 6-15. SHASTA R NR YREKA CA (11517500) - Hydrology calibration: Average normalized monthly streamflow.

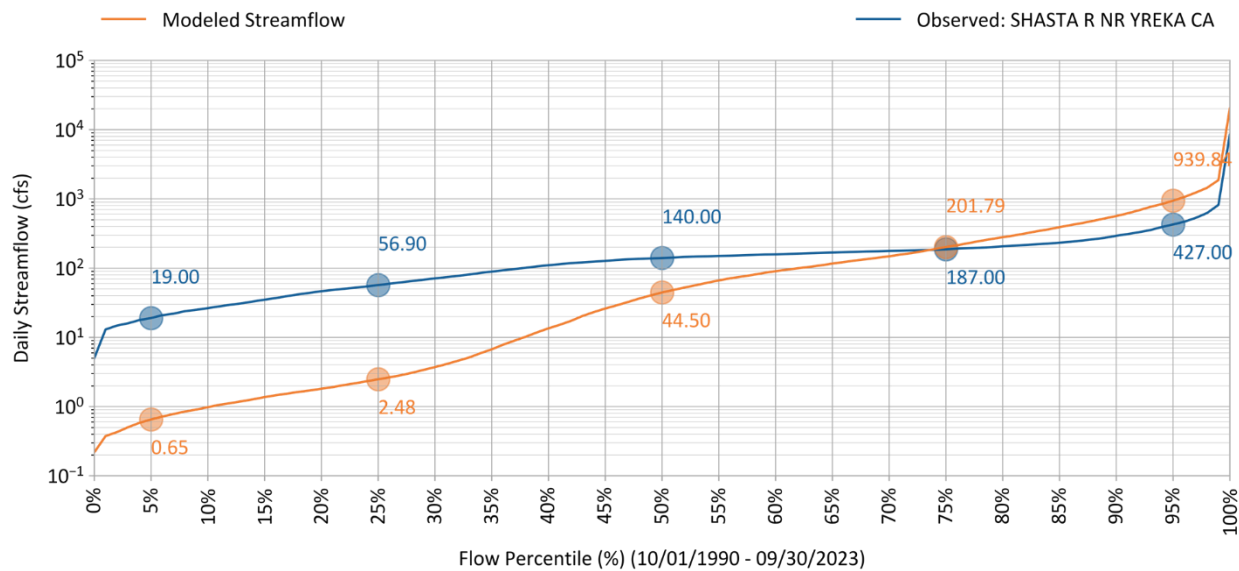


Figure 6-16. SHASTA R NR YREKA CA (11517500) - Hydrology calibration: Simulated vs. observed streamflow duration curves.

6.6 MODFLOW Calibration

The MODFLOW groundwater model was calibrated in conjunction with the LSPC model as part of the integrated modeling process. Groundwater calibration focused on reducing the difference between observed and predicted streamflow and groundwater elevations. Target MODFLOW baseflows were established by subtracting the sum of modeled surface (SURO) and interflow (IFWO) volumes from observed USGS flows. Flow exchange between aquifers and streams, via the SFR package of the groundwater model, were reverted to the LSPC model. The LSPC and MODFLOW model simulations were performed in a loop to match the available streamflow data at various gages distributed throughout the model domain. Calibrating the model to groundwater heads alone may systematically bias the calibrated parameters and skew water budgets. However, including streamflow measurements as a calibration target in combination with groundwater head measurements provides a constraint on simulated water budgets in the system which in turn reduces bias in the model. Additionally, retaining aquifer properties within a reasonable range provides additional constraints on water budgets. The approach used in the calibration process appropriately conserves water balance in the surface water – groundwater system and provides water budgets across the model domain. The calibration process was facilitated by the parameter estimation software PEST (Doherty, 2009).

6.6.1 Groundwater Heads

6.6.1.1 Initial Heads

Initial heads are needed in the model to provide a starting condition for the groundwater simulation. For a large and dynamic hydrologic system such as the Shasta Valley it is challenging to generate a reasonable set of initial groundwater elevation values. As an approximation, average WY 1991-2023 boundary conditions were applied, particularly the groundwater recharge boundary, and a steady-state solution was obtained.

The initial heads thus generated were assessed qualitatively by examining transient water level changes in the available well hydrographs. The trends generated by the simulated hydrographs in majority of the groundwater elevation wells matched with observed data. These trends indicate that the initial conditions obtained using a steady-state assumption were reasonable.

The initial conditions were also compared to the groundwater head contours provided by Mack (1960, Plate 1) for Spring 1954. Note that the initial conditions generated in the model represent average conditions at the beginning of WY 1991, however, these heads were compared to contours from Spring of 1954 for a qualitative assessment of groundwater heads. As shown in Figure 6-17, it is noted that the two sets of head contours generally agree well in terms of their shape indicating appropriate flow direction and gradients in the model. Differences such as localized drawdown may be attributed to the differences between conditions in 1954 and early WY 1991. Based on the contours presented by Mack (1960) there are other important aspects that are noted in relevant sections below.

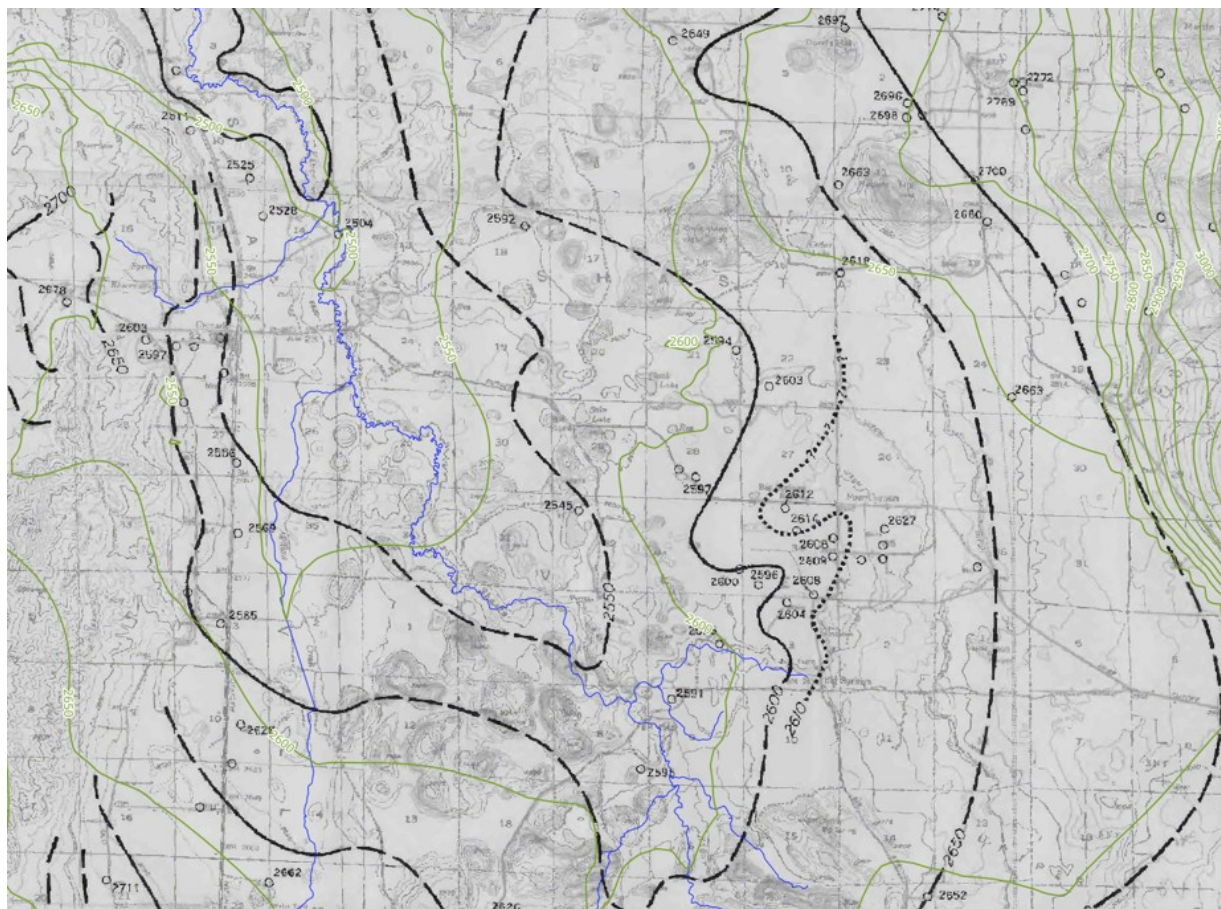


Figure 6-17. Head contours comparing observed data for Spring 1954 (Mack, 1960) (Black Lines) and model generated steady-state conditions (Green Lines) representing initial conditions for WY 1991.

6.6.1.2 Calibration

MODFLOW calibration was performed by adjusting aquifer conductivity and storage parameters within each of the aquifer zones (depicted in Section 4). Other calibration parameters included streambed and lakebed conductance. Calibration targets included groundwater head measurements and streamflow measurements. Observed groundwater elevation data were provided by LWA obtained from the ongoing model development extending the work presented in Siskiyou County GSA (2021) and relied upon for calibration purposes.

The layer assignment in the model for almost all observations were also used as assigned by LWA in support of Siskiyou County GSA (2021). For calibration purposes, selected groundwater-level observations were assigned zero weight and therefore not used in the calibration. These wells include c_40, c_39, and c_44. For well c_40, observed water levels were approximately 160 ft higher than neighboring measurements. For wells c_39 and c_44, simulated water levels were elevated relative to observations, likely due to unrepresented localized pumping effects. In addition, all groundwater-level observations from 1993 and earlier were zero-weighted to avoid potential issues associated with approximate initial water-level conditions.

Figure 6-18 shows a scatterplot of simulated and observed monthly groundwater heads. Considering the complex hydrogeology characterized by lave tubes, basalts, and highly heterogeneous volcanic

units, the scatterplot shows a good agreement between the observed and simulated head values. This demonstrates that the model can create head gradients along the streams, where groundwater data are available. The lack of groundwater head data away from the streams creates uncertainty in the model performance in the areas where head data are unavailable. All individual groundwater head hydrographs are provided in Appendix G. The statistics presented in the scatterplot are two different ways to quantify the ‘goodness-of-fit’ of the modeled data as compared to the observed groundwater elevation data. The statistics follow methods presented by Legates and McCabe (1999). The coefficient of efficiency, R^2 , was calculated as 0.98 and the index of agreement, d , was 0.99; both statistics indicating good agreement between modeled and observed values.

Several groundwater-level hydrographs do not exhibit a pronounced irrigation-related response because pumping was represented as spatially distributed rather than assigned to specific well locations. For example, see the hydrograph for sha_03 in Appendix G. Site-specific well location information was not available; therefore, pumping was applied over the spatial footprint of irrigation service areas. This distributed representation results in a muted drawdown signal at individual observation wells. As more detailed pumping and well-location information becomes available, the simulated groundwater-level responses are expected to improve.

In the vicinity of the Little Shasta River, simulated groundwater levels locally rise above land surface, indicating areas of potential discharge. This is consistent with the presence of known spring systems, which can partly explain the overestimated heads in the model by representing focused groundwater emergence that may not be fully or accurately captured spatially. However, another plausible explanation is unaccounted or underestimated groundwater pumping in the area, which could lower actual water levels relative to simulated conditions, thereby contributing to the apparent overestimation in modeled heads. As more site-specific information becomes available such as spring locations, discharge rates, and pumping data, the model can be refined to better represent these processes and improve agreement with observed conditions.

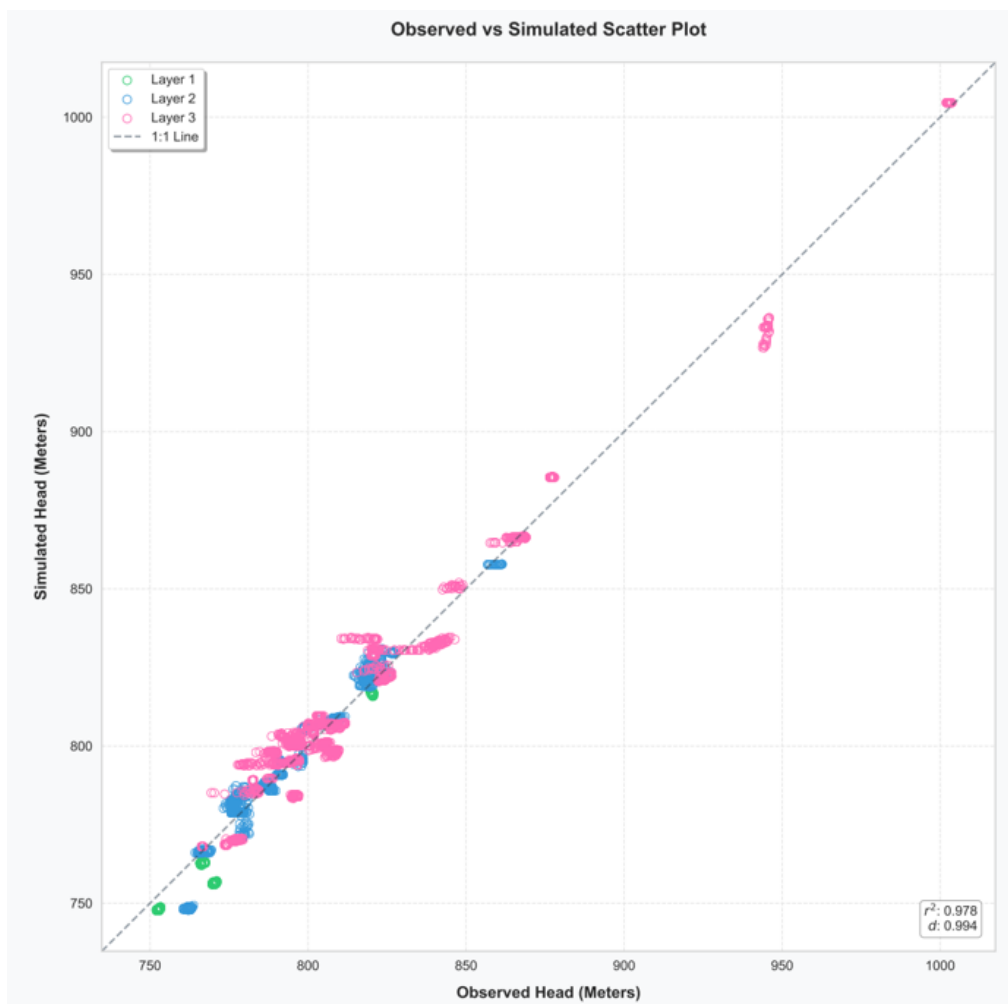


Figure 6-18. Simulated and observed monthly groundwater head values. The coefficient of efficiency, R^2 , and the index of agreement, d , were calculated following methods presented by Legates and McCabe (1999).

6.6.2 Lake Shastina

MODFLOW calibration was performed by adjusting aquifer conductivity, storage parameters, and lakebed and streambed conductance values within each of the aquifer zones (designated in Section 4), to obtain a match between observed and simulated lake volumes. Observed and simulated lake volumes are shown in Figure 6-19. The simulated values capture the average lake volumes over the simulation period although the model does not capture all the oscillations observed in the field estimates. Stream inflow and outflow (to Lower Shasta River and diversion to the MWCD canal) are major components of the lake water budget. Inaccuracies in simulating these terms are reflected in the simulated lake volume change over time.

Simulated lake water budgets were calculated and average budgets for Water Years 1991-2023 are shown in Figure 6-20. Simulated lake storage losses or increases can get up to approximately 30,000 AFY. The range of these losses and increases is similar to the range of 6,500 to 42,000 AFY, suggested by previous studies (NCRWQCB, 2006; Paulsen, 1963).

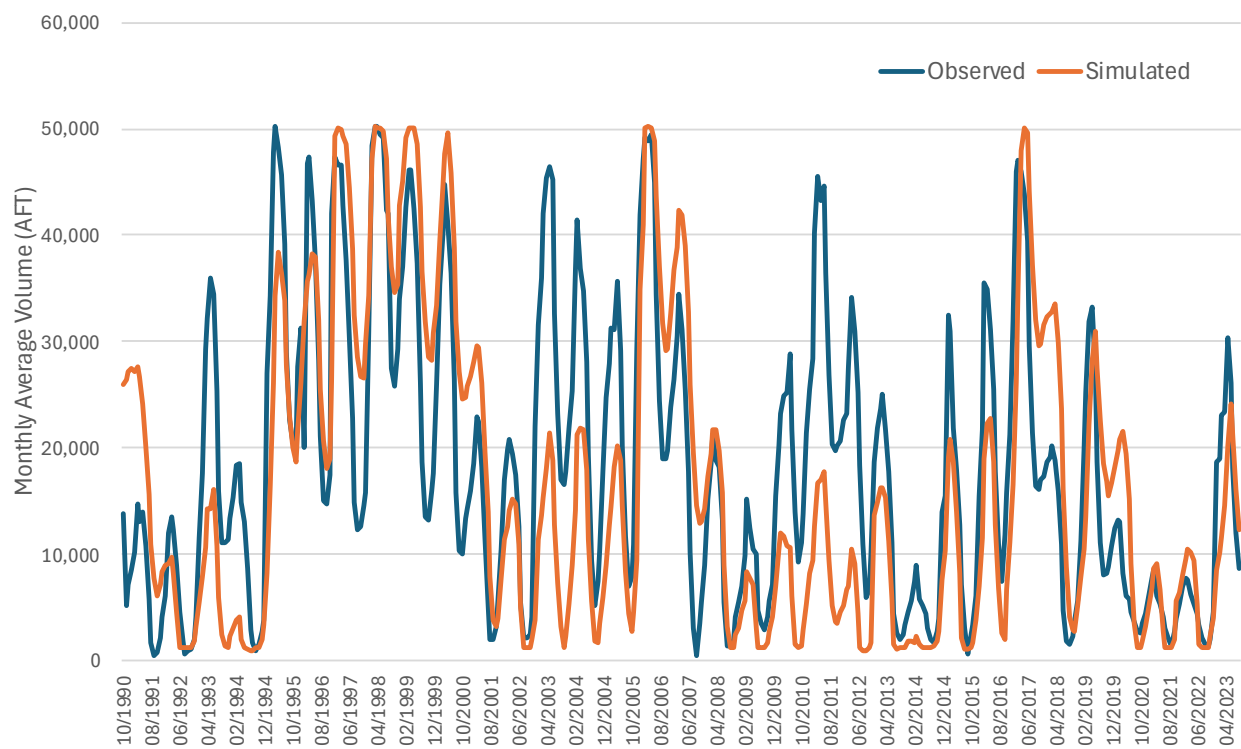


Figure 6-19. Lake Shastina observed and simulated values.

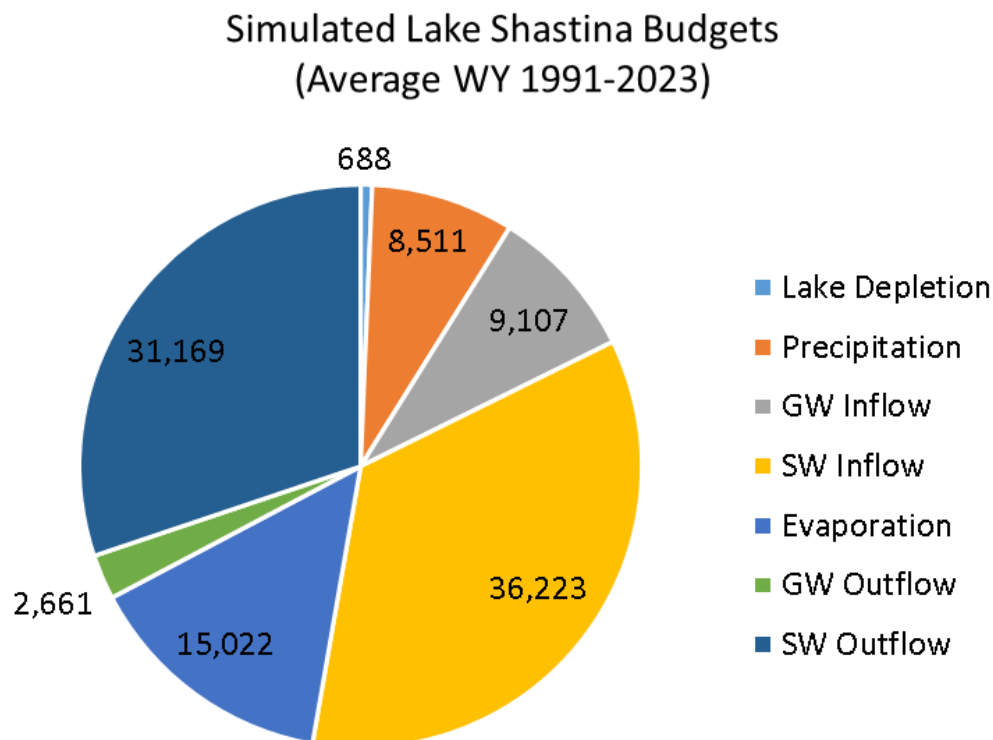


Figure 6-20. Simulated water budget for Lake Shastina.

6.6.3 Minor Spring Flow

The largest spring system in the model is Big Springs and given the high magnitude of flow rates and the amount of data available for Big Springs it was treated as a streamflow gage within LSPC and is not discussed here. Several other springs, demarcated as high priority, for which flow estimates are available only at specific times or as estimated averages were compared to simulated average spring flow rates. These spring flow estimates were not used for calibration purposes but were used to assess the model performance at these spring flow sites; to identify the areas that reproduce estimated spring flows within a reasonable range and the model areas that are deficient in reproducing stream flows with the current model structure. Figure 6-21 shows the locations of these springs and identifies the springs as either being represented as stream segments of the SFR boundary or as DRN boundary.

Average simulated flow within the stream or the drain boundaries associated with springs were compared to estimated values and are shown in Table 6-8. The discrepancies noted in the comparison of spring flows can be attributed to the regional scale of the model and its limitations in representing small scale features. Additionally, the springs are likely fed by high conductivity zones within the aquifer that are not well represented in the model due to the lack of information on the locations of such underground high conductivity formations in the southern portions of the valley.

The Little Shasta River is sustained by a combination of spring-fed groundwater discharge and seasonal inputs such as precipitation runoff, with groundwater providing critical baseflow. Elevation gradients control the spatial distribution and timing of recharge. Geologic conditions, particularly contrasts between highly permeable volcanic units and lower-permeability formations, govern how

recharge is stored, transmitted, and discharged, leading to focused spring systems and spatially variable stream–aquifer interactions. The model captures this overall conceptual behavior, including groundwater contributions and spring flow; however, the specific locations and distribution of flow along the river are not matched in detail. Incorporating more detailed local data such as reach-specific streamflow measurements, mapped spring locations, elevations, and discharge rates, and any potential unrepresented diversions would help refine the representation of the Little Shasta River system and improve simulation of where and how flow occurs.

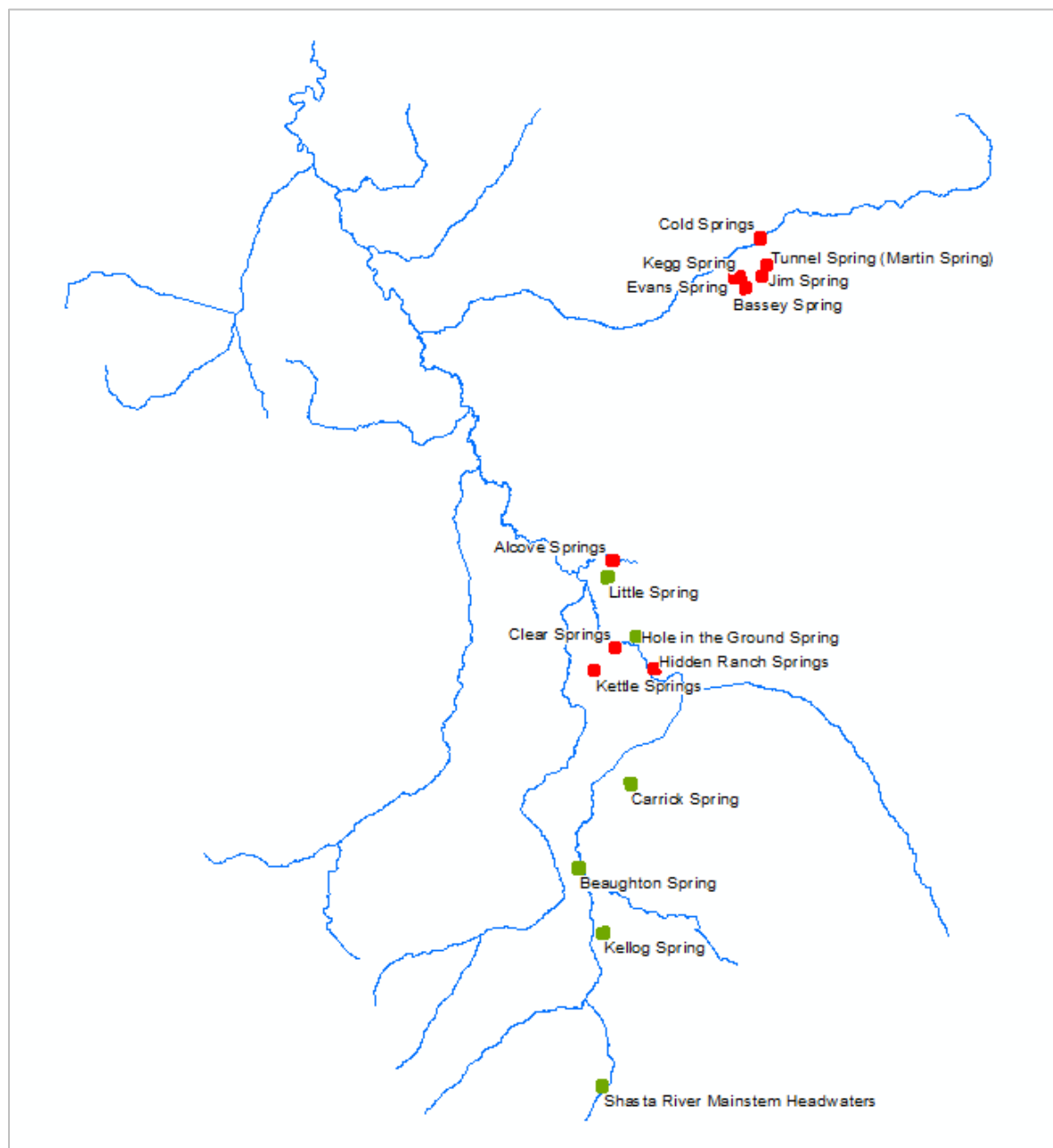


Figure 6-21. Location of springs represented as drain (red) or streams (green) in MODFLOW.

Table 6-8. Observed and simulated flow rates for springs (drains or streams) within the MODFLOW model

Boundary Type	Name	Average Spring Flow Rates (cfs)	
		Observed	Simulated
Drains	Evans	2.4	0.1
	Martin	3.1	0.1
	Cold	13.0	0.0
	Kettle	7.1	0.8
	Hidden Ranch	3.6	0.0
	Alcove	47.0	0.0
	Clear	2.0	0.0
	Jim	2.3	0.0
	Bassey	6.0	0.2
	Kegg	0.3	0.0
	Little	8.0	0.5
Streams	Carrick	8.5	9.3
	Beaughton	8.0	7.7
	Kellog	1.6	1.3
	Hole in the Ground	5.5	1.1
	Shasta Headwaters	10.6	1.7

6.6.4 Aquifer Parameters

Aquifer parameter zonation in the model relied on the zonation provided by Siskiyou County GSA (2021). Calibrated parameters were analyzed to ensure that the values were within a plausible range. Changes in parameter values during the calibration process were monitored to guide the boundary conditions, and therefore, assisted the model development process by providing feedback on potential water budget issues in the system.

Table 6-9 shows the calibrated aquifer parameters. The zone representing Pluto's Cave Basalt, has a very high conductivity value as it represents the high-conductivity zone that supplies water to Big Springs. The other zones range in horizontal and vertical conductivity from 0.01 to 136.05 feet/day and from 0.00025 to 13.55 feet/day, respectively. The wide range, respectively. The wide range of conductivity values is reflective of the diverse system of aquifer formations present in the groundwater system. After the Pluto's Cave Basalt, the aquifer zone representing the Pleistocene Volcanic rocks, that is approximately present in the southeast quadrant of the model, has the highest horizontal conductivity of about 4,000 feet/day. Lava tubes are also expected to be present within this zone. The high conductivity value calibrated for the Pleistocene Volcanic rocks, represents the average bulk transmissivity of the conductivity for Pleistocene Volcanic zone and the high transmissivity of the network of conduits. The bulk transmissivity resulting from calibration is similar to an equivalent porous medium approach commonly used in fractured flow and solute transport.

Low vertical hydraulic conductivity values in the Klamath Mountains, Western Cascades Pliocene Volcanic Rocks, and Western Cascade Volcanics indicate a low potential for groundwater recharge in these areas. Specific storage in the model ranges from 1.9×10^{-7} to 1.3×10^{-4} and specific yield ranges from 0.05 to 0.28. These storage values are within plausible ranges for the aquifers in Shasta Valley.

Table 6-9. Calibrated aquifer parameters used in the Shasta River watershed MODFLOW model

Geological Group	Horizontal Hydraulic Conductivity				Vertical Hydraulic Conductivity				Specific Storage	Specific Yield
	(feet/day)				(feet/day)				(1/feet)	
	Layer 1	Layer 2	Layer 3	Layer 4	Layer 1	Layer 2	Layer 3	Layer 4	All Layers	All Layers
Klamath Mountains	9.94	0.030	0.030	0.030	1.99	0.00025	0.00025	0.00025	6.23E-07	0.14
Hornbrook Formation	0.0084	0.0084	0.0084	0.0084	0.00055	0.00055	0.00055	0.00055	1.89E-05	0.055
Western Cascades Pliocene Volcanic	1.85	1.85	1.85	---	0.031	0.031	0.031	---	1.41E-05	0.12
Alluvium	136.05	27.53	27.53	27.53	13.549	4.03	4.03	4.03	1.70E-06	0.20
Glacial Deposits	0.46	0.46	0.46	---	0.011	0.011	0.011	---	5.82E-06	0.056
Pleistocene Volcanic	38.72	38.72	38.72	---	7.74	7.74	7.74	---	1.06E-04	0.28
Shasta Valley Volcanic	7.65	7.65	7.65	---	0.44	0.44	0.44	---	1.87E-07	0.28
Western Cascades Volcanic	0.41	0.27	0.27	0.27	0.04	0.05	0.05	0.05	1.88E-06	0.28
Pluto's Cave Basalt	---	3,652.47	---	---	---	379.49	---	---	1.25E-04	0.28

6.7 Calibration: Coupled LSPC-MODFLOW Streamflow

Calibration of the coupled LSPC-MODFLOW model was performed for Water Years 2013-2018 (October 1 through September 30) at the Shasta River near Yreka CA USGS gage. These years were chosen to ensure that the model simulation includes a timeframe that coincides with the most recent information on consumptive use and land cover patterns.

The hydrology calibration results in a series of graphical outputs and statistical metrics that were previously described in Section 5.3. The calibration outputs are a result of a series of iterative parameter adjustments in LSPC after incorporating the final MODFLOW active groundwater timeseries based on investigation into model performance compared to observations. The calibration process focused on achieving a reasonable annual and seasonal water budget at the downstream Shasta River near Yreka CA USGS gage, as this location represents the culmination of all watershed activities that impact hydrology. Model performance was also evaluated at and all other intermediate gages with available data (Section 6.9) and further validated using long-term observed data at the Shasta River near Montague, CA (11517000), as presented in Appendix I.

The coupled LSPC-MODFLOW model helped to (1) refine the temporal response during low-flow periods and (2) evaluate spatial impacts of groundwater pumping on summer low flows. Figure 6-22 through Figure 6-25 present time series and summary graphics showing model performance over the calibration period. Model PBIAS for daily flows for the Shasta River near Yreka gage is summarized and presented for the *Wet Season* (October-April), *Dry Season* (May-September), and *All Seasons* (October-September) and by flow condition (e.g., Highest 10% of Flows, Baseflow Periods) in Table 6-10. Model performance metrics for monthly flows for the Shasta River near Yreka gage is summarized in Table 6-11. Additional plots and tables summarizing R-squared and NSE values are presented in Appendix H.

Some notable observations from reviewing the figures and performance metrics include:

- ▼ The Shasta River at Yreka CA gage achieved Good to satisfactory (Fair) performance for total volume in all seasons (including the *Wet*, *Dry* and *All Seasons* categories).
- ▼ *All Seasons* category shows satisfactory (Fair) or better values of PBIAS across all flow conditions and similar results were exhibited for *Wet Season* except for condition describing Storm Flow days.
- ▼ During the *Dry Season*, the model generally performed satisfactorily or worse, apart from baseflow conditions where PBIAS showed Very Good results. In summary, the calibrated model tended to overestimate flows in the *Dry Season*.
- ▼ For monthly flows, the calibrated model was Very Good across metrics and seasons, except for PBIAS, which exhibited Good to satisfactory performance for all seasons.

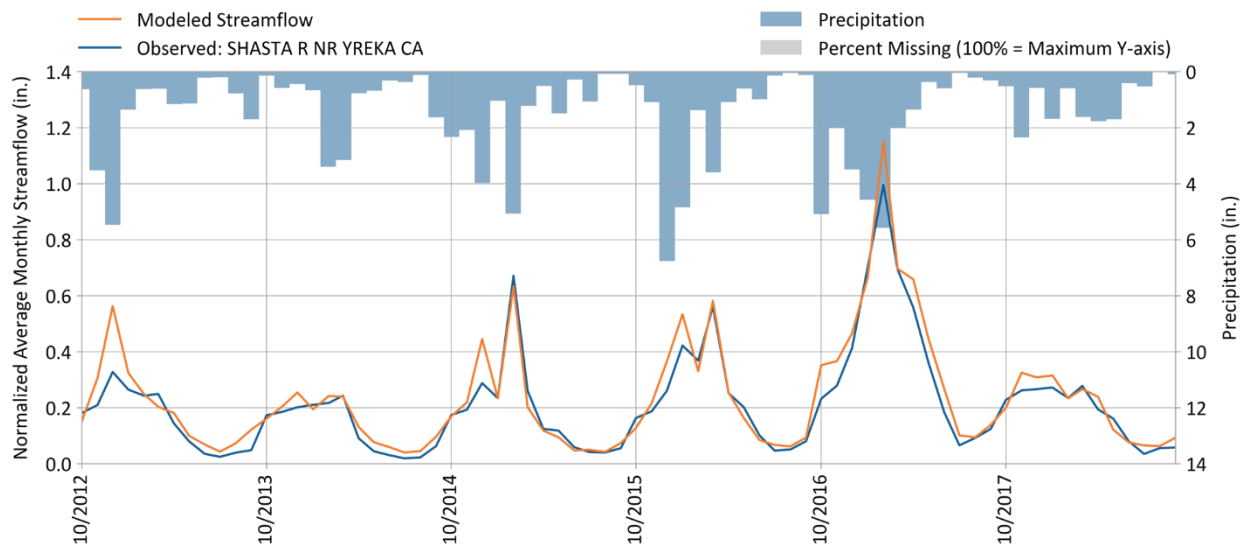


Figure 6-22. SHASTA R NR YREKA CA (11517500) - Hydrology calibration: Simulated vs. observed normalized monthly streamflow.

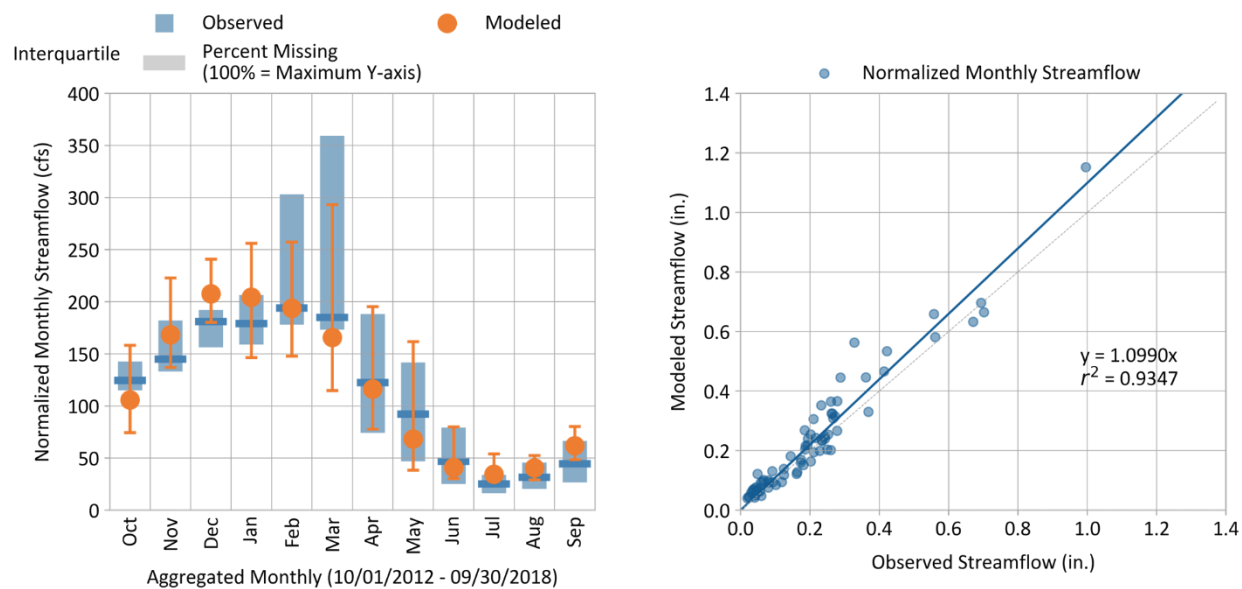


Figure 6-23. SHASTA R NR YREKA CA (11517500) - Hydrology calibration: Simulated vs. observed normalized monthly streamflow.

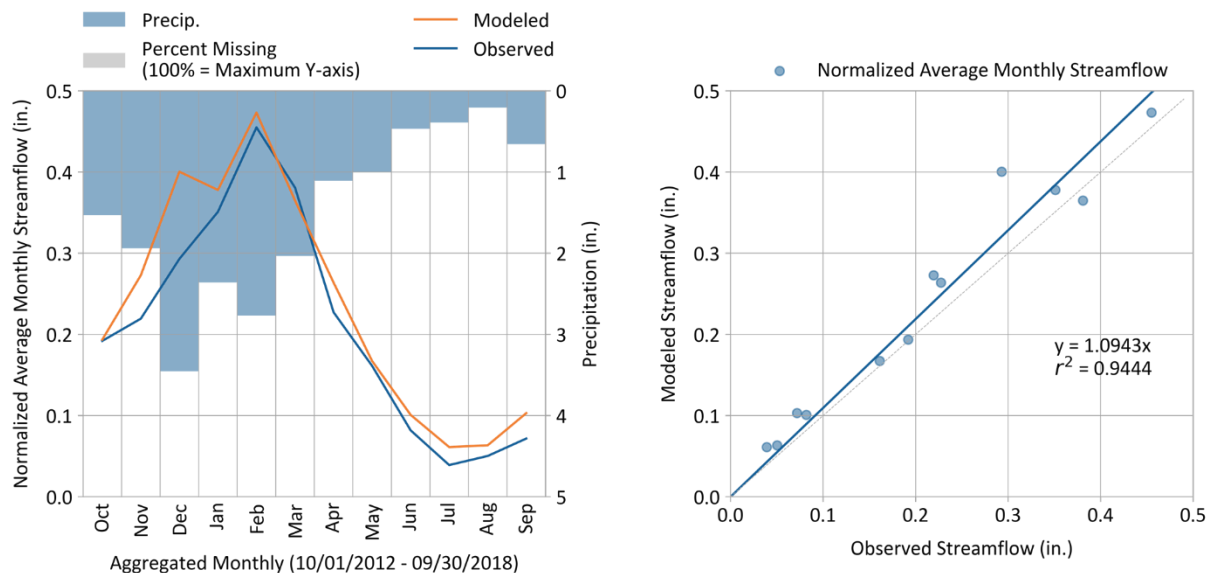


Figure 6-24. SHASTA R NR YREKA CA (11517500) - Hydrology calibration: Average normalized monthly streamflow.

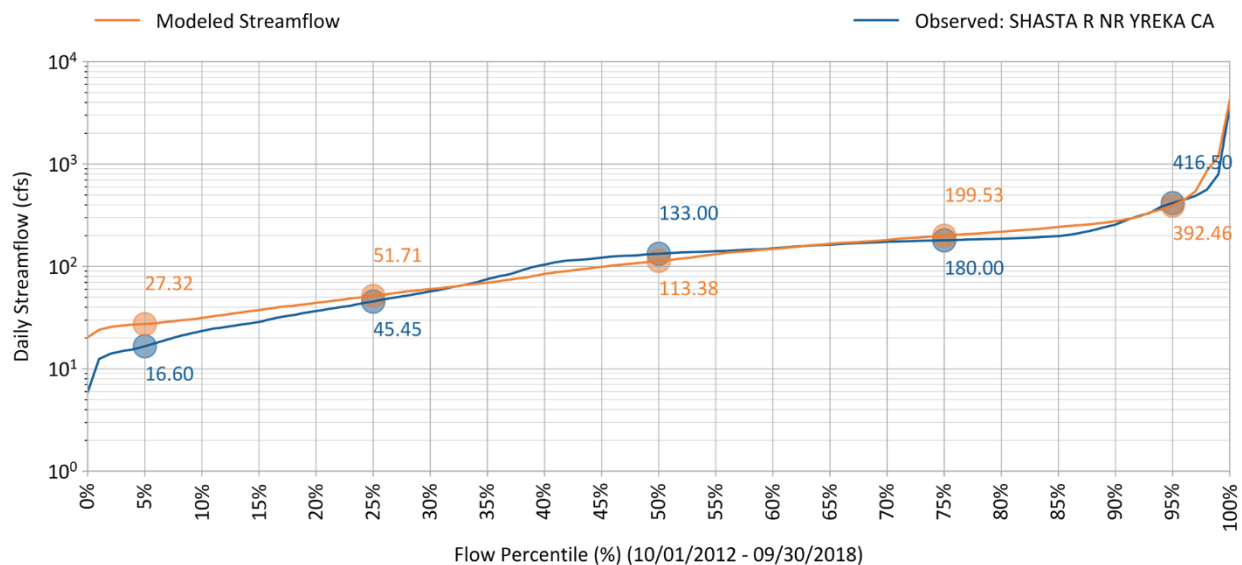


Figure 6-25. SHASTA R NR YREKA CA (11517500) - Hydrology calibration: Simulated vs. observed streamflow duration curves.

Table 6-10. SHASTA R NR YREKA CA (11517500) - Hydrology calibration: Percent bias statistical metric for predicted vs observed volumes

Calibration Metrics for Daily Flow (10/01/2012 - 09/30/2018)	Percent Bias (PBIAS)		
	All Seasons	Wet Season	Dry Season
All Conditions	-12.7%	-10.8%	-22.7%
Highest 10% of Daily Flow Rates	-14.1%	-13.4%	-26.9%
Lowest 50% of Daily Flow Rates	-12.8%	4.3%	-26.0%
Days Categorized as Storm Flow	-26.2%	-25.1%	-31.5%
Days Categorized as Baseflow	9.7%	12.3%	-5.8%
Baseflow Recession Rate ¹	3.5%	N/A	N/A

Calibration Metrics (10/01/2012 - 09/30/2018)	Recommended Error Criteria				Reference
	Very Good	Good	Fair	Poor	
All Conditions	<5%	5% - 10%	10% - 15%	>15%	Based on HSPF experience by A.A. Donigian, Jr., prepared for USEPA (2000)
Seasonal Flows	<10%	10% - 15%	15% - 25%	>25%	
Highest 10% of Daily Flow Rates					
Lowest 50% of Daily Flow Rates					
Days Categorized as Storm Flow					
Days Categorized as Baseflow					
Baseflow Recession Rate					

1: Sorted percentile values of recession rates were used.

Table 6-11. SHASTA R NR YREKA CA (11517500) - Hydrology calibration: Statistical metric for monthly predicted vs observed volumes

Calibration Metrics for Monthly Flow (10/01/2012 - 09/30/2018)	Hydrological Condition		
	All (n = 72)	Wet Season (n = 42)	Dry Season (n = 30)
Percent Bias (PBIAS)	-12.7%	-10.8%	-22.7%
R-Squared (R ²)	0.94	0.91	0.86
Nash-Sutcliffe Efficiency (NSE)	0.9	0.85	0.75
RMSE-Std-Dev_Ratio (RSR ¹)	0.32	0.39	0.5

Calibration Metrics (10/01/2012 - 09/30/2018)	Recommended Error Criteria				Reference
	Very Good	Good	Fair	Poor	
PBIAS (All Conditions)	<5%	5% - 10%	10% - 15%	>15%	Based on HSPF experience by A.A. Donigian, Jr., prepared for USEPA (2000); Moriasi et al. (2015)
PBIAS (Seasonal Flows)	<10%	10% - 15%	15% - 25%	>25%	
R ² (All Conditions)	>0.85	0.75 - 0.85	0.60 - 0.75	≤0.60	
R ² (Seasonal Flows)	>0.75	0.60 - 0.75	0.50 - 0.60	≤0.50	
NSE (All Conditions)	>0.80	0.70 - 0.80	0.50 - 0.70	≤0.50	
NSE (Seasonal Flows)	>0.70	0.50 - 0.70	0.40 - 0.50	≤0.40	
RSR (All Conditions)	≤0.50	0.50 - 0.60	0.60 - 0.70	>0.70	
RSR (Seasonal Flows)	≤0.60	0.60 - 0.70	0.70 - 0.80	>0.80	

1: Sorted percentile values of recession rates were used.

6.8 Validation: Coupled LSPC-MODFLOW Streamflow

After calibrating the coupled model (Section 6.7), its performance was validated using data for a separate period at the Shasta River near Yreka, CA USGS gage to ensure consistent results. The validation period selected was the 17 years prior to the model calibration from October 1, 1995 through September 30, 2012. Systematic validation using high-quality long-term records was conducted for the entire simulation period (October 1, 1990 through September 30, 2023) for two mainstream gages (Yreka [11517500] and Montague [11517000]). The exhibits for additional validation are presented in Appendix I.

The hydrology validation includes a series of graphical outputs and statistical metrics as previously described in Section 5.3. The validation represents the calibrated parameters in the LSPC model along with the final MODFLOW active groundwater timeseries. No additional parameter adjustments were made. The validation process also evaluated the annual and seasonal water budget at the downstream Shasta River near Yreka CA USGS gage. Additional validation checks using other streamflow gages in the watershed are presented in Section 6.9.

The coupled LSPC-MODFLOW model helped to (1) refine the temporal response during low-flow periods and (2) evaluate spatial impacts of groundwater pumping on summer low flows. Figure 6-26 through Figure 6-29 present time series and summary graphics showing model performance over the validation period. Model PBIAS for daily flows for the Shasta River near Yreka gage is summarized and presented for the *Wet Season* (October-April), *Dry Season* (May-September), and *All Seasons* (October-September) and by flow condition (e.g., Highest 10% of Flows, Baseflow Periods) in Table 6-12. Model performance metrics for monthly flows for the Shasta River near Yreka gage is summarized in

Table 6-13. Additional plots and tables summarizing R-squared and NSE values are presented in Appendix I.

Some notable observations from reviewing the figures and performance metrics include:

- ▼ The Shasta River at the Yreka, CA gage demonstrated Very Good performance in total volume across all seasonal categories (*Wet*, *Dry*, and *All Seasons*). The calibrated model performed satisfactory or better for every season and flow condition, except for the top 10% and low 50% of flows during the *Dry Season*, where it tended to underpredict and overpredict respectively.
- ▼ During the validation phase, the *Wet Season* PBIAS was notably low at around -1.8%. For *All Seasons*, PBIAS increased slightly to around -2.4%, primarily due to flow overprediction observed in the *Dry Season* (-4.7%). Importantly, all seasons exhibited lower PBIAS values compared to the calibration period, reflecting a reduced tendency for overprediction relative to observed flows.
- ▼ For monthly averaged flows, the calibrated model achieved Very Good ratings for all metrics and seasons, except in the *Dry Season*, where the NSE was classified as Good.

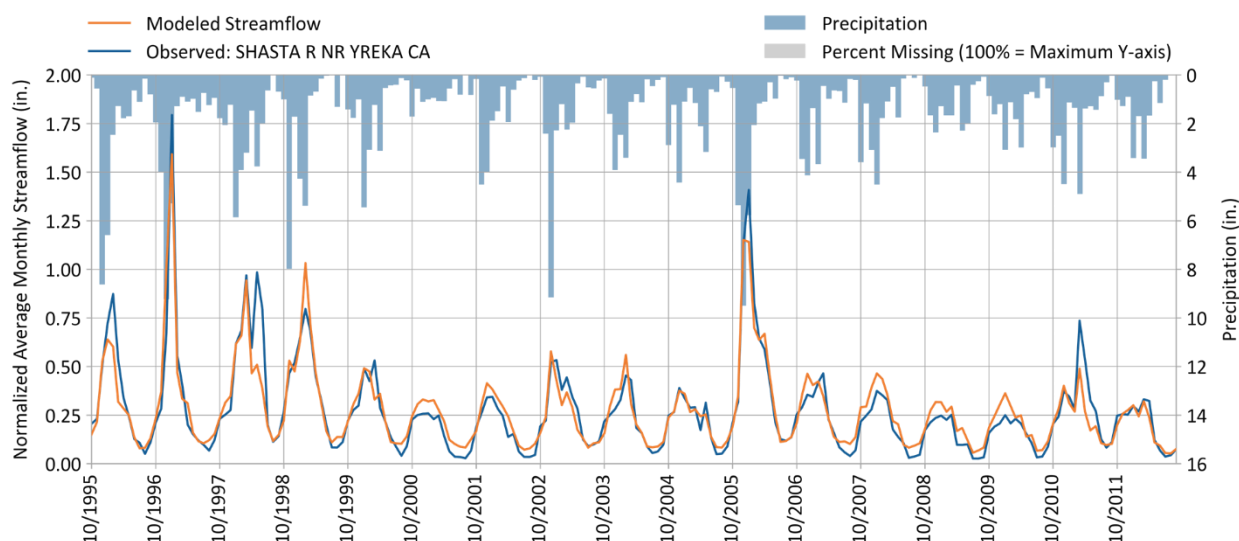


Figure 6-26. SHASTA R NR YREKA CA (11517500) - Hydrology validation: Simulated vs. observed normalized monthly streamflow.

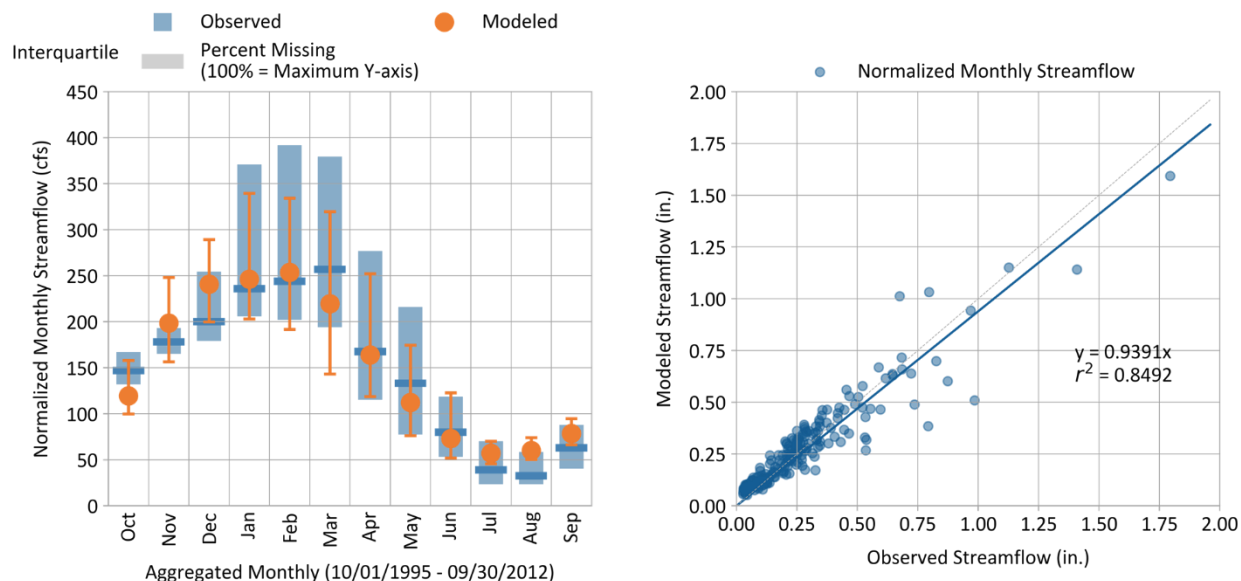


Figure 6-27. SHASTA R NR YREKA CA (11517500) - Hydrology validation: Simulated vs. observed normalized monthly streamflow.

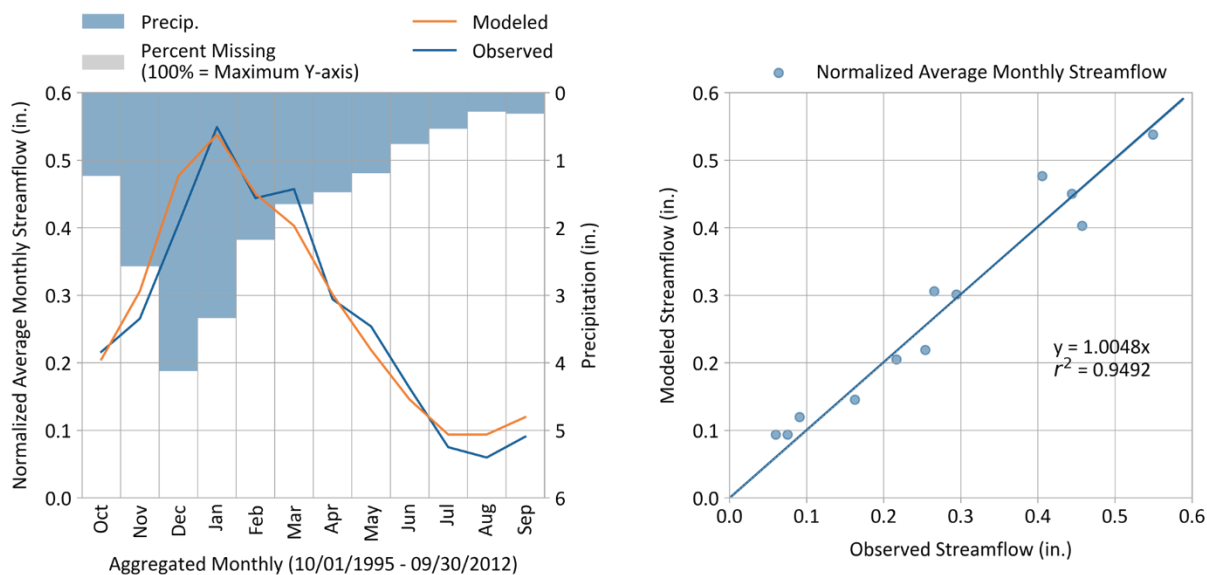


Figure 6-28. SHASTA R NR YREKA CA (11517500) - Hydrology validation: Average normalized monthly streamflow.

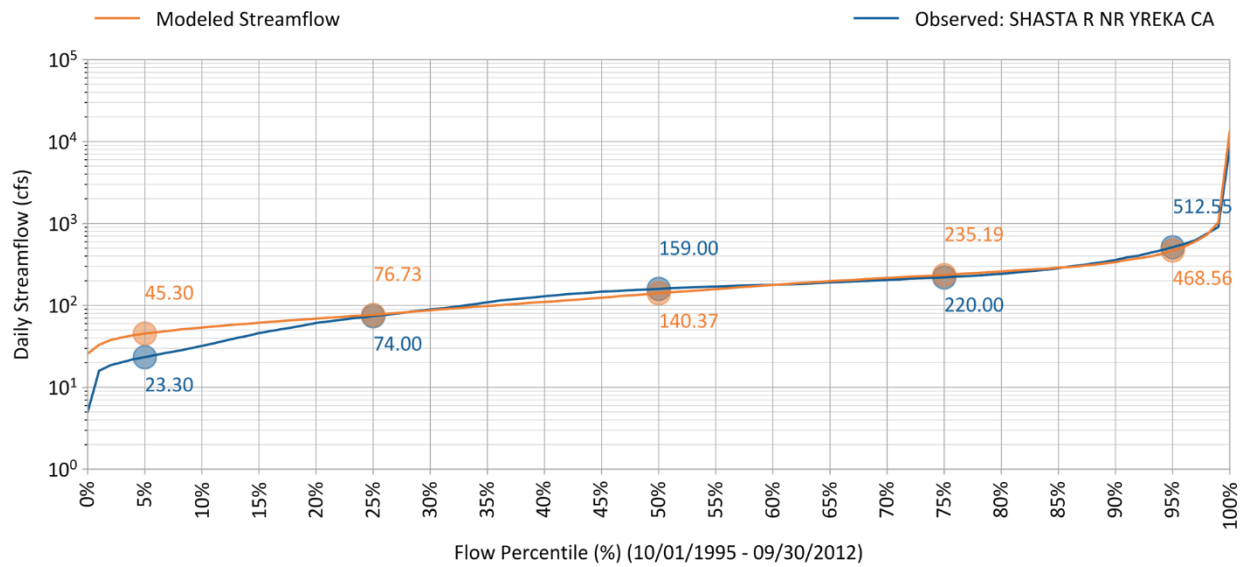


Figure 6-29. SHASTA R NR YREKA CA (11517500) - Hydrology validation: Simulated vs. observed streamflow duration curves.

Table 6-12. SHASTA R NR YREKA CA (11517500) - Hydrology validation: Percent bias statistical metric for predicted vs observed volumes

Calibration Metrics for Daily Flow (10/01/1995 - 09/30/2012)	Percent Bias (PBIAS)		
	All Seasons	Wet Season	Dry Season
All Conditions	-2.4%	-1.8%	-4.7%
Highest 10% of Daily Flow Rates	8.5%	4.0%	49.8%
Lowest 50% of Daily Flow Rates	-19.0%	-9.1%	-26.4%
Days Categorized as Storm Flow	-12.3%	-12.3%	-12.1%
Days Categorized as Baseflow	14.0%	15.5%	7.7%
Baseflow Recession Rate ¹	3.5%	N/A	N/A

Calibration Metrics (10/01/1995 - 09/30/2012)	Recommended Error Criteria				Reference
	Very Good	Good	Fair	Poor	
All Conditions	<5%	5% - 10%	10% - 15%	>15%	Based on HSPF experience by A.A. Donigian, Jr., prepared for USEPA (2000)
Seasonal Flows	<10%	10% - 15%	15% - 25%	>25%	
Highest 10% of Daily Flow Rates					
Lowest 50% of Daily Flow Rates					
Days Categorized as Storm Flow					
Days Categorized as Baseflow					
Baseflow Recession Rate					

1: Sorted percentile values of recession rates were used.

Table 6-13. SHASTA R NR YREKA CA (11517500) - Hydrology calibration: Statistical metric for monthly predicted vs observed volumes

Calibration Metrics for Monthly Flow (10/01/1995 - 09/30/2012)	Hydrological Condition		
	All (n = 204)	Wet Season (n = 119)	Dry Season (n = 85)
Percent Bias (PBIAS)	-2.4%	-1.8%	-4.7%
R-Squared (R ²)	0.88	0.86	0.82
Nash-Sutcliffe Efficiency (NSE)	0.87	0.86	0.68
RMSE-Std-Dev_Ratio (RSR ¹)	0.36	0.37	0.56

Calibration Metrics (10/01/1995 - 09/30/2012)	Recommended Error Criteria				Reference
	Very Good	Good	Fair	Poor	
PBIAS (All Conditions)	<5%	5% - 10%	10% - 15%	>15%	Based on HSPF experience by A.A. Donigian, Jr., prepared for USEPA (2000); Moriasi et al. (2015)
PBIAS (Seasonal Flows)	<10%	10% - 15%	15% - 25%	>25%	
R ² (All Conditions)	>0.85	0.75 - 0.85	0.60 - 0.75	≤0.60	
R ² (Seasonal Flows)	>0.75	0.60 - 0.75	0.50 - 0.60	≤0.50	
NSE (All Conditions)	>0.80	0.70 - 0.80	0.50 - 0.70	≤0.50	
NSE (Seasonal Flows)	>0.70	0.50 - 0.70	0.40 - 0.50	≤0.40	
RSR (All Conditions)	≤0.50	0.50 - 0.60	0.60 - 0.70	>0.70	
RSR (Seasonal Flows)	≤0.60	0.60 - 0.70	0.70 - 0.80	>0.80	

1: Sorted percentile values of recession rates were used.

6.9 Validation: Intermediate Network Locations

Because diversions can have an impact on the ability of the coupled model to represent observed streamflow at specific sites, model calibration and validation focused on the Shasta River at Yreka CA gage to represent the global water budget for the Shasta River. This prevented the model calibration from compensating for a missing source or sink had the intermediate streamflow gages been used. Instead, these intermediate streamflow gages with heavy influence of diversions and withdrawals were evaluated as an additional check on model performance (Table 6-14). The exhibits for additional validation on these intermediate locations are presented in Appendix J.

Big Springs Creek was considered a key evaluation point in the network as a lot of effort during model development focused on the Big Springs Water Conservation District and representing spring flows through the lava tubes from Mount Shasta. Flows at the confluence of Big Springs Creek represent a considerable amount of water with flows ranging between 50 cfs and 100 cfs on average. Figure 6-30 and Figure 6-31 present the average monthly modeled vs. observed flows and the flow duration curve, respectively, for the Big Springs Creek at Water Wheel gage. Before coupling to MODFLOW, this gage consistently underpredicted volumes with modeled flows an order of magnitude less than the observations. Table 6-15 presents the model PBIAS versus the observed data. PBIAS performs well across seasons and most flow conditions except for the highest 10% of flows. Interestingly, *Dry Season*

shows exceptionally good results for all flow conditions. One note about the flows as Big Springs Creek is they do not vary by orders of magnitude like other streamflow gages typically do as the contributions from the springs help regulate the volume; Therefore, there is not much variation in magnitude across the flow duration curve.

Table 6-14. Summary of PBIAS by season and flow regime for additional validation gages

Hydrology Monitoring Locations	Station ID	Start Date	End Date	PBIAS							
				Season			Flow Condition				
				All	Wet Season	Dry Season	All	>10th %ile Flows	Storm Flows	<50th %ile Flows	Baseflow
Big Springs Creek Water Wheel	105SRBSWW	10/1/2013	9/30/2018	0.1	0.2	0.0	0.1	0.4	0.1	0.0	0.1
SHASTA R NR MONTAGUE CA	11517000	10/1/1995	9/30/2018	-0.1	0.1	0.1	-0.1	0.2	0.1	0.0	0.1
SHASTA R NR YREKA CA	11517500	10/1/1995	9/30/2018	0.0	0.0	-0.1	0.0	0.0	-0.2	-0.2	0.1
Shasta River near Grenada	F21370	1/27/2005	9/30/2018	0.1	-0.2	0.3	0.1	0.0	0.1	0.2	0.1
Little Shasta River Nr Montague	11516900	7/21/2017	9/30/2018	0.6	0.7	0.5	0.6	0.8	0.6	0.4	0.6
Shasta River near Edgewood (lower)	F21675	10/1/2004	9/30/2018	0.6	0.5	0.6	0.6	0.6	0.5	0.6	0.6

Very Good
Good
Fair
Poor

- Overpredicts
 + Underpredicts

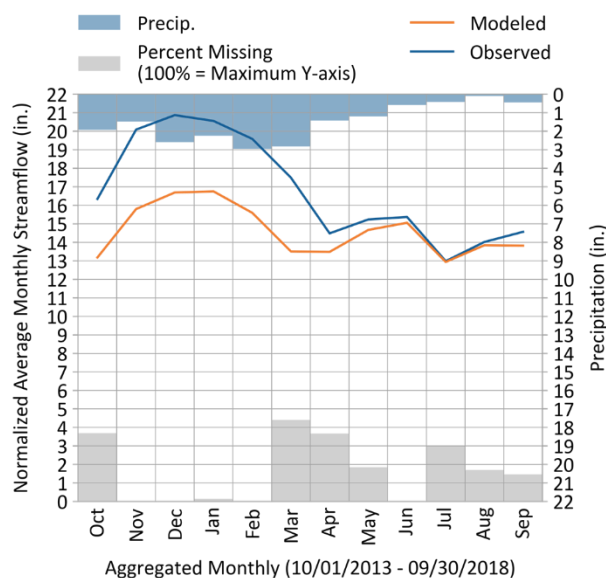


Figure 6-30. Big Springs Creek Water Wheel (105SRBSWW) - Hydrology calibration: Average normalized monthly streamflow

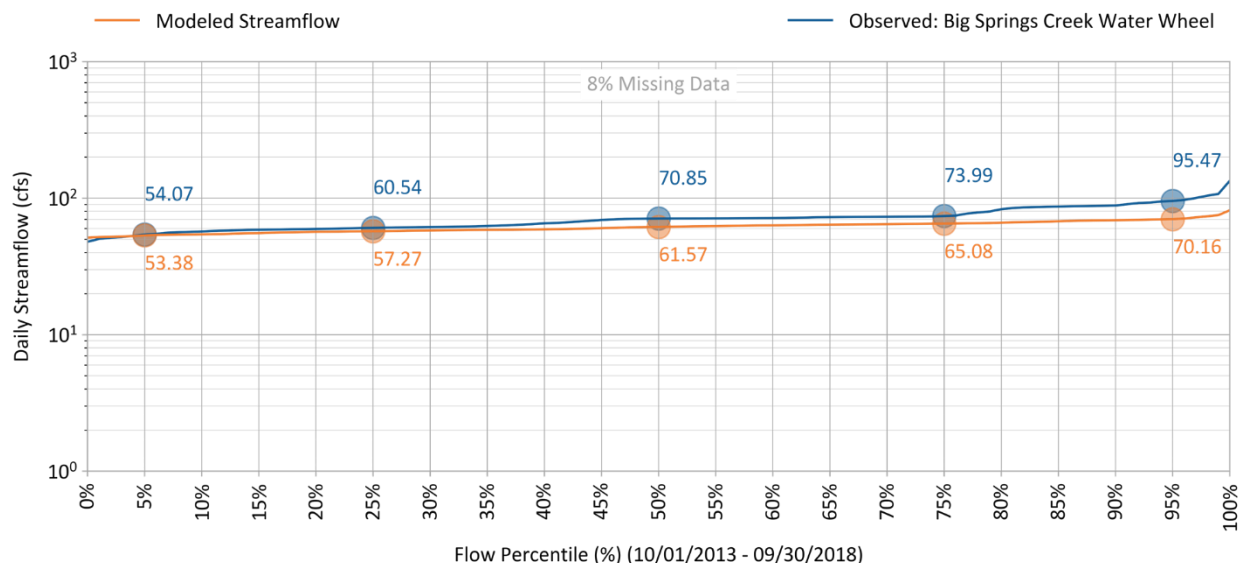


Figure 6-31. Big Springs Creek Water Wheel (105SRBSWW) - Hydrology calibration: Simulated vs. observed streamflow duration curves

Table 6-15. Big Springs Creek Water Wheel (105SRBSWW) - Hydrology calibration: Percent bias statistical metric for predicted vs observed volumes

Calibration Metrics for Daily Flow (10/01/2013 - 09/30/2018)	Percent Bias (PBIAS)		
	All Seasons	Wet Season	Dry Season
All Conditions	13.0%	18.9%	2.6%
Highest 10% of Daily Flow Rates	39.6%	39.6%	N/A
Lowest 50% of Daily Flow Rates	3.2%	7.7%	1.4%
Days Categorized as Storm Flow	14.1%	19.6%	4.0%
Days Categorized as Baseflow	12.2%	18.3%	1.4%
Baseflow Recession Rate ¹	-0.5%	N/A	N/A

Calibration Metrics (10/01/2013 - 09/30/2018)	Recommended Error Criteria				Reference
	Very Good	Good	Fair	Poor	
All Conditions	<5%	5% - 10%	10% - 15%	>15%	Based on HSPF experience by A.A. Donigian, Jr., prepared for USEPA (2000)
Seasonal Flows	<10%	10% - 15%	15% - 25%	>25%	
Highest 10% of Daily Flow Rates					
Lowest 50% of Daily Flow Rates					
Days Categorized as Storm Flow					
Days Categorized as Baseflow					
Baseflow Recession Rate					

1: Sorted percentile values of recession rates were used.

One of the applications of the model is to estimate flows at Big Springs under unimpaired conditions. References such as Deas (2006) indicate that flows during 1922–1923 were on the order of 100–125

cfs, whereas the model simulates average flows on the order of 50–100 cfs. An analysis was therefore undertaken to evaluate whether this difference can be partly explained by long-term changes in hydrologic conditions. The analysis uses groundwater recharge as a proxy for flow to Big Springs; as an approximation, lag times between recharge and spring discharge were not explicitly considered. Recharge was quantified over the contributing subsurface area draining toward Big Springs, as shown in Figure 6-32, using results from the Basin Characterization Model (BCM; Flint et al, 2021). The assessment emphasizes century-scale variability based on historical data and is intended as a qualitative evaluation of broad trends rather than a precise reconstruction.

The results indicate a clear long-term decline in recharge, with notable variability across different periods. Average recharge during the early 1900s was higher than in recent decades, with current conditions showing a reduction of approximately 15–20 cfs. These findings suggest that while hydrology is inherently variable, there has been a shift toward lower recharge in recent decades. This shift provides a plausible explanation for why historically reported higher flows may not be representative of present-day unimpaired conditions. In addition, increases in diversions and groundwater pumping over time may have further reduced observed flows.

Overall, the model captures the subsurface routing of recharge and its contribution to spring flow, including flow directions, magnitudes, and timing. The results support the conclusion that the model appropriately represents unimpaired flow conditions under recent hydrologic regimes, while also providing context for differences between historical and present-day flow estimates.

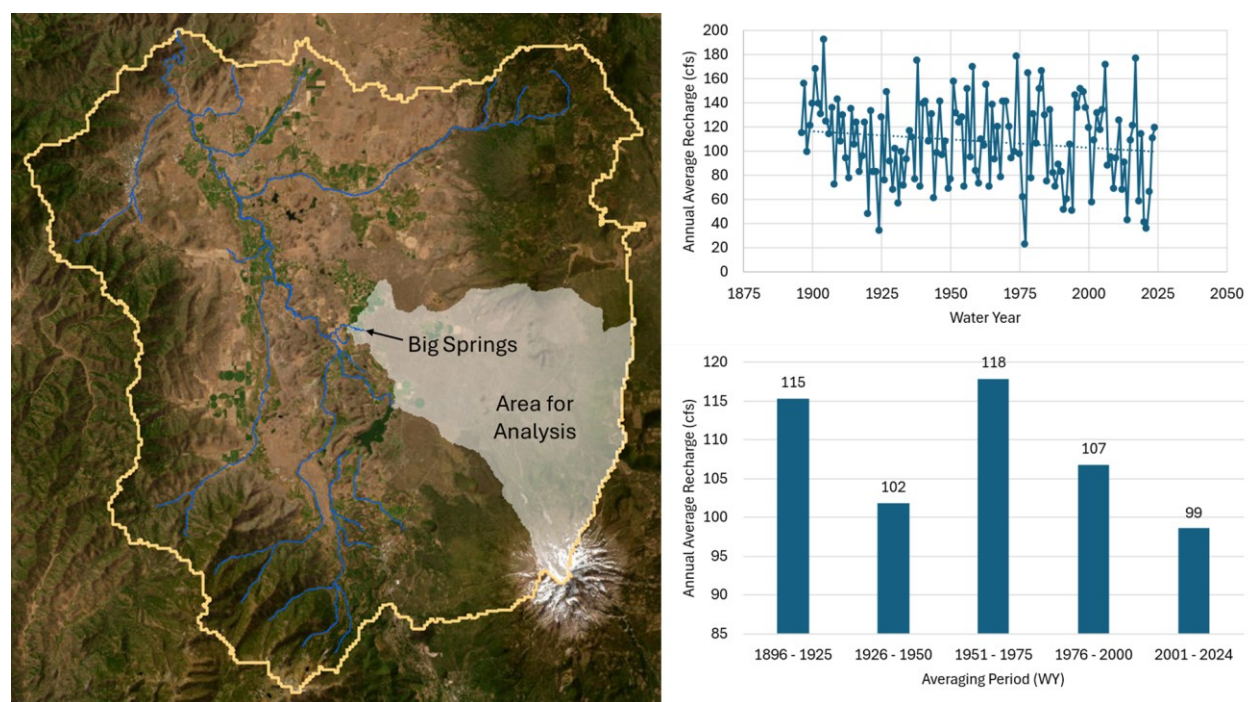


Figure 6-32. Long-term Trends in Groundwater Recharge (1896-2024).

The Shasta River near Montague USGS gage is located about two-thirds of the way down the mainstem of the Shasta River just south of the City of Montague and just downstream of the confluence with Little Shasta. While the Shasta River at Yreka gage near the outlet of the watershed is ultimately downstream of all flows, regardless of the magnitude of diverted flows, the Shasta River near Montague gage is heavily influenced by diversion from the Grenada Water Conservation District,

the Shasta Water Association, and the Montague Water Conservation District diversion through the Parks Creek cross-over channel to Lake Shastina.

The representation of these movements in the model is based on the best available information; However, there is still a degree of uncertainty about the timing, magnitude, and ultimate target for these diversions through time due to gaps in observed diversion data or reliance on operational rules that may be executed slightly different in practice than how they are represented in the model. Mismatches in representing these volumes during different hydrologic periods can lead to difficulties in the model matching observed data across the lower end of the flow duration curve.

Figure 6-33 presents an example of the flow duration curve for the Shasta River at Montague gage modeled vs. observed data.

Table 6-16 presents a summary of model PBIAS performance values. The model generally performs satisfactory or better for all seasons and flow conditions. This assessment confirms that the calibrated model is overall effective in capturing the water movement within the Shasta River watershed.

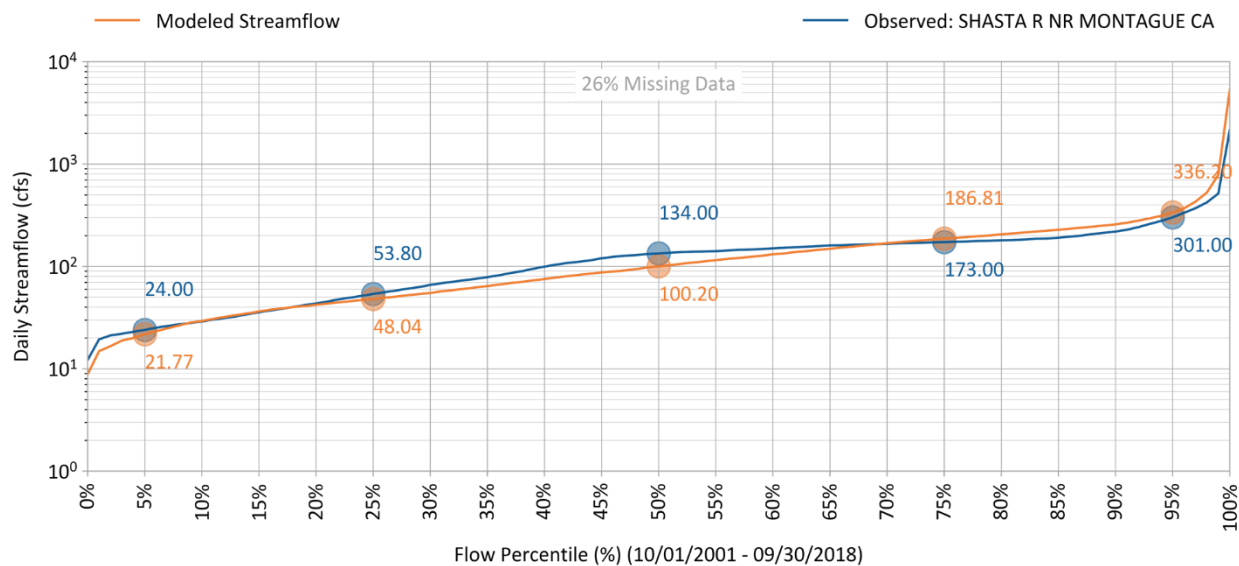


Figure 6-33. SHASTA R NR MONTAGUE CA (11517000) - Hydrology calibration: Simulated vs. observed streamflow duration curves

Table 6-16. SHASTA R NR MONTAGUE CA (11517000) - Hydrology calibration: Percent bias statistical metric for predicted vs observed volumes

Calibration Metrics for Daily Flow (10/01/2001 - 09/30/2018)	Percent Bias (PBIAS)		
	All Seasons	Wet Season	Dry Season
All Conditions	-6.2%	-9.4%	7.0%
Highest 10% of Daily Flow Rates	-16.4%	-19.2%	15.8%
Lowest 50% of Daily Flow Rates	0.9%	-1.8%	2.5%
Days Categorized as Storm Flow	-14.7%	-18.5%	0.3%
Days Categorized as Baseflow	8.5%	6.0%	19.3%
Baseflow Recession Rate ¹	5.5%	N/A	N/A

Calibration Metrics (10/01/2001 - 09/30/2018)	Recommended Error Criteria				Reference
	Very Good	Good	Fair	Poor	
All Conditions	<5%	5% - 10%	10% - 15%	>15%	Based on HSPF experience by A.A. Donigian, Jr., prepared for USEPA (2000)
Seasonal Flows	<10%	10% - 15%	15% - 25%	>25%	
Highest 10% of Daily Flow Rates					
Lowest 50% of Daily Flow Rates					
Days Categorized as Storm Flow					
Days Categorized as Baseflow					
Baseflow Recession Rate					

1: Sorted percentile values of recession rates were used.

7 UNIMPAIRED FLOW SCENARIO

Unimpaired flow is the flow that would have occurred had the natural flow regime remained unaltered in rivers instead of being stored in reservoirs, imported, exported, diverted, or pumped from the subsurface. Unimpaired flow is a modeled flow generally based on historical gage data with factors applied to primarily remove the effects of dams and diversion within the watersheds. Unimpaired flow differs from full natural flow in that the modeled unimpaired flow does not remove changes that have occurred such as channelization and levees, loss of floodplain and wetlands, deforestation, and urbanization. Where no diversion, storage, or consumptive use exists in the watershed, the historical gage data is often assumed to represent unimpaired flow.

The calibrated Shasta River Watershed model was utilized as the baseline scenario (i.e. the existing historical conditions). To simulate unimpaired flow, all anthropogenic elements that influence stream flows were systematically removed from the model. This process involved eliminating the Dwinnell Reservoir, groundwater pumping, irrigation diversions, Flying L and Pacey pumps, as well as non-irrigation consumptive uses and the Parks Creek diversion. By removing these hydrologic features from the baseline scenario, the model is able to reflect the flow conditions that would occur in the

absence of human interventions, thereby providing a counterfactual representation of unimpaired flow within the watershed.

Comparing the baseline and the unimpaired flow scenarios isolates the human-induced effects on the flow system. Figure 7-1 illustrates the flow locations chosen to compare unimpaired flows with the baseline scenario. Figure 7-2 to Figure 7-7 present selected location comparisons, generally showing higher unimpaired flows than baseline.

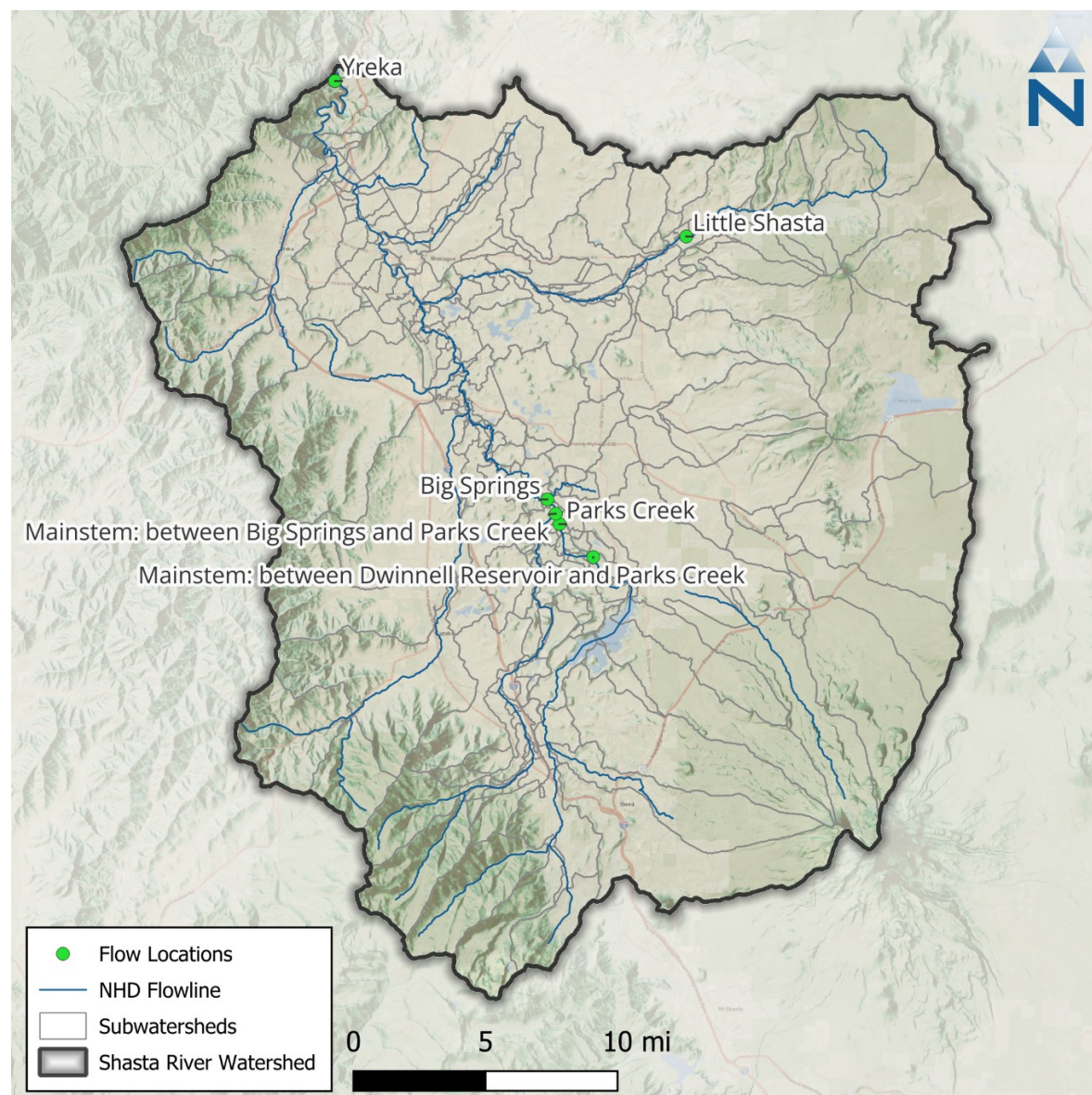


Figure 7-1. Selected unimpaired flow locations within Shasta River Watershed.

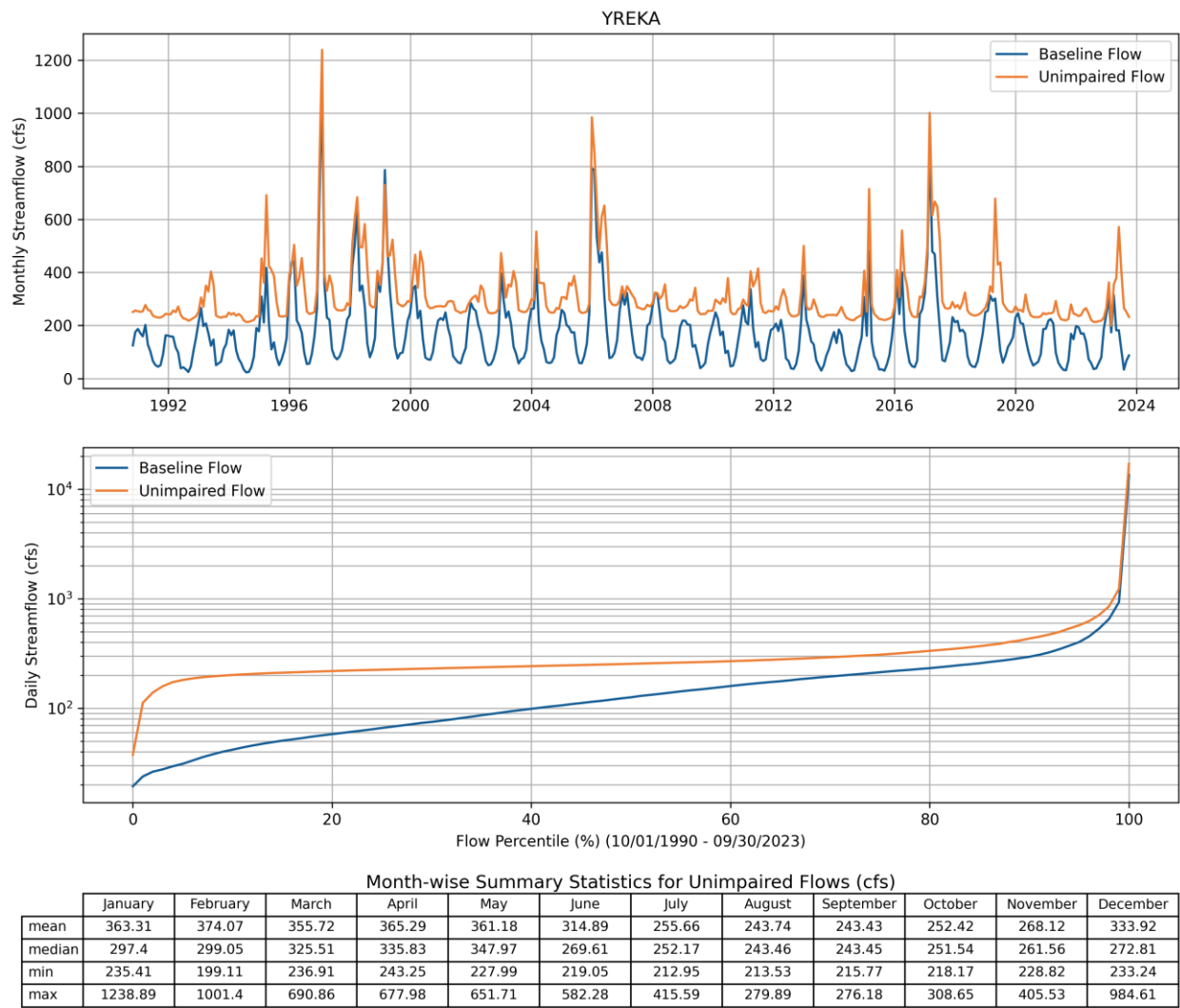


Figure 7-2. Flow at Yreka: comparison between unimpaired and baseline flow conditions.

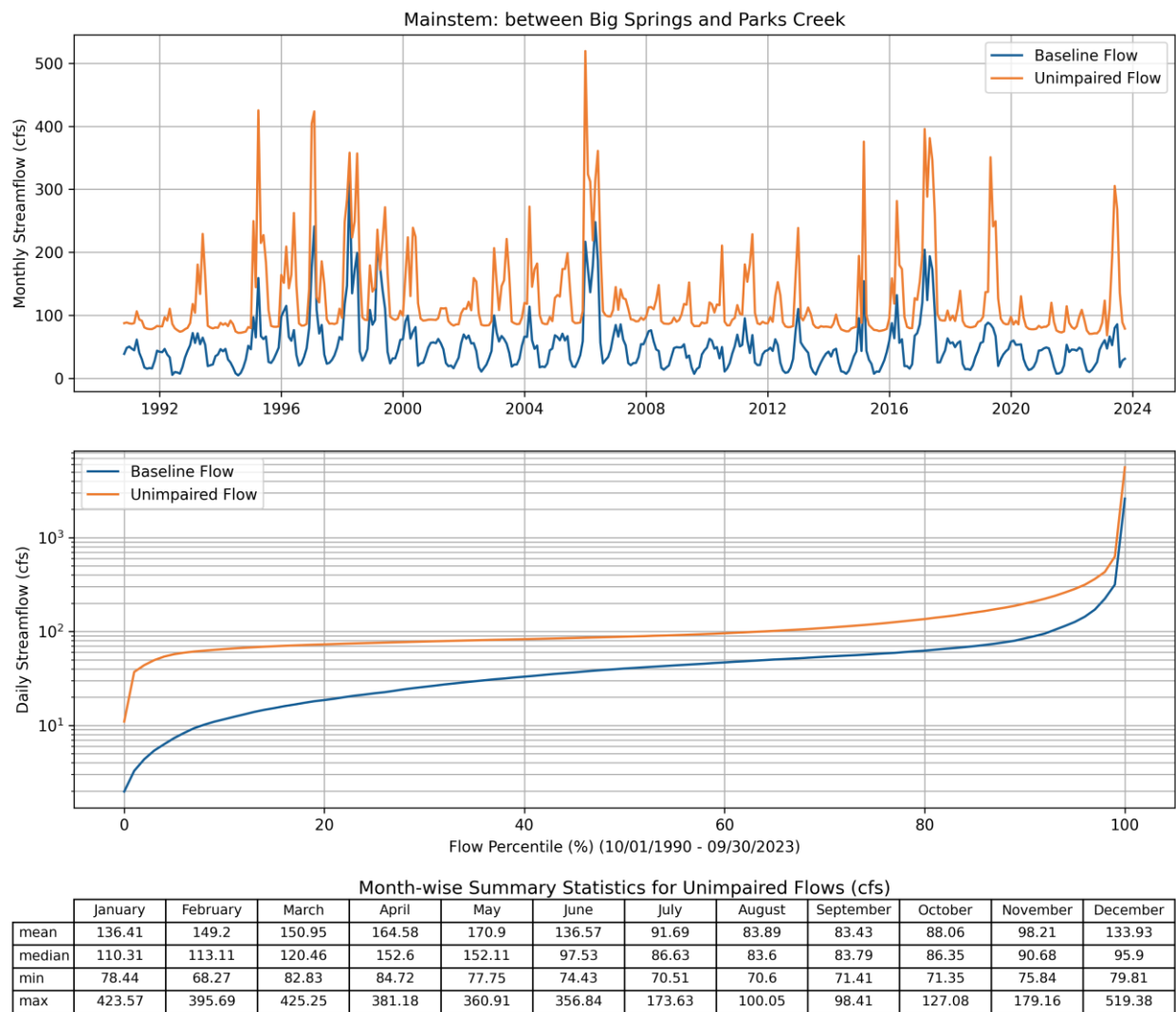


Figure 7-3. Flow at mainstem between Big Springs and Parks Creek: comparison between unimpaired and baseline flow conditions.

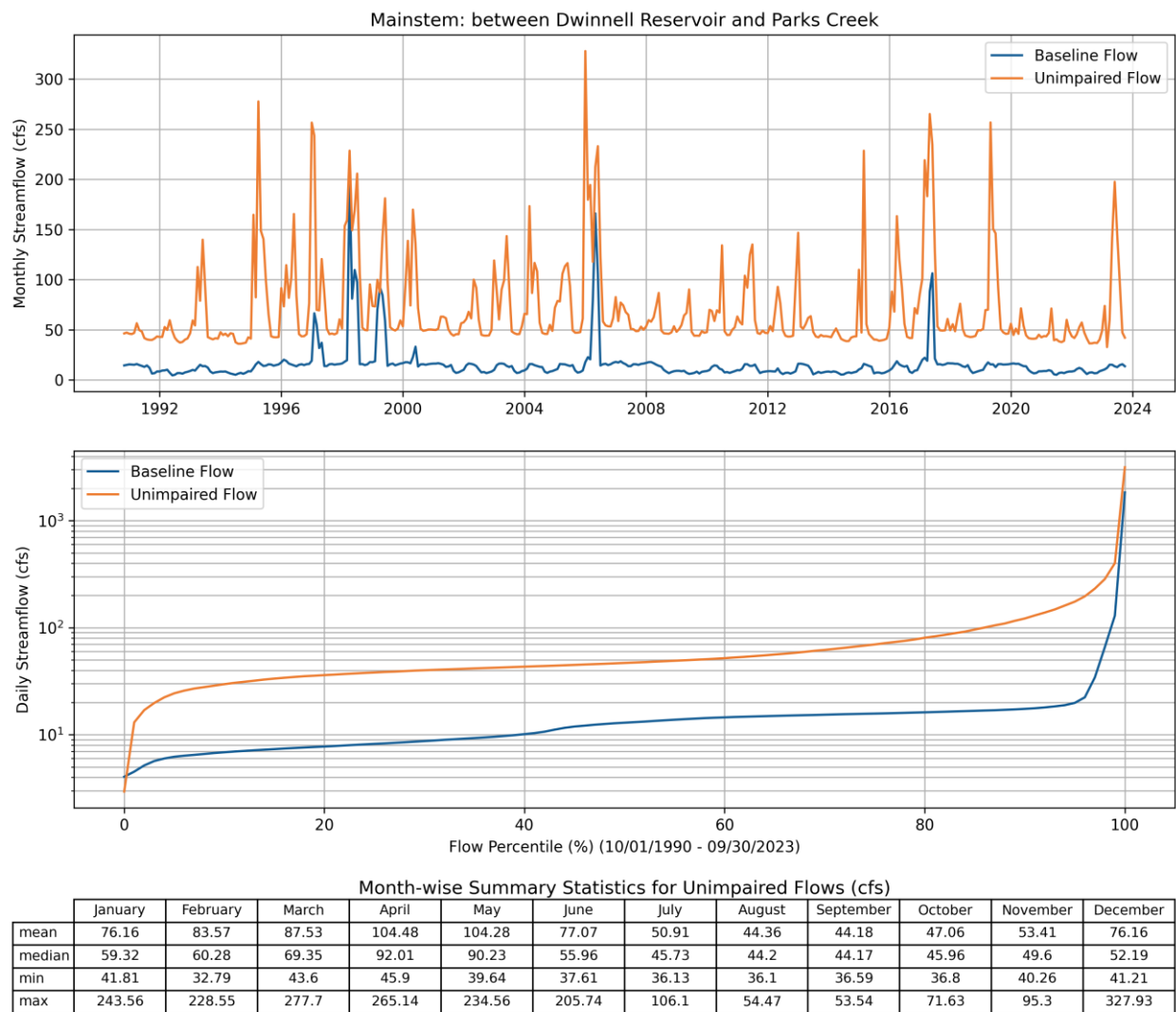


Figure 7-4. Flow at mainstem between Dwinnell Reservoir and Parks Creek: comparison between unimpaired and baseline flow conditions.

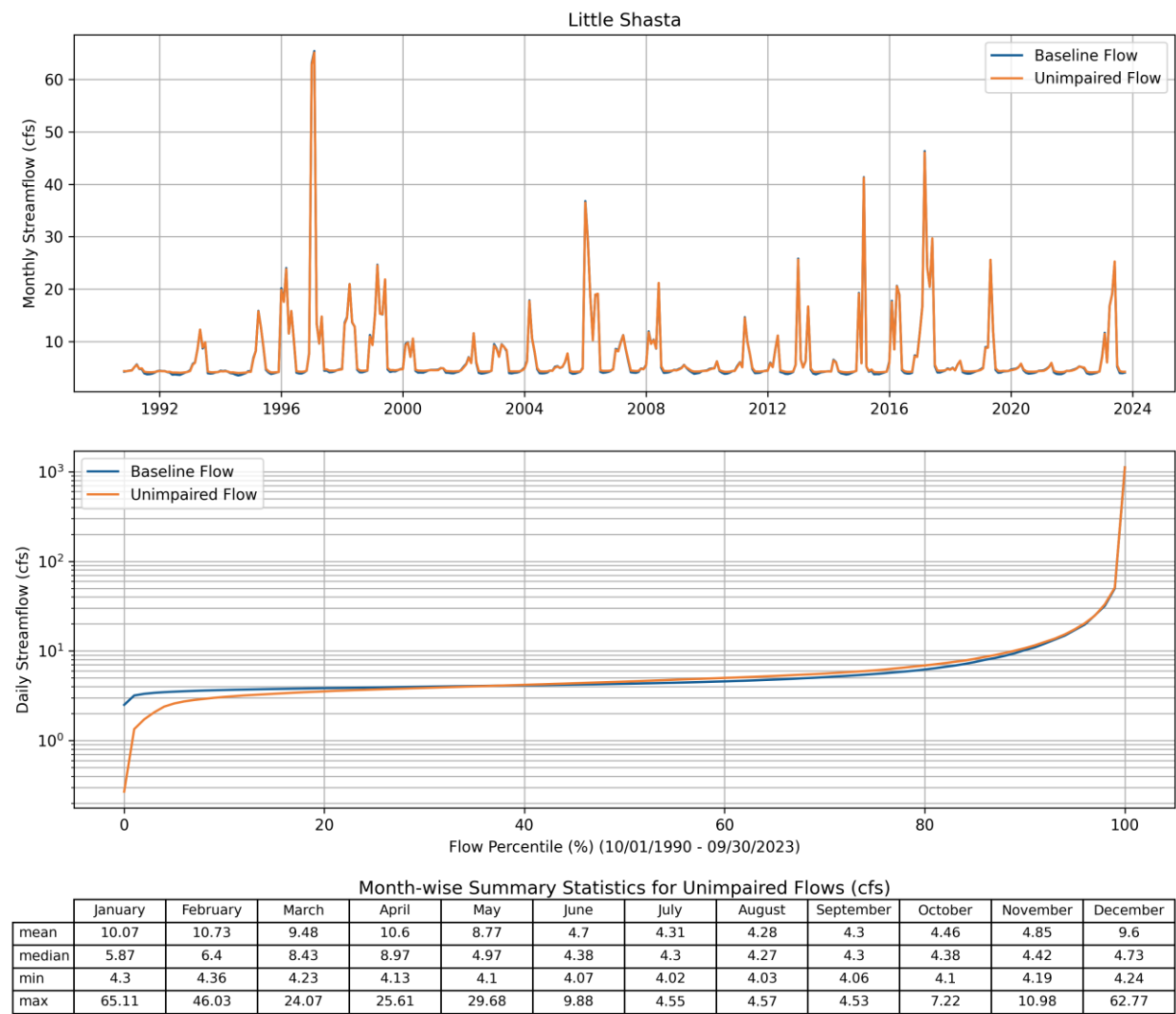


Figure 7-5. Flow at Little Shasta River Near Montague Gage: comparison between unimpaired and baseline flow conditions.

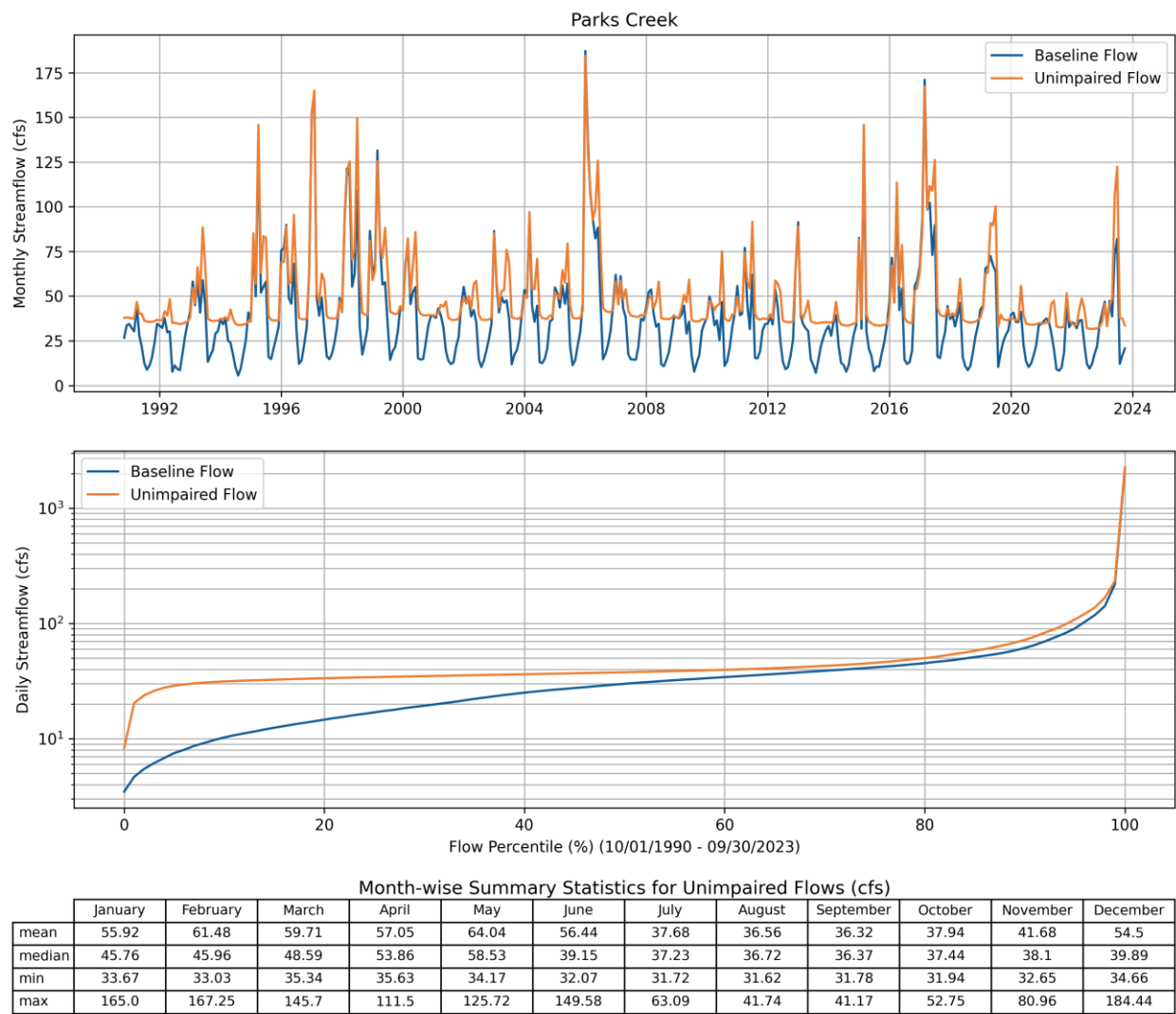


Figure 7-6. Flow at Parks Creek location: comparison between unimpaired and baseline flow conditions.

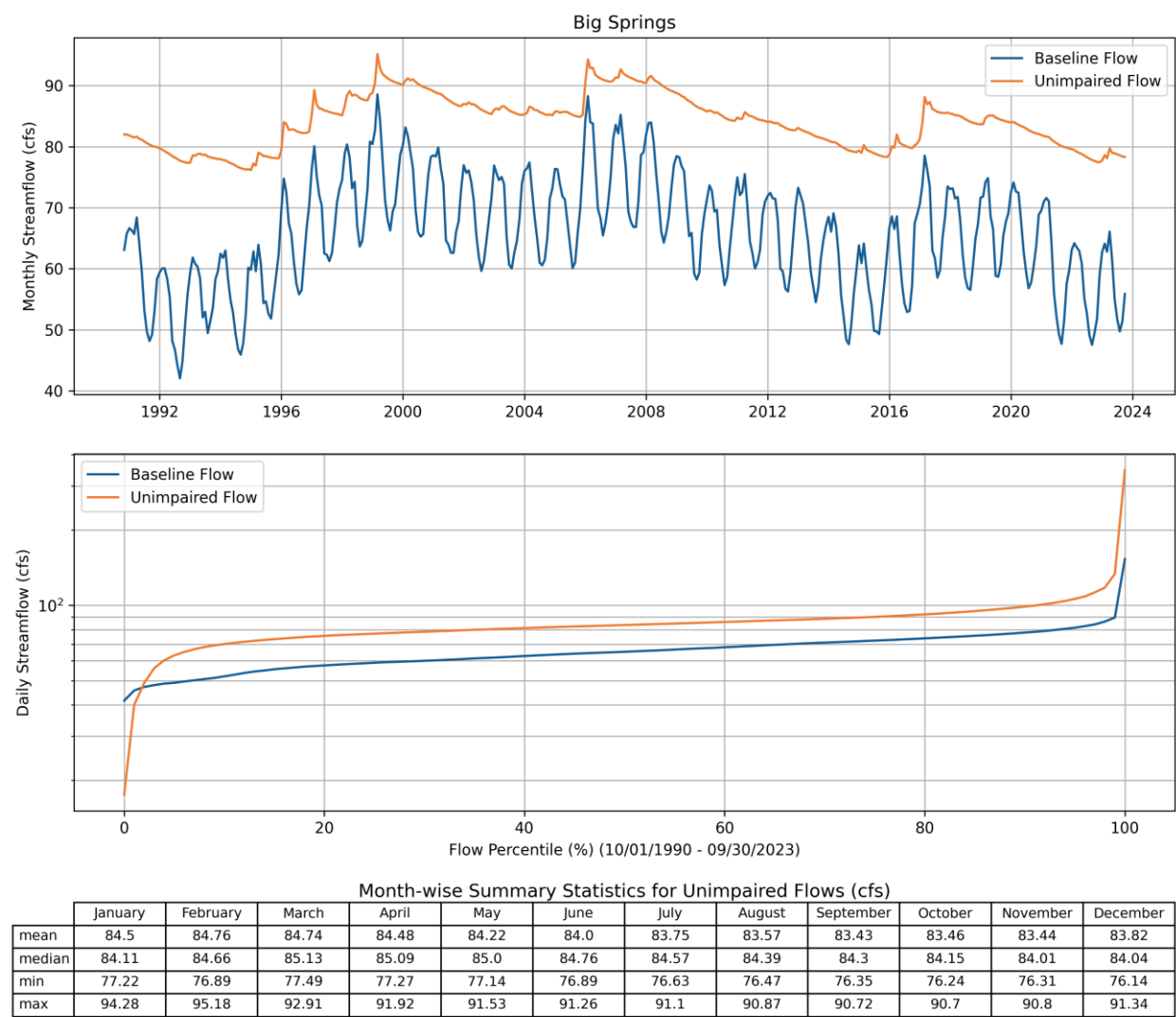


Figure 7-7. Flow at Big Springs: comparison between unimpaired and baseline flow conditions.

8 APPLICATION GUIDELINES AND CONSIDERATIONS

Several improvements have been made to the coupled LSPC-MODFLOW model to improve its predictive capability.

- The southwestern area features predominantly sandy loam soils intermixed with clay layers, which are underlain by volcanic bedrock and alluvial deposits. These soil types influence water movement, limiting infiltration and contributing to higher surface runoff. The local geology is characterized by fractured basalt formations interspersed with sedimentary strata, impacting groundwater flow and recharge rates.
- The surface hydrology calibration in LSPC was refined to reduce infiltration in the southwestern area as described above, and MODFLOW conductivity was also adjusted to better represent subsurface gradients. As a result, shallow groundwater discharge predictions now align with known high water table zones, springs, and surface impoundments in the Shasta Valley.
- The model was also revised to better represent irrigation practices within subwatersheds, enabling some HRUs to be irrigated using surface water and others using groundwater. This approach replaces the previous method of assigning a single irrigation source per subcatchment based on the predominant source. By differentiating irrigation sources at the HRU level, the model provides enhanced spatial and temporal resolution of water use, resulting in more representative estimates of both surface water diversions and groundwater pumping volumes.
- Pacey Pumping volumes were varied for wet, normal and dry years, with pumping estimates derived from the shortfall in potential demand during dry and normal years. This improves the temporal representation of those pumping activities and the overall model calibration during low flow periods.
- The model's representation of the Big Springs area was also improved. Subsurface flow pathways were adjusted within the model to better account for the unique groundwater movement and discharge characteristics of these volcanic features, as well as the impact of pumping on streamflows.

Below are some key considerations when applying the model to evaluate management scenarios.

- An average monthly distribution pattern for irrigation is assumed in the model, with irrigation volumes estimated by adjusting the relative footprints of irrigated versus non-irrigated land. This method was developed to match the spatial and temporal scale of available irrigation demand data, as individual landowner activity is not known or explicitly modeled. While this approach estimates long-term irrigation volumes, it may not capture small-scale variability or short-term fluctuations as precisely.
- To run curtailment scenarios that reflect spatial variability in irrigation activities, the modeler should first update the irrigated and non-irrigated footprint areas for each subwatershed to represent the desired restrictions and update the associated "Landuse" table in the model. Because the HRU footprint remains constant throughout a simulation, the modeler would need to compare results from the updated scenario to those from the baseline run using the original HRU footprints to evaluate the impact of curtailment on water use and distribution.

- Coupling with MODFLOW allows the model to capture the volumes at Big Springs; however, MODFLOW simulates those volumes at a monthly timestep. Hourly AGWO distributions were used to disaggregate MODFLOW predicted volumes in LSPC, but given the large difference in volume, they do not always capture behavior observed at the small temporal scale. This means that while the model can represent overall monthly trends in groundwater discharge, it may miss important short-term fluctuations that occur within a single month. As a result, management decisions requiring finer temporal resolution should consider these limitations when interpreting the model outputs.
- Hydrology plays a key role in temperature modeling within LSPC. Water temperature is stratified by layer and calibrated to observed data: surface water is warmest, while interflow and active groundwater are cooler, with active groundwater outflow being the coolest and relatively constant over time (e.g., 10–11 °C). Sources of cool water to streams include: (1) pumped groundwater that routed to the stream, (2) springs, or (3) infiltrated surface water that ultimately returns as baseflow. Those sources all contribute to cooling the receiving water. Cooling depends on the volume of that water relative to the water in the stream.

The model development process is an effective way to learn about gaps in understanding of the system. Below are some ideas and considerations for future model refinements.

- Expand the calibration dataset by integrating additional field observations such as groundwater level measurements, streamflow records, and water quality data from various locations throughout the watershed. Greater spatial and temporal data coverage will improve model accuracy and confidence in predictions.
- Revisit model calibration for baseflow and unimpaired flow in the Little Shasta River by integrating any additional data, if available. Likewise, future refinements may include calibrating Dwinnell Reservoir storage through the incorporation of detailed reservoir operation rules, if these data are available. These improvements will strengthen the effectiveness and applicability of the integrated model.
- Implement scenario analyses that account for future land use changes, including urban expansion, restoration projects, or shifts in agricultural practices. Updating land use assumptions will ensure that the model remains current and accurately reflects evolving watershed conditions.
- Incorporate climate change scenarios into future model runs to assess the potential impacts of altered precipitation patterns and temperature regimes on groundwater recharge, surface runoff, and irrigation demand. This can help inform long-term water management strategies and enhance the model's relevance for adaptive planning.
- When using the model for management scenario evaluation, ensure that stakeholder input is solicited during scenario development to capture local knowledge, values, and priorities. Collaborative scenario design can improve the relevance and acceptance of model results.
- Regularly update model input datasets and refine model calibration parameters as new information becomes available, such as revised irrigation practices, updated geological data, or improved remote sensing products. Keeping the model current will enhance its predictive capability and usefulness for ongoing watershed management.

9 SUMMARY AND CONCLUSIONS

This report presents the development, configuration, and calibration of an integrated surface and groundwater model for the Shasta River watershed, designed to advance three primary objectives: ensuring reliable water supplies, restoring critical species and habitats, and building a resilient, sustainably managed water resources system that encompasses water supply, quality, flood protection, and environmental integrity. The modeling framework couples LSPC for surface hydrology with MODFLOW for groundwater processes, enabling a comprehensive assessment of watershed hydrology including snowfall/snowmelt, evapotranspiration, surface water diversions, and groundwater pumping.

The model was calibrated using a range of metrics. It frequently demonstrated satisfactory or better performance in reproducing observed conditions at the downstream Shasta River at Yreka and the Montague USGS gages. The coupled model improved the predictive capability for baseflows, though simulating dry season and low flow conditions remain challenging due to anthropogenic influences and model sensitivity to even small changes in low flows. For example, there are small-scale practices like on-lot ponding that may have a collective impact on hydrology; however, they are not explicitly modeled. The coupled model yielded some estimates of shallow groundwater recharge, which spatially aligned with regions of the model where those types of activities are known to occur. Overall, the model provides valuable support for evaluating management scenarios impacts across the watershed.

The model development process itself is an effective way to identify gaps in understanding of the system and areas for future refinement. Some ideas and considerations for future refinements include expanding calibration datasets with additional field observations, updating land use assumptions to reflect changes in urbanization and agricultural practices, evaluating climate change scenarios, and regularly updating model inputs and calibration parameters as new data become available. Such enhancements will further support adaptive planning and strengthen the model's utility for long-term water management.

In conclusion, the coupled LSPC/MODFLOW model stands as a robust foundation for achieving the original objectives of improved water reliability, ecosystem restoration, and sustainable resource management in the Shasta River watershed. Continued refinement and stakeholder engagement will ensure the model remains a relevant and effective tool for guiding decisions in the face of evolving pressures and uncertainties.

10 REFERENCES

- Behnke, R., Vavrus, S., Allstadt, A., Albright, T., Thogmartin, W. E., & Radloff, V. C. (2016). Evaluation of downscaled, gridded climate data for the conterminous United States. *Ecological Applications*, 26(5), 1338–1351. <https://doi.org/10.1002/15-1061>
- Bent, G. C., & Waite, A. M. (2013). Equations for Estimating Bankfull Channel Geometry and Discharge for Streams in Massachusetts. U.S. Geological Survey Scientific Investigations Report 2013–5155. 62. <https://doi.org/https://doi.org/10.3133/sir20135155>
- Bicknell, B. R., Imhoff, J. C., Kittle, J. L., Jobes, T. H., & Donigan, A. S. 1997. Hydrological Simulation Program—FORTRAN (HSPF) User's Manual for Release 11 (EPA/600/R-

- 97/080). U.S. Environmental Protection Agency, National Exposure Research Laboratory, Athens, GA.
- Blodgett, B. J. C., Poeschel, K. R., & Thornton, J. L. (1988). Water-Resources Investigations Report 87-4239 Sacramento, California Denver, CO 80225.
- Buck, C. R. (2013). Managing Groundwater for Environmental Stream Temperature. University of California Davis.
- CDFFP (California Department of Forestry and Fire Protection). (2005). California Forest Practice Rules. Title 14, California Code of Regulations: Chapters 4, 4.5, and 10. Prepared by California Department of Forestry and Fire Protection Resource Management, Forest Practice Program, Sacramento, California, for California Lic.
- CDMG (California Division of Mines and Geology). (1997). Factors Affecting Landslides in Forested Terrain. Note 50.
- Chow, V. Te. (1959). Open Channel Hydraulics. McGraw-Hill.
- Cosgrove, B. A., Lohmann, D., Mitchell, K. E., Houser, P. R., Wood, E. F., Schaake, J. C., Robock, A., Marshall, C., Sheffield, J., Duan, Q., Luo, L., Higgins, R. W., Pinker, R. T., Tarpley, J. D., & Meng, J. (2003). Real-time and retrospective forcing in the North American Land Data Assimilation System (NLDAS) project. *Journal of Geophysical Research: Atmospheres*, 108(22), 8842. <https://doi.org/10.1029/2002jd003118>
- Coulston, J. W., Jacobs, D. M., King, C. R., & Elmore, I. C. (2013). The influence of multi-season imagery on models of canopy cover: A case study. *Photogrammetric Engineering and Remote Sensing*, 79(5), 469–477. <https://doi.org/10.14358/PERS.79.5.469>
- Crandell, D. R. (1989). Gigantic Debris Avalanche of Pleistocene Age From Ancestral Mount Shasta Volcano, California, and Debris-Avalanche Hazard Zonation.
- Crandell, D. R., Miller, C. D., Glicken, H. X., Christiansen, R. L., & Newhall, C. G. (1984). Catastrophic debris avalanche from ancestral Mount Shasta volcano, California. *Geology*, 12(3), 143–146. [https://doi.org/10.1130/0091-7613\(1984\)12<143:CDAFAM>2.0.CO;2](https://doi.org/10.1130/0091-7613(1984)12<143:CDAFAM>2.0.CO;2)
- Crawford, N. H., & Linsley, R. K. 1966. Digital Simulation in Hydrology: Stanford Watershed Model IV (Technical Report No. 39). Department of Civil Engineering, Stanford University, Stanford, CA.
- Daly, C., Halbleib, M., Smith, J. I., Gibson, W. P., Doggett, M. K., Taylor, G. H., Curtis, J., & Pasteris, P. P. (2008). Physiographically sensitive mapping of climatological temperature and precipitation across the conterminous United States. *International Journal of Climatology*, 28(15), 2031–2064. <https://doi.org/10.1002/joc.1688>
- Daly, C., Neilson, R. P., & Phillips, D. C. (1994). A Statistical-Topographic Model for Mapping Climatological Precipitation over Mountainous Terrain. *Journal of Applied Meteorology and Climatology*, 33(2), 140–158. https://journals.ametsoc.org/view/journals/apme/33/2/1520-0450_1994_033_0140_astmfm_2_0_co_2.xml
- Daly, C., Taylor, G., & Gibson, W. (1997). The Prism Approach to Mapping Precipitation and Temperature. 10th AMS Conf. on Applied Climatology, 10–12.

<http://citeseerx.ist.psu.edu/viewdoc/download?doi=10.1.1.730.5725&rep=rep1&type=pdf>

- Davids Engineering. (2020). Shasta Valley Basin Evapotranspiration and Applied Water Estimates, Technical Memorandum.
- Deal, R. L., & Harrington, C. A. (2006). Red Alder: A State of Knowledge. Gen. Tech. Rep. PNW-GTR-669. Portland, OR.
- Deas, M. 2006. Big Springs Creek and Spring Complex – Estimated Quantification. Technical Memorandum prepared for the North Coast Regional Water Quality Control Board. Davis, CA.
- Deas, M., Abbott, A., & Bale, A. (2003). Shasta River Flow and Temperature Modeling Project, Sponsored by the Shasta Valley Resource Conservations District with funding from the California Department of Fish and Game. https://www.waterboards.ca.gov/northcoast/water_issues/programs/tmdls/shasta_river/060707/32appendixeeshastariverflowandtemperaturemodelingproject.pdf
- Devine, W. D., & Harrington, C. A. (2007). Release of Oregon white oak from overtopping Douglas-fir: Effects on soil water and microclimate. Northwest Science, 81(2), 112–124. <https://doi.org/10.3955/0029-344X-81.2.112>
- Doherty, J. (2009). PEST: Model independent parameter estimation. Watermark Numerical Computing, Queensland, Australia. <http://www.pesthomepage.org>
- Donigian, A. S. (2000). Watershed Model Calibration and Validation : Issues and Procedures.
- DWR (California Department of Water Resources). (2011). Shasta Valley, Siskiyou County, Groundwater Data Needs Assessment-Final Draft.
- DWR (California Department of Water Resources). (2019). Statewide Crop Mapping - Datasets - California Natural Resources Agency Open Data. <https://data.cnra.ca.gov/dataset/statewide-crop-mapping>
- DWR (Department of Water Resources). (2003). California's Groundwater. In Bulletin 118. http://www.water.ca.gov/groundwater/bulletin118/docs/Bulletin_118_Update_2003.pdf
- EPA (U.S. Environmental Protection Agency). (2000). BASINS Technical Note 6 Estimating Hydrology and Hydraulic Parameters for HSPF. In Office of Water 4305. EPA-823-R00-012 (Issue July).
- EPA (U.S. Environmental Protection Agency). (2002). Guidance for Quality Assurance Project Plans for Modeling.
- Esposito, C. (n.d.). Personal Communication with Cab Esposito of Larry Walker Associates to John Riverson [Email].
- Fenn, M. E., & Bytnerowicz, A. (1997). Summer throughfall and winter deposition in the San Bernardino mountains in southern California. Atmospheric Environment, 31(5), 673–683. [https://doi.org/10.1016/S1352-2310\(96\)00238-5](https://doi.org/10.1016/S1352-2310(96)00238-5)

- Flint, L.E., Flint, A.L., Stern, M.A., and Seymour, W.A., 2021, The Basin Characterization Model - A monthly regional water balance software package (BCMv8) data release and model archive for hydrologic California (ver. 5.0, June 2025): U.S. Geological Survey data release, <https://doi.org/10.5066/P9PT36UI>.
- Gesch, D. B., Oimoen, M. J., & Evans, G. A. (2014). Accuracy Assessment of the U.S. Geological Survey National Elevation Dataset, and Comparison with Other Large-Area Elevation Datasets-SRTM and ASTER Open-File Report 2014-1008. <https://doi.org/10.3133/ofr20141008>
- Gibson, W. P., Daly, C., Kittel, T., Nychka, D., Johns, C., Rosenbloom, N., McNab, A., & Taylor, G. H. (2002). Development of a 103-Year High-Resolution Climate Data Set for the Conterminous United States. Proceedings of the 13th AMS Conference on Applied Climatology, 181–183. http://www.prism.oregonstate.edu/pub/prism/docs/appclim02-103yr_hires_dataset-gibson.pdf
- Henn, B., Newman, A. J., Livneh, B., Daly, C., & Lundquist, J. D. (2018). An assessment of differences in gridded precipitation datasets in complex terrain. *Journal of Hydrology*, 556, 1205–1219. <https://doi.org/10.1016/j.jhydrol.2017.03.008>
- Homer, C., Dewitz, J., Yang, L., Jin, S., Danielson, P., Xian, G., Coulston, J., Herold, N., Wickham, J., & Megown, K. (2015). Completion of the 2011 National Land Cover Database for the Conterminous United States-Representing a Decade of Land Cover Change Information. *Photogrammetric Engineering and Remote Sensing*, 81(5), 345–354. <https://doi.org/10.14358/PERS.81.5.345>
- Hotz, P. E. (1977). *Geology of the Yreka Quadrangle , Siskiyou County , California*.
- Irwin, W. P. (1981). Tectonic accretion of the Klamath Mountains. In E. W.G. (Ed.), *The geotectonic development of California* (Volume 1, pp. 29–49). Prentice Hall, Inc.
- Jeffres, C. A., Buckland, E. M., Deas, M. L., Hammock, B. G., Kiernan, J. D., King, A. M., Krigbaum, N. Y., Mount, J. F., Moyle, P. B., Nichols, D. L., & Null, S. E. (2008). Baseline Assessment of Salmonid Habitat and Aquatic Ecology of the Nelson Ranch , Shasta River , California Water Year 2007. In Report prepared for: United States Bureau of Reclamation, Klamath Area Office.
- Jeffres, C. A., Dahlgren, R. A., Deas, M. L., Kiernan, J. D., King, A. M., Lusardi, R. A., Mount, J. M., Moyle, P. B., Nichols, A. L., Null, S. E., Tanaka, S. K., & Willis, A. D. (2009). Baseline Assessment of Physical and Biological Conditions Within Waterways on Big Springs Ranch, Siskiyou County, California. In Report prepared for: California State Water Resources Control Board.
- Keter, T. S., & Busam, H. (1997). Growing the Forest Backwards Virtual Prehistory on the North Fork of the Eel River. Paper Presented to the Society for California Archaeology, March 27, 1997, Rohnert Park, California. <http://solararch.org/Papers/SCA1997GISvegmappingintheNorthFork.pdf>
- Legates, D. R., & McCabe, G. J. (1999). Evaluating the use of “goodness-of-fit” Measures in hydrologic and hydroclimatic model validation. *Water Resources Research*, 35(1), 233–241. <https://doi.org/10.1029/1998WR900018>

- Link, P., Simonin, K., Maness, H., Oshun, J., Dawson, T., & Fung, I. (2014). Species differences in the seasonality of evergreen tree transpiration in a Mediterranean climate: Analysis of multiyear, half-hourly sap flow observations. *Water Resources Research*, 50(3), 1869–1894. <https://doi.org/10.1002/2013WR014023>
- Mack, S. (1960). *Geology and Groundwater Features of Shasta Valley, Siskiyou County California*. Geological Survey Water-Supply Paper 1484.
- McCandless, T. L. (2003a). Maryland stream survey: Bankfull discharge and channel characteristics in the Allegheny Plateau and the Valley and Ridge hydrologic region.
- McCandless, T. L. (2003b). Maryland Stream Survey: Bankfull Discharge and Channel Characteristics in the Coastal Plain Hydrologic Region. www.fws.gov/r5cbfo
- McCandless, T. L., & Everett, R. A. (2002). Maryland stream survey: Bankfull discharge and channel characteristics in the Piedmont hydrologic region.
- McLaughlin, R. J., Ellen, S. D., Blake, M. C., Jayko, A. S., Irwin, W. P., Aalto, K. R., Carver, G. A., & Clarke, S. H. J. (2000). *Geology of the Cape Mendocino, Eureka, Garberville, and Southwestern part of the Hayfork 30 X 60 minute quadrangles and adjacent offshore area, Northern California*.
- McNab, W. H., & Avers, P. E. (1994). *Ecological subregions of the United States: WOWSA-5*.
- Mitchell, K. E., Lohmann, D., Houser, P. R., Wood, E. F., Schaake, J. C., Robock, A., Cosgrove, B. A., Sheffield, J., Duan, Q., Luo, L., Higgins, R. W., Pinker, R. T., Tarpley, J. D., Lettenmaier, D. P., Marshall, C. H., Entin, J. K., Pan, M., Shi, W., Koren, V., ... Bailey, A. A. (2004). The multi-institution North American Land Data Assimilation System (NLDAS): Utilizing multiple GCIP products and partners in a continental distributed hydrological modeling system. *Journal of Geophysical Research: Atmospheres*, 109(7). <https://doi.org/10.1029/2003jd003823>
- Moriasi, D. N., Gitau, M. W., Pai, N., & Daggupati, P. (2015). Hydrologic and water quality models: Performance measures and evaluation criteria. *Transactions of the ASABE*, 58(6), 1763–1785. <https://doi.org/10.13031/trans.58.10715>
- Murphy, M. S. (2008). *Edaphic Controls Over Succession In Former Oak Savanna, Willamette Valley, Oregon* [University of Oregon]. <http://scholarsbank.uoregon.edu/xmlui/handle/1794/7887>
- MWCD. (2020). Site Plan Agreement between Montague Water Conservation District, NOAA's National Marine Fisheries Service (NMFS), and California Department of Fish and Wildlife (CDFW) for the Template Safe Harbor Agreement for Conservation of Coho Salmon in the Shasta R. <https://media.fisheries.noaa.gov/2021-03/montague-water-conservation-district-site-plan.pdf>
- MWCD. (2021). Montague Water Conservation District Water Operation Plan March 2021. https://www.waterboards.ca.gov/waterrights/water_issues/programs/drought/scott_shasta_rivers/docs/mwcd-water-operation-plan.pdf

- Nash, J. E., & Sutcliffe, J. V. (1970). River flow forecasting through conceptual models part I - A discussion of principles. *Journal of Hydrology*, 10(3), 282–290. [https://doi.org/10.1016/0022-1694\(70\)90255-6](https://doi.org/10.1016/0022-1694(70)90255-6)
- NCRWQCB (California North Coast Regional Water Quality Control Board). (2006). Report for the Action Plan for the Shasta River Watershed Temperature and Dissolved Oxygen Total Maximum Daily Loads. 1123.
- Nichols, A.L., Jeffres, C. ., Willis, A. D., Corline, N. J., King, A. M., Lusardi, R. A., Deas, M. L., Mount, J. F., & Moyle, P. B. (2010). Longitudinal Baseline Assessment of Salmonid Habitat Characteristics of the Shasta River , March through September , 2008.
- Nichols, Andrew Larsen. (2008). Geological Mediation of Hydrologic Process , Channel Morphology and Resultant Planform Response to Closure of Dwinnell Dam , Shasta River , California (Issue December 2008). University of California Davis.
- Niswonger, R. G., Panday, S., & Ibaraki, M. (2011). MODFLOW-NWT, A Newton formulation for MODFLOW-2005: U.S. Geological Survey Techniques and Methods 6-A37. <https://doi.org/https://doi.org/10.3133/tm6A45>
- NMFS (National Marine Fisheries Service). (2000). Salmonid guidelines for forestry practices in California.
- NRCS (Natural Resources Conservation Service). (2016a). Soil Survey Geographic (SSURGO) Database. USDA. <https://sdmdataaccess.sc.egov.usda.gov>
- NRCS (Natural Resources Conservation Service). (2016b). U.S. General Soil Map (STATSGO2). USDA. <https://sdmdataaccess.sc.egov.usda.gov>
- NSIDC (National Snow & Ice Data Center). (2021). Snow Data Assimilation System (SNODAS) Data Products at NSIDC, Version 1. <https://nsidc.org/data/g02158>
- Pace Engineering. (2016). City of Yreka 2015 Urban Water Management Plan, Job No. 69.47.102. https://wuedata.water.ca.gov/uwmp_plans.asp
- Paradigm Environmental. (2022). Draft Temperature Modeling Report for the Shasta River Watershed.
- Paulsen, W. W. (1963). Geologic investigation for [Dwinell] reservoir leakage and groundwater development.
- PGS (Peninsula Geological Society). (2001). Peninsula Geological Society and Stanford GES-052Q combined field trip , Mount Shasta-Klamath- northern Coast Range area , NW California.
- Phillips, N., Bond, B. J., McDowell, N. G., Ryan, M. G., & Schauer, A. (2003). Leaf area compounds height-related hydraulic costs of water transport in Oregon White Oak trees. *Functional Ecology*, 17(6), 832–840. <https://doi.org/10.1111/j.1365-2435.2003.00791.x>
- Saleeby, J. B., Harper, G. D., Snoke, A. W., & Sharp, W. D. (1982). Time relations and structural-stratigraphic patterns in ophiolite accretion west central Klamath Mountains, California. *Journal of Geophysical Research*, 87(B5), 3831–3848. <https://doi.org/10.1029/JB087iB05p03831>

- Shasta Valley Resource Conservation District. (2017). Lower Shasta River Water Balance : September 2016 (Issue January).
- Silva, I. C., & Rodriguez, H. G. (2001). Interception loss, throughfall and stemflow chemistry in pine and oak forests in northeastern Mexico. *Tree Physiology*, 21(12–13), 1009–1013. <https://doi.org/10.1093/treephys/21.12-13.1009>
- Siskiyou County Flood Control and Water District Groundwater Sustainability Agency [Siskiyou County GSA]. (2021). Shasta Valley Groundwater Sustainability Plan (Public Draft). <https://www.co.siskiyou.ca.us/naturalresources/page/sustainable-groundwater-management-act-sigma>
- Stubblefield, A., Kaufman, M., Blostrom, G., & Rogers, J. (2012). Summer water use by mixed-age and young forest stands, Mattole River, northern California, U.S.A. In R. B. Standiford, T. J. Weller, D. D. Piirto, & J. D. Stuart (Eds.), *Proceedings of coast redwood forests in a changing California: symposium for scientists and managers* (pp. 183–193). USFS, USDA. <https://www.fs.usda.gov/treearch/pubs/41298>
- Sutherland, R. C. (2000). Methods for Estimating the Effective Impervious Area of Urban Watersheds, Technical Note 58. In T. R. Scueler & H. K. Holland (Eds.), *The Practice of Watershed Protection* (pp. 193–195). Center for Watershed Protection.
- Tague, C., & Grant, G. E. (2004). A geological framework for interpreting the low-flow regimes of Cascade streams, Willamette River Basin, Oregon. *Water Resources Research*, 40(4), 1–9. <https://doi.org/10.1029/2003WR002629>
- Tague, C. L., Farrell, M., Grant, G., Lewis, S., & Rey, S. (2007). Hydrogeologic controls on summer stream temperatures in the McKenzie River basin, Oregon. *Hydrological Processes*, 21(24), 3288–3300. <https://doi.org/10.1002/HYP.6538>
- U.S. Environmental Protection Agency (USEPA). 2017a. LSPC user’s manual (Version 5.0). U.S. Environmental Protection Agency. <https://github.com/USEPA/LSPC-Loading-Simulation-Program/blob/master/Document/LSPC%20Version%205.0%20User%20Manual%20DRAFT%2012-6-17.pdf>
- U.S. Environmental Protection Agency (USEPA). 2017b. LSPC: Loading Simulation Program [Computer software]. GitHub. <https://github.com/USEPA/LSPC-Loading-Simulation-Program>
- U.S. Geological Survey. (2018). NHDPlus Version 2. https://nhdplus.com/NHDPlus/NHDPlusV2_home.php
- Vignola, E., & Deas, M. (2005). Lake Shastina Limnology. In Prepared for the North Coast Regional Water Quality Control Board.
- Wagner, D. L., & Saucedo, G. J. (1987). Geologic map of the Weed Quadrangle. California Division of Mines and Geology, Regional Geologic Map Series Map No. 4A, 1-250,000.
- Ward, M., & Eaves, N. (2011). Shasta Valley, Siskiyou County Groundwater Data Needs Assessment.
- Willis, A., & Deas, M. (2009). LAKE SHASTINA WATER BALANCE.

- Willis, A., & Deas, M. (2010). MONTAGUE MAIN CANAL CONVEYANCE EFFICIENCY STUDY.
- Xia, Y., Mitchell, K., Ek, M., Cosgrove, B., Sheffield, J., Luo, L., Alonge, C., Wei, H., Meng, J., Livneh, B., Duan, Q., & Lohmann, D. (2012). Continental-scale water and energy flux analysis and validation for North American Land Data Assimilation System project phase 2 (NLDAS-2): 2. Validation of model-simulated streamflow. *Journal of Geophysical Research Atmospheres*, 117(3). <https://doi.org/10.1029/2011JD016051>
- Xia, Y., Mitchell, K., Ek, M., Sheffield, J., Cosgrove, B., Wood, E., Luo, L., Alonge, C., Wei, H., Meng, J., Livneh, B., Lettenmaier, D., Koren, V., Duan, Q., Mo, K., Fan, Y., & Mocko, D. (2012). Continental-scale water and energy flux analysis and validation for the North American Land Data Assimilation System project phase 2 (NLDAS-2): 1. Intercomparison and application of model products. *Journal of Geophysical Research Atmospheres*, 117(3), 3109. <https://doi.org/10.1029/2011JD016048>
- Xian, G., Homer, C., Demitz, J., Fry, J., Hossain, N., & Wickham, J. (2011). Change of Impervious Surface Area Between 2001 and 2006 in the Conterminous United States. *Photogrammetric Engineering and Remote Sensing*, 77(8), 758–762.